

For Reference

NOT TO BE TAKEN FROM THIS ROOM

Ex LIBRIS
UNIVERSITATIS
ALBERTAEASIS





Digitized by the Internet Archive
in 2022 with funding from
University of Alberta Library

<https://archive.org/details/Nielsen1977>

THE UNIVERSITY OF ALBERTA

RELEASE FORM

NAME OF AUTHOR Peter A. Nielsen

TITLE OF THESIS Metamorphic Petrology and Mineralogy of the
Arseno Lake Area, N.W.T.

DEGREE FOR WHICH THESIS WAS PRESENTED Ph.D.

YEAR THIS DEGREE GRANTED 1977

Permission is hereby granted to THE UNIVERSITY OF
ALBERTA LIBRARY to reproduce single copies of this
thesis and to lend or sell such copies for private,
scholarly or scientific research purposes only.

The author reserves other publication rights, and
neither the thesis nor extensive extracts from it may
be printed or otherwise reproduced without the author's
written permission.

THE UNIVERSITY OF ALBERTA
METAMORPHIC PETROLOGY AND MINERALOGY OF THE
ARSENO LAKE AREA, N.W.T.

by



PETER A. NIELSEN

A THESIS
SUBMITTED TO THE FACULTY OF GRADUATE STUDIES AND
RESEARCH IN PARTIAL FULFILMENT OF THE REQUIREMENTS
FOR THE DEGREE OF DOCTOR OF PHILOSOPHY

DEPARTMENT OF GEOLOGY

EDMONTON, ALBERTA
SPRING, 1977

THE UNIVERSITY OF ALBERTA
FACULTY OF GRADUATE STUDIES AND RESEARCH

The undersigned certify that they have read, and
recommend to the Faculty of Graduate Studies and Research,
for acceptance, a thesis entitled Metamorphic Petrology and
Mineralogy of the Arseno Lake area, N.W.T.
submitted by Peter A. Nielsen
in partial fulfilment of the requirements for the degree of
Doctor of Philosophy
in Geology.

ABSTRACT

A suite of aluminous Proterozoic Snare Group metasediments and polymetamorphic remobilised Archean paragneisses from the Arseno Lake area, Northwest Territories, Canada have been examined. The metamorphic grade ranged from the chlorite zone in the eastern part of the study area to the cordierite-almandine-K-feldspar zone in the west. Based on the spatial distribution of mineral assemblages observed in thin sections, the following isograds have been mapped:

1. Biotite in.
2. Andalusite in.
3. Cordierite in - muscovite + chlorite out.
4. Sillimanite in - andalusite out.
5. Sillimanite + K-feldspar in - muscovite + quartz out.
6. Almandine + K-feldspar ± cordierite in - biotite + sillimanite out.

This sequence of mineral assemblages corresponds to the 'low pressure' facies series of Miyashiro (1961).

Microprobe analysis of the ferro-magnesian silicates show that the scale of equilibrium in the cordierite-almandine-K-feldspar zone is on the order of 1 mm. This small scale of equilibrium is most probably a result of the CO₂ rich nature of the metamorphic fluid in the area.

The available cordierite-garnet-biotite geothermometers have been tested and it is shown that the data of Thompson (1976a,b) are internally consistant and agree well with P - T conditions estimated from experimentally determined equilibria in the system $\text{FeO}-\text{MgO}-\text{SiO}_2-\text{Al}_2\text{O}_3-\text{K}_2\text{O}-\text{H}_2\text{O}$.

The conditions of metamorphism in the Arseno Lake area range from 350° C. @ 2.0 kbar and $X_{\text{H}_2\text{O}} = 1$ in the chlorite zone to $T \sim 630^\circ \text{ C.}$ @ 3.2 kbar and $X_{\text{H}_2\text{O}} = .5$ for the almandine-cordierite-K-feldspar zone.

ACKNOWLEDGEMENTS

Dr. R. St. J. Lambert suggested this project to me and has been the principal advisor throughout. I am most grateful to him and to Drs. H. Baadsgaard, J. Krupicka, R. D. Morton, C. M. Scarfe, and D. G. W. Smith, who advised me on aspects of the study. Dr. Smith also spent many hours instructing me in the use of the microprobe and he and Mr. C. M. Gold taught me the use of the data reduction program, EDATA. Mr. D. A. Tomlinson and S. Launspach assisted in the microprobe laboratory. Mr. F. Dimitrov assisted in the drafting of many diagrams and Mr. A. Stelmach analysed several bulk rock samples and instructed me in the use of the P. E. Model 503 Atomic Absorption Spectrophotometer. Mr. W. Day provided me with the Rb/Sr data for the isochron shown in Figure 3. Drs. C. R. Ramsay, S. Winzer, and N. B. W. Harris provided valuable discussion. Mr. R. Hornal, of the Department of Indian and Northern Affairs in Yellowknife, lent me equipment for use in the field and generously assisted with air transport. Dr. W. Paghman provided helpful discussion in the field. Messrs. D. Frichman and G. Wahl, Ms. G. Hoffman, and my wife assisted in the field.

I received direct financial support from the Boreal Institute for Northern Studies of the University of Alberta, from teaching assistantships in the Department of Geology, and from an Izaak Walton Killam Predoctoral Fellowship

and a National Research Council Scholarship. I also received indirect support from National Research Council of Canada grants to staff members in the Department of Geology, most notably support of the microprobe laboratory by grants to Dr. D. G. W. Smith.

I am especially indebted to my wife, BJ, without whom this thesis would never have been written, for assisting in the field, for typing the thesis, and for understanding the many evenings and weekends spent on the research.

For advice, guidance, and support from all of these sources, I am most grateful. All errors are my own.

TABLE OF CONTENTS

	Page
<u>ABSTRACT</u>	iv
<u>ACKNOWLEDGEMENTS</u>	vi
<u>PART I: INTRODUCTION</u>	1
STATE OF THE ART	4
PREVIOUS WORK.....	10
GENERAL GEOLOGIC CHARACTER OF THE STUDY AREA.	11
General Lithologies.....	14
Structure in Relation to Metamorphism	18
Metamorphism	19
<u>PART II: PETROLOGY</u>	21
GENERAL DESCRIPTION.....	21
The Chlorite Zone	21
The Biotite Zone.....	21
The Cordierite-Andalusite Zone.....	23
The Cordierite-Sillimanite Zone.....	26
The Cordierite-Almandine-K-Feldspar Zone..	27
The Archean Paragneisses	28
The Facies Series	28
The Sample Series	32
CONTROLS ON MINERAL COMPOSITION	33
Permissive Controls	33
Modifying Controls	34
BIOTITE ZONE MINERAL CHEMISTRY.....	39
Biotite.....	39
Chlorite	43
Muscovite	47
Oxides.....	47
CONTROLS OF BIOTITE ZONE MINERAL CHEMISTRY...	53
Metamorphic Grade.....	53
Rock Composition.....	56
Mineral Assemblages Present.....	59
THE BIOTITE FORMING REACTION	59

<u>PART III: CONDITIONS OF METAMORPHISM</u>	127
COMPARISON OF THE METAMORPHISM OF THE ARSENO LAKE AREA AND THE ABUKUMA PLATEAU.....	127
RESTRICTIONS OF THE METAMORPHIC FLUID COMPOSITION IN THE ARSENO LAKE AREA	130
Fluid Inclusions.....	130
Absence of Anatexis.....	131
Scale of Equilibration.....	136
Mineral Assemblages Present.....	136
GARNET - BIOTITE - CORDIERITE GEOTHERMOMETRY..	137
Garnet-Biotite Geothermometry.....	137
Garnet-Cordierite Geothermometry.....	142
Biotite-Cordierite Geothermometry.....	147
Evaluation and Discussion.....	150
GARNET - CORDIERITE - PLAGIOCLASE GEOBAROMETRY.....	155
Garnet-Cordierite-Sillimanite-Quartz.....	155
Garnet-Plagioclase-Al ₂ SiO ₅ -Quartz	157
Evaluation and Discussion.....	161
RESTRICTIONS OF PRESSURE AND TEMPERATURES OF METAMORPHISM	162
The Aluminosilicate Phase Diagram	163
Dehydration Reactions.....	165
Anatexis.....	169
Cordierite Stability.....	169
Oxygen Fugacity.....	170
THE NATURE OF THE HEAT SOURCE.....	175
THE CONDITIONS OF METAMORPHISM IN THE ARSENO LAKE AREA	175
The Biotite Zone.....	176
The Cordierite-Andalusite Zone.....	178
The Cordierite-Sillimanite Zone.....	179
The Biotite-Cordierite-K-feldspar- Sillimanite Zone.....	179
The Cordierite-Almandine-K-feldspar Zone...	180
Origin of the CO ₂ Rich Fluid Phase	181
<u>PART IV: CONCLUSION</u>	186
CONTROLS ON MINERAL COMPOSITION.....	187
The Cordierite Amphibolite Facies.....	191

Geological Evolution.....	195
Scales of Equilibrium.....	196
<u>BIBLIOGRAPHY</u>	200
<u>APPENDIX: METHODOLOGY</u>	217
MINERAL ANALYSES.....	217
Equipment and Operating Conditions.....	217
Precision and Accuracy of Energy Dispersive Analyses.....	220
Standards.....	222
Sample Damage.....	223
MAPS AND SAMPLING.....	226
Maps.....	226
Grade Index.....	226
Samples.....	228
Petrographic Methods.....	228
FLUID INCLUSION STUDIES.....	228
NUMERICAL METHODS AND SAMPLE CALCULATIONS.....	232
Calculation of Fe ⁺³ in Spinel.....	232
Thompson Geothermometry.....	233
Currie Geothermometry.....	233

LIST OF TABLES

Table		Page
1	Commonly observed mineral assemblages from single thin sections.	29
2	Microprobe analyses and structural formulae of BIOTITE from the biotite zone, Arseno Lake area.	40
3	Microprobe analyses and structural formulae of CHLORITE from the biotite zone, Arseno Lake area.	44
4	Microprobe analyses and structural formulae of MUSCOVITE from the Arseno Lake area.	48
5	Microprobe analyses and structural formulae of RUTILE from the Arseno Lake area.	49
6	Microprobe analyses and structural formulae of ILMENITE from the Arseno Lake area.	50
7	Feldspar analyses from the Arseno Lake area.	57
8	Microprobe analyses and structural formulae of BIOTITE from the cordierite zone.	63
9	Microprobe analyses and structural formulae of CORDIERITE from the cordierite zone.	66
10	Microprobe analyses and structural formulae of BIOTITE from the cordierite-garnet zone.	76
11	Microprobe analyses and structural formulae of CORDIERITE from the cordierite-garnet zone.	83
12	Microprobe analyses and structural formulae of GARNET from the cordierite-garnet zone.	86

Table		Page
13	Variation in mineral composition in sample 73252.	94
14	Microprobe analyses and structural formulae of GARNET from the biotite zone.	97
15	Microprobe analyses and structural formulae of BIOTITE from remobilised Archean paragneiss.	103
16	Microprobe analyses and structural formulae of CORDIERITE from remobilised Archean paragneiss.	108
17	Microprobe analyses and structural formulae of SPINEL from remobilised Archean paragneiss.	113
18	Microprobe analyses and structural formulae of GARNET from remobilised Archean paragneiss.	123
19	Comparison of the Arseno Lake area with the central Abukuma Plateau.	128
20	Composition of primary fluid inclusions observed in quartz.	132
21	Temperatures calculated for co-existing biotite and garnet.	140
22	Temperatures calculated for co-existing garnet and cordierite.	144
23	Temperatures calculated for co-existing biotite and cordierite.	148
24	Pressures calculated for co-existing garnet and cordierite.	159
25	Estimated limits of oxygen fugacity.	172
26	Pressure temperature conditions at metamorphism of the Arseno Lake area.	177
27	Bulk rock analyses from the Arseno Lake area.	185

Table	Page
A-1 Comparison of results obtained by energy dispersive and wavelength dispersive analysis of trace amounts of Zn and V for minerals from the Arseno Lake area.	221
A-2 Standards used in microprobe analysis.	224
A-3 Standard compositions.	225
A-4 Rb-Sr data for the samples plotted on figure 3.	230
A-5 Microprobe analyses (weight %) and structural formulae (based on 20 oxygen ions) of alumino silicate minerals from the Arseno Lake area.	231

LIST OF FIGURES

Figure		Page
1	Locality diagram.	2
2	Generalised geology of the Arseno Lake area.	12
3	Rb/Sr reference line.	15
4	Isograds map.	22
5	Controls of mineral composition.	38
6	Relation of biotite composition to metamorphic grade, biotite zone.	41
7a	Relation of chlorite composition to metamorphic grade, biotite zone.	45
7b	Chlorite classification diagram.	46
8a	Relation of ilmenite composition to metamorphic grade, biotite zone.	54
8b	Relation of ilmenite composition to metamorphic grade, almandine-cordierite-K-feldspar zone.	55
9	Relation of biotite composition to metamorphic grade, cordierite zone.	64
10	Relation of cordierite composition to metamorphic grade, cordierite zone.	67
11a	Relation of biotite composition to metamorphic grade, almandine-cordierite-K-feldspar zone for biotite adjacent to cordierite.	80
11b	Relation of biotite composition to metamorphic grade, almandine-cordierite-K-feldspar zone for biotite adjacent to garnet.	81
12	Relation of cordierite composition to metamorphic grade, almandine-cordierite-K-feldspar zone.	85
13a	Relation of garnet composition to metamorphic grade, almandine-cordierite-K-feldspar zone.	91
13b	Chemical zoning of garnet from the almandine-cordierite-K-feldspar zone.	92

Figure		Page
14	Chemical zoning of garnet from the biotite zone.	98
15	Relation of biotite composition to metamorphic grade remobilised Archean paragneiss.	106
16a	Relation of cordierite composition to metamorphic grade, remobilised Archean paragneiss for cordierite adjacent to biotite.	111
16b	Relation of cordierite composition to metamorphic grade, remobilised Archean paragneiss for cordierite adjacent to spinel.	112
17a	Relation of spinel composition to metamorphic grade, remobilised Archean paragneiss for garnet free assemblages.	116
17b	Relation of spinel composition to metamorphic grade, remobilised Archean paragneiss for garnet bearing assemblages.	117
18	Relation of garnet composition to metamorphic grade, remobilised Archean paragneiss.	124
19	Garnet-biotite thermometry.	141
20	Garnet-cordierite geothermometry.	145
21	Biotite-cordierite geothermometry.	149
22	Calibration of garnet- Al_2SiO_5 geobarometer.	158
23	Garnet-cordierite geobarometry.	160
24	Pressure-temperature conditions deduced for the Arseno Lake area.	164
25	Block diagram of the Arseno Lake area.	184
26	AKFM tetrahedron.	192

Figure	Page
27 A'F'M' diagram for the almandine-cordierite-K-feldspar zone.	193
28 A'F'M' diagram for the remobilised Archean paragneiss.	194
29 Tectonic model for the Arseno Lake area.	197

LIST OF PLATES

Plate		Page
I	Photomicrographs of biotite zone features.	25
II	Photomicrographs of almandine-cordierite-K-feldspar textures.	90
III	Photomicrographs showing spinel-cordierite-sillimanite relations.	120
IV	Photomicrographs of fluid inclusions	135

PART I: INTRODUCTION

The Arseno Lake area is located on the Bear-Slave Province boundary, 260 km north-northwest of Yellowknife, Northwest Territories, Canada, and is roughly bounded by $115^{\circ} 30'$ to $116^{\circ} 00'$ West longitude and $64^{\circ} 15'$ to $64^{\circ} 45'$ North latitude (Fig. 1). East of the boundary, the bedrock consists of the Yellowknife Group and related intrusive rocks of Archean age (Lord, 1942; McGlynn and Ross, 1963; Ross and McGlynn, 1965). West of the boundary, the bedrock is predominantly metamorphosed Proterozoic Snare Group sediments, with sporadic occurrences of remobilised Archean ortho- and paragneiss (Lord, 1942; Frith and Leatherbarrow, 1975; Nielsen, 1975). The meta-sediments of the area west of the Bear-Slave Province boundary were studied with the principal objectives of elucidating their metamorphic evolution and of unraveling the relationships between the Bear and Slave provinces.

To those ends, all of the available geologic, geochronologic and geophysical data for the area were compiled and evaluated in an attempt to gain additional controls on the area's evolution. The geologic maps of Lord (1942), McGlynn and Ross (1963), and Frith et al. (1974) served as base maps for planning of traverse lines and for plotting the resultant petrographic observations. K/Ar radiometric dating, by the Geological Survey of Canada (Wanless et al., 1965, 1966, 1968, 1970) established an age of

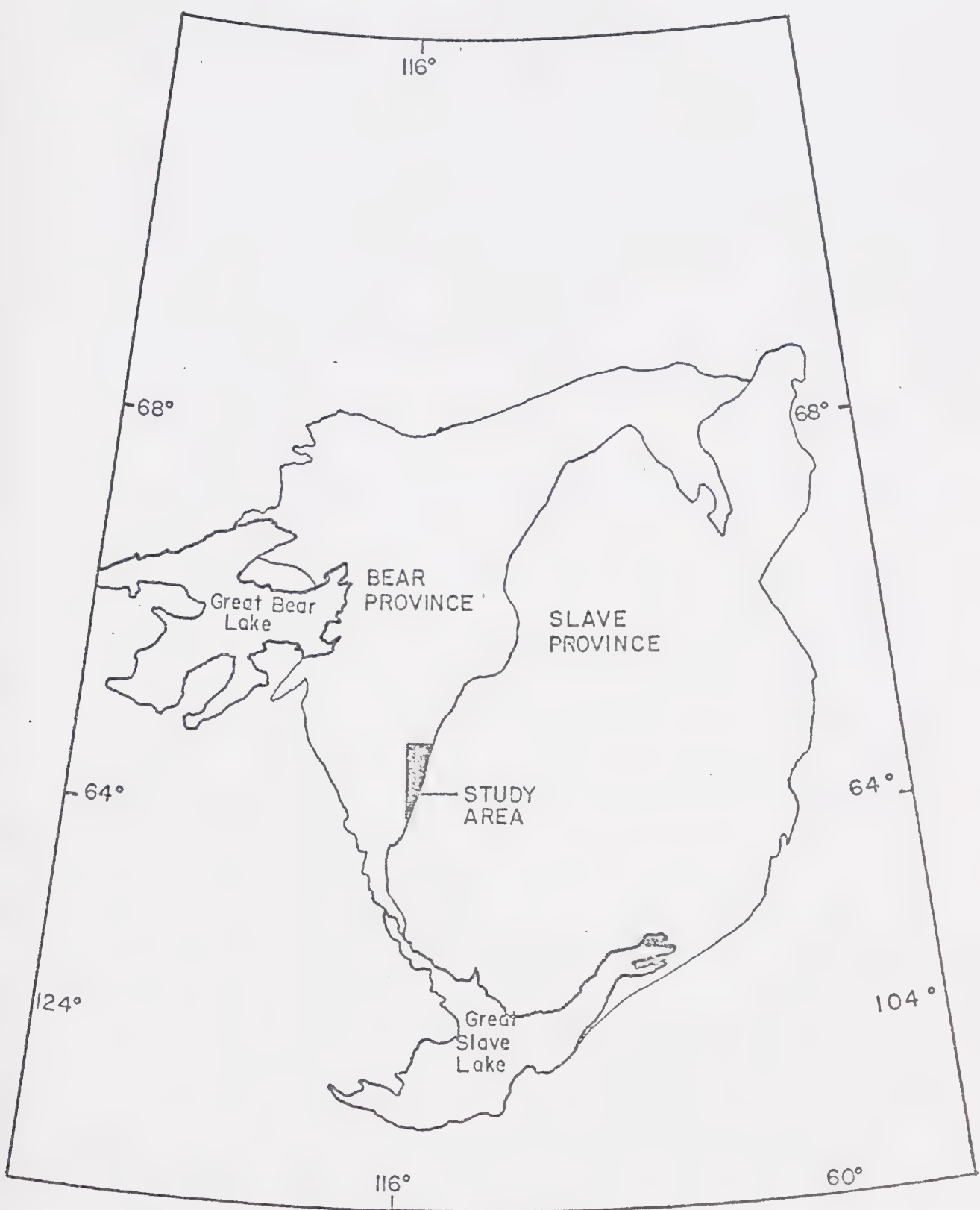


FIGURE 1: Location map.

1815 m.y. for the age of metamorphism of the Snare Group.

The preliminary Rb/Sr dating reported by Frith et al.

(1974) established a minimum age of 2712 ± 89 m.y. for the granitoid core of the gneiss dome in the western half of the area. The only geophysical data available were aeromagnetic anomaly maps (Map 2918G, 2930G), and a regional gravity map compiled from an eight mile grid. The resolution of the gravity survey is too poor to aid in interpreting this area, and the aeromagnetic survey reflects only near surface magnetism.

This particular area was selected for study because of the following reasons:

1. The lithologic character of the rocks favored the presence of an Al_2SiO_5 mineral developing during prograde metamorphism.

This was deemed to be essential for deducing the metamorphic facies series represented in the area.

2. The Bear-Slave Province boundary in this area is relatively uncomplicated and is generally represented by a fault contact between Snare and Yellowknife Group rocks, or locally as an unconformity on the Yellowknife Group, overlain by a basal quartz pebble comglomerate of the Snare Group (Lord, 1942; McGlynn and Ross, 1963; Ross and McGlynn, 1965).

3. The range of metamorphic grade is sufficiently large to permit deduction of the thermal gradient and the general nature of the metamorphic fluid.

It will be shown in Part IV that a detailed metamorphic study of this type of terrain, when integrated with structural and geochronologic data, can provide the necessary data to unravel the complex geological evolution to which the area was subjected.

Field work was conducted during June and July of 1972 and 1973. A total of fourteen weeks was spent in sampling the metasediments along parallel traverses perpendicular to metamorphic gradient, and along accessible lake shores where time and weather permitted. Traverses were spaced 1.0 to 1.75 km apart in the biotite zone and were generally less than 1 km apart in the amphibolite facies zone. Sampling was biased in favor of pelitic and amphibolitic compositions, because such lithologies are most likely to contain 'indicator' mineral assemblages which would be diagnostic of the P-T conditions encountered in this study.

STATE OF THE ART

The field of metamorphism and the methods used in studying metamorphic petrology have, in the last few years, undergone a transformation. A well developed framework was left by early workers for present investigators to

build upon, and their classical studies and the methods they employed are now being supplemented and supplanted by new techniques and additional observations.

The early studies of Barrow (1893), Eskola (1915, 1920), Tilley (1926), and others were primarily concerned with erecting a framework or grid onto which metamorphic assemblages could be related to one another and to an orderly increase in pressure and temperature conditions. The technique used was petrographic examination of thin sections, coupled with bulk rock chemical analyses and analyses of some mineral separates. More recent studies (Miyashiro, 1958; Lambert, 1959; Chinner, 1960, 1962), examined the response of mineral composition to changes in metamorphic grade. Mineral chemical data used in these studies were obtained by wet chemical analyses done on mineral separates. These data, while presenting good totals, represent an average composition of the mineral being analysed, along with 2 - 5% of impurities which could not be separated from the bulk fraction.

With the development of the electron microprobe and an understanding of the quantification of X-ray spectrographic data, mineral analyses without contamination from included impurities became possible. With the widespread availability of the microprobe, more mineral analyses are now routinely collected and a great deal of inhomogeneity and zoning have been detected in minerals which appeared to be homogeneous on the basis of petro-

graphic data. For zoned minerals, there still remained a minor component of inaccuracy and imprecision, affected by the necessity to return to the analytical area repeatedly in order to collect both peak and background counts for each element being analysed.

The development of energy dispersive microprobe analysis enabled the investigator to collect all of the necessary data from a single point in a relatively short time and therefore allowed for a greater confidence in the major element concentrations measured. Thus a method which produces rapid quantitative mineral analyses is now routinely available to the metamorphic petrologist.

Experimental investigation of relatively simple systems relevant to assemblages encountered in metamorphic terrains have also provided insight into metamorphism and the petrogenetic grid. Early studies examined three and four component systems and had no controls on f_{O_2} and the CO_2/H_2O ratio of the fluid pressure medium (e.g. Bowen and Tuttle, 1949). A major step in experimental studies was taken when buffer assemblages were evaluated and routinely applied in investigating mineral assemblage stability fields. These include oxygen buffers in the system Fe-O (Eugster and Wones, 1962; Wones and Eugster, 1965), the C-O system buffers (French and Eugster, 1965), and buffers in the system C-O-H (French, 1966). At the same time, techniques were developed for studying the effect of CO_2 partial pressures on dehydration reactions (Kerrick,

1972) and of H_2O on decarbonation reactions (Greenwood, 1963, 1967). This, therefore, quantitatively assessed the effect of fluid composition on the equilibrium conditions for dehydration reactions encountered during prograde metamorphism.

The experimental study of the key 'isograd' reactions encountered in the metamorphism of pelitic rocks has helped to locate the commonly observed mineral assemblage transitions on the petrogenetic grid. These works include:

1. The muscovite + quartz stability field
(Evans, 1965; Kerrick, 1972)
2. The muscovite + chlorite stability field
(Seifert, 1970; Bird and Fawcett, 1973)
3. The almandine + sillimanite + quartz stability field (Currie, 1971; Hensen and Green, 1971, 1972, 1973; Weisbrod, 1973a,b)
4. The stability fields of the Al_2SiO_5 polymorphs (Richardson, Gilbert, and Bell, 1969; Zen, 1969 (review paper); Holdaway, 1971)

The metamorphic petrologist may also utilize two other methods for obtaining the information present in standard and polished thin sections. The first of these is to examine primary fluid inclusions to obtain information on the gas composition of the fluid phase which was trapped during the host mineral's crystallization. It is relatively simple to determine whether the trapped

fluid is pure CO_2 , pure H_2O , or a two or more component mixture. The second method is to examine the 'opaque' minerals in reflected light or with the microprobe. These observations allow the investigator to estimate which of the phases buffered f_{O_2} during the metamorphism. If good estimates of pressure and temperature are available, f_{O_2} can be determined within a few orders of magnitude.

Therefore, with these analytical techniques and a large data base of experimental work, the approach to evaluating a metamorphic terrain has changed and enlarged relative to the approach employed by early investigators. This multifaceted approach enables the investigator to reach more quantitative conclusions concerning the actual physical conditions of metamorphism. Thus, recently published work (e.g. Henry, 1974; Berg, 1975; Tracey et al., 1975; Thompson, 1976a,b) include detailed evaluation of pressure, temperature, and the fugacity of several components in the fluid phase within well defined limits. These define the metamorphic conditions much more precisely than a general subfacies description could do. The current trend towards an integrated study, making use of all of the current techniques available, marks the transition of metamorphic petrology from a descriptive qualitative branch of geology to a much more quantitative, definitive science which is capable of producing reliable data that can be used in more clearly defin-

ing the tectonic evolution of metamorphic terrains.

This study extends the use of the microprobe to examine small scale equilibrium in upper amphibolite facies rocks. It will be shown that such an approach is necessary in investigations of this type of metamorphic terrain, and that the conclusions reached are important in understanding and evaluating the metamorphic evolution of an original sedimentary series. For example, the analysis of biotite from the several distinct 'domains' in single polished thin sections has shown that equilibration of iron and magnesium between adjacent phases has occurred only at a scale of a few millimeters (see page 94). (The term domain refers to the mineral assemblage in contact with the analysed biotite.)

The methods used in this study, then, differ slightly from previous investigations in similar terrains (e.g. Folinsbee, 1942; Miyashiro, 1958; Lambert, 1959). The steps taken to evaluate the area were:

1. Detailed sampling of pelitic and amphibolitic lithologies.
2. Petrographic examination of the above samples.
3. Microprobe analysis of ferro-magnesian phases in a suite of samples which were selected on the basis of the total phase assemblage present and a low degree of

alteration.

4. Examination of primary fluid inclusions in order to estimate the CO₂/H₂O ratio in the metamorphic fluid.
5. Application of mineral chemical data to published geothermometric and geobarometric calculations (e.g. Saxena, 1969; Currie, 1971; Hensen and Green, 1971, 1972, 1973; Hutcheon et al., 1974; Thompson, 1975a, 1976a,b).
6. Synthesis of all of the above data to produce a geologic history and proposed tectonic evolution of the study area.

PREVIOUS WORK

Prior to the regional mapping by C. S. Lord and J. T. Wilson of the Geological Survey of Canada, the Arseno Lake area had been examined only by prospectors in search of gold. Wilson mapped the southern part of the Arseno Lake area in 1939 at a scale of 1:253,440. C. S. Lord extended Wilson's work to the north in 1940 and these maps were published as a G. S. C. memoir by Lord in 1942.

A more detailed study was undertaken by J. C. McGlynn and J. V. Ross in their 1:63,360 mapping project in the east half of the Arseno Lake map area (McGlynn and Ross, 1963). They studied the structural style and stra-

tigraphy of the Yellowknife Group and the overlying Snare Group metasediments. The western boundary of their study corresponds to the cordierite isograd of this study. Ross and McGlynn (1965) summarized the Snare-Yellowknife relations along the known length of the Snare Group, from Basler Lake in the south to Arseno Lake in the north. They noted a change in structural style from open concentric folding in the south to more steeply dipping upright to westerly dipping folds in the north.

R. A. Frith in 1972 began a 1:50,000 scale structural study in the western half of the Arseno Lake map area (Frith, 1973; Frith et al., 1974; Frith and Leatherbarrow, 1975; Leatherbarrow and Frith, 1975). Figure 2 shows the generalized geologic map of the study area.

GENERAL GEOLOGIC CHARACTER OF THE STUDY AREA

The area studied was characterised by a low pressure, Abukuma type, metamorphic series. It ranged in grade from the chlorite zone in the eastern part of the area, just west of the Bear-Slave boundary, to upper amphibolite grade rocks in the west. The thermal gradient was not uniform, but appears to have steepened as the gneiss dome in the west central portion of the area was approached and to have levelled off across the gneiss dome. Rocks in the eastern part of the area, below the andalusite isograd, show well preserved bedding. These metasediments are correlative with the lower Epworth

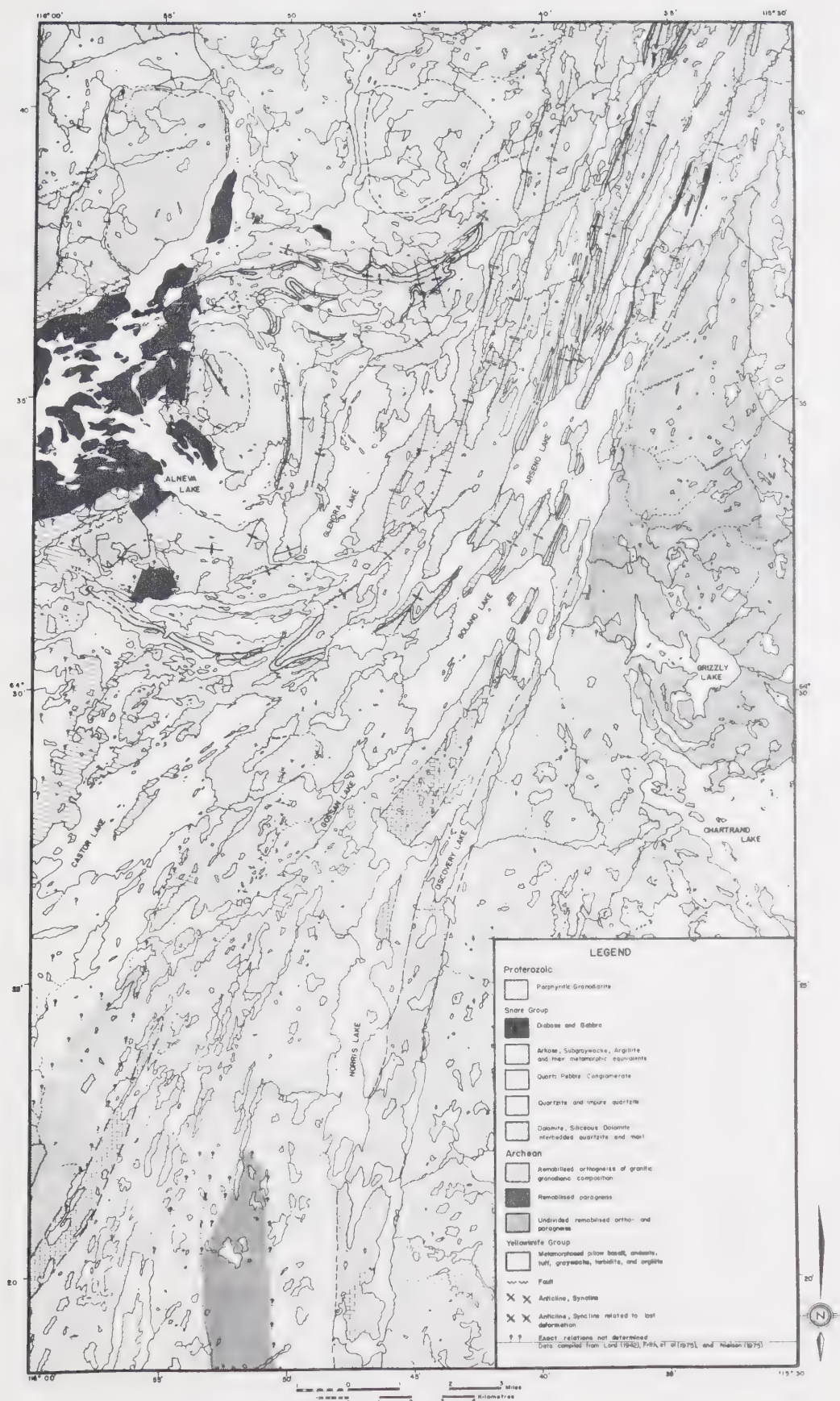


FIGURE 2: Generalised geology of the Arseno Lake area

Group (Hoffman, 1970), which is exposed 100 km north of the Arseno Lake area. Above the andalusite isograd, primary textures and features have been obscured by penetrative structures associated with D_1 and D_2 phases of deformation (Frith and Leatherbarrow, 1975), and only cryptic chemical differences can be used to define some of the original lithological units.

The gneiss dome exposed in the central part of the area plunges to the southwest and is exposed for more than 25 km along strike. It is cored by remobilised Kenoran granodiorites (Frith *et al.*, 1974), and Archean paragneiss is exposed in the western and southern portions of the dome. (The term 'Archean paragneiss', as used in this study, refers to polymetamorphic rocks whose first metamorphism predates the Hudsonian Snare event. At present, there are not sufficient data to establish a definite age for these rocks.)

Thus the area as a whole shows an Abukuma facies series type metamorphism in the Proterozoic (middle Aphebian) sediments in the east, which is superimposed upon a mixed assemblage of Proterozoic sediments and remobilised Kenoran ortho- and paragneiss in the west.

Distinction between the Proterozoic metasediments and remobilised Archean paragneisses was made on the basis of:

1. The polymetamorphic nature of the latter, which contain relic grains of high P-T

minerals that could not have resulted from the Proterozoic metamorphism.

2. The presence of similar grade paragneisses in the Ghost Lake area of the Slave craton (Folinsbee, 1940, 1941, 1942).
3. A Rb/Sr whole rock reference isochron (Fig. 3) which had an initial ratio of .704 and an age of > 2100 m.y.

General Lithologies

The lithology of the region consists of a sedimentary sequence with a near basal siliceous dolomite, overlain by interbedded thin bands of siltstone and shale, graded bands of siltstone and shale, subgraywacke, and rusty pyritic shale with occasional horizons of quartzites, intraformational conglomerate and calcareous argillite. These are all members of the Snare Group (Lord, 1942).

In the higher grade portion of the area, local pegmatites, minor injection migmatites and remobilised Archean granitoid rocks are found, along with retrograded Archean paragneisses, which are similar to those described by Folinsbee (1940, 1941, 1942).

The basement rocks of the Snare Group metasediments are the Yellowknife Group metasediments and metavolcanics, although in some locations, Kenoran intrusive rocks are overlain by Snare sediments. Throughout much

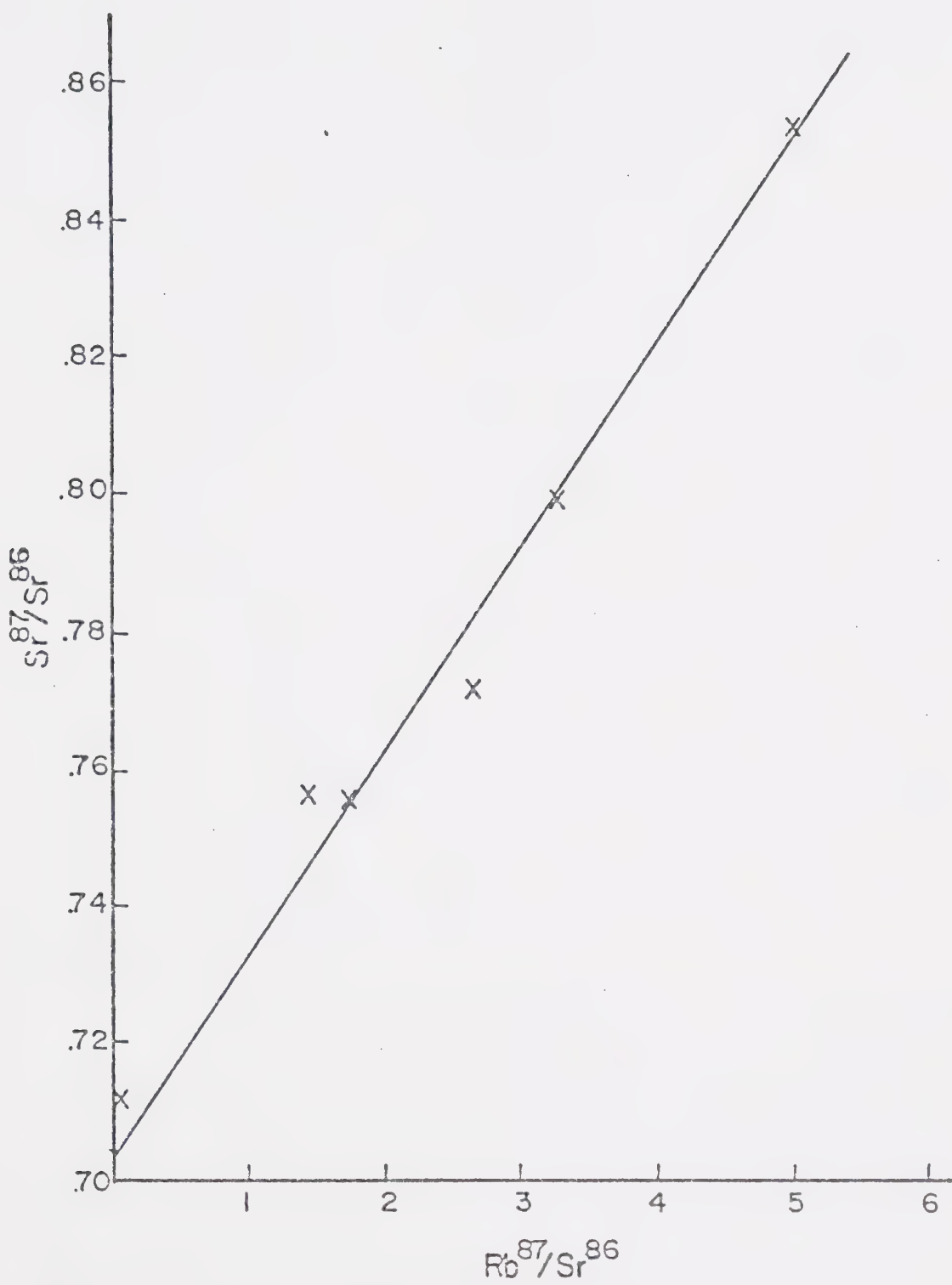


FIGURE 3: Diagram showing the Rb/Sr data available for the remobilised Archean paragneiss. The line shown is a 2110 m.y. reference isochron.

of the central area, only the Proterozoic Snare Group metasediments are exposed. Basement in the western part of the area consists of remobilised Archean granodiorites and pre-Snare paragneisses which together define the core of the gneiss dome shown in Figure 2.

Metapelites. Interbedded shales and argillites and their metamorphic equivalents comprise the bulk of the Snare Group sediments. At low grades of metamorphism, original bedding is preserved, with beds approximately 1 cm thick, giving the rock a laminated appearance. Buff silty bands alternate with medium grey shaly bands. Locally, however, the thickness of individual beds can exceed 10 to 20 cm. The shale is dominantly comprised of white mica, chlorite, quartz, and plagioclase. The argillites have more quartz and plagioclase and less white mica and chlorite. At higher grades of metamorphism, biotite, andalusite, cordierite, sillimanite, K-feldspar, and garnet have appeared, while muscovite and chlorite have disappeared.

Siliceous Carbonates. On the eastern margin of the Snare Group, basal carbonates lie unconformably upon, or in fault contact with, the Yellowknife Group metavolcanics. They generally consist of recrystallised granular or crystalline carbonates with varying amounts of quartz, epidote, zoisite, tremolite, phlogopite, sphene, biotite, and diopside. The type and amount of accessory

minerals is a function of metamorphic grade and original composition.

Metapsammites. These units range from less than 1 meter to several meters in thickness and are interbedded with shale, argillite, calcareous argillite, and pyritic black shale. The quartzites are generally impure and contain minor plagioclase, white mica, and some chlorite. The conglomerates consist of quartz rich clasts in a matrix of chlorite, white mica, and finer grained quartz. At higher metamorphic grade, the matrix has recrystallised and developed biotite while retaining the original plagioclase and K-feldspar.

Granitic Rocks. Granitic rocks of two ages are present in the study area. Within the Bear Province, older granitic rocks of 2710 m.y. (Frith et al., 1974) occur as remobilised material coring the central gneiss dome. To the north and west, granodiorite of the Hepburn Batholith type (~ 1800 m.y.) occurs.

Other Intrusive Rocks. The Snare Group meta-sediments are cut by dikes and sills (?) of medium to fine grained, rusty weathering metagabbro. Higher grade Snare rocks are also cut by aplite dikes and coarse grained, garnet bearing pegmatites. The whole of the central and western part of the area is domed up by remobilised Archean granodiorites and pre-Snare paragneisses. Quartz veins and minor pegmatites cut many of the higher

grade Snare Group paragneisses. Some of the pegmatites are derived from the Snare rocks, and others near the gneiss dome are derived from the remobilised Archean (Kenoran) granodiorite. These yield a Rb/Sr isochron of 1808 m.y. with an initial $\text{Sr}^{87}/\text{Sr}^{86}$ ratio of 0.7142 (Frith et al., 1975).

Structure in Relation to Metamorphism

Deformation of the Snare metasediments differed from east to west, and the cordierite isograd approximates the boundary between the two domains. East of the cordierite isograd, where metamorphic grade was in the biotite zone or lower, the fold axes trend approximately 020° , plunging northwards, and form a zone of closely spaced, upright to westerly dipping folds. These are primarily isoclinal folds, formed by simple or pure shear (McGlynn and Ross, 1963).

West of the cordierite isograd, the first phase of deformation (D_1) was much like that in the east, and a second phase of deformation (D_2) is evident. Where D_2 was not too intense, the folds strike 080° . D_2 was much less intense than D_1 and is generally expressed as gentle open folds which plunge to the south or southwest (Frith and Leatherbarrow, 1975). D_1 was more intense, and caused the development of biotite schistosity and elongation and flattening of mineral grains. Porphyroblasts on axial planar structures developed as a result of the penetrative

nature of the first phase of deformation.

Metamorphism

The metamorphism of the Proterozoic Snare Group sediments and remobilised Archean paragneisses was a low pressure type event, similar to that in the Abukuma Plateau (Miyashiro, 1958). The average thermal gradient was approximately $66^{\circ}/\text{km}$ and ranged from less than $38^{\circ}/\text{km}$ to $75^{\circ}/\text{km}$. The maximum thermal gradient occurred on the eastern flanks of the gneiss dome above the cordierite isograd. The metamorphic grade increased from east to west and ranged from the chlorite zone at the base of the Snare sediments to the upper amphibolite facies (almandine-K-feldspar-cordierite-sillimanite) in the west. Sample density and mineral assemblage data have defined the following isograds:

1. Biotite in, muscovite + chlorite out.
2. Andalusite in.
3. Cordierite in.
4. Sillimanite in, andalusite out.
5. Sillimanite + K-feldspar in, muscovite + quartz out.
6. Coexistence of cordierite + garnet.

Locally, the first appearance of garnet in rocks of the appropriate composition occurs between the biotite and andalusite isograds.

In addition to the prograde sequence noted above,

a series of retrograde reactions have been inferred from observations of thin sections from the remobilised Archean paragneiss. These include:

1. Spinel + quartz \rightarrow cordierite.
2. Garnet + K-feldspar + H₂O \rightarrow biotite + Al₂SiO₅.
3. Orthopyroxene + Al₂SiO₅ + K-feldspar \rightarrow biotite + quartz.
4. Orthopyroxene + Al₂SiO₅ + quartz \rightarrow cordierite.

PART II: PETROLOGY

GENERAL DESCRIPTION

The Chlorite Zone

The lowest grade metamorphic rocks sampled lie immediately west of the Bear-Slave boundary and extend between 0.2 and 1.2 km into the Bear Province. The samples from this narrow zone contain chlorite, white mica, quartz, and detrital feldspars, as well as ilmenite and minor authigenic pyrite. These rocks are very fine grained with quartz and plagioclase clasts set in a matrix of recrystallized quartzo-feldspathic material and interleaved chlorite and white mica. Westward from this zone, biotite appears in all of the rock types present except for the most mafic compositions, where a blue green actinolitic amphibole is present (Fig. 4).

The Biotite Zone

The biotite zone ranges in width from 2.6 km in the northern part of the area, east of the gneiss dome, to up to 8 km south of the outcrop limits of the gneiss dome. The upper limit of the biotite zone is defined by the cordierite isograd and the lower limit by the first appearance of biotite from the reaction of chlorite + white mica.

Metapelites. The pelitic rocks in the lowest part of the biotite zone are very fine grained and are

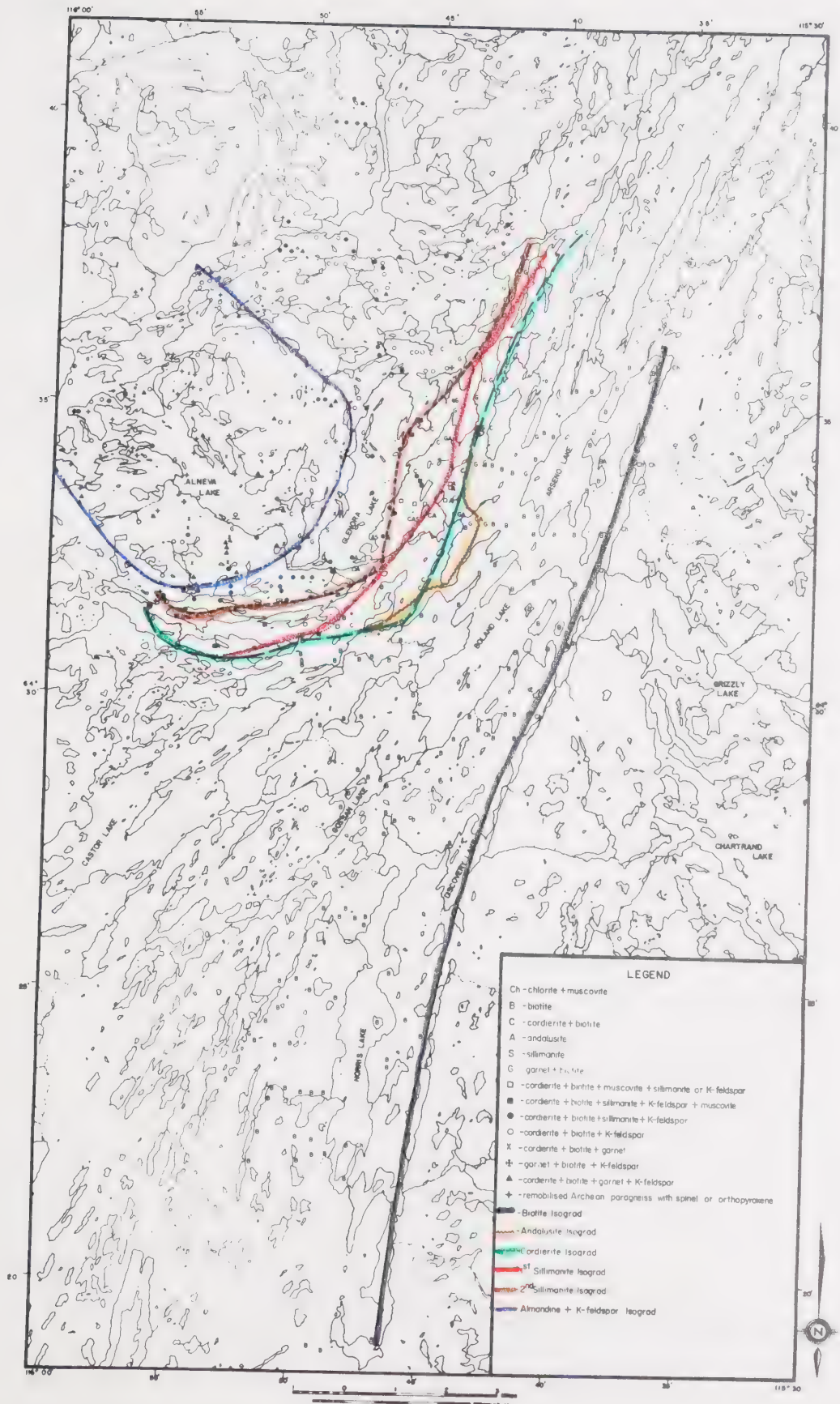


FIGURE 4: Isograd map

characterised by a phyllitic or lepidoblastic arrangement of chlorite and white mica in fine grained granoblastic quartz and feldspar. Large ragged porphyroblasts of biotite cut across this foliation and commonly contain a network of rutile needles (see Plate I). Ilmenite, graphite, and minor pyrite are also present.

In rocks of higher grade, biotite is often interleaved with chlorite or muscovite and as it becomes a major phase, biotite alignment defines the foliation.

Metagraywackes. These are blastopsammitic rocks with similar mineralogy to the metapelites. The biotite is less abundant and is present as scattered anhedral flakes. The plagioclase clasts are commonly altered to white mica at low grade. In higher grade rocks, the plagioclase shows evidence of variable degrees of recrystallisation.

In the uppermost part of the biotite zone, andalusite appears as larger porphyroblasts (up to 3 cm) and most of the plagioclase and quartz has recrystallized to an equilibrium texture characterised by triple point junctions and straight line boundaries. In rocks of the appropriate composition, spessartine rich poikiloblastic garnets are present (see Plate I).

The Cordierite - Andalusite Zone

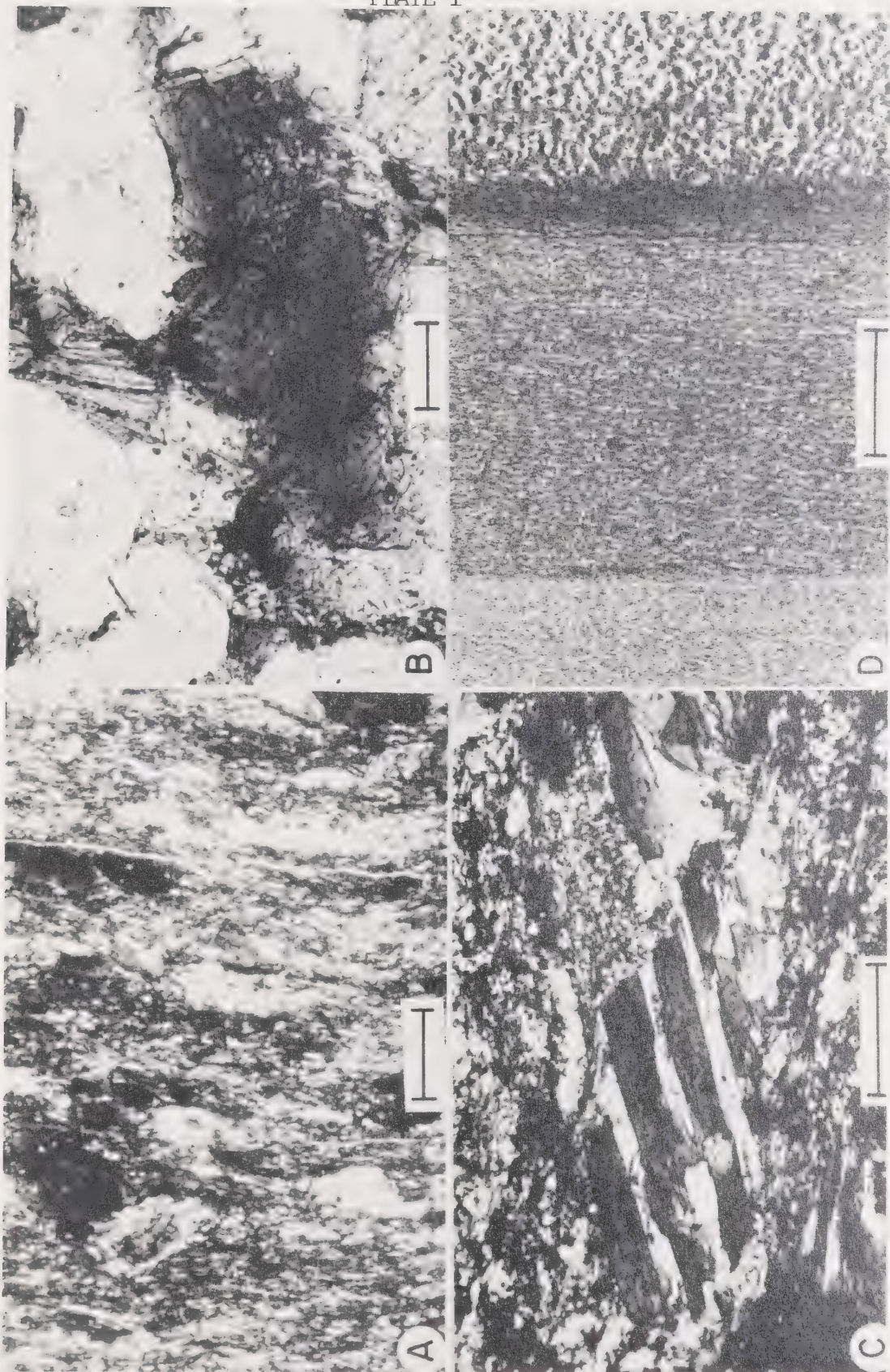
Cordierite porphyroblasts first appear in the pelitic rocks at the same time as andalusite in the northern

PLATE I

Features of the biotite zone.

- A. Sample 7223 showing fine grained muscovite-chlorite-quartz matrix with ilmenite and sulfide grains and dusty graphite. Large white areas are quartz light grey areas are biotite. Crossed nicols. Scale bar = 125 microns.
- B. Sample 7273 showing a coarse biotite flake in a quartz matrix. Chlorite grain in upper center of photomicrograph. The dark lines in the biotite are rutile needles which are thought to have grown epitaxially in the biotite as a product of reaction 3. Crossed nicols. Scale bar = 50 microns.
- C. Sample 7215, a spotted biotite slate showing large clots of biotite + quartz in a fine grained matrix of chlorite, muscovite, plagioclase, ilmenite and graphite crossed nicols. Scale bar = 50 microns.
- D. Sample 7269 showing the control of initial sediment composition on the mineral assemblage formed. The 3 bands are composed of differing amounts of biotite and muscovite ± garnet. The band at the right margin is composed of garnet (dark grey) + quartz + plagioclase. Plane light. Scale bar = 4 mm.

PLATE I



part of the area. East and southeast of the gneiss dome, cordierite first appears between 0.2 and 1.0 km above the first appearance of andalusite. Cordierite and biotite are present from the upper limit of the biotite zone to the western edge of the study area. The upper limit of the cordierite zone is defined by the presence of garnet in hand specimen with cordierite and biotite. The cordierite zone ranges in width between 1.0 and 3.5 km.

Rocks from the cordierite zone are nodular in appearance. This is caused by the presence of large diffuse cordierite poikiloblasts as well as euhedral andalusite porphyroblasts. Chlorite and muscovite are mutually exclusive. Biotite is ubiquitous and abundant. The rock is much more massive than specimens from the biotite zone and cleavage and well defined foliation are much less common, except in the most biotite rich rocks.

The Cordierite - Sillimanite Zone

In the upper part of the cordierite zone, andalusite is replaced by sillimanite and a well defined first sillimanite isograd has been mapped. At the first appearance of sillimanite, the rocks take on a rusty weathering appearance.

The second sillimanite isograd, marked by the reaction of muscovite + quartz \rightarrow sillimanite + K-feldspar + H_2O , brackets the upper part of the cordierite zone in the

southern and southeastern part of the gneiss dome, but does not appear until well into the garnet zone in the northeastern part of the area. Pelitic and peraluminous rocks from above the second sillimanite isograd are massive, rusty weathering and nodular in appearance. The knots are cordierite porphyroblasts and bundles of fine sillimanite (variety fibrolite) or large prisms of coarsely crystalline sillimanite. The rocks are much more gneissic. This gneissosity is defined by an alternation of leucocratic and melanocratic bands formed by metamorphic segregation.

The Cordierite - Almandine - K-feldspar Zone

This is the highest grade of metamorphism recorded in the Snare Group metasediments. Cordierite and garnet, along with biotite, quartz, ilmenite, rutile, plagioclase, K-feldspar, and sillimanite are the dominant minerals. Sillimanite is commonly found within cordierite, but never in contact with garnet. Cordierite is present in all but the most magnesium poor metasediments and biotite is ubiquitous. In the central part of the cordierite-almandine-K-feldspar zone, minor injection migmatites and local anatetic pegmatites are found. The garnets are euhedral to anhedral. The anhedral garnets are rimmed by biotite and fine grained plagioclase, indicating the retrograde reaction of garnet + K-feldspar + H₂O → biotite + plagioclase. Table 1 presents commonly observed

mineral assemblages from the above zones in the Arseno Lake area.

The Archean Paragneisses

In the western part of the gneiss dome, polymetamorphic rocks crop out. They were retrograded to the cordierite-almandine assemblage by the Hudsonian metamorphism, but relic grains of hercynite spinel solid solution and iron rich orthopyroxene (Fs 53-55) persist. The presence of spinel enclosed by cordierite and cordierite + sillimanite, and the occurrence of embayed orthopyroxene, leads to the conclusion that these samples were originally metamorphosed under granulite facies conditions and were retrograded to the upper amphibolite facies during the Hudsonian.

The Facies Series

The zonal series described above closely approximates an Abukuma facies series (Miyashiro, 1958). The observed zonal succession is:

biotite → andalusite → cordierite →
sillimanite → almandine garnet.

Conditions of Metamorphism. This facies series, characterised by a low pressure, high temperature gradient, suggests that the pressure of metamorphism ranged from about 2 kbar in the biotite zone to about 3.5 to 4 kbar in the cordierite-almandine zone, and temperature ranged from approximately 350° C. in the biotite zone to

TABLE 1: Commonly observed mineral assemblages from single thin sections

Chlorite Zone

chlorite-sericite-quartz-plagioclase-ilmenite ±
detrital K-feldspar and pyrite

calcite-dolomite-quartz-tremolite

Biotite Zone

biotite-sericite-chlorite-quartz-plagioclase-
ilmenite-rutile ± detrital K-feldspar and pyrite

biotite-muscovite-spessartine garnet-quartz-
plagioclase-rutile-ilmenite

biotite-muscovite-quartz-plagioclase-ilmenite-
rutile

Andalusite Zone

biotite-muscovite-andalusite-quartz-plagioclase-
ilmenite-rutile

biotite-chlorite-andalusite-quartz-plagioclase-
ilmenite-rutile

Cordierite Zone

biotite-muscovite-cordierite-andalusite-quartz-
plagioclase-rutile-ilmenite

biotite-cordierite-andalusite-quartz-plagioclase-
ilmenite-rutile

biotite-cordierite-fibrolite-andalusite-plagioclase-
ilmenite-rutile

biotite-cordierite-sillimanite-fibrolite-plagioclase-
ilmenite-rutile

biotite-cordierite-muscovite-orthoclase-plagioclase-
ilmenite-rutile-quartz

TABLE 1 (Continued)

Second Sillimanite Zone

biotite-cordierite-sillimanite-microcline-quartz-
plagioclase ± ilmenite ± rutile

biotite-cordierite-sillimanite-microcline-quartz-
plagioclase-garnet ± ilmenite ± rutile

biotite-cordierite-garnet-microcline-quartz-
plagioclase ± ilmenite ± rutile

biotite-garnet-microcline-quartz-plagioclase ±
ilmenite ± rutile

Retrograded Archean Paragneiss

biotite-cordierite (spinel-sillimanite)-K-feldspar-
plagioclase-quartz ± ilmenite ± rutile

biotite-cordierite (spinel)-K-feldspar-plagioclase-
quartz ± ilmenite ± rutile

biotite-cordierite (spinel)-garnet-K-feldspar-
plagioclase-quartz ± ilmenite ± rutile

biotite-cordierite (spinel-sillimanite)-garnet-
K-feldspar-plagioclase-quartz ± ilmenite ± rutile

biotite-cordierite-garnet-orthopyroxene-K-feldspar-
plagioclase-quartz ± ilmenite ± rutile

biotite-orthopyroxene-plagioclase-quartz-K-feldspar
± ilmenite ± rutile

calcite-serpentine (forsterite)-ilmenite

700° C. in the cordierite-almandine zone (see Part III, page 164, 177).

The general absence of anatexis and the close spacing of the first and second sillimanite isograds suggests that for higher grades of the metamorphism, $P_{H_2O} < P_f$. This has been substantiated by preliminary fluid inclusion studies and is further substantiated by the lack of large scale equilibration noted at higher grades of metamorphism (see Part III, page 130-36, Part IV, page 196).

Assignment of Metamorphic Grade. For many of the observations developed below, a non-mineralogical index of metamorphic grade is required. Ramsay (1973 a) defined such a grade index as the distance above or below the cordierite isograd. In this study, such a grade index proved to be unsatisfactory due to the asymmetrical nature of the cordierite isograd. The grade index chosen is defined as the radial distance from the thermal dome (as measured on the map of sample localities (see map pocket)), divided by the distance along the same radial line to the almandine-K-feldspar isograd. The thermal dome is defined by contouring the mole per cent gahnite in spinels from the remobilised Archean paragneiss. The area enclosed by the contour of lowest mole per cent gahnite was chosen as the thermal high because the spinels have reequilibrated with the host cordierite at the highest temperatures (see Part II, page 107,ff).

This dimensionless grade index is believed to be superior to an unscaled index because it takes into account variations in the dip of the contact between the heat source and the metamorphosed country rock. This, then, compensates for the asymmetrical shape of the heat source and the isotherms resulting from it.

The Sample Series

All of the 893 samples collected were examined in thin section. From this group, 100 samples were selected for further study. These samples were chosen on the basis of:

1. The mineral assemblage present, with those having two or more ferromagnesian silicates chosen in order to use the various geothermometers based on compositions of coexisting cordierite, garnet, and/or biotite.
2. The presence of fresh unaltered minerals.
3. The presence of relict orthopyroxene or spinel.

The spinel bearing samples were studied to observe the reaction relationship between spinel and the cordierite surrounding it. These 100 samples were studied in reflected and transmitted light and areas of interest were noted for microprobe analysis. 350 mineral analyses were made using an ARL-EMX Scanning Electron Microprobe equipped with an energy dispersive X-ray analyser. The compo-

sitions obtained are used in the discussion below.

CONTROLS ON MINERAL COMPOSITION

There are two types of controls in metamorphic systems which determine a mineral's composition:

1. Those which permit the existence of a mineral (permissive controls).
2. Those which modify its composition (modifying controls) (Fig. 5).

Permissive Controls

Energetic. The most important permissive controls are energetic. Whether or not a mineral is stable is absolutely dependent upon the physical conditions of metamorphism. These factors include pressure, temperature, and the fugacities of mobile components.

Compositional. Coupled with the energetic controls is the need for the presence of an adequate supply of the required chemical components in the proper concentrations to form the mineral. The adequate supply is a function of:

1. Bulk rock composition.
2. The ease of transport of the chemical components to the nucleation and growth centers.
3. Metasomatic introduction or loss of one or more components, thus altering the bulk rock composition.

4. Whether the phase which is forming is a product of a continuous or discontinuous reaction.

Modifying Controls

For minerals of a fixed composition, or minerals which are the dominant phase for one or more components (e.g., Ti in rutile or ilmenite), the permissive controls are sufficient to determine the presence or absence of that mineral. For other minerals whose composition is variable, the permissive controls determine the appearance of a mineral, but not its exact composition.

There are several important modifying controls operating simultaneously to determine mineral compositions. The relative importance of these factors differs for each mineral group within a metamorphic complex and may differ between metamorphic complexes.

Internal Crystal Chemistry. One of the most important internal modifying controls is the partitioning of two or more elements between coexisting phases. In rocks of similar composition, but with different mineral assemblages, mineral composition is determined by equilibrium partitioning between phases with common chemical components. This is a second order compositional modifier and is related to cation-oxygen bond strengths of the coexisting phases and the free energy of each component in all phases. Experimental studies of metamor-

phic minerals in model systems strongly suggests that the distribution coefficients relating two components and two phases may be temperature dependent (Hensen and Green, 1971, 1972, 1973). The presence of a third phase competing for the same common components would further restrict the compositions of the coexisting phases. The change in composition with the introduction of an additional phase may reflect a shift in a continuous reaction in which the fluid may also be a participant.

Crystal field restrictions form a second internal modifying control. Ion exchange between minerals is not always possible over a broad range of compositions. For example, crystal field restrictions governing the M-sites in staurolite limit magnesium solid solution in staurolite and restrict staurolite to an iron rich composition. Thus, staurolite composition is controlled by crystal field factors. Any Fe-Mg phase coexisting with staurolite would also have its composition defined because of the limited amount of Fe-Mg exchange with staurolite which could occur. Reactions involving staurolite are most likely to be discontinuous reactions.

A third control is that electrical neutrality must be maintained. When a mineral's composition is changed by one of the above factors, the demands of electrical neutrality must sometimes result in modification of the mineral composition. If, for example, an increase in temper-

ature results in the substitution of Al^{+3} for Mg^{+2} in a muscovite, there would be a simultaneous change in other elements (Al^{+3} for Si^{+4}) to preserve neutrality.

External. For a given set of metamorphic conditions and system bulk chemistry, growth and diffusion kinetics exert a strong influence on a mineral's composition. If growth or diffusion rates are slow, or if the time for attainment of equilibration is short, then a mineral's composition may vary on a small scale (see Part II, page 94). The situation is still one of attainment of equilibrium, although if reaction rates had been faster or the time for equilibration longer, different mineral compositions would have been attained.

A major factor affecting diffusion is the length of time that the system is at local peak conditions. The longer a system is held at a fixed set of metamorphic conditions, the greater the chance of attaining equilibrium, and the larger the scale of equilibration. This can readily be seen in contact metamorphic aureoles, where the extent of the aureole is a function of the total heat content of the intrusive rock. Similarly, regional metamorphism may be reflected by broad or narrow mineral assemblage zones and large or small scales of equilibration.

A second factor affecting diffusion is the nature of the fluid phase. As mentioned above, the fugacity of

the mobile components is a permissive control. In addition to that role, the fluid phase may exert a strong influence on mineral composition, even if the components of the fluid are not part of the phase composition. A fluid with a low mole fraction of H_2O will be a much poorer medium for diffusion of cations or cation complexes which move from the reactants to the products during a reaction (continuous or discontinuous). The lower the rate of intergranular diffusion, the smaller the scale of equilibration will be for a given time. This situation is discussed further in Part III.

A third factor affecting diffusion is the nature of the crystal lattice of phases participating in a reaction. It is well known that certain minerals, garnets for example, are much more refractory than other minerals. The more refractory minerals have a much slower rate of self diffusion, as is shown by zoning preserved in both prograde and retrograded garnets (Grant and Weiblen, 1971; Bethune and Laduron, 1975). If the refractory phase is present in a greater volume per cent than the other phases with which it is equilibrating, then the resultant mineral compositions will not reflect equilibria representative of the bulk rock composition, but will represent equilibria defined by the active composition. This does not include the material effectively isolated in the non-reactive inner regions of refractory minerals.

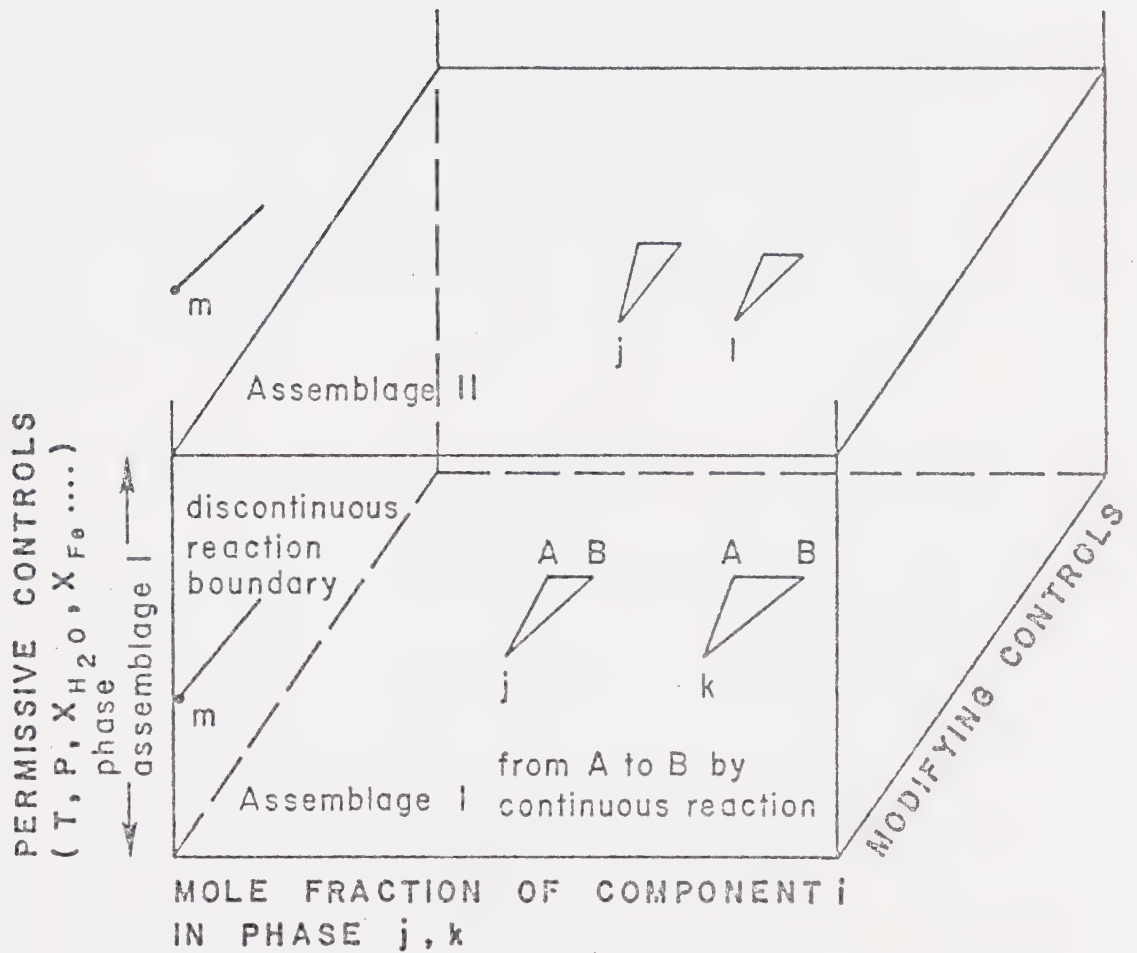


FIGURE 5: Diagram illustrating the relative roles of permissive and modifying controls on mineral composition. See text for discussion of the modifying controls. Points m, j, k, and i all lie on one vertical plane and represent mineral compositions that would be attained at perfect equilibrium (i.e., the chemical potential for any given species is identical in all phases containing that species). Where perfect equilibrium is not attained due to kinetic restrictions or limited intergranular diffusion, then a mineral's composition may vary along the area kAB. The exact location in the area kAB can be related to the cumulative effects of all of the modifying controls.

BIOTITE ZONE MINERAL CHEMISTRY

The most abundant rock type in the biotite zone is metapelite with minor metagraywacke. At the lowest grade in the biotite zone, the rocks are spotted biotite slates with patchy eyes of biotite + quartz in a finer grained matrix of plagioclase, sericite, and chlorite. At slightly higher grade, there is a well developed schistosity defined by alignment of biotite flakes. Phyllosilicates comprise more than 50% of the rock volume (Plate I).

Biotite

Analyses and structural formulae of six biotites from the biotite zone are presented in Table 2. The compositional variability is small and is shown in Figure 6. There is an increase in Mg and a decrease in Fe, Ti, and the Fe/Mg ratio.

Influence of Metamorphic Grade. Within this rather restricted compositional field, there are limited systematic trends related to metamorphic grade. The main points are:

1. There is a systematic increase in Mg and decreases in Fe and Ti. Mn content is variable, but no systematic variation is apparent.
2. Other elements in the Y-site, most notably Al^{VI}, show no systematic trend. There

TABLE 2 : Microprobe analyses (weight %) and structural formulae (based on 22 oxygen ions) of BIOTITES from the Biotite zone, Arseno Lake area

Sample Number	72271	7218	727	7217	7248G	7255G
Grade Index	4.07	2.95	2.87	2.82	2.39	1.99
SiO ₂	35.59	34.80	33.31	35.95	34.75	36.23
TiO ₂	2.18	2.17	1.79	1.34	1.70	0.70
Al ₂ O ₃	19.37	18.40	19.11	18.56	18.50	19.17
FeO* ₃	18.01	20.72	22.14	21.13	20.23	21.08
MgO	10.40	7.27	8.20	7.01	9.35	10.11
MnO	0.18	0.10	0.07	0.11	0.23	-----
CaO	0.06	0.22	0.23	0.26	0.27	0.19
K ₂ O	8.91	7.94	7.78	8.10	8.83	5.52
Total	94.70	91.62	92.61	93.46	93.86	93.00
Si	5.390	5.506	5.261	5.627	5.394	5.540
Al ^{IV}	2.610	2.494	2.739	2.373	2.606	2.460
Al ^{VI}	0.848	0.938	0.818	1.051	0.779	0.994
Ti	0.249	0.258	0.213	0.158	0.198	0.081
Fe	2.281	2.742	2.925	2.766	2.626	2.695
Mg	2.348	1.714	1.930	1.635	2.163	2.304
Mn	0.023	0.014	0.009	0.015	0.031	-----
Ca	0.010	0.037	0.038	0.044	0.045	0.030
K	1.721	1.602	1.568	1.617	1.748	1.076
Σ Y-site	5.756	5.666	5.895	5.625	5.797	6.074
Σ X-site	1.731	1.639	1.606	1.661	1.793	1.116
Fe/Mg	0.97	1.60	1.52	1.69	1.21	1.18
mole % annite	40	48	50	49	45	44

mole % annite is defined as Fe/ Y-site

*total Fe as FeO

G = spessartine rich garnet present

----- = not detected

For this and all subsequent tables of mineral analyses, the elements Na-Zn (except Ar), Zr, and Ba were sought using the energy dispersive data reduction program EDATA. Elements present in concentrations less than .03 weight % are not reported. For a full discussion of mineral analysis, the reader is referred to the appendix, and to the Short Course Notes from the MAC Short Course in Microbeam Techniques, Edmonton, Alta., 1976, edited by D.G.W. Smith.

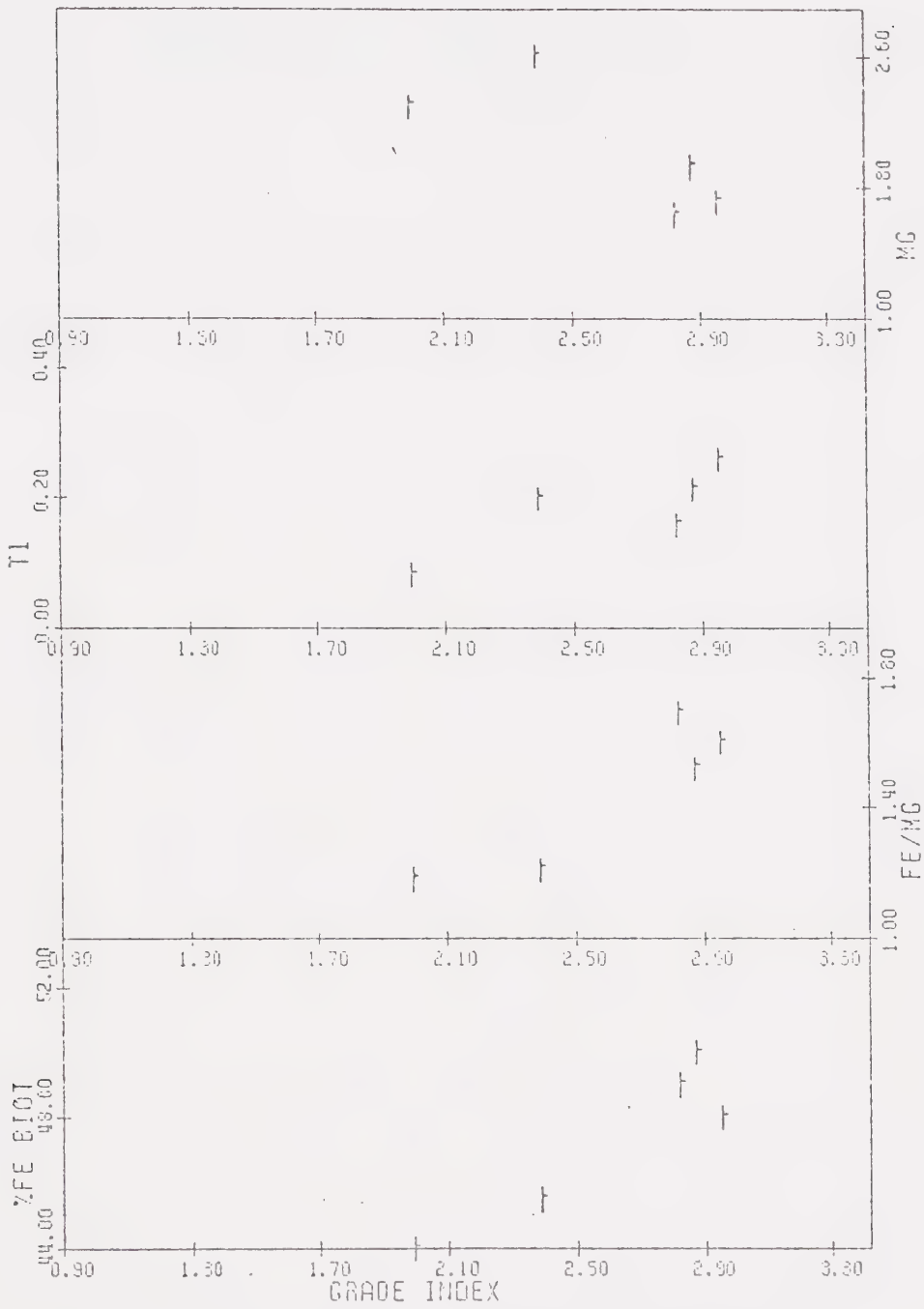


FIGURE 6: Diagram illustrating the relationship of biotite composition (atomic proportions) to grade index for biotites from the biotite zone. The symbol size is $\pm .5$ SD for the quantity plotted on the ordinate and 1 SD for the Grade Index. Grade Index increases with decreasing metamorphic grade.

is also no trend apparent in the total Y-site occupancy.

Comparative Discussion. The biotites from the biotite zone analysed in this study are similar to those reported by Ramsay (1973 a,b,c). All of the above biotites are from metapelites and, as discussed by Ramsay, there is little variation in biotite composition in green-schist grade metapelites.

Abundant data on biotites from greenschist facies are available in the literature (e.g. Lambert, 1959; Brown, 1967; Butler, 1967; Mather, 1970; Pinson, 1971; Pinson and Smith, 1975). The Arseno Lake biotites are compositionally similar to those reported in the above studies except that they have slightly higher magnesium contents and lower X-site totals. The problem with the X-site totals is discussed in the appendix on analytical methods.

Aside from X-site deficiency caused by alkali migration during microprobe analysis, it is most probable that hydronium ions substitute for the vacant lattice sites in the biotite structure. The other possibility is that the oxygen framework has several defects in sites corresponding to the location of the X ions in the biotite structure.

The variation of biotite composition in response to increasing pressure and temperature has been discussed

by several authors (e.g. Lambert, 1959; Butler, 1967; Guidotti, 1970), but most of the data are for higher grades of metamorphism and higher pressure metamorphic series than those presented here. The Al^{IV} increase described by Butler (1967) is present in this study, although there is no increase in Al^{VI}, as was the case in Butler's study.

Chlorite

Analyses of four chlorites and their structural formulae are given in Table 3. There is a limited compositional range. Figure 7 shows that all of the chlorites are ripidolites. There is a limited range of Al/(Fe + Mg + Mn) ratios and a slightly larger range in the Mg/(Fe + Mn) ratio and the Si/Al ratio.

Influence of Metamorphic Grade. Grade has a smaller influence on chlorite composition than on biotite. The main features are:

1. The Fe/Mg ratio tends to decrease towards the cordierite isograd, although the number of samples is too limited to establish this trend conclusively.
2. There is a small increase in the Al^{IV} content and a decrease in Si/Al^{IV}.

Comparative Discussion. The composition of these chlorites is similar to those reported from other greenschist facies metapelites (Brown, 1967; Mather,

TABLE 3 : Microprobe analyses (weight %) and structural formulae (based on 28 oxygen ions) of CHLORITES from the Arseno Lake area

Sample Number	7224	7218	727	7248G
Grade Index	3.2	2.95	2.87	2.82
SiO ₂	25.22	23.33	23.13	23.61
TiO ₂	0.06	-----	0.13	0.10
Al ₂ O ₃	19.32	22.27	22.82	
FeO*	27.05	27.82	28.30	26.52
MgO	12.92	10.47	11.99	14.06
MnO	0.17	0.29	0.15	0.40
K ₂ O	0.05	0.09	0.15	-----
Total	84.79	84.27	86.60	87.07
Si	5.570	5.215	5.036	5.068
Al ^{IV}	2.430	2.785	2.964	2.932
Al ^{VI}	2.598	3.184	2.893	2.732
Ti	0.009	-----	0.021	0.016
Fe	4.996	5.201	5.154	4.762
Mg	4.252	3.489	3.888	4.500
Mn	0.032	0.055	0.027	0.073
K	0.014	0.008	0.023	-----
ΣY-site	11.920	11.937	12.003	12.083

* total iron as FeO

G = spessartine rich garnet present

----- element not detected

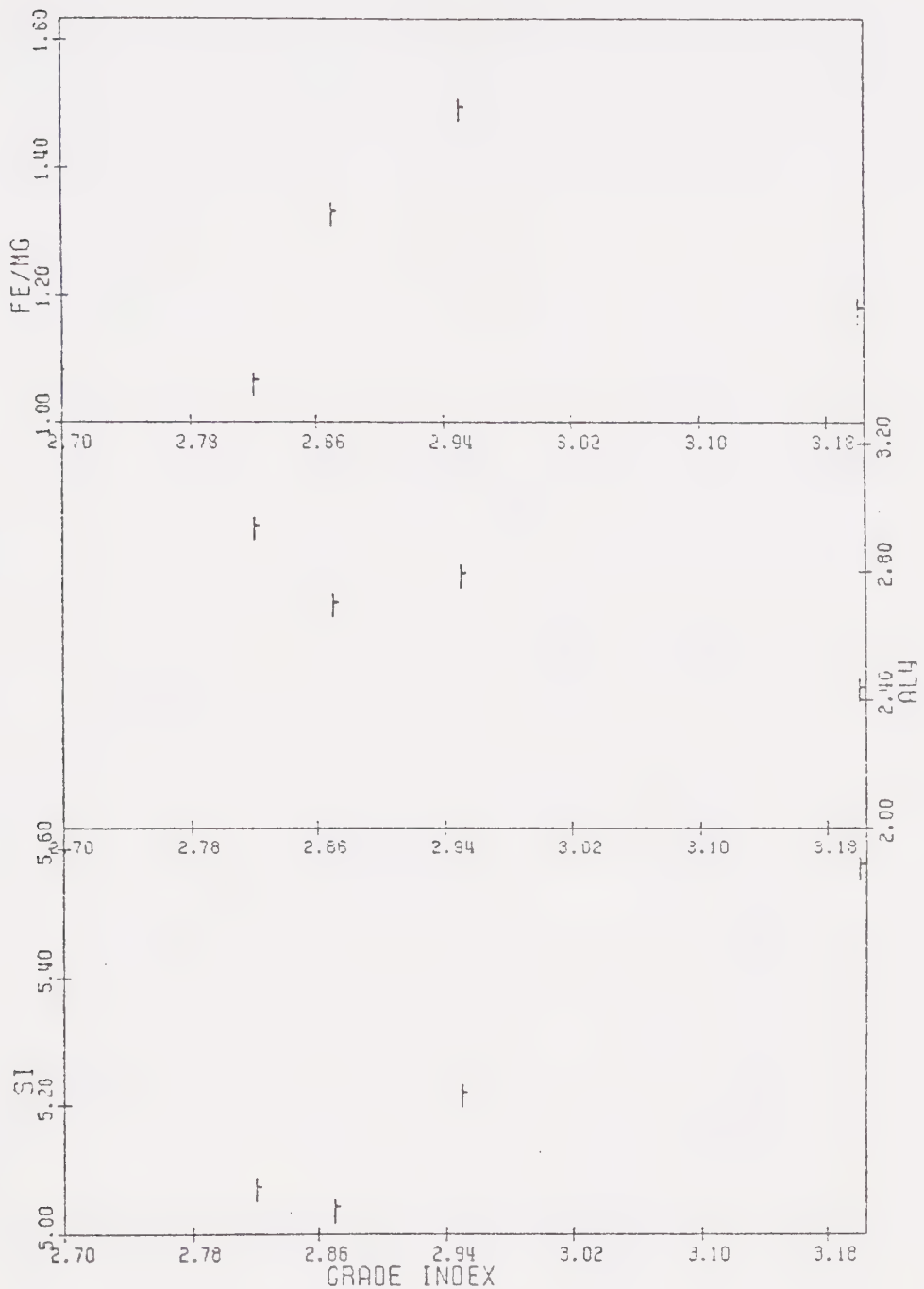


FIGURE 7a: Diagram illustrating the relationship of chlorite composition (atomic proportions) to grade index for chlorites from the biotite zone.

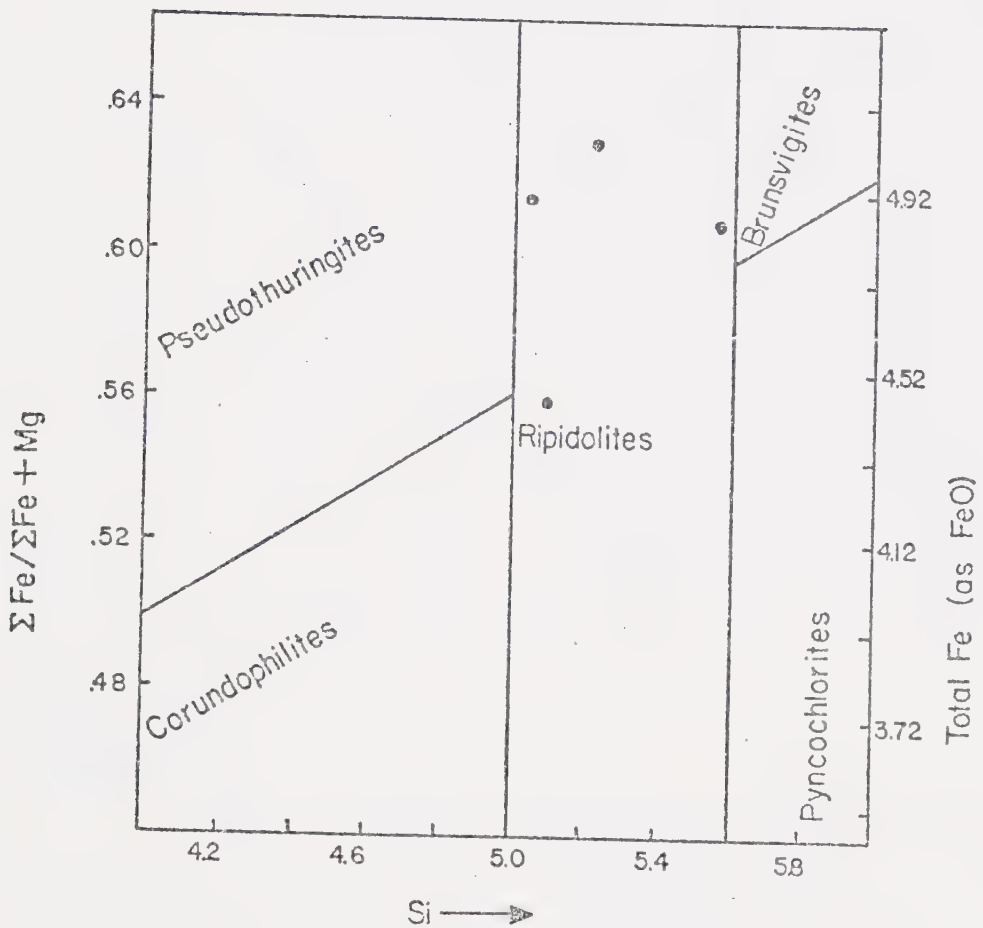


FIGURE 7b: Diagram showing that all of the biotite zone chlorites are ripidolites. (Modified after Hey, 1954)

1970; PinSENT, 1971; Ramsay, 1973), although they are less magnesium rich than Ramsay's (1973). The compositional variability, especially $\text{Fe}/(\text{Fe} + \text{Mg} + \text{Mn})$, is similar to that reported by Brown (1967).

Muscovite

Muscovite is a common phase in the chlorite zone and in the biotite zone. Due to its fine grained nature (5-10 microns) and the fact that it is commonly interleaved with biotite and chlorite, muscovite analyses from the biotite zone are not reported. A table of muscovite analyses from the upper part of the biotite zone, and the cordierite-andalusite and cordierite-sillimanite zones, is discussed elsewhere (Table 4). The analytical techniques used in this study (see appendix) were not suited to analyzing very fine grained, unstable materials. Since the aim of this study was to examine mineral equilibria on a fine scale, an average of short counts on several muscovite grains would not have added relevant data to the project.

Oxides

Opaque minerals comprise up to 5% of the mode of the biotite zone rocks. Rutile and ilmenite are the oxides present; no magnetite has been observed. Microprobe analyses of these phases are given in Tables 5 and 6.

Rutile occurs as needles in biotite and as porphyroblastic aggregates. In the presence of biotite,

TABLE 4 : Microprobe analyses (weight %) and structural formulae (based on 22 oxygen ions) of MUSCOVITES from the Arsenic Lake area

Sample Number	72271	7248G	73394	73308	7259	7347	73227
Grade Index	4.07	2.39	2.22	1.86	1.80	1.07	0.29
SiO ₂	44.97	44.77	45.49	46.46	48.45	44.01	44.76
TiO ₂	1.29	0.32	-----	0.30	0.10	0.64	0.16
Al ₂ O ₃	35.22	34.75	34.09	35.62	32.25	33.95	34.92
Cr ₂ O ₃	0.06	-----	-----	-----	-----	0.05	-----
V ₂ O ₃	0.11	-----	-----	0.06	0.06	0.13	-----
FeO*	0.94	1.09	2.39	0.95	2.19	3.11	3.00
MgO	0.33	0.12	2.10	0.35	0.83	0.35	0.55
BaO	0.34	0.15	-----	0.49	-----	-----	-----
CaO	0.59	0.29	0.38	0.35	0.25	0.32	0.16
K ₂ O	9.94	9.66	10.70	10.19	8.46	10.05	8.72
Na ₂ O	-----	-----	0.46	0.62	-----	0.46	-----
Total	93.79	91.15	95.61	95.39	92.59	93.17‡	92.27
Si	6.082	6.174	6.115	6.180	6.509	6.063	6.134
Al _{IV}	1.918	1.826	1.885	1.820	1.491	1.937	1.866
Al _{VI}	3.696	3.822	3.517	3.763	3.615	3.576	3.775
Cr	0.006	-----	-----	-----	-----	0.006	-----
V	0.011	-----	-----	-----	-----	0.006	-----
Ti	0.132	0.033	-----	0.006	0.006	0.014	-----
Fe	0.107	0.126	0.260	0.106	0.010	0.066	0.016
Mg	0.067	0.024	0.421	0.070	0.167	0.071	0.112
Ba	0.018	0.006	-----	0.025	-----	-----	-----
Ca	-----	0.043	0.055	0.050	0.036	0.047	0.050
K	1.715	1.699	1.727	1.729	1.449	1.765	1.524
Na	-----	-----	0.120	0.160	-----	0.123	0.112
Σ X-site	1.715	1.750	1.902	1.954	1.485	1.935	1.636
Σ Y-site	4.019	4.005	4.206	3.905	4.043	4.092	4.247
Fe/Mg	1.597	5.250	0.640	1.510	1.467	5.056	3.050

*total Fe as FeO

----- = not detected

G = spessartine rich garnet present

‡contains 0.1% F, .003F = 0

TABLE 5 : Microprobe analyses (weight %) and structural formulae
 (based on 2 oxygen ions) of RUTILE from the Arseno Lake
 area

Sample Number	7218	7219	727	7255G	73450	73451	73501
Grade Index	2.95	2.90	2.87	1.99	0.90	0.79	0.76
SiO ₂	0.34	0.56	-----	0.18	0.20	0.11	0.39
TiO ₂	95.48	95.12	95.48	95.24	98.11	98.23	97.99
Cr ₂ O ₃	-----	0.09	-----	-----	0.44	-----	0.59
V ₂ O ₃	0.83	1.50	0.66	0.65	3.07	0.67	3.99
FeO*	0.22	0.12	0.56	0.41	0.14	0.69	0.18
MnO	-----	-----	-----	-----	-----	0.10	-----
Total	96.87	97.39	96.70	96.48	101.96	99.80	103.14
Si	0.005	0.008	-----	0.002	0.008	0.001	0.005
Ti	0.987	0.978	0.991	0.990	0.906	0.998	0.957
Cr	-----	0.001	-----	-----	0.014	-----	0.006
V	0.009	0.016	0.007	0.007	0.097	0.024	0.037
Fe	0.002	0.001	0.006	0.005	0.005	0.009	0.004
Mn	-----	-----	-----	-----	-----	0.001	-----

----- = not detected

*total Fe as FeO

G = spessartine rich garnet present

TABLE 6 : Microprobe analyses (weight %) and structural formulae
 (based on 6 oxygen ions) of ILMENITE from the Arseno
 Lake area

Sample Number	7224	7218	727	7217	7248G	73407	73376
Grade Index	3.2	2.95	2.87	2.82	2.39	2.03	2.03
SiO ₂	1.04	0.08	0.71	-----	-----	0.14	-----
TiO ₂	50.14	52.97	51.04	53.27	50.56	51.72	54.86
Al ₂ O ₃	-----	-----	0.55	-----	-----	-----	-----
Cr ₂ O ₃	0.06	-----	-----	-----	-----	0.08	-----
V ₂ O ₃	0.88	0.70	0.62	0.71	0.42	1.06	0.25
FeO*	28.98	42.70	43.34	42.60	29.38	45.89	45.06
MnO	15.18	1.86	1.72	1.35	16.54	0.93	0.70
Total	96.28	98.41	97.98	97.93	96.90	99.82	100.87
Si	0.054	0.004	0.036	-----	-----	0.007	-----
Ti	1.952	2.026	1.957	2.040	1.980	1.968	2.044
Al	-----	-----	0.033	-----	-----	-----	-----
Cr	0.002	-----	-----	-----	-----	-----	-----
V	0.036	0.029	0.025	0.029	0.017	-----	0.010
Fe	1.254	1.816	1.843	1.814	1.280	1.942	1.867
Mn	0.669	0.080	0.075	0.058	0.734	0.040	0.033
mole % pyrophanite	34.8	4.2	3.9	3.1	36.0	2.0	1.7

*total Fe as FeO

G = spessartine garnet present in phase assemblage

----- = not detected

TABLE 6 (Continued)

Sample Number	73402	7255G	72385	7347	73478	73451	73501
Grade Index	2.02	1.99	1.21	1.07	0.93	0.79	0.76
SiO ₂	0.22	0.37	-----	-----	0.28	-----	0.21
TiO ₂	52.46	52.46	53.88	53.37	51.49	52.83	53.61
Al ₂ O ₃	-----	-----	-----	-----	-----	-----	-----
Cr ₂ O ₃	-----	-----	0.08	-----	0.05	0.07	0.21
V ₂ O ₃	-----	0.58	-----	-----	0.60	0.60	2.02
FeO*	44.88	43.51	46.22	45.08	45.02	44.14	45.32
MnO	0.81	0.29	0.25	0.89	1.66	1.89	1.16
Total	98.37	97.21	100.43	99.34	99.10	99.53	102.53
Si	0.011	0.019	-----	-----	0.014	-----	0.010
Ti	2.005	2.022	2.026	2.028	1.969	2.006	1.972
Al	-----	-----	-----	-----	-----	-----	-----
Cr	-----	0.003	0.003	-----	0.002	0.003	0.008
V	-----	0.024	-----	-----	0.024	0.017	0.079
Fe	1.907	1.865	1.934	1.905	1.919	1.863	1.854
Mn	0.035	0.013	0.012	0.038	0.071	0.081	0.048
mole % pyrophanite	1.8	0.69	0.62	1.96	3.57	4.17	2.52

TABLE 6 (Continued)

Sample Number	73239	73185	73205	72351	73171	72345	72356
Grade Index	0.67	0.66	0.53	0.50	0.17	0	0
SiO ₂	-----	0.16	0.24	-----	-----	-----	-----
TiO ₂	53.55	52.24	52.82	53.26	51.34	52.23	54.17
Al ₂ O ₃	-----	-----	-----	-----	-----	-----	-----
Cr ₂ O ₃	-----	0.16	0.11	-----	0.05	-----	0.05
V ₂ O ₃	0.71	0.75	1.04	0.52	0.07	0.35	0.58
FeO*	44.62	44.75	45.12	45.30	45.85	46.21	45.75
MnO	0.73	0.52	0.64	0.40	2.87	0.96	0.56
Total	99.61	98.58	99.96	99.48	100.18	99.75	101.11
Si	-----	0.008	0.012	-----	-----	-----	-----
Ti	2.020	2.000	1.993	2.020	1.961	1.976	2.020
Al	-----	-----	-----	-----	-----	-----	-----
Cr	-----	0.006	0.004	-----	0.002	-----	0.002
V	0.028	0.030	0.042	0.020	0.003	0.014	0.023
Fe	1.878	1.906	1.893	1.912	1.947	1.987	1.899
Mn	0.028	0.022	0.027	0.017	0.124	0.041	0.023
mole % pyrophanite	1.47	1.14	1.41	0.88	5.99	2.02	1.20

rutile is also found as a reaction rim around ilmenite. It is fairly uniform in composition and contains minor amounts of iron and vanadium. Under the electron beam, it exhibits a pale blue cathodoluminescence, perhaps caused by the presence of niobium and tantalum in the rutile structure (Deer, Howie, and Zussman, 1962).

Ilmenite has a more variable composition between samples and also between individual grains within a single thin section. Minor amounts of silicon and vanadium are present. The manganese oxide content ranges from 0.287% to 16.54%, thus displaying the high pyrophanite content characteristic of metamorphic ilmenites (Rumble, 1971).

There is no apparent grade dependence of rutile composition in the biotite zone, however, the pyrophanite content of ilmenite shows a systematic decrease with increasing grade (Fig. 8).

CONTROLS OF BIOTITE ZONE MINERAL CHEMISTRY

Metamorphic Grade

From the compositional data presented above, it is apparent that there is no strong correlation between metamorphic grade and biotite zone mineral chemistry. The trends observed between mineral composition and metamorphic grade are:

1. A decrease in Fe/Mg and a decrease in Si/Al^{IV} in chlorite.

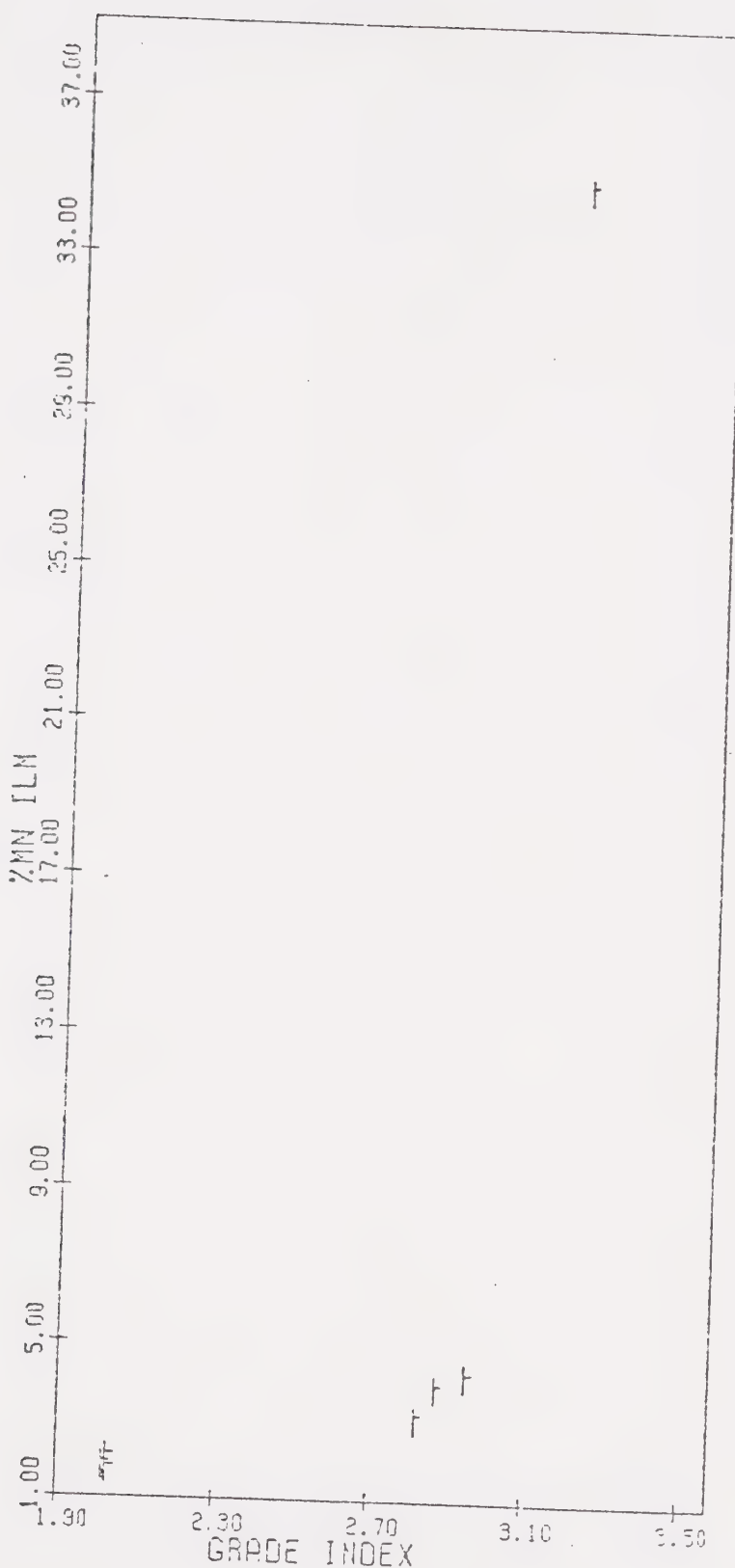


FIGURE 8a: Diagram illustrating the relationship between the pyrophanite content of ilmenite and grade index for ilmenite from the biotite zone.

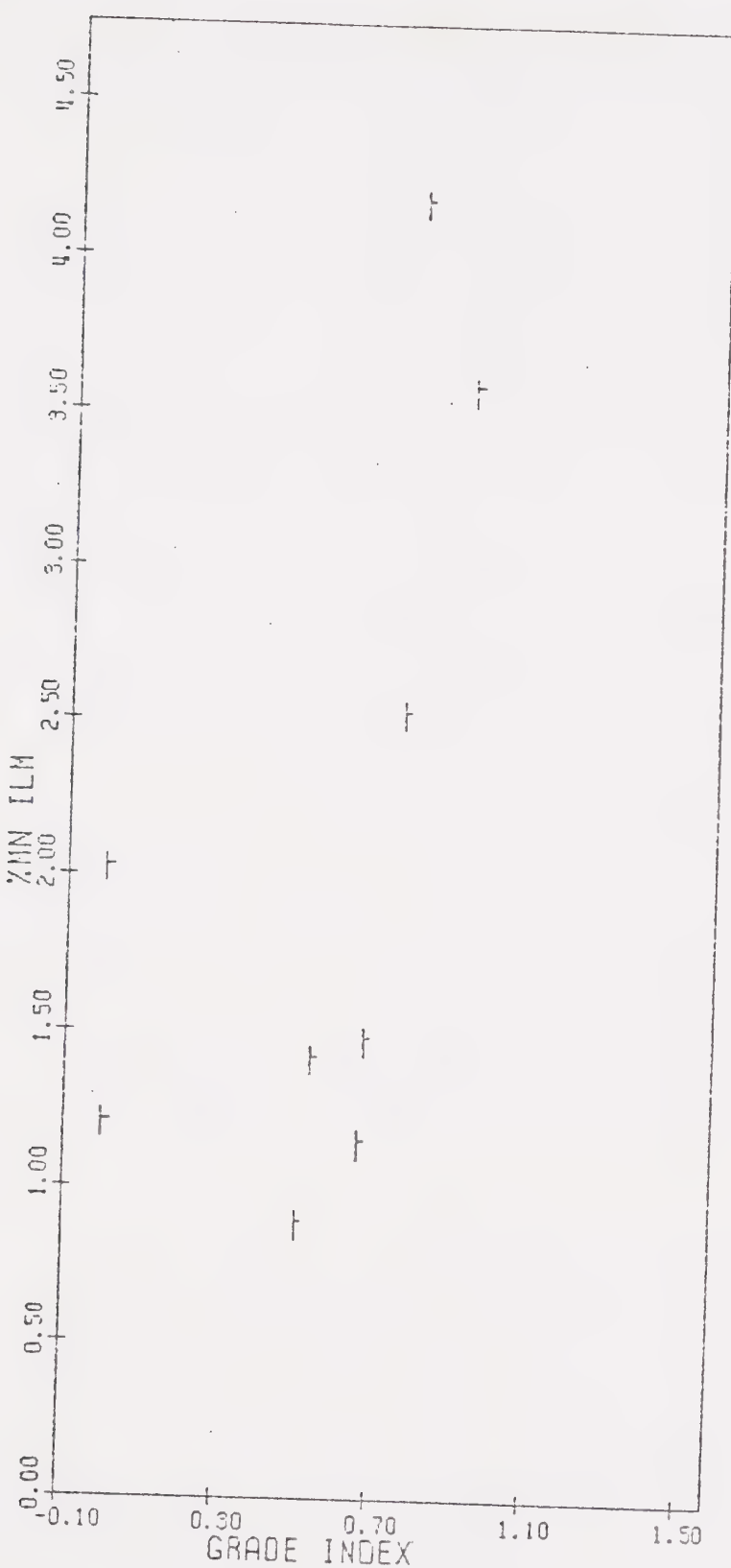


FIGURE 8b: Diagram illustrating the relationship between the pyrophanite content of ilmenite and grade index for ilmenite from the almandine-cordierite-K-feldspar zone.

2. A decrease in Fe/Mg and a decrease in Si/Al^{IV} in biotite.

Thus, across the biotite zone, there appears to be a progressive Mg enrichment in biotite and the remaining chlorite. The same trend has been reported in biotite zone rocks from the Buchan (D) section of the eastern Scottish Dalradian (Harte, 1975).

Rock Composition

The range of composition of the biotite zone minerals, and the absence of compositional dependency on grade (except as noted above), suggests that bulk rock composition was the major factor in determining mineral composition. This is most obvious from the oxide minerals rutile and ilmenite, where there is strong variation from sample to sample and also from grain to grain within a single sample. Most notable are the Mn, V, and Si contents of ilmenite and the Si, V, and Fe contents of rutile.

A limited number of qualitative microprobe analyses of plagioclase showed variation from sample to sample and suggests that host rock composition and the composition of detrital plagioclase were the dominant controls of plagioclase composition. Plagioclase ranges from An₁₃ to An₃₀ in the biotite zone (Table 7). The high An content of some plagioclase probably reflects their clastic origin.

TABLE 7 : Feldspar analyses from the Arseno Lake area

Sample Number	7224	7219	7217	73280	73376	73407	73402	7253
Grade Index	3.2	2.9	2.82	2.51	2.03	2.03	2.02	1.91
Plagioclase								
Ab	64.3	75.7	52.9	73.5	85.4	66.1	73.5	
An	33.9	23.7	47.1	26.1	13.4	33.3	25.9	85.8
Or	1.8	0.6	0	0.4	1.2	0.6	0.6	13.4
K-feldspar								
Ab								
An								
Or								
Cs								
Ab								
An								
Or								
Cs								
Sample Number	73171	72385	7347	73145	73153	73416	73478	73162
Grade Index	1.28	1.21	1.07	1.0	1.0	0.98	0.93	0.92
Plagioclase								
Ab								
An								
Or								
K-feldspar								
Ab								
An								
Or								
Cs								

All of the analyses presented in this table were collected using beam scanning over an area of $\sim 16 \times 20 \mu\text{m}$ in order to prevent alkali loss over long counting times. The analyses are therefore averages of these areas. This explains the occurrence of plagioclase analyses reported here whose composition falls in the peristerite gap.

TABLE 7 (Continued)

Sample Number	73450	73451	73501	73239	73185	73180	73157	73206
Grade Index	0.90	0.79	0.76	0.68	0.66	0.64	0.54	0.53
Plagioclase								
Ab	74.8	49.2	92.1	71.1	73.6	63.4	54.5	62.2
An	24.7	49.9	7.8	27.8	25.6	0.5	44.9	37.3
Or	0.5	0.9	0.1	1.1	0.8	36.1	0.6	0.5
K-feldspar								
Ab								
An								
Or								
Cs								

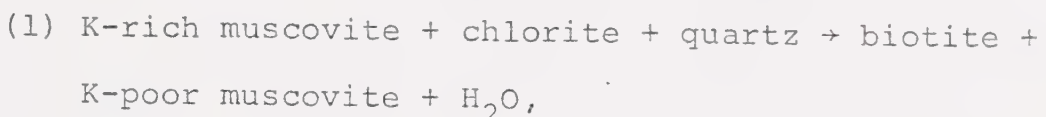
Sample Number	73155	72351	73202	73195	73226	73171	72345	72356
Grade Index	0.53	0.50	0.46	0.41	0.31	0.17	0	0
Plagioclase								
Ab	57.8	67.0	74.9	49.3	66.8	73.0	58.9	70.7
An	40.5	32.0	24.7	50.1	31.5	26.4	40.6	28.2
Or	1.8	1.0	0.4	0.6	1.7	0.6	0.5	1.1
K-feldspar								
Ab								
An								
Or								
Cs								

Mineral Assemblages Present

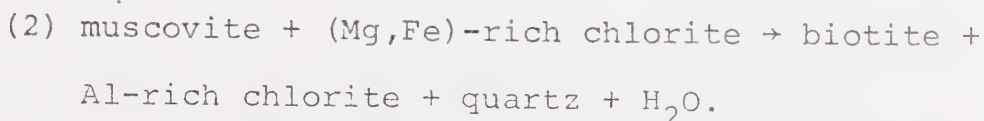
A third control of biotite zone mineral chemistry, especially the compositions of biotite and chlorite, is the total mineral assemblage present. Two biotite zone samples contained garnet as a third ferro-magnesian aluminum silicate, and the Fe/Mg ratio of biotite adjacent to garnet is lower than that of biotite in garnet free rocks.

THE BIOTITE FORMING REACTION

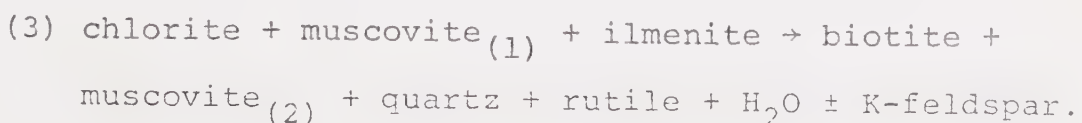
Since 1926, when C. E. Tilley proposed that biotite was formed by the reaction:



there has been substantial controversy over the nature of the biotite forming reaction in pelitic rocks. More recently, Ramberg (1952), Barth (1962), Winkler (1965), and Turner (1968) have suggested that biotite forms by the following reaction:



The most definitive study in Abukuma facies series rocks to date is that of Ramsay (1973 a,b,c), who deduced the biotite forming reaction in rocks of similar composition and metamorphic setting to be:



Muscovite₍₁₎ is richer in the phengite components and muscovite₍₂₎ is closer to the ideal muscovite formula. The major role of muscovite, however, is to provide potassium for the product biotite. K-feldspar may or may not be produced, depending on whether or not potassium and aluminum are present in excess.

The present study has arrived at similar conclusions, especially concerning the role of ilmenite as a reactant and the observation that quartz and rutile are products of the biotite forming reaction. In all of the samples examined where biotite has formed, ilmenite grains are rimmed by rutile, and rutile has frequently grown epitaxially within biotite. Biotite + quartz intergrowths are also common (see Plate I).

THE CORDIERITE - AMPHIBOLITE FACIES

The most abundant rock type in the cordierite-amphibolite facies, as in the biotite zone, is metapelite with subordinate metagraywacke. Cordierite first appears simultaneously, or just after, the first appearance of andalusite. There is an increase in grain size of all the minerals present, indicating that nearly complete recrystallization has occurred. In the low grade part of the cordierite zone, minor amounts of chlorite are still present, but within 0.5 km above the cordierite isograd, all of the primary chlorite has been consumed. Across the cordierite zone, plagioclase changes in composition from

sodic oligoclase to oligoclase-andesine. The rocks lose the schistosity characteristic of the upper biotite zone and become gneissic.

Samples from the cordierite zone are divided into two major groups based on the mineral assemblages present. Group I samples are characterised by the presence of andalusite, sillimanite, and/or muscovite along with cordierite, biotite, quartz, plagioclase, ilmenite, and rutile. Group II samples are less aluminous and lack alumina rich phases such as Al_2SiO_5 and muscovite.

Andalusite is replaced by sillimanite as the stable Al_2SiO_5 polymorph in the middle of the cordierite zone. Sillimanite occurs in two habits. The most common is as groups of acicular, small ($1 \times 20 \mu\text{m}$) crystals distinguished as sillimanite (variety fibrolite). Fibrolite most commonly occurs in biotite grains and less frequently as inclusions in cordierite. More coarsely crystalline sillimanite occurs at slightly higher grade, often replacing the fibrous variety. Reconnaissance microprobe analyses showed no compositional differences between the two types of sillimanite or between sillimanite and andalusite. It is most likely that the andalusite persists into the sillimanite stability field because of very small differences in entropy between andalusite and sillimanite of 0.7 cal/degree (Pankratz and Kelley, 1964; Holdaway, 1971).

Muscovites from the cordierite zone are very pure, having Fe + Mg totals in the Y-site of less than 0.5 (Table 4). Rutile and ilmenite (Tables 5 and 6) show the same range in composition as described for the biotite zone, except that the amount of manganese in ilmenite has a smaller range of values and the pyrophanite content is much lower.

In the upper part of the cordierite zone, muscovite is consumed by a discontinuous reaction with quartz to form sillimanite plus K-feldspar (the second sillimanite isograd of Figure 4). Above the second sillimanite isograd, sillimanite and K-feldspar coexist with cordierite, biotite, quartz, plagioclase, and the titaniiferous oxides.

CORDIERITE ZONE MINERAL CHEMISTRY

Biotite

Analyses and structural formulae for eight biotites are presented in Table 8.

Influence of Metamorphic Grade. Analysed biotites from the cordierite zone exhibit the following trends:

1. There is a tendency for Fe and the Fe/Mg ratio to increase with increasing metamorphic grade coupled with a sympathetic decrease in Mg.
2. Ti also increases with increasing meta-

TABLE 8 : Microprobe analyses (weight %) and structural formulae (based on 22 oxygen ions) of BIOTITE from the Cordierite zone

Sample Number	73269	73394	73407	73308	73131	72385*	73449	73450
Grade Index	2.70	2.22	2.03	1.86	1.28	1.21	0.94	0.90
SiO ₂	35.98	36.39	34.92	35.38	34.55	35.74	35.19	36.47
TiO ₂	1.62	3.20	3.97	2.53	2.60	3.29	3.22	3.23
Al ₂ O ₃	20.31	19.48	18.31	19.63	19.09	18.81	19.42	18.67
FeO*	17.86	16.07	20.41	19.74	18.48	19.56	19.51	14.32
MgO	9.34	10.22	7.68	8.27	7.98	9.15	7.84	11.41
MnO	0.08	0.07	0.08	0.09	0.08	-----	0.05	0.05
CaO	0.34	0.38	0.30	0.35	0.24	0.27	-----	0.28
K ₂ O	9.41	9.72	9.35	9.29	8.21	9.71	9.24	8.80
Na ₂ O	-----	0.16	-----	-----	-----	-----	-----	-----
Total	94.94	95.53	95.02	95.28	91.23	97.21	94.47	93.23
Si	5.431	5.421	5.353	5.378	5.436	5.319	5.389	5.492
Al ^{IV}	2.569	2.579	2.647	2.622	2.564	2.681	2.611	2.508
Al ^{VI}	1.044	0.842	0.661	0.895	0.976	0.618	0.894	0.806
Ti	0.184	0.358	0.458	0.289	0.308	0.368	0.370	0.366
Fe	2.254	2.002	2.615	2.508	2.431	2.435	2.498	1.804
Mg	2.102	2.263	1.754	1.873	1.871	2.030	1.790	2.561
Mn	0.010	0.009	0.010	0.011	0.010	-----	0.006	0.007
Ca	0.055	0.060	0.049	0.057	0.041	0.043	-----	0.045
K	1.812	1.847	1.829	1.801	1.647	1.844	1.805	1.690
Na	-----	0.045	-----	-----	-----	-----	-----	-----
Σ Y-site	5.594	5.474	5.498	5.776	5.813	5.526	5.558	5.544
Σ X-site	1.871	1.952	1.878	1.858	1.688	1.887	1.805	1.735
Fe/Mg	1.07	0.88	1.49	1.34	1.3	1.2	1.40	0.70
mole % annite	40	37	48	43	42	44	45	33

*total Fe as FeO; *contains 0.68% F, .018 F = 0; ----- = not detected

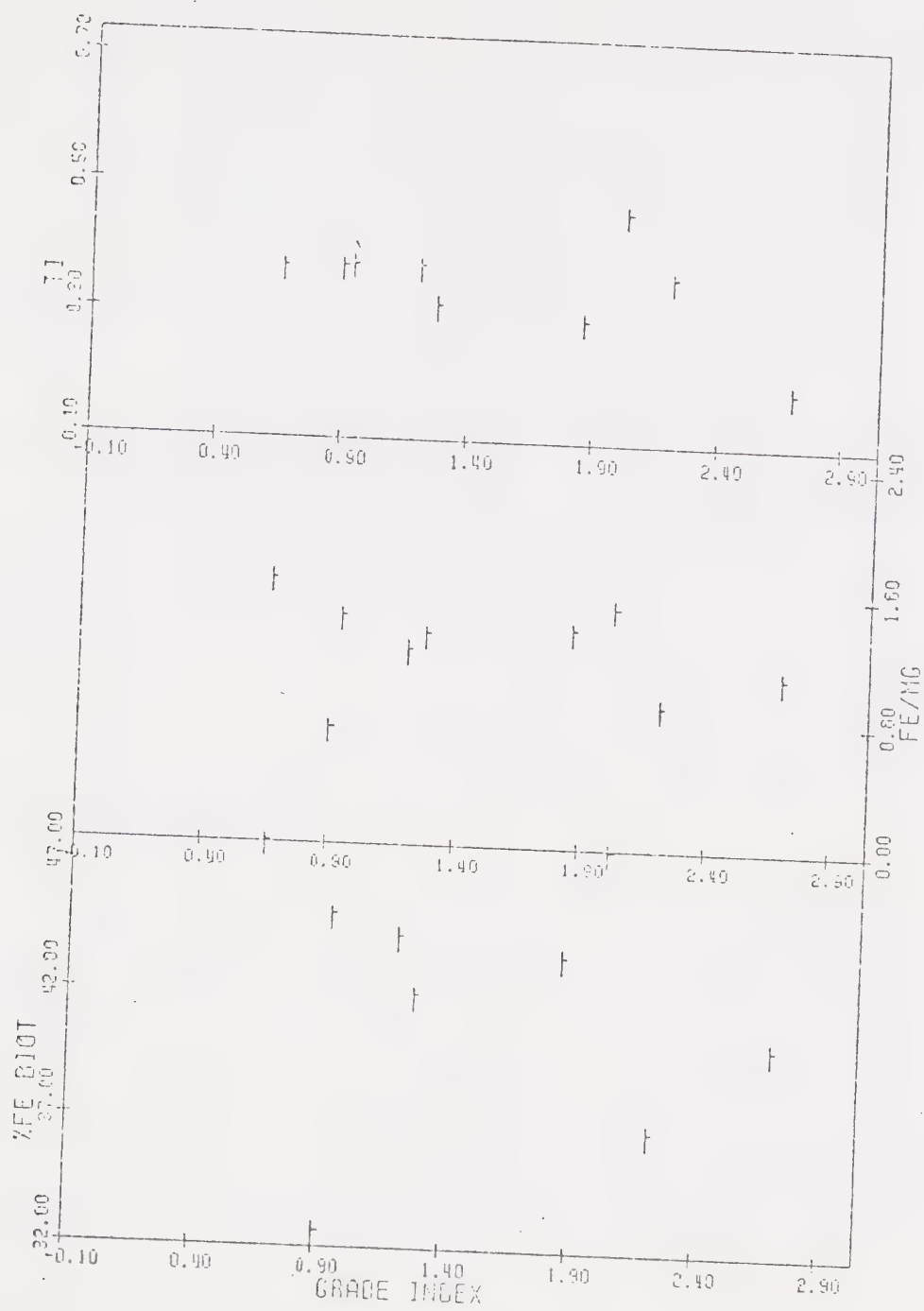


FIGURE 9: Diagram illustrating the relationship of biotite composition (atomic proportions) to grade index for biotite from the cordierite zone.

morphic grade. There is no apparent grade dependence of the other Y-site cations, nor in the X-site. There may be a slight increase in Al^{IV} and a decrease in the $\text{Si}/\text{Al}^{\text{IV}}$ ratio, but there is too little data to establish this conclusively.

These data are shown in Figure 9.

Comparative Discussion. There are few published data on biotite compositions from cordierite zone mineral assemblages. The bulk of reported analyses of biotite coexisting with cordierite come from higher grade assemblages where garnet is also present. These garnet-cordierite-biotite assemblages are discussed under the cordierite-garnet zone.

Ramsay (1973 a,b,c) presented data on biotites from the cordierite zone in the metamorphic aureole of the Prosperous Lake area, which, like the present study, is a low pressure, intermediate temperature facies series. The trend of increasing Fe and decreasing Mg in biotite from this study is in agreement with Ramsay's data.

Cordierite

Analyses and structural formulae for nine cordierites are presented in Table 9. These data are summarized on Figure 10.

Influence of Metamorphic Grade. Analysed cordierites from the cordierite zone exhibit the following trends:

TABLE 9 : Microprobe analyses (weight %) and structural formulae (based on 18 oxygen ions) of CORDIERITE from the Cordierite zone, Arseno Lake area

Sample Number	73269	73394	73407	73308	7259	72385	73449	73450	73185
Grade Index	2.70	2.22	2.03	1.86	1.80	1.21	0.94	0.90	0.66
SiO ₂	48.42	49.69	48.17	48.33	48.75	49.05	48.49	49.04	48.80
Al ₂ O ₃	32.75	33.29	32.75	32.80	32.79	32.31	32.96	32.99	32.78
FeO*	8.83	7.58	9.25	9.52	8.27	10.76	9.10	6.32	9.50
MgO	7.75	8.50	7.20	7.25	7.31	6.82	7.18	8.97	7.02
MnO	0.22	0.15	0.19	0.24	0.44	0.09	0.24	0.10	0.13
K ₂ O	0.13	0.05	----	0.04	0.04	----	0.08	----	----
Na ₂ O	0.25	0.22	----	0.23	----	----	----	0.10	----
Total	98.30	99.48	97.56	98.41	97.60	99.03	98.05	97.42	98.33
Si	5.003	5.036	5.016	5.003	5.051	5.060	5.022	5.040	5.044
Al ^{IV}	0.997	0.964	0.984	0.997	0.949	0.940	0.978	0.960	0.956
Al ^{VI}	2.992	3.012	3.035	3.005	3.055	2.988	3.044	3.006	3.040
Fe	0.763	0.643	0.806	0.825	0.717	0.935	0.788	0.544	0.821
Mg	1.194	1.284	1.118	1.119	1.128	1.053	1.108	1.374	1.081
Mn	0.020	0.013	0.017	0.021	0.038	0.008	0.021	0.009	0.020
K	0.017	0.007	----	0.005	0.005	----	0.011	----	----
Na	0.049	0.042	----	0.046	----	----	----	0.013	----
Σ Y-site	5.035	5.001	4.976	5.021	4.943	4.985	4.972	4.933	4.967
Fe/Mg	0.639	0.501	0.721	0.737	0.636	0.888	0.711	0.396	0.759
mole % Fe Cordierite	39	33	42	42	39	47	42	28	43

*total Fe as FeO; ---- = not detected

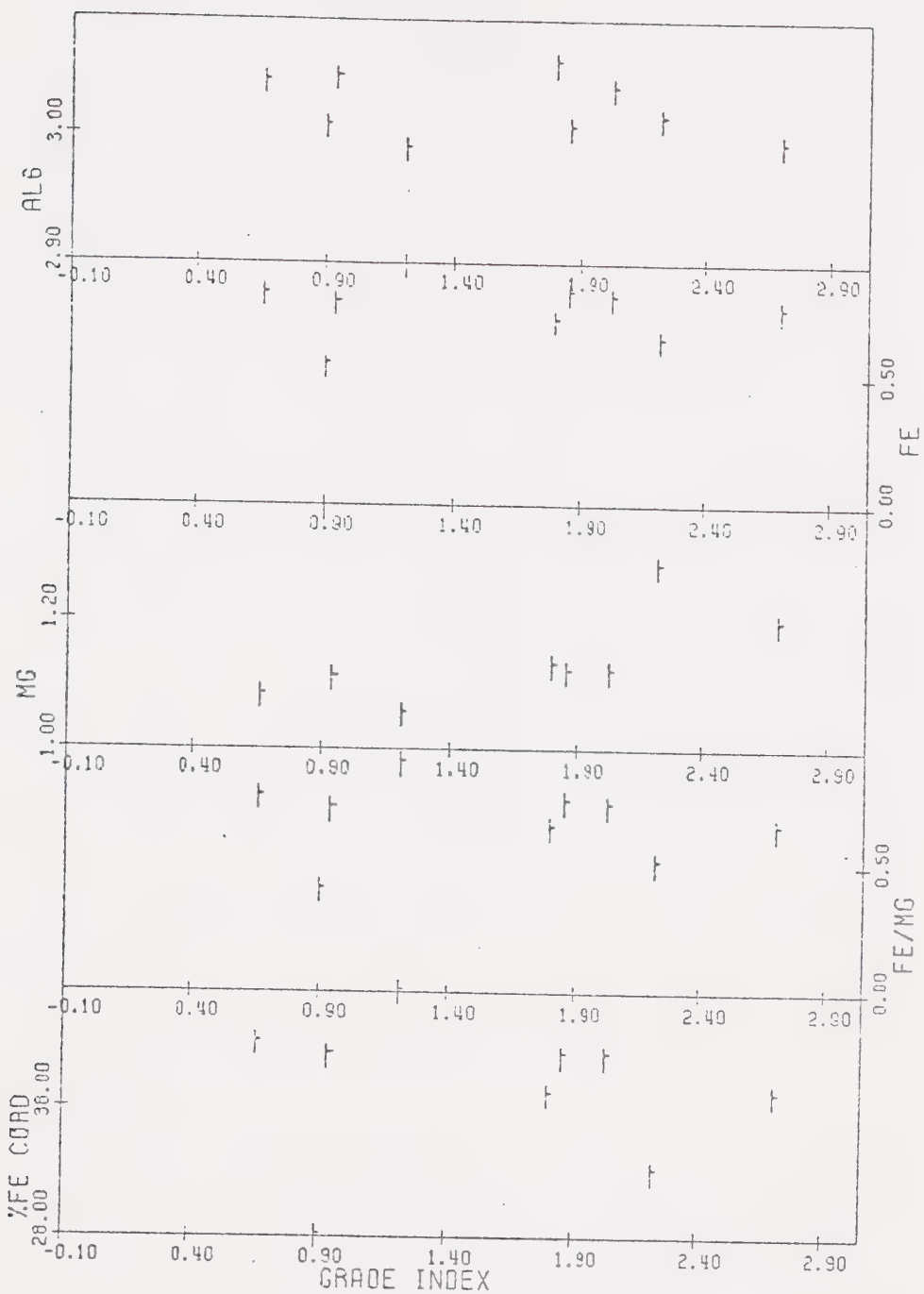


FIGURE 10: Diagram illustrating the relationship of cordierite composition (atomic proportions) to grade index for cordierites from the cordierite zone.

1. There is a systematic increase in Fe with increasing metamorphic grade.
2. There is a corresponding decrease in Mg and an increase in the Fe/Mg ratio.

No trends related to tetrahedral site occupancy have been observed, and there is no relationship between Mn or the presence of K and Na and metamorphic grade.

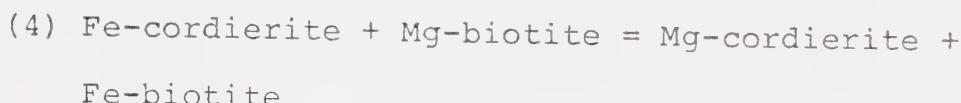
Discussion. The data presented on Figures 9 and 10 show the general trends outlined above. Two samples display anomalous Fe, Mg contents for both biotite and cordierite. These samples differ from the others in that there is less biotite and cordierite present, and alumina rich phases such as the Al_2SiO_5 minerals or muscovite are absent. These two samples (73450 and 73394) are apparently metagraywackes whereas the other samples are metapelites.

CONTROLS OF CORDIERITE ZONE MINERAL CHEMISTRY

Metamorphic Grade

Across the cordierite zone, in the pelitic rocks, there is a tendency for both biotite and cordierite to become slightly more iron rich in composition. This may reflect the role of ilmenite as a reactant in the biotite and cordierite forming reaction. The slight increase in Ti in biotite indicates that a Ti bearing phase (ilmenite) is a reactant. There is a tendency for the distribution coefficients for iron and magnesium between

biotite and cordierite to increase with increasing metamorphic grade. This suggests that a continuous reaction of the type:



was occurring and modifying the compositions of coexisting biotite and cordierite.

Bulk Rock Composition

As has been noted earlier, major differences in bulk rock composition are reflected in the mineral assemblages present and in the compositions of those minerals. The points which lie away from the trends shown on Figures 9 and 10 are from semi-pelitic to graywacke compositional environments. The Fe and Mg contents of coexisting biotite and cordierite from these samples, as well as the K_D for iron and magnesium, are clearly different from the pelitic assemblages.

The range of compositions in the biotite tetrahedral and X-sites and the cordierite tetrahedral site, as well as the aluminum content of both cordierite and biotite, show no relationship to metamorphic grade. It is therefore suggested that minor variations in bulk rock composition may have, at least in part, controlled these aspects of mineral composition.

Mineral Assemblages Present

The mineral assemblages present in the cordierite

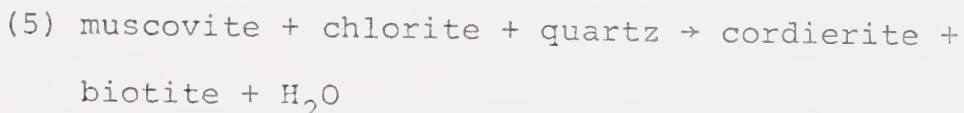
zone apparently do not play a major role in controlling the compositions of biotite and cordierite. The limited data from the cordierite zone suggests that a continuous iron-magnesium exchange reaction producing a Mg-richer cordierite and an Fe-richer biotite occurred. This type of continuous reaction, which results in the slow disappearance of one phase, is illustrated by the Zn content of spinel which is discussed below.

Conclusions

From the limited data presently available, it appears that within the cordierite zone of the low pressure, intermediate temperature facies series, the permissive controls are more important than modifying controls in defining the compositions of the ferro-magnesian silicates present.

THE CORDIERITE FORMING REACTION

There are numerous possible reactions which could account for the appearance of cordierite in pelitic schists. The reaction:



is perhaps the most frequently suggested. This reaction has been studied in many metamorphic terrains as well as in several experimental studies (Tilley, 1924; Schreyer and Yoder, 1961; Hess, 1969; Schreyer and Seifert, 1969; Seifert, 1970; Bird and Fawcett, 1971). The Fe/Mg ratio

of the bulk rock, as well as Al_2O_3 content, restrict the simultaneous first appearance of cordierite plus biotite. If the $\text{Fe}/(\text{Mg} + \text{Fe})$ ratio of the bulk rock exceeds 0.75, staurolite will occur in place of cordierite (Hoschek, 1969).

The experimental studies to date in haplopelitic systems have neglected the minor components titanium, sodium, and manganese. As a consequence, the above experimentally determined reaction is unlikely to represent the total reaction isograd occurring in real pelitic systems. The above reaction also does not reflect the fact that in most low pressure facies series, biotite appears before cordierite.

In the Arseno Lake area, many samples just below the cordierite isograd contain minor amounts of muscovite and chlorite as well as biotite. Thus, the first appearance of cordierite in some samples probably resulted from a reaction similar to that discussed above, except that ilmenite should be added as a reactant and rutile as a product. The role of ilmenite in the reaction was the same as it was in the biotite forming reaction.

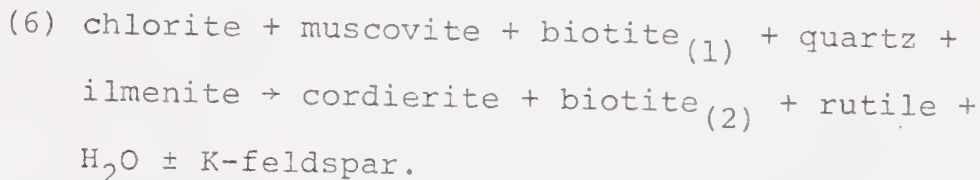
The compositional relationships between coexisting biotite and cordierite also provide some insight into the cordierite forming reaction. As biotite shows no strong decrease modally in the cordierite zone, it is suggested that biotite was modified in composition as

the cordierite forming reaction proceeded, especially in the upper part of the cordierite zone.

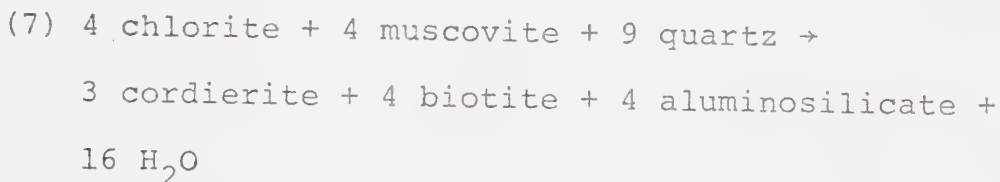
An examination of all of the mineral assemblages present in the cordierite zone (Table 1) leads to the conclusion that more than one reaction probably produced cordierite, as is discussed below.

The Cordierite Isograd

The reaction which first produces cordierite, and which defines the cordierite isograd of this study, is similar to that of Ramsay (1973 a, 1974):

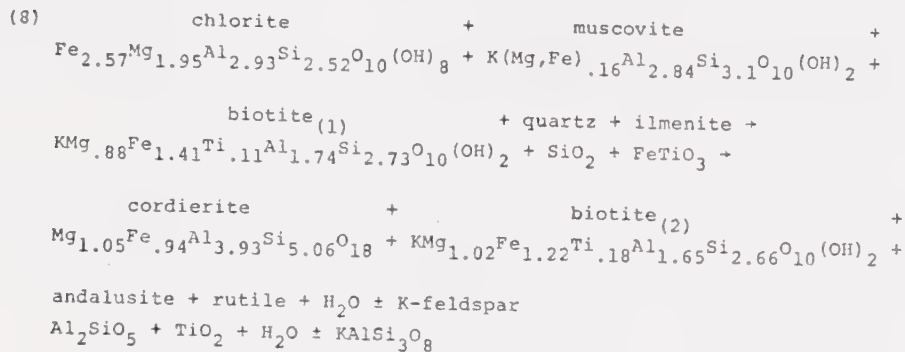


Biotite₍₂₎ is richer in Fe and Mn and depleted in Mg relative to biotite₍₁₎. Hirschberg and Winkler (1968) investigated the reaction:



and the equilibrium conditions attained suggest that the cordierite + andalusite assemblage formed in the Arseno Lake area at a temperature of $\sim 540^\circ \text{ C.}$ at a pressure of 3.2 kbars. Application of the equilibrium data for the above reaction to this area is limited because biotite occurs before cordierite and because ilmenite is a reactant.

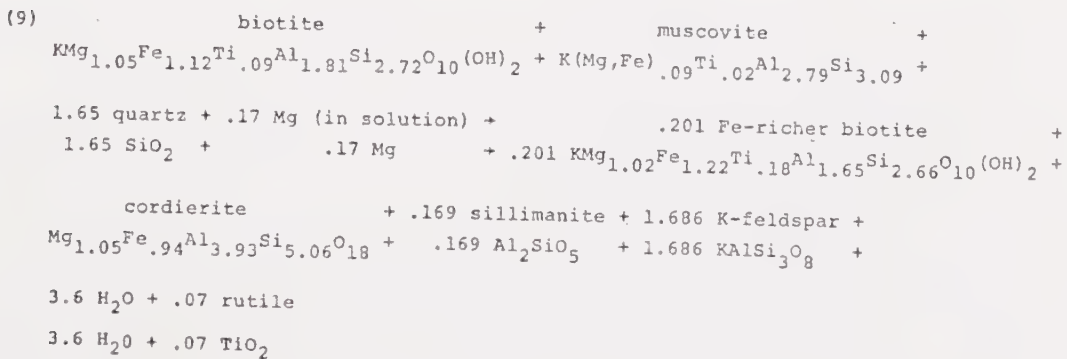
The reaction suggested for the cordierite isograd in the Arseno Lake area, therefore, is:



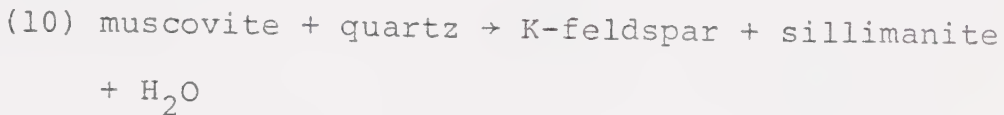
This reaction is a coupled reaction combining reactions (3) and (7).

Reactions at Higher Grade

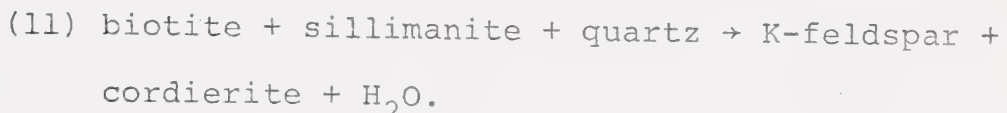
At higher grades of metamorphism in the cordierite zone, after chlorite has been consumed by reaction, a new cordierite forming reaction must have taken place. Biotite was the sole remaining source of Fe + Mg and aluminosilicate and K-feldspar increase in abundance. Muscovite disappeared as well. It is therefore suggested that the cordierite forming reaction at higher grade was:



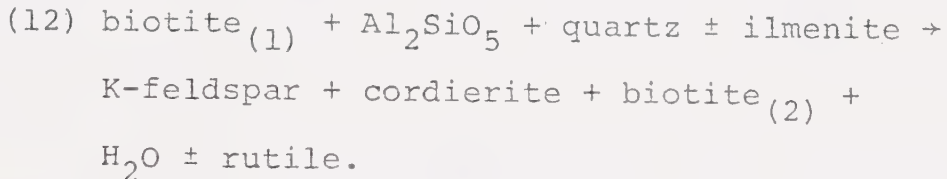
For clarity, this reaction can be considered as two coupled reactions. The first defines the second sillimanite isograd:



and the second reaction is:



At higher grade within the cordierite zone, above the second sillimanite isograd where muscovite is no longer present, the cordierite forming reaction appears to have been a continuous reaction in which the biotite composition was modified as follows:



The product biotite ($\text{biotite}_{(2)}$) is depleted in aluminum and enriched in iron relative to the reactant biotite.

THE CORDIERITE - ALMANDINE - K-FELDSPAR ZONE

The major rock type present is metapelite with subordinate amounts of metagraywacke. Garnet first appears in the metapelites. Biotite, cordierite, quartz, plagioclase (oligoclase-andesine), microcline, ilmenite and/or rutile, and sillimanite are also present in varying proportions, depending on the bulk rock composition.

Garnet was observed in about 40% of the samples from this zone. The majority of the garnets show minor late stage retrograde reaction to biotite and plagioclase which is more calcic than the matrix plagioclase (up to An₅₀). In addition, garnet has not been observed in contact with sillimanite. Where sillimanite is included in the total mineral assemblage, it is most frequently bordered by cordierite and the felsic minerals quartz, plagioclase, and microcline. It is only infrequently observed in contact with biotite plus quartz. This is in contrast to the common association of biotite and sillimanite in the cordierite zone.

CORDIERITE - ALMANDINE - K-FELDSPAR ZONE MINERAL CHEMISTRY

Biotite

Table 10 presents 24 analyses of biotite from the cordierite-almandine-K-feldspar zone. Biotite composition varies as a function of the Fe-Mg silicate with which it is in contact. Single grains of biotite are homogenous, but ΣAl , Ti and Fe/Mg vary from grain to grain within a single section. Biotite associated with cordierite is richer in ΣAl and Fe and lower in Ti and Mg than biotite in equilibrium with garnet and orthopyroxene. The following relationships of biotite composition, which is a function of the phase in local

TABLE 10: Microprobe analyses (weight %) and structural formulae
 (based on 22 oxygen ions) of BIOTITE from the Cordierite-
 Garnet zone

Sample Number	73280C	73402G	73402C	73366C	7345G	73153C	73153G	73162C
Grade Index	2.51	2.02	2.02	1.64	1.0	1.0	1.0	0.92
SiO ₂	35.84	34.11	34.65	35.28	33.90	33.99	34.15	34.80
Al ₂ O ₃	20.47	18.68	18.93	16.61	18.75	19.24	19.34	20.05
TiO ₂	2.56	2.70	2.90	3.91	3.00	2.98	2.73	3.05
Cr ₂ O ₃	0.06	----	0.13	----	----	0.06	0.05	0.20
V ₂ O ₃	0.10	0.11	0.08	----	0.05	0.07	0.07	0.08
FeO*	19.85	20.44	22.08	22.30	20.84	22.14	21.74	22.03
MgO	7.96	8.07	6.71	8.68	7.23	6.19	6.64	5.91
MnO	0.07	----	----	----	0.11	0.15	0.18	0.20
K ₂ O	8.04	9.07	8.12	9.00	8.39	8.49	7.93	7.96
CaO	----	----	0.26	----	----	----	0.26	----
Total	94.95	93.18	93.86	95.78	92.27	93.31	93.09	94.28
Si	5.398	5.336	5.393	5.414	5.319	5.332	5.356	5.365
Al ^{IV}	2.602	2.664	2.607	2.386	2.681	2.668	2.644	2.635
Al ^{VI}	1.032	0.780	0.866	0.613	0.785	0.890	0.930	1.008
Cr	0.007	----	0.016	----	----	0.007	0.006	0.024
V	0.012	0.014	0.010	----	0.007	0.009	0.008	0.010
Ti	0.290	0.317	0.340	0.452	0.354	0.352	0.322	0.354
Fe	2.500	2.675	2.874	2.860	2.734	2.906	2.851	2.840
Mg	1.788	1.881	1.556	1.983	1.691	1.448	1.552	1.358
Mn	0.009	----	----	----	0.014	0.020	0.024	0.027
K	1.550	1.810	1.611	1.760	1.680	1.699	1.581	1.565
Ca	----	----	0.043	----	----	----	0.044	----
Σ Y-site	5.638	5.667	5.662	5.918	5.585	5.632	5.693	5.621
Fe/Mg	1.40	1.42	1.85	1.44	1.62	2.01	1.84	2.09
mole % annite	44	47	51	48	49	52	50	51

C = biotite adjacent to cordierite

G = biotite adjacent to garnet

*total Fe as FeO

TABLE 10 (Continued)

Sample Number	73451G	73185C	73157G	73155C	73206C	73202C	73202G	73195C
Grade Index	0.79	0.66	0.54	0.53	0.53	0.46	0.46	0.41
SiO ₂	34.44	35.91	37.15	35.35	35.56	36.23	34.67	34.99
Al ₂ O ₃	16.60	18.85	18.72	19.22	19.03	18.93	17.53	17.40
TiO ₂	3.82	3.15	2.20	2.66	2.95	3.13	3.23	4.52
Cr ₂ O ₃	0.07	0.14	-----	0.22	0.16	0.06	0.13	0.11
V ₂ O ₃	0.12	0.22	0.10	0.13	0.28	0.10	0.12	0.15
FeO*	19.93	21.34	18.90	20.72	18.03	20.28	20.23	19.40
MgO	9.20	7.35	11.32	7.25	8.67	8.76	8.35	8.54
MnO	0.11	0.07	0.12	-----	-----	0.07	0.08	0.11
K ₂ O	8.94	6.83	5.85	8.56	9.37	6.61	8.16	9.10
CaO	-----	0.20	-----	-----	0.29	0.20	-----	0.25
Total	93.23	94.06	94.46	94.11	94.34	94.37	92.50	94.46
Si	5.386	5.496	5.539	5.441	5.435	5.483	5.436	5.389
Al _{IV}	2.614	2.504	2.461	2.559	2.565	2.517	2.564	2.611
Al _{VI}	0.446	0.897	0.829	0.928	0.863	0.861	0.673	0.547
Cr	0.009	0.017	-----	0.027	0.019	0.007	0.017	0.013
V	0.016	0.027	0.012	0.016	0.034	0.012	0.016	0.018
Ti	0.451	0.363	0.246	0.308	0.340	0.356	0.382	0.547
Fe	2.608	2.731	2.356	2.667	2.305	2.567	2.656	2.498
Mg	2.146	1.676	2.516	1.663	1.975	1.977	1.952	1.960
Mn	0.015	0.009	0.016	-----	-----	0.009	0.011	-----
K	1.783	1.334	1.113	1.680	1.828	1.277	1.634	1.787
Ca	-----	0.033	-----	-----	0.047	0.032	-----	0.041
Σ Y-site	5.681	5.720	5.975	5.609	5.536	5.889	5.747	5.589
Fe/Mg	1.22	1.63	0.94	1.60	1.17	1.30	1.36	1.27
mole % annite	46	48	39	48	42	44	46	45

TABLE 10 (Continued)

Sample Number	73221C	73221G	73226C ₁	73226C ₂	73227C	73229C	73171C	73255C
Grade Index	0.33	0.33	0.31	0.31	0.29	0.27	0.17	0.05
SiO ₂	34.78	34.91	35.95	35.85	34.95	35.30	35.89	35.35
Al ₂ O ₃	17.51	16.97	18.09	18.32	18.57	16.83	17.31	17.26
TiO ₂	4.58	4.78	4.35	4.16	4.31	3.45	2.79	4.63
Cr ₂ O ₃	0.06	----	0.09	----	0.10	0.08	0.08	0.08
V ₂ O ₃	0.20	0.21	0.15	0.12	0.12	0.12	0.12	0.15
FeO*	21.31	22.13	16.63	16.08	19.61	18.10	19.39	20.40
MgO	7.89	8.09	10.22	10.09	7.19	9.47	11.08	8.01
MnO	----	----	----	----	0.08	0.06	0.07	0.05
K ₂ O	8.45	9.06	9.38	9.65	9.20	9.26	9.38	9.25
Total	94.78	96.15	94.86	94.27	94.13	94.47	96.11	95.18
Si	5.363	5.348	5.423	5.435	5.395	5.388	5.408	5.424
Al ^{IV}	2.637	2.652	2.577	2.565	2.605	2.612	2.592	2.576
Al ^{VI}	0.545	0.412	0.640	0.708	0.773	0.739	0.483	0.545
Cr	0.007	----	0.017	----	0.012	0.010	0.010	0.009
V	0.025	0.026	0.019	0.014	0.015	0.014	0.014	0.019
Ti	0.531	0.551	0.494	0.474	0.500	0.396	0.316	0.535
Fe	2.748	2.835	2.098	2.039	2.531	2.310	2.443	2.617
Mg	1.814	1.846	2.297	2.280	1.655	2.151	2.487	1.832
Mn	----	----	----	----	0.011	0.008	0.008	0.007
K	1.662	1.771	1.804	1.867	1.811	1.802	1.802	1.811
Ca	----	----	----	----	----	----	----	----
Σ Y-site	5.670	5.670	5.559	5.515	5.497	5.638	5.761	5.555
Fe/Mg mole %	1.51	1.54	0.91	0.89	1.53	1.07	0.98	1.13
annite	48	50	38	37	46	41	42	47

equilibrium with it, are based upon the data for sample 73252:

Element in Biotite*	Concentration of Element in Biotite Adjacent to:
Ti	garnet > cordierite > orthopyroxene
Al	orthopyroxene > cordierite > garnet
Fe	cordierite > garnet > orthopyroxene
Mg	orthopyroxene > garnet > cordierite
Fe/Mg	garnet > cordierite > orthopyroxene

The relationships between biotite associated with cordierite and with garnet still hold when pyroxene is absent.

Influence of Metamorphic Grade. Systematic variation of biotite composition across the cordierite-almandine-K-feldspar zone occurs in the Y-site components Ti, Mg, and Fe. The data shown on Figure 11 are only for biotite adjacent to cordierite. There are two major trends noted for these biotite:

1. There is an increase in Mg and a decrease in the Fe/Mg ratio with increasing metamorphic grade.
2. There is a tendency for Ti to increase.

*This table should be read as follows: The concentration of Ti in biotite adjacent to garnet is greater than the concentration of Ti in biotite adjacent to cordierite is greater than the concentration of Ti in biotite adjacent to orthopyroxene, etc.

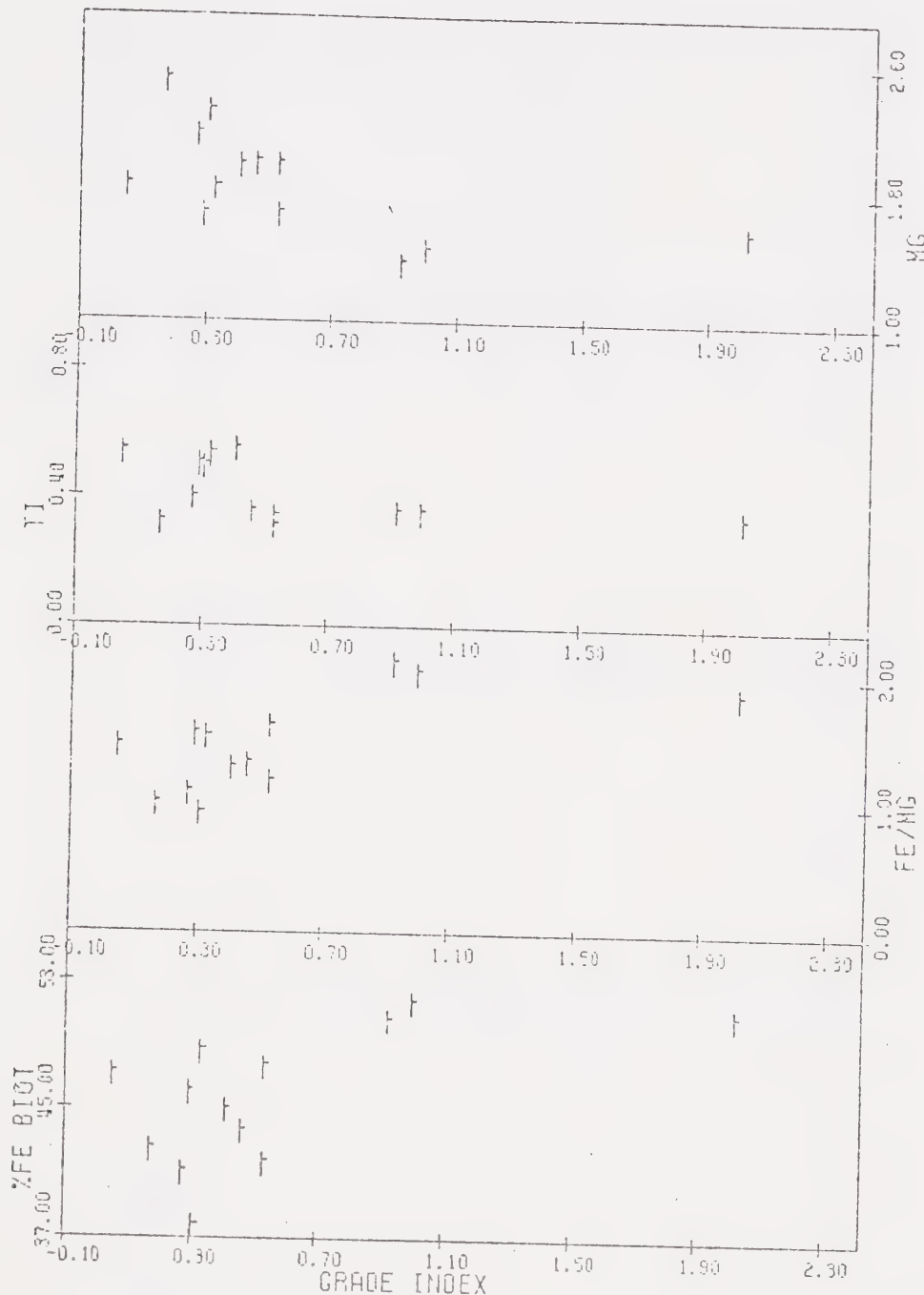


FIGURE 11a: Diagram illustrating the relationship of biotite composition (atomic proportions) to grade index for biotites from the almandine-cordierite-K-feldspar zone adjacent to cordierite.

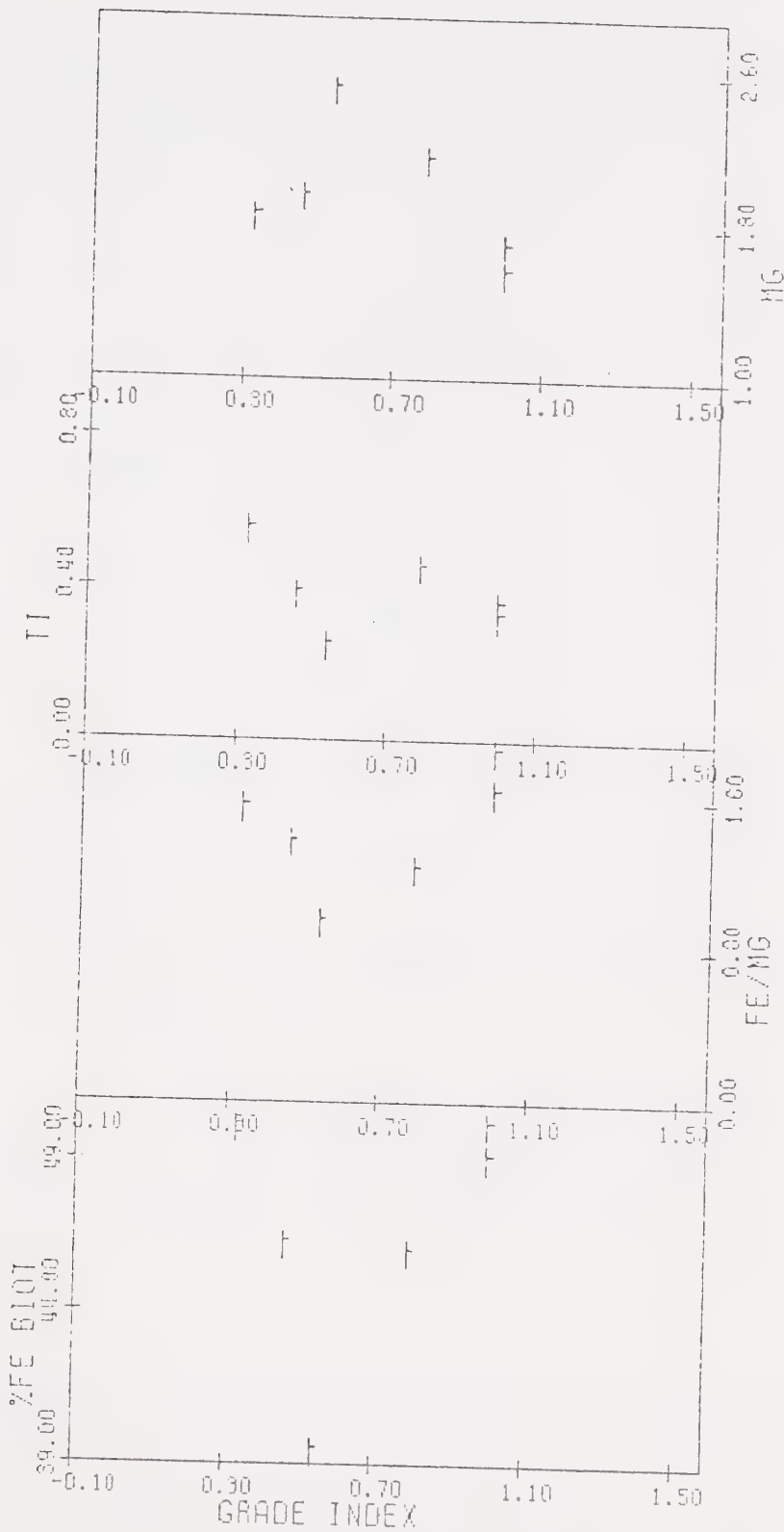


FIGURE 11b: Diagram illustrating the relationship of biotite composition (atomic proportions) to grade index for biotites from the almandine-cordierite-K-feldspar zone adjacent to garnet.

There are fewer data for biotite adjacent to garnet, but the available data suggest that the above changes in Mg and Fe/Mg are more intense.

Cordierite

Table 11 presents 13 analyses of cordierite from the cordierite-almandine-K-feldspar zone. The cordierites analysed are homogeneous within single grains and are of nearly constant composition in single thin section. Cordierite is associated with biotite, the feldspars, quartz, and sillimanite and has not been observed in direct contact with garnet.

Influence of Metamorphic Grade. Cordierite shows a systematic variation in composition with increasing metamorphic grade. The observed trends are:

1. An increase in Mg with increasing metamorphic grade.
2. A decrease in Fe and the Fe/Mg ratio.

There is no systematic change in Mn or the Si/Al^{IV} ratio, although these components do vary.
(Fig. 12)

Garnet

Table 12 presents 18 analyses of garnet from the cordierite-almandine-K-feldspar zone. Garnet is variable in composition across the zone, but no systematic chemical changes related to metamorphic grade have been observed. All are greater than 70% almandine, from core

TABLE 11: Microprobe analyses (weight %) and structural formulae (based on 18 oxygen ions) of CORDIERITE from the Cordierite - Garnet zone

Sample Number	73402	73153	73162	73185N	73155N	73202	73195
Grade Index	2.02	1.00	0.92	0.66	0.53	0.46	0.41
SiO ₂	47.19	48.43	48.31	48.80	48.87	48.37	48.51
Al ₂ O ₃	32.51	32.64	32.57	32.78	32.80	32.69	32.94
FeO*	10.27	10.90	11.00	9.50	10.08	8.68	9.11
MgO	6.29	6.06	5.73	7.12	6.70	7.50	7.64
MnO	0.19	0.52	0.97	0.13	0.21	0.28	0.11
K ₂ O	-----	-----	-----	0.10	-----	0.06	-----
Total	96.45	98.55	98.53	98.43	98.66	97.58	98.31
Si	5.031	5.032	5.032	5.044	5.046	5.025	5.006
Al ^{IV}	0.969	0.968	0.968	0.956	0.954	0.975	0.994
Al ^{VI}	3.054	3.030	3.030	3.040	3.028	3.028	3.016
Fe	0.902	0.947	0.958	0.821	0.870	0.754	0.787
Mg	0.984	0.939	0.889	1.081	1.031	1.161	1.176
Mn	0.017	0.046	0.086	0.120	0.018	0.025	0.009
K	-----	-----	-----	0.013	-----	0.006	-----
Σ Y-site	4.958	4.962	4.963	4.967	4.957	4.974	4.983
Fe/Mg	0.92	1.01	1.08	0.76	0.84	0.65	0.67
mole % Fe Cordierite	48	50	52	43	46	39	40

*total Fe as FeO

N = garnet absent from total assemblage

TABLE 11 (Continued)

Sample Number	73221	73226N	73227N	73229N	73171	73255N
Grade Index	0.32	0.31	0.29	0.27	0.17	0.05
SiO ₂	48.66	49.26	48.22	48.82	49.67	48.80
Al ₂ O ₃	32.95	33.66	32.82	33.25	32.80	33.10
FeO*	9.62	7.23	9.84	7.93	7.44	8.99
MgO	7.36	8.83	6.80	7.99	8.78	7.47
MnO	-----	0.10	0.27	0.21	0.18	0.24
K ₂ O	0.06	0.14	0.06	0.08	-----	0.06
Total	98.65	99.22	98.01	98.28	98.87	98.66
Si	5.014	4.998	5.014	5.016	5.059	5.019
Al ^{IV}	0.986	1.002	0.986	0.984	0.941	0.981
Al ^{VI}	3.016	3.023	3.037	3.042	2.999	3.032
Fe	0.829	0.613	0.856	0.681	0.634	0.774
Mg	1.131	1.335	1.054	1.223	1.333	1.145
Mn	-----	0.008	0.024	0.019	0.016	0.021
K	0.008	0.018	0.008	0.011	-----	0.008
Σ Y-site	4.984	4.997	4.979	4.976	4.982	4.980
Fe/Mg	0.73	0.46	0.81	0.56	0.48	0.68
mole % Fe Cordierite	42	31	45	36	32	40

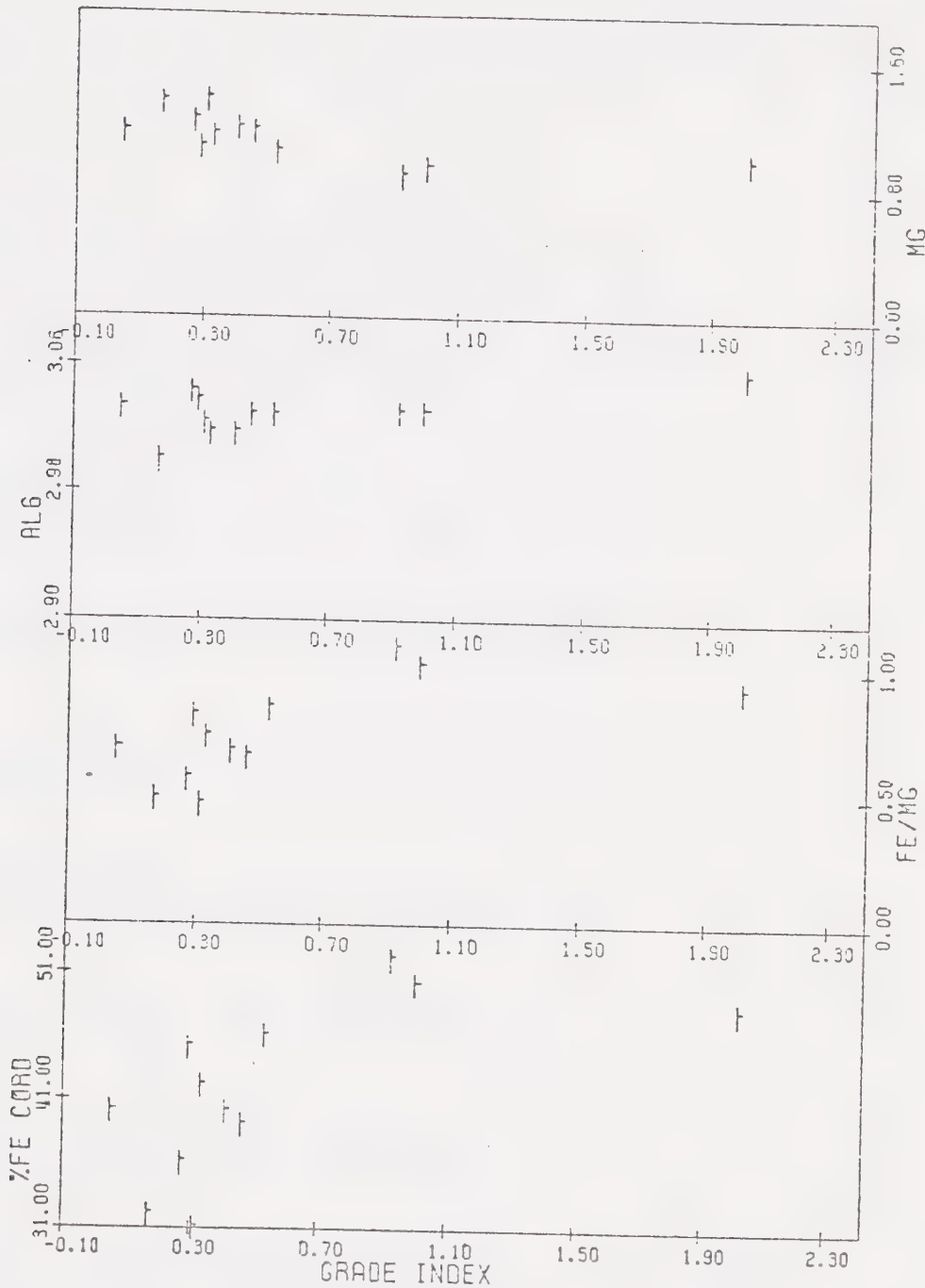


FIGURE 12: Diagram showing the relationship between cordierite composition (atomic proportions) and grade index for cordierites from the almandine-cordierite-K-feldspar zone.

TABLE 12: Microprobe analyses (weight %) and structural formulae (based on 24 oxygen ions) of GARNET from the Cordierite - Garnet zone

Sample Number	73280	73402	73366C	73366R	7345	73153C	73153R	73416C	73416R
Grade Index	2.51	2.02	1.64	1.64	1.0	1.0	1.0	0.98	0.98
SiO ₂	38.35	36.19	37.75	37.48	37.39	36.97	36.84	37.79	37.53
Al ₂ O ₃	20.94	20.62	21.24	21.24	20.57	21.01	20.72	21.29	21.14
Cr ₂ O ₃	0.06	-----	-----	-----	-----	0.05	0.06	0.11	0.09
FeO*	35.12	36.50	35.98	35.56	34.28	34.15	34.05	35.37	36.28
MgO	2.66	1.96	3.23	2.74	1.95	1.53	1.01	3.47	2.52
MnO	3.61	1.96	2.00	2.04	5.14	5.99	6.93	1.28	1.51
CaO	1.10	1.00	1.27	1.34	1.01	0.63	0.58	2.02	2.12
Total	101.94	98.23	101.47	100.20	100.34	100.33	100.19	101.33	101.19
Si	6.077	5.990	5.993	5.984	6.056	6.005	6.020	5.993	5.998
AlIV	-----	0.010	0.007	0.016	-----	-----	-----	0.007	0.002
AlVI	3.910	4.012	3.968	3.980	3.926	4.022	3.990	3.972	3.979
Cr	0.007	-----	-----	-----	-----	0.006	0.008	0.013	0.012
Fe	4.667	5.051	4.778	4.881	4.643	4.639	4.653	4.691	4.849
Mg	0.668	0.484	0.764	0.651	0.471	0.370	0.245	0.821	0.600
Mn	0.448	0.276	0.270	0.277	0.710	0.829	0.964	0.173	0.205
Ca	0.187	0.177	0.215	0.230	0.175	0.110	0.101	0.342	0.362
Σ X-site	5.970	5.988	6.068	6.049	5.999	5.948	5.963	6.027	6.016
Fe/Mg mole %	6.99	10.44	6.25	7.50	9.86	12.54	18.99	5.71	8.08
Alm	78.2	84.4	79.3	80.8	77.4	78.0	78.0	77.8	80.6
mole %	11.2	8.1	12.7	10.8	7.9	6.2	4.1	13.6	10.0
Py									
mole %	7.5	4.6	4.5	4.6	11.8	13.9	16.2	2.9	3.4
Sp									
mole %	3.1	2.9	3.5	3.8	2.9	1.9	1.7	5.7	6.0
Gr + An									

*total Fe as FeO
 C = garnet core
 R = garnet rim

TABLE 12 (continued)

Sample Number	73451C	73451R	73157C	73157R	73202C	73202R	73221C	73221R	73171
Grade Index	0.79	0.79	0.54	0.54	0.462	0.462	0.325	0.325	0.167
SiO ₂	36.84	37.13	37.94	37.62	37.26	37.12	37.82	37.44	38.38
Al ₂ O ₃	21.05	21.04	21.00	21.18	20.88	20.99	21.50	21.34	21.16
Cr ₂ O ₃	0.06	0.06	0.06	0.06	0.06	0.11	0.11	0.11	0.11
FeO*	33.39	33.53	32.37	33.31	33.05	32.62	36.67	37.06	34.38
MgO	3.31	2.83	3.26	2.69	3.15	3.18	3.70	3.10	3.18
MnO	2.41	3.15	4.91	5.03	3.52	3.47	0.59	0.62	3.33
CaO	1.71	1.67	1.15	1.02	0.95	1.03	1.15	1.34	1.05
Total	98.77	99.41	100.69	100.85	98.81	98.57	101.43	100.90	101.48
Si	5.986	6.010	6.050	6.023	6.051	6.035	5.988	5.983	6.075
Al _{IV}	0.014	-----	-----	-----	-----	-----	0.012	0.017	-----
Al _{VI}	4.017	4.015	3.947	3.996	3.996	4.022	4.001	4.002	3.947
Cr	0.008	0.007	0.008	0.008	0.008	0.015	0.015	0.015	-----
Fe	4.536	4.539	4.317	4.459	4.488	4.435	4.856	4.953	4.552
Mg	0.802	0.683	0.775	0.641	0.763	0.770	0.873	0.737	0.751
Mn	0.333	0.434	0.667	0.686	0.488	0.488	0.080	0.085	0.448
Ca	0.298	0.290	0.196	0.174	0.166	0.188	0.195	0.229	0.178
$\Sigma X\text{-site}$	5.969	5.946	5.955	5.960	5.905	5.854	6.004	6.004	5.929
Fe/Mg mole	5.66	6.65	5.57	6.96	5.88	5.76	5.56	6.72	6.06
mole	8	76.0	76.3	72.5	74.8	76.0	75.5	80.9	76.8
Alm	mole	8	13.4	11.5	13.0	10.8	12.9	13.1	14.5
Py	mole	8	5.6	7.3	11.2	11.5	8.3	8.2	1.3
Sp	mole	8	5.0	4.9	3.3	2.9	2.8	3.2	3.8
Gr + An									3.0

to rim, but the pyrope, spessartine, and grossular molecules vary from sample to sample. This suggests that the initial chemical environment in which the garnet formed was the major control on its composition. Nearly all of the garnets examined are zoned, with the pyrope component greater in the core and decreasing toward the rim, coupled with a sympathetic increase in almandine and spessartine away from the core. The garnet rim composition is in part controlled by the phases with which it is in contact. Thus biotite had caused a depletion of the pyrope molecule while plagioclase had caused the grossular molecule to decrease as calcium was incorporated into the plagioclase. The garnet rim composition is further altered by late stage resorption of garnet to produce biotite and plagioclase (Fig. 13, Plate II).

CONTROLS OF CORDIERITE - ALMANDINE - K-FELDSPAR ZONE MINERAL CHEMISTRY

Well defined trends in the Fe/Mg ratios of co-existing cordierite and biotite indicate that the compositions of these two phases were controlled by more than just energetic factors.

Metamorphic Grade

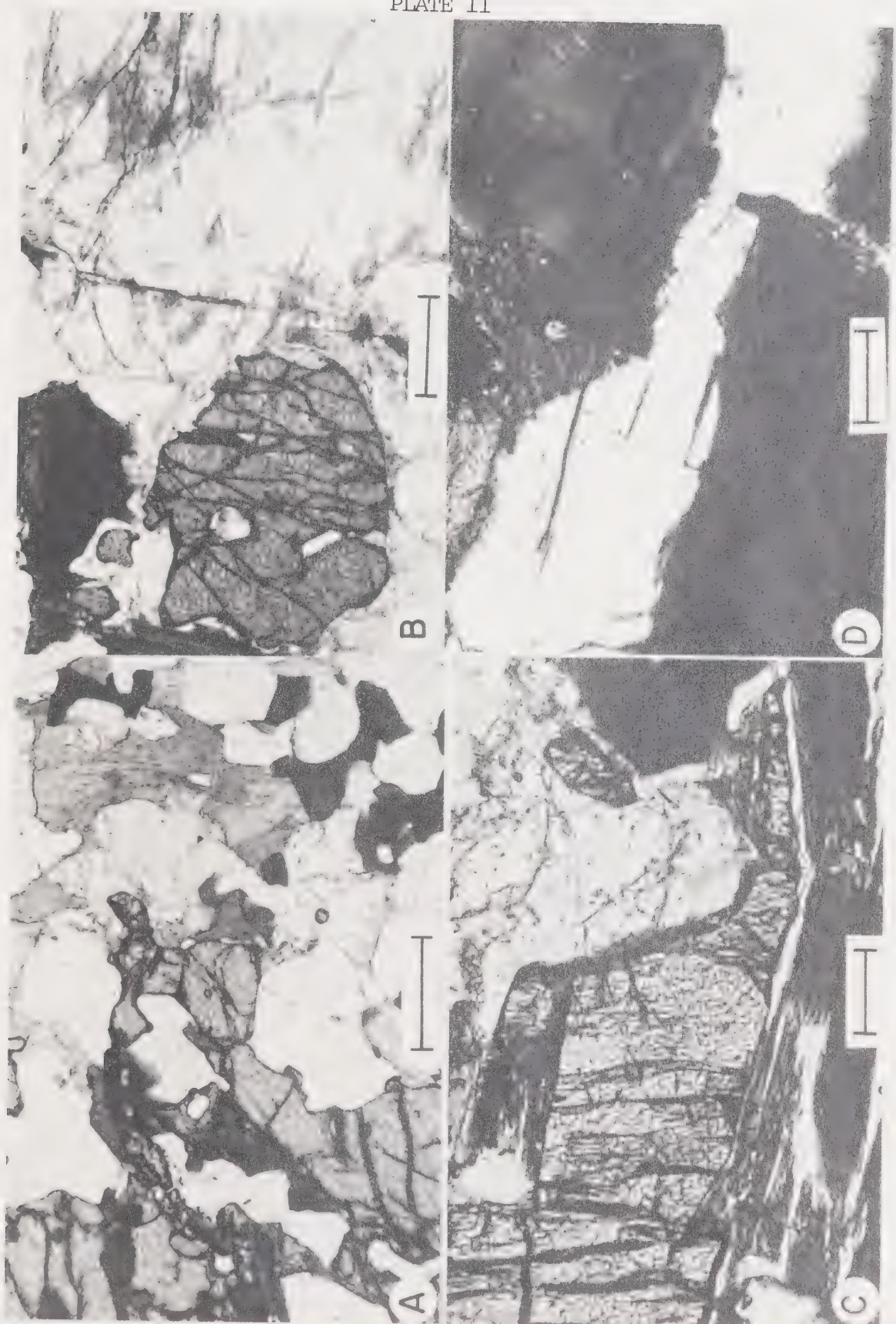
The role of metamorphic grade in determining the mineral compositions in the cordierite-almandine-K-feldspar zone is complex. Garnet is present across the

PLATE II

Features of the almandine-cordierite-K-feldspar zone.

- A. Sample 73483. Garnet-high relief, biotite - dark gray, quartz-clear, K-feldspar - light gray, cloudy and cordierite - clear - rimmed by pinnite. Plane polarised light. Scale bar = 250 microns.
- B. Sample 73496. Garnet-high relief, biotite - dark gray, K-feldspar - cloudy, quartz-white. Plane polarised light. Scale bar = 250 microns.
- C. Sample 73252. Garnet-high relief, biotite - dark gray to black, quartz clear, cordierite cloudy and light gray. A grain of K-feldspar is shown in the upper right hand corner. Plane polarised light. Scale bar = 100 microns.
- D. Sample 73483. Garnet black, cordierite - light gray and cloudy, quartz-white, K-feldspar dark gray (upper right hand corner) and biotite-speckled. Crossed nicols. Scale bar = 50 microns.

PLATE II



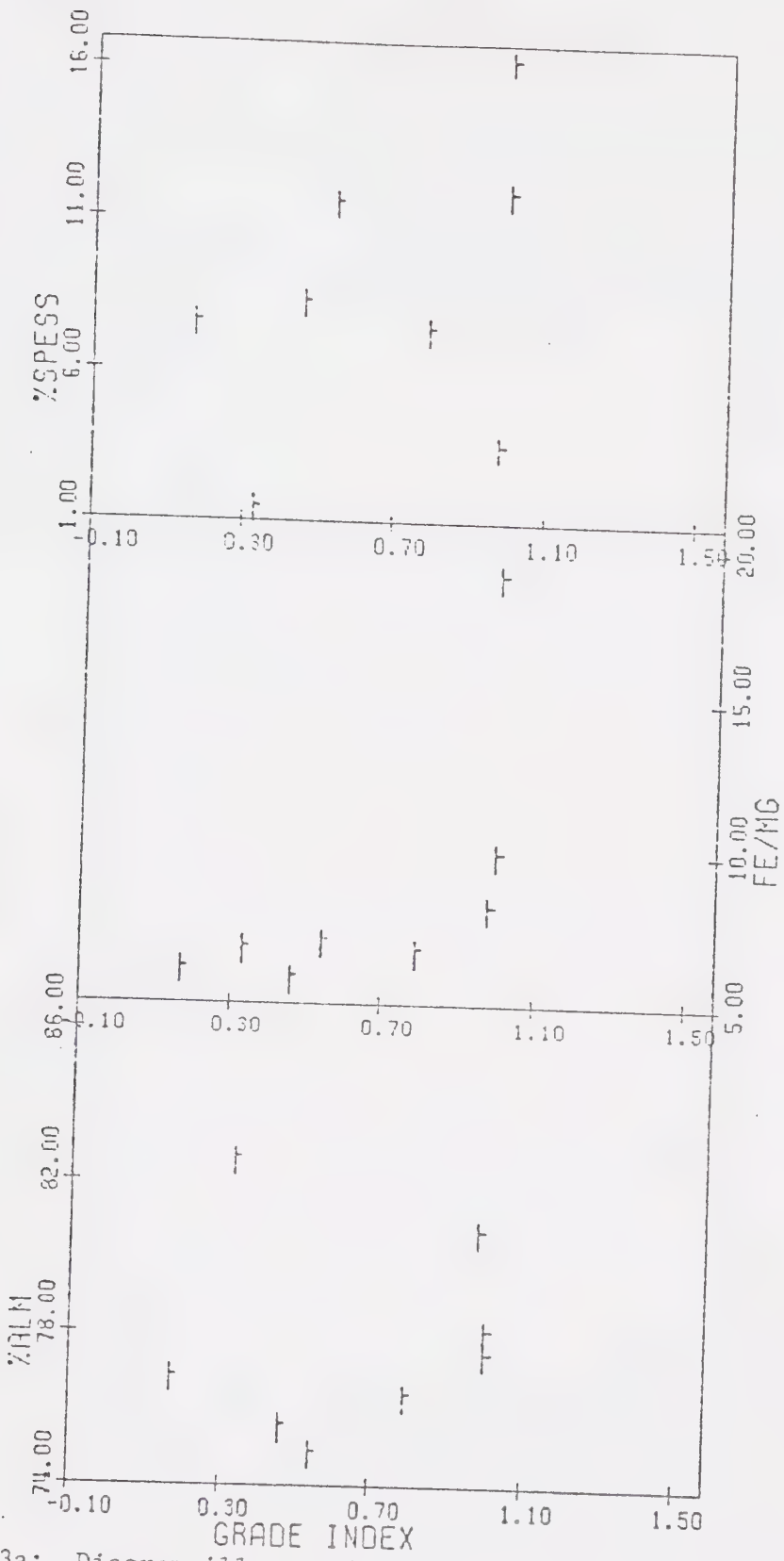


FIGURE 13a: Diagram illustrating the relationship of garnet composition (atomic proportions) to grade index for garnets from the almandine-cordierite-K-feldspar zone.

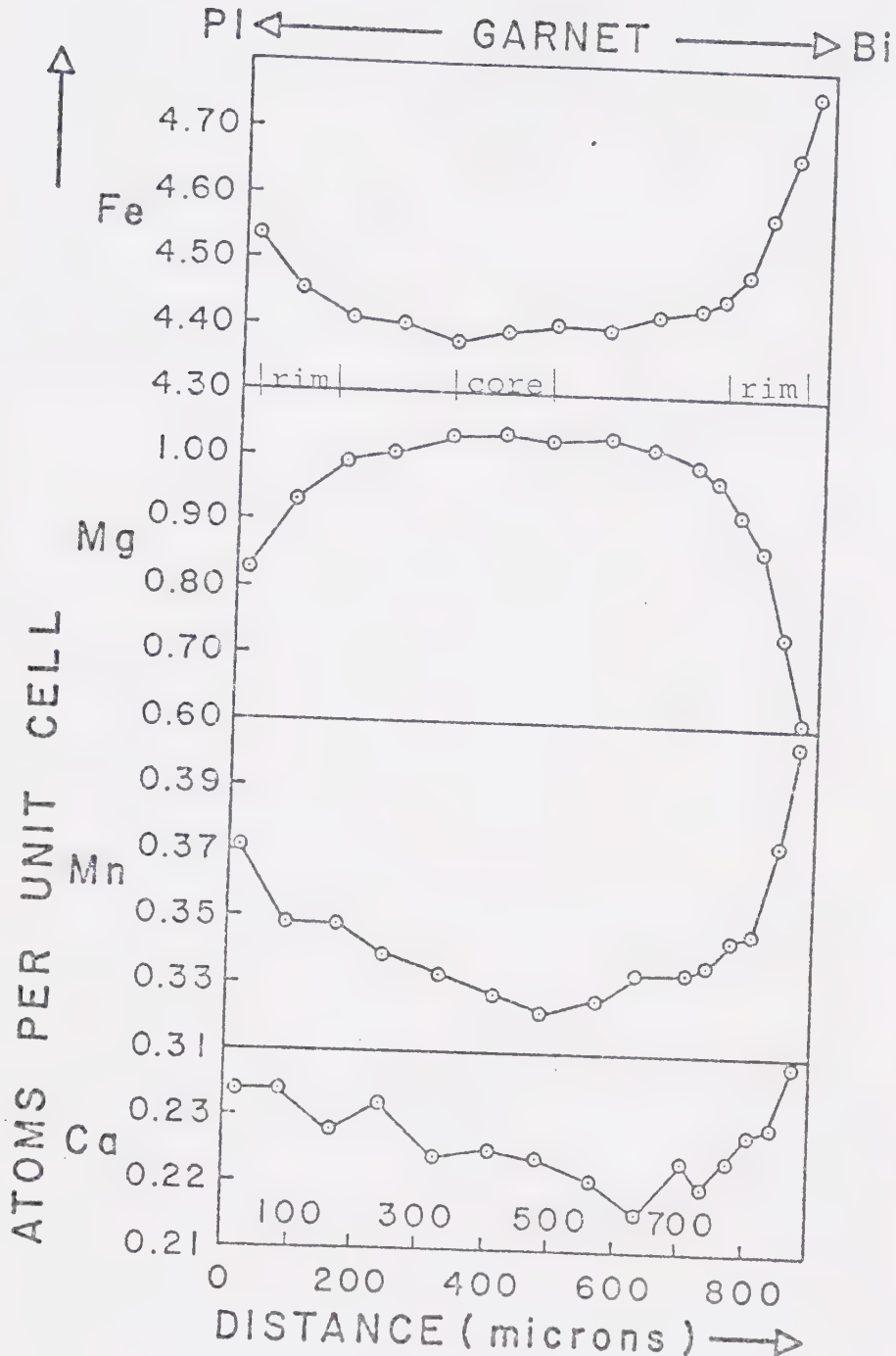


FIGURE 13b: Diagram showing the reverse zoning profile shown by garnets from the almandine-cordierite-K-feldspar zone.

entire zone, but is always present in smaller amounts than biotite + cordierite. As discussed above, the non-systematic variation of garnet composition suggests that for garnet, other controls were of greater importance. Biotite and cordierite display good grade dependent trends, and metamorphic grade was an important control in determining their compositions.

Bulk Rock Composition

The non-systematic variation of the $\text{Si}/\text{Al}^{\text{IV}}$ ratio in biotite and cordierite, as well as the components Mn and Na, suggest that minor variation in bulk rock composition controlled these aspects of mineral chemistry. Also, the presence or absence of garnet is apparently controlled by the relative amounts of iron plus magnesium to aluminum.

Mineral Assemblage Present

The most important control of cordierite-almandine-K-feldspar zone mineral chemistry appears to have been the mineral assemblage present. This is especially well shown by the biotite and orthopyroxene compositions obtained from sample 73252 (Table 13), where the analysed minerals vary in composition as a function of the other ferro-magnesian silicates with which they are in local equilibrium. All of the samples, where more than two analyses of a mineral are available, display this effect.

TABLE 13: Variation in mineral composition in Sample 73252

	Biotite with Ortho- pyroxene	Biotite with Garnet	Biotite with Cordi- erite	Ortho- pyroxene with Biotite	Ortho- pyroxene with Cordierite
SiO ₂	36.51	35.73	36.04	50.23	49.83
TiO ₂	2.46	4.37	3.22	-----	-----
Al ₂ O ₃	17.05	16.48	16.73	2.01	2.59
V ₂ O ₃	0.10	0.13	0.10	-----	-----
FeO*	18.91	19.21	19.43	32.13	32.69
MgO	11.53	10.77	10.48	15.35	14.42
MnO	-----	-----	0.06	0.64	0.74
CaO	-----	0.05	-----	0.07	0.07
K ₂ O	9.44	8.71	9.13	-----	-----
Total	96.00	95.54	95.19	100.43	100.34
<u>Structural Formulae</u>					
Si ⁺⁴	5.500	5.415	5.492	1.952	1.944
Al ^{IV}	2.500	2.585	2.508	0.048	0.056
Al ^{VI}	0.528	0.359	0.497	0.044	0.063
V ⁺³	0.012	0.015	0.012	-----	-----
Ti ⁺⁴	0.279	0.498	0.369	-----	-----
Fe ⁺²	2.383	2.434	2.476	1.044	1.067
Mg ⁺²	2.588	2.437	2.381	0.889	0.838
Mn ⁺²	-----	-----	0.007	0.021	0.025
Ca ⁺²	-----	0.007	-----	0.003	0.003
K	1.815	1.685	1.774	-----	-----
Number of Anions	22	22	22	6	6
Σ Y-site	5.890	5.743	5.737		
Σ X-site	1.815	1.692	1.774		
Σ Al	3.028	2.944	3.005		
Fe/Mg mole %	0.92	0.99	1.039	1.174	1.273
anaite	40	42	43		

*total Fe as FeO

----- = not detected

At this point, it should be stressed that with the exception of garnet, all of the ferro-magnesian silicates are homogeneous within single grains.

Conclusions

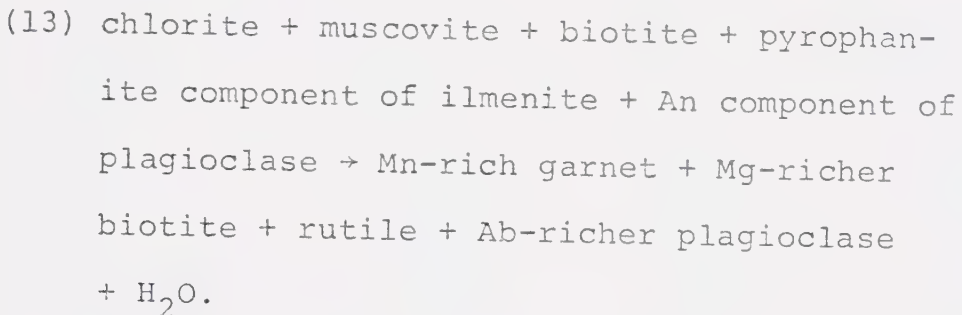
From the data available for the cordierite-almandine-K-feldspar zone, the modifying controls appear to have been most important in determining mineral composition. The most important internal control appears to have been the equilibrium partitioning of iron and magnesium between biotite and cordierite and biotite and garnet. The external control of diffusion also played an important role. This is shown by the small scale system within which equilibrium was attained. If components had not been effectively isolated by slow intergranular diffusion, garnet would have been a more abundant phase and the iron-magnesium ratios of the various ferro-magnesian silicates would have been different.

THE GARNET FORMING REACTIONS

In this section, two separate garnet forming reactions are discussed, corresponding to the two different environments in which garnet has been observed. The first reaction refers to the rather sporadic occurrences of garnet below the andalusite isograd. The second reaction is the one which formed garnet in the cordierite-almandine-K-feldspar zone.

Reaction at Low Grade

The garnets below the andalusite isograd are very rich in the spessartine molecule (> 25 mole per cent) and show prograde zonation, with Mg enrichment in the rim and a strong decrease in Mn from core to rim (Fig. 14). The presence of garnet at this grade of metamorphism is most probably a function of the bulk rock MnO content, thus only local horizons contain garnet (Plate I). This garnet most probably arose from the reaction:



The garnets are formed in the biotite zone, below the andalusite isograd, and are stable because of their high Mn content. The garnet most probably was able to nucleate because the ilmenite, which was a reactant in the biotite forming reaction, also released Mn to the fluid phase. Table 14 presents analyses for garnets from two biotite zone samples. Another feature to note in these garnets is their relatively high Ca content. The calcium in these garnets was probably made available through breakdown of clastic plagioclase.

TABLE 14 : Microprobe analyses (weight %) and structural formulae (based on 24 oxygens) of GARNETS from the biotite zone

Sample Number	7248C	7248R	7255R
Grade Index	2.39	2.39	1.99
SiO ₂	37.15	36.69	36.61
Al ₂ O ₃	20.55	20.48	20.57
FeO*	20.44	28.19	37.22
MgO	.35	1.12	2.50
MnO	16.53	11.31	.61
CaO	4.87	1.53	1.46
Total	99.89	99.32	98.97
Si	6.044	6.027	5.998
Al ^{IV}	-----	-----	.002
Al ^{VI}	3.941	3.966	3.968
Fe	2.781	3.873	5.098
Mg	.084	.273	.610
Mn	2.291	1.583	.085
Ca	.816	.269	.256
Σ X-site	5.972	5.998	6.049
Fe/Mg	33.1	14.2	8.36
mole %			
Alm	46.5	64.6	84.3
mole %			
Py	1.4	4.6	10.11
mole %			
Sp	38.4	26.4	1.4
mole %			
Gr + An	13.7	4.4	4.21

* Total Fe as FeO

C garnet core

R garnet rim

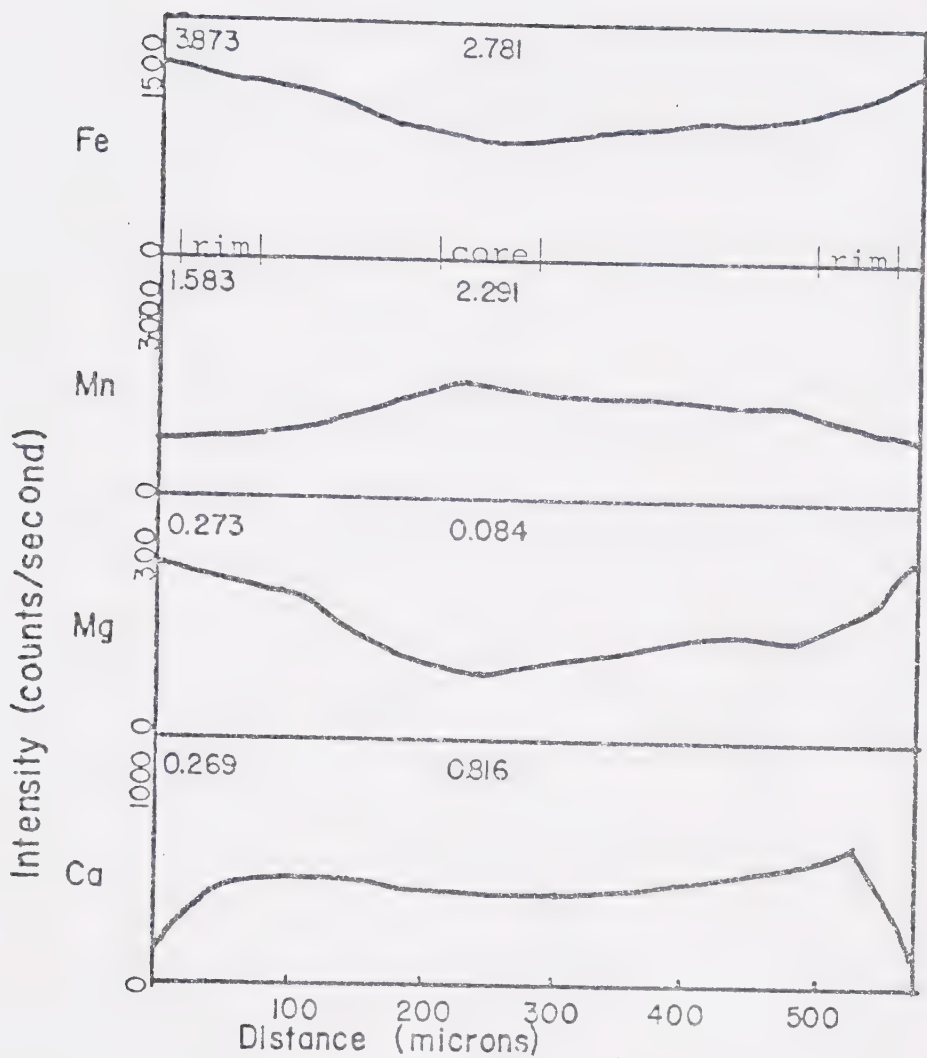
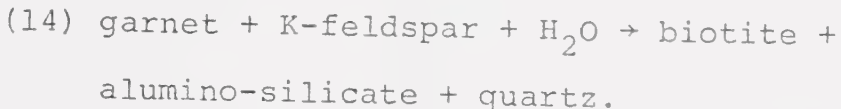


FIGURE 14: Diagram illustrating the 'prograde' zoning profile shown by garnets from the biotite zone.

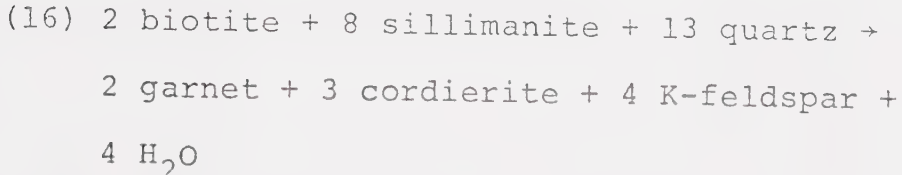
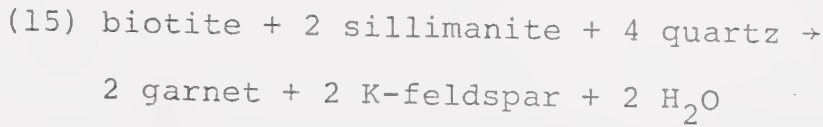
Reaction at Higher Grade

The major garnet forming reaction occurred above the second sillimanite isograd and defines the transition from the cordierite-sillimanite zone to the cordierite-almandine-K-feldspar zone. These garnets are characterised by a much lower Ca and Mn content than the biotite zone garnets.

The larger garnets are characterised by a large homogeneous core, approximately 500 - 700 μm in diameter, rimmed by a retrograde zone of 100 - 200 μm in width, which shows Mg depletion and Ca, Mn, and Fe enrichment. (Grant and Weiblen, 1971). This outer compositional zonation is thought to record retrograde iron-magnesium exchange with biotite, coupled with the reverse of the garnet forming reaction:



Two reactions producing garnet are given below. Reaction (15) consumes less Al_2SiO_5 than reaction (16).



The garnet producing reactions in the Arseno Lake area differ from the above reactions because:

1. Biotite is not totally consumed, but changes in composition (a continuous reaction).
2. Ilmenite is one of the reactants and rutile is one of the products.

The proposed garnet forming reactions in the cordierite-almandine-K-feldspar zone for the Arseno Lake area are:

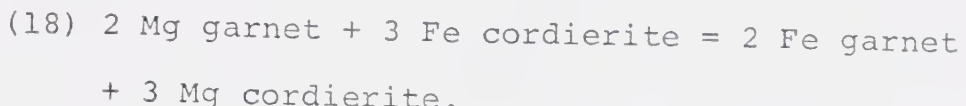
- (15a) biotite + sillimanite + quartz + ilmenite →
garnet + Mg,Ti-richer biotite + K-feldspar
+ rutile + H₂O
- (16a) biotite + sillimanite + quartz + ilmenite →
garnet + cordierite + Mg,Ti-richer biotite
+ K-feldspar + rutile + H₂O

Reaction (15a) apparently proceeded in rocks with a lower aluminum/iron + magnesium ratio and led to cordierite free assemblages. In rocks with a higher aluminum/iron + magnesium ratio, reaction (16a) would have occurred and produced the common assemblage with both cordierite and garnet present.

There is no evidence that the stability field of cordierite was exceeded. This is supported by the absence of coexisting garnet + sillimanite + quartz, which would have formed if the following reaction had proceeded:



Apparently, the only influence that cordierite had on garnet development was as a compositional modifier by the exchange reaction:



THE REMOBILISED ARCHEAN PARAGNEISS

The major rock type exposed in the remobilised Archean paragneiss is metapelite. Unlike the other mineral zones discussed, samples here are from more than one mineral zone, spanning the cordierite zone and the cordierite-almandine-K-feldspar zone in metamorphic grade. These samples are discussed separately because of their polymetamorphic history. When individual minerals are examined, certain aspects of their composition appear to have remained unchanged by the Hudsonian metamorphism. Three orthopyroxene and seventeen spinel bearing samples have been examined in detail. Individual samples contain from two to four ferro-magnesian silicates, along with quartz, plagioclase, microcline, perthite, ilmenite, and occasional rutile. Some of the cordierite knots have been retrograded and the products include diaspore. Spinel is always enclosed within cordierite and varies in abundance from sample to sample.

MINERAL CHEMISTRY OF THE REMOBILISED ARCHEAN PARAGNEISS

Biotite

Table 15 presents 22 analyses of biotite from the remobilised Archean paragneiss. There is a wide range in composition and only one trend has been defined.

Influence of Metamorphic Grade. Unlike the biotite discussed above, the biotites in the remobilised Archean paragneiss show a strong trend in the tetrahedral site. There is a decrease in Al^{IV} and an increase in the $\text{Si}/\text{Al}^{\text{IV}}$ ratio across the zone. No systematic changes are apparent in the Y-site components, as was characteristic of the metamorphosed Snare Group. It is therefore suggested that the trend in Al^{IV} observed is a relic from the original Archean metamorphism (Fig. 15).

Cordierite

Table 16 presents analyses of 24 cordierites from the remobilised Archean paragneiss. There is a wide variation in the composition of cordierite in equilibrium with spinel, but no systematic variation is seen. However, cordierite coexisting with biotite does exhibit trends.

Influence of Metamorphic Grade. The three trends noted in cordierite adjacent to biotite are:

1. An increase in Al^{IV} with increasing

TABLE 15: Microprobe analyses (weight %) and structural formulae (based on 22 oxygen ions) of BIOTITE from remobilised Archean paragneisses

Sample Number	73377C	73376C	73498C	7347C [#]	73416G	73478C	73453C	73501C
Grade Index	2.05	2.03	1.52	1.07	0.98	0.93	0.89	0.76
SiO ₂	35.19	35.57	35.12	35.24	34.74	33.00	35.62	34.91
TiO ₂	2.36	2.64	2.46	3.02	4.85	2.28	3.35	3.83
Al ₂ O ₃	19.80	18.95	19.10	19.05	15.43	20.74	19.18	18.07
Cr ₂ O ₃	0.20	0.10	0.05	0.07	0.10	-----	0.09	0.20
V ₂ O ₃	0.22	0.15	0.25	0.09	0.32	0.07	0.23	0.35
FeO*	18.42	19.82	20.82	19.81	22.53	21.63	18.08	18.98
MgO	8.78	8.89	7.59	8.25	8.35	7.43	7.93	8.09
MnO	-----	-----	-----	0.04	-----	-----	-----	-----
CaO	-----	-----	-----	-----	-----	-----	-----	-----
K ₂ O	8.43	9.01	9.15	9.35	8.82	9.53	9.00	9.03
Total	93.40	95.13	94.54	95.50	95.14	94.68	93.48	93.78
Si _{IV}	5.403	5.301	5.417	5.350	5.389	5.125	5.470	5.401
Al _{VI}	2.597	2.699	2.583	2.650	2.611	2.875	2.530	2.599
Al _{VII}	0.985	0.727	0.890	0.759	0.210	0.925	0.942	0.696
Cr	0.024	0.012	0.006	0.008	0.012	-----	0.011	0.024
V	0.028	0.018	0.031	0.011	0.040	0.010	0.029	0.044
Ti	0.272	0.305	0.285	0.346	0.568	0.271	0.387	0.445
Fe	2.365	2.542	2.685	2.515	2.924	2.811	2.322	2.456
Mg	2.010	2.033	1.745	1.866	1.932	1.721	1.814	1.865
Mn	-----	-----	-----	0.006	-----	-----	-----	-----
Ca	-----	-----	-----	-----	-----	-----	-----	0.052
K	1.651	1.763	1.800	1.814	1.747	1.891	1.764	1.782
Σ Y-site	5.684	5.637	5.642	5.511	5.686	5.738	5.505	5.530
Fe/Mg	1.18	1.25	1.54	1.35	1.51	1.63	1.28	1.32
mole % annite	42	45	48	46	51	49	46	44

*total Fe as FeO

----- = not detected

-contains 0.58% F, .015 F = 0

C = biotite adjacent to cordierite

G = biotite adjacent to garnet

TABLE 15 (Continued)

Sample Number	73239C	73238C	73208C	73205C	72351C	73433P	73211C
Grade Index	0.68	0.56	0.50	0.50	0.49	0.42	0.31
SiO ₂	33.88	34.35	35.02	35.46	35.50	35.00	35.83
TiO ₂	4.52	3.93	5.05	3.91	2.87	2.72	3.02
Al ₂ O ₃	17.22	18.34	18.25	18.26	18.74	17.95	17.74
Cr ₂ O ₃	0.07	0.18	0.07	-----	0.15	-----	0.07
V ₂ O ₃	0.20	0.20	0.10	0.15	0.20	0.09	0.12
FeO*	20.78	21.11	19.80	19.89	18.36	20.84	19.26
MgO	9.26	7.36	7.60	8.45	10.11	9.03	9.33
MnO	-----	-----	-----	-----	-----	0.17	0.05
CaO	-----	-----	-----	-----	-----	-----	-----
K ₂ O	9.56	9.23	9.01	9.04	8.75	9.30	9.15
Total	95.49	94.70	94.90	95.16	94.68	95.10	94.57
Si _{IV}	5.217	5.320	5.360	5.408	5.380	5.389	5.486
Al _{VI}	2.783	2.680	2.640	2.592	2.620	2.611	2.514
Al _{VII}	0.383	0.667	0.651	0.691	0.737	0.646	0.687
Cr	0.008	0.021	0.009	-----	0.018	-----	0.009
V	0.025	0.025	0.012	0.018	0.024	0.011	0.015
Ti	0.515	0.457	0.582	0.456	0.329	0.315	0.348
Fe	2.673	2.734	2.534	2.536	2.329	2.683	2.467
Mg	2.125	1.698	1.735	1.922	2.286	2.072	2.130
Mn	-----	-----	-----	-----	-----	-----	0.006
Ca	-----	-----	-----	-----	-----	-----	-----
K	1.882	1.823	1.759	1.758	1.695	1.826	1.786
Σ Y-site	5.729	5.602	5.523	5.623	5.723	5.727	5.662
Fe/Mg mole %	1.26	1.61	1.46	1.32	1.02	1.29	1.16
annite	47	49	46	45	41	47	44

P = biotite adjacent to orthopyroxene

TABLE 15 (Continued)

Sample Number	73212C	73252C ^a	72344G	72344C	72356C	73178C ^{\$}	72345C
Grade Index	0.31	0.21	0.04	0.04	0	0	0
SiO ₂	37.15	36.51	35.61	35.20	34.12	35.26	34.13
TiO ₂	1.92	2.46	3.87	3.98	3.98	4.02	3.80
Al ₂ O ₃	19.28	17.05	18.73	19.38	18.22	17.58	18.62
Cr ₂ O ₃	-----	-----	-----	-----	0.07	0.24	0.13
V ₂ O ₃	0.05	0.10	0.08	0.06	0.13	0.24	0.23
FeO*	18.84	18.91	20.91	20.76	20.75	19.93	20.47
MgO	9.77	11.53	7.72	7.25	9.13	8.79	8.21
MnO	-----	-----	0.06	0.10	-----	0.05	0.08
CaO	-----	-----	-----	-----	-----	-----	-----
K ₂ O	8.91	9.44	9.50	9.37	9.15	8.74	8.62
Total	95.92	96.00	96.56	96.10	95.55	94.85	94.29
Si	5.552	5.500	5.390	5.343	5.224	5.400	5.269
Al ^{IV}	2.448	2.500	2.610	2.657	2.776	2.600	2.731
Al ^{VI}	0.949	0.528	0.730	0.810	0.593	0.574	0.659
Cr	-----	-----	-----	-----	0.008	0.030	0.015
V	0.006	0.012	0.009	0.007	0.016	0.030	0.028
Ti	0.216	0.279	0.441	0.455	0.465	0.463	0.444
Fe	2.355	2.383	2.647	2.636	2.656	2.552	2.645
Mg	2.155	2.588	1.742	1.639	2.083	2.007	1.888
Mn	-----	-----	0.008	0.013	-----	0.007	0.011
Ca	-----	-----	-----	-----	-----	-----	-----
K	1.700	1.815	1.834	1.815	1.790	1.708	1.706
Σ Y-site	5.681	5.790	5.577	5.560	5.821	5.663	5.690
Fe/Mg mole %	1.09	0.92	1.52	1.61	1.27	1.27	1.40
annite	4]	4]	47	47	46	45	46

^{\$} contains 0.04% Cl, .001 Cl = 0^a see Table 13 for additional analyses

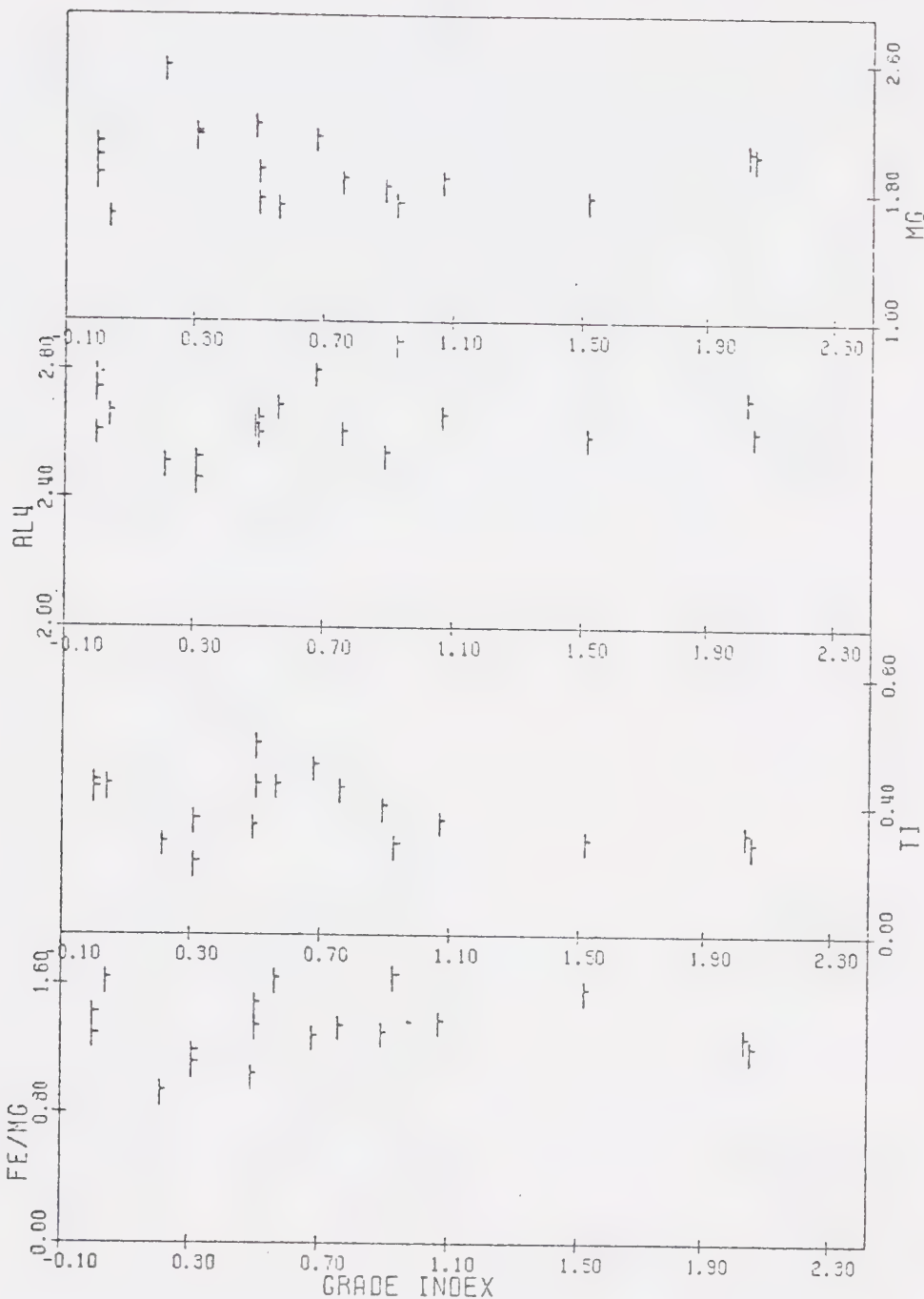


FIGURE 15: Diagram illustrating the relationship between biotite composition (atomic proportions) and grade index for biotites from the remobilised Archean paragneiss.

metamorphic grade.

2. An increase in Mn.
3. A decrease in Mg and a corresponding increase in the Fe/Mg ratio.

These data are shown in Figure 16, along with similar data for cordierite coexisting with spinel.

The high value of the correlation coefficient for Al^{IV} increase with increasing metamorphic grade, coupled with the decrease in Mg suggests that:

1. Cordierite and biotite exchanged iron and magnesium during the Hudsonian metamorphism.
2. The trend in Al^{IV} may be a relic of the Archean metamorphism.

The evidence for (1) above is that with the exception of the remobilised Archean paragneiss samples, biotite and cordierite show the same trends for Mg and the Fe/Mg ratio. The evidence for (2) is that this is the only suite of cordierites to show any trend in Al^{IV}.

Spinel

Table 17 presents 19 spinel analyses from the remobilised Archean paragneiss. These spinels are dominantly hercynite, with spinel, gahnite, and locally chromite as additional components in the solid solution series. Magnetite solid solution is less than 5% and, with the exception of two localities, chromite is

TABLE 16: Microprobe analyses (weight %) and structural formulae
 (based on 18 oxygen ions) of CORDIERITE from remobilised
Archean paragneiss

Sample Number	73377S	73377B	73376S	7347S	73478S	73453S	73453B	73501S
Grade Index	2.05	2.05	2.03	1.07	0.93	0.89	0.89	0.76
SiO ₂	47.42	48.44	49.46	49.37	46.73	48.84	48.85	48.34
Al ₂ O ₃	32.64	32.99	32.57	32.47	32.55	33.13	32.80	32.59
FeO*	9.49	9.21	9.55	10.57	11.18	8.90	9.07	9.17
MgO	6.62	7.17	7.44	7.00	6.89	7.69	7.52	7.22
MnO	0.11	0.13	0.13	0.16	0.26	0.12	0.13	0.32
K ₂ O	0.07	0.05	-----	-----	-----	-----	0.10	-----
Na ₂ O	-----	0.18	-----	-----	-----	-----	-----	-----
Total	96.55	98.17	99.15	99.57	97.61	98.68	98.47	97.64
Si	5.007	5.014	5.069	5.063	4.920	5.016	5.034	5.034
Al ^{IV}	0.993	0.986	0.931	0.937	1.080	0.984	0.966	0.966
Al ^{VI}	3.069	3.038	3.004	2.988	2.963	3.026	3.018	3.034
Fe	0.837	0.798	0.819	0.908	0.985	0.765	0.782	0.798
Mg	1.042	1.106	1.137	1.071	1.083	1.177	1.156	1.121
Mn	0.010	0.012	0.013	0.015	0.024	0.010	0.011	0.012
K	0.009	0.007	-----	-----	-----	-----	0.013	-----
Na	-----	0.036	-----	-----	-----	-----	-----	-----
Σ Y-site	4.967	4.897	4.973	4.972	5.055	4.978	4.980	4.965
Fe/Mg	0.80	0.72	0.72	0.85	0.91	0.65	0.68	0.71
mole % Fe Cordierite	45	42	42	46	48	39	40	42

*total Fe as FeO

S = cordierite adjacent to spinel

B = cordierite adjacent to biotite

TABLE 16 (Continued)

Sample Number	73239S	73238S	73238B	73208S	73208B	73205S	73205B	72351S
Grade Index	0.68	0.56	0.56	0.50	0.50	0.50	0.50	0.50
SiO ₂	47.36	48.49	48.45	48.72	48.76	49.02	49.10	47.07
Al ₂ O ₃	33.13	32.91	32.63	33.15	32.89	33.37	32.92	32.82
FeO*	8.88	9.08	9.22	9.62	9.35	9.86	9.62	10.07
MgO	8.75	7.45	7.30	7.18	7.31	7.66	7.60	7.78
MnO	0.19	0.16	0.19	0.08	0.08	0.07	0.10	0.11
K ₂ O	-----	0.04	0.11	0.09	0.13	0.05	0.09	-----
Na ₂ O	-----	-----	-----	-----	-----	-----	-----	-----
Total	98.31	98.13	97.90	98.84	98.52	100.03	99.43	97.85
Si	4.902	5.015	5.029	5.013	5.025	4.991	5.024	4.915
Al ^{IV}	1.098	0.985	0.971	0.987	0.975	1.009	0.976	1.085
Al ^{VI}	2.945	3.027	3.021	3.034	3.019	2.995	2.994	2.954
Fe	0.763	0.786	0.800	0.828	0.866	0.840	0.813	0.880
Mg	1.352	1.149	1.130	1.101	1.123	1.162	1.159	1.211
Mn	0.016	0.014	0.016	0.007	0.007	0.006	0.008	0.010
K	-----	0.005	0.014	0.012	0.017	0.007	0.012	-----
Na	-----	-----	-----	-----	-----	-----	-----	-----
Σ Y-site	5.076	4.981	4.981	4.982	5.032	5.010	4.986	5.055
Fe/Mg	0.56	0.68	0.71	0.75	0.77	0.72	0.70	0.73
mole % Fe Cordierite	36	41	41	43	44	42	41	42

TABLE 16 (Continued)

Sample Number	73211S	73212S	73212B	73252B	72344S	72344B	72356S	72345S
Grade Index	0.31	0.31	0.31	0.21	0.04	0.04	0	0
SiO ₂	48.33	49.18	48.88	49.23	48.10	48.37	47.19	47.36
Al ₂ O ₃	32.55	33.22	33.29	33.08	33.08	32.84	33.21	32.95
FeO*	11.83	11.20	11.26	8.41	10.66	10.24	9.73	9.24
MgO	6.27	6.44	6.38	8.41	6.91	6.95	8.06	8.18
MnO	0.11	0.11	0.09	0.21	0.29	0.35	0.17	0.26
K ₂ O	0.07	0.09	0.05	0.04	0.07	0.07	-----	-----
Na ₂ O	-----	-----	-----	-----	-----	-----	-----	-----
Total	99.16	100.24	99.95	99.38	99.11	98.82	98.36	97.99
Si	5.012	5.024	5.009	5.014	4.970	5.002	4.898	4.923
Al ^{IV}	0.988	0.976	0.991	0.986	1.030	0.998	1.102	1.077
Al ^{VI}	2.990	3.023	3.030	2.985	2.999	3.004	2.963	2.962
Fe	1.026	0.957	0.965	0.726	0.921	0.885	0.845	0.803
Mg	0.969	0.981	0.975	1.277	1.065	1.072	1.248	1.268
Mn	0.009	0.009	0.008	0.018	0.026	0.031	0.016	0.023
K	0.009	0.012	0.006	-----	0.009	0.009	-----	-----
Na	-----	-----	-----	0.055	-----	-----	-----	-----
Σ Y-site	5.003	4.982	4.984	5.061	5.020	5.001	5.072	5.056
Fe/Mg	1.06	0.98	0.99	0.57	0.86	0.83	0.68	0.63
mole % Fe Cordierite	51	49	50	36	46	45	40	39

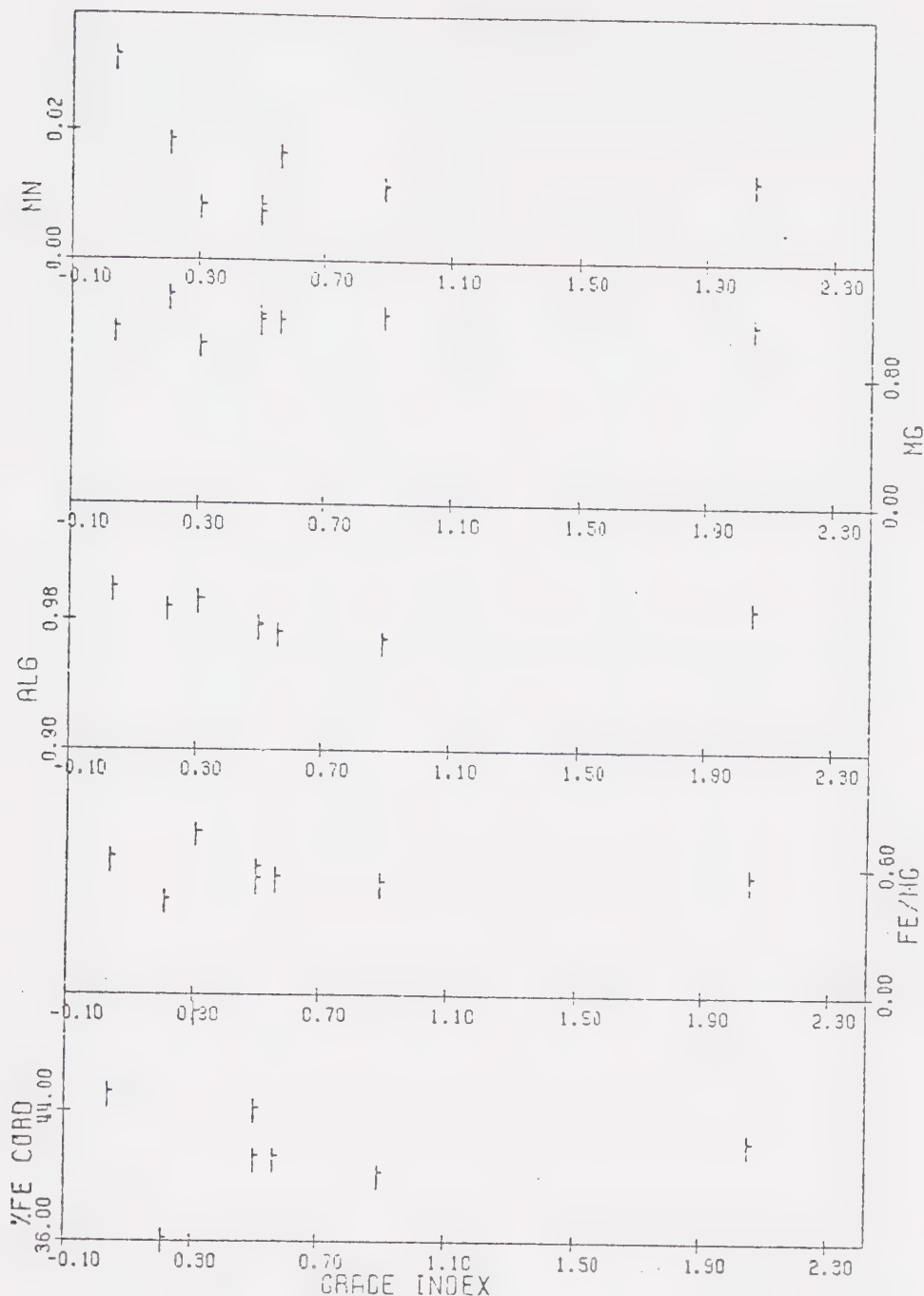


FIGURE 16a: Diagram illustrating the relationship between cordierite composition (atomic proportions) and grade index for cordierite adjacent to biotite from the remobilised Archean paragneiss.

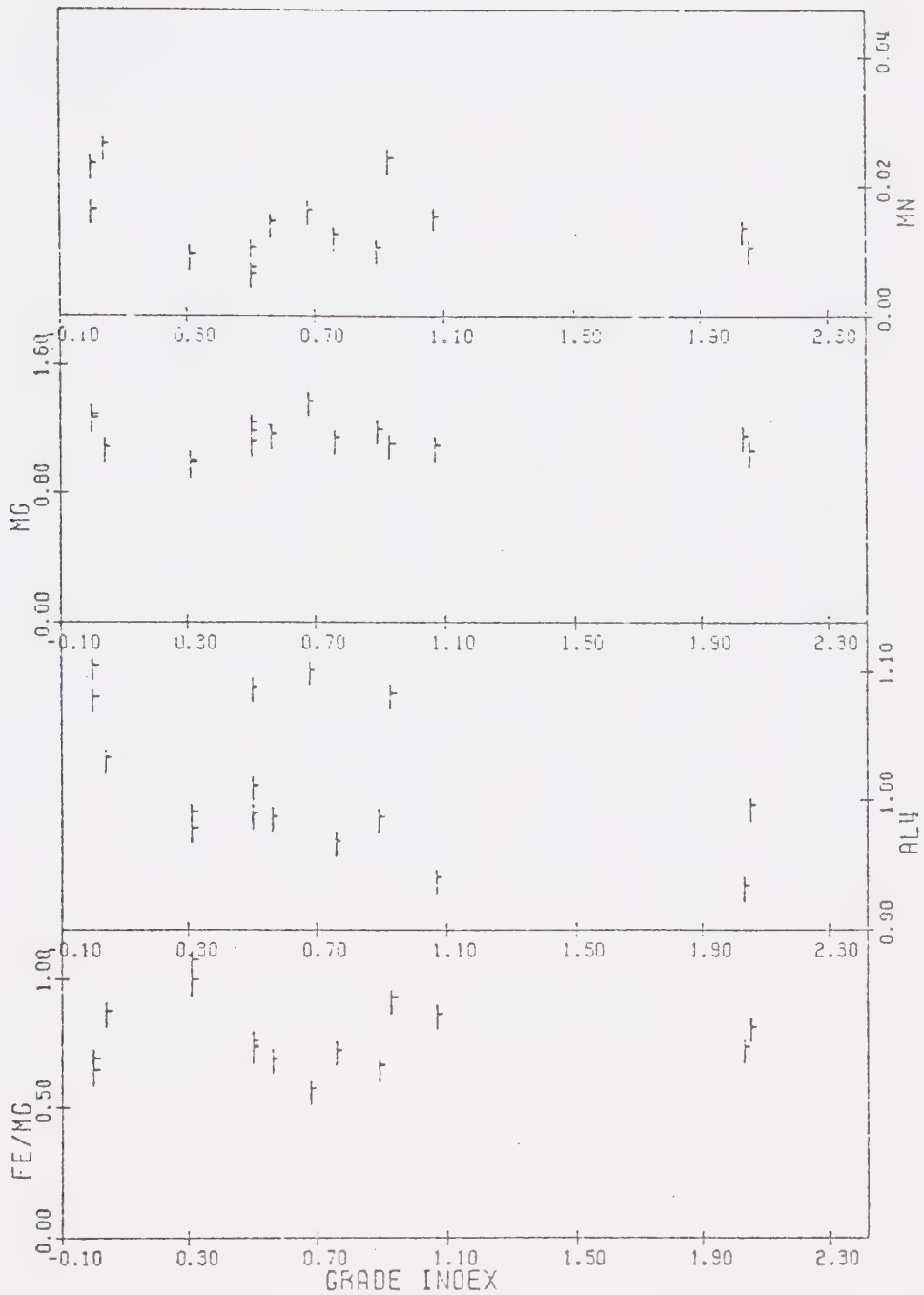


FIGURE 16b: Diagram illustrating the relationship between cordierite composition (atomic proportions) and grade index for cordierites surrounding spinel from the remobilised Archean paragneiss.

TABLE 17: Microprobe analyses (weight %) and structural formulae
 (based on 32 oxygen ions) of SPINEL from remobilised
 Archean paragneiss

Sample Number	73377	73376	73498C	7347	73478	73453	73239
Grade Index	2.05	2.03	1.52	1.07	0.93	0.89	0.68
Al ₂ O ₃	58.01	58.17	48.42	59.28	58.12	59.24	58.93
Fe ₂ O ₃ *	-----	0.11	0.21	0.53	0.48	0.05	1.70
Cr ₂ O ₃	0.29	0.21	8.46	0.08	0.53	0.07	0.15
V ₂ O ₃	0.48	0.46	1.66	0.06	0.07	0.19	0.30
FeO	26.70	23.05	37.08	25.22	33.19	31.06	33.89
MgO	1.95	2.04	0.86	2.70	1.90	2.89	3.55
MnO	0.09	0.08	-----	0.10	0.14	0.13	0.14
NiO	0.16	0.04	0.04	0.05	0.15	0.09	0.08
ZnO	11.72	16.53	0.88	13.47	5.37	6.19	2.36
Total	99.40	100.69	99.61	101.49	99.95	99.91	101.10
Al	15.918	15.847	13.841	15.883	15.781	15.945	15.630
Fe ⁺³	-----	0.025	0.214	0.091	0.084	0.009	0.288
Cr	0.054	0.039	1.622	0.015	0.097	0.012	0.027
V	0.090	0.089	0.323	0.011	0.014	0.035	0.054
Fe ⁺²	5.260	4.452	7.522	4.795	6.393	5.932	6.377
Mg	0.677	0.703	0.312	0.915	0.651	0.983	1.190
Mn	0.017	0.015	-----	0.019	0.028	0.024	0.027
Ni	0.030	0.008	0.008	0.010	0.028	0.017	0.014
Zn	2.016	2.822	0.158	2.261	0.913	1.044	0.392
Fe/Mg	7.77	6.33	24.11	5.24	9.82	6.03	5.36
Zn/ Σ X ⁺²	0.252	0.353	0.020	0.283	0.114	0.131	0.049
mole %	0	0.16	1.34	0.57	0.53	0.06	1.80
magne- tite							

*Fe⁺³ calculated to the ideal spinel structural formula
 C = chromium rich spinel
 ----- = not detected

TABLE 17 (Continued)

Sample Number	73238C	73208	73205	72351	73211	73212	72344*
Grade Index	0.56	0.50	0.50	0.50	0.31	0.30	0.04
Al ₂ O ₃	57.22	59.59	60.06	58.42	58.25	59.58	58.55
Fe ₂ O ₃ *	1.76	0.68	1.60	0.43	1.65	0.33	2.42
Cr ₂ O ₃	0.22	-----	-----	0.46	0.15	0.33	0.06
V ₂ O ₃	0.13	0.05	0.09	0.30	0.05	0.19	-----
FeO	34.18	35.16	33.76	33.96	30.89	36.31	36.19
MgO	2.44	2.60	2.82	2.34	1.75	2.15	2.45
MnO	0.21	0.08	0.04	0.14	0.12	0.05	0.28
NiO	0.21	0.22	0.14	0.15	0.08	0.22	0.20
ZnO	2.77	2.53	5.04	3.91	8.63	2.15	1.53
Total	99.14	100.91	101.55	100.11	98.37	101.31	101.68
Al	15.606	15.879	15.719	15.762	15.680	15.852	15.579
Fe ⁺³	0.306	0.116	0.266	0.073	0.283	0.055	0.411
Cr	0.041	-----	-----	0.083	0.027	0.059	0.010
V	0.025	0.009	0.015	0.055	0.010	0.034	-----
Fe ⁺²	6.615	6.646	6.223	6.501	5.910	6.855	6.832
Mg	0.843	0.876	0.925	0.798	0.597	0.724	0.825
Mn	0.041	0.015	0.008	0.028	0.023	0.010	0.053
Ni	0.039	0.040	0.024	0.028	0.014	0.040	0.035
Zn	0.473	0.423	0.821	0.660	1.456	0.359	0.250
Fe/Mg	7.85	7.73	6.73	8.15	9.90	9.47	8.28
Zn/ Σ X ⁺²	0.059	0.053	0.103	0.083	0.182	0.045	0.031
mole %	1.91	0.73	1.66	0.46	1.77	0.34	2.57
magne-tite							

*core

TABLE 17 (Continued)

Sample Number	72344\$	73178C	73178	72345	72356
Grade Index	0.04	0	0	0	0
Al ₂ O ₃	58.93	52.55	59.48	59.09	59.39
Fe ₂ O ₃ *	2.32	1.56	0.99	1.49	0.99
Cr ₂ O ₃	0.06	5.95	0.11	0.15	-----
V ₂ O ₃	-----	0.28	0.06	0.08	-----
FeO	36.55	35.14	35.84	34.44	35.04
MgO	2.42	2.20	3.15	3.27	3.19
MnO	0.27	0.33	0.25	0.28	0.07
NiO	0.14	0.15	0.25	0.22	0.15
ZnO	1.51	1.24	0.73	1.87	1.55
Total	101.20	99.40	100.86	100.89	100.38
Al ⁺³	15.597	14.566	15.772	15.706	15.832
Fe ⁺³	0.392	0.276	0.167	0.253	0.168
Cr	0.011	1.106	0.020	0.027	-----
V	-----	0.052	0.011	0.014	-----
Fe ⁺²	6.863	6.912	6.743	6.496	6.627
Mg	0.810	0.771	1.058	1.098	1.074
Mn	0.052	0.065	0.048	0.054	0.014
Ni	0.025	0.028	0.046	0.041	0.027
Zn	0.255	0.215	0.121	0.312	0.258
Fe/Mg ⁺²	8.47	8.96	6.37	5.92	6.17
Zn/ Σ X ⁺²	0.032	0.027	0.015	0.039	0.032
mole % magne- tite	2.45	1.67	1.04	1.58	1.05

\$_{rim}

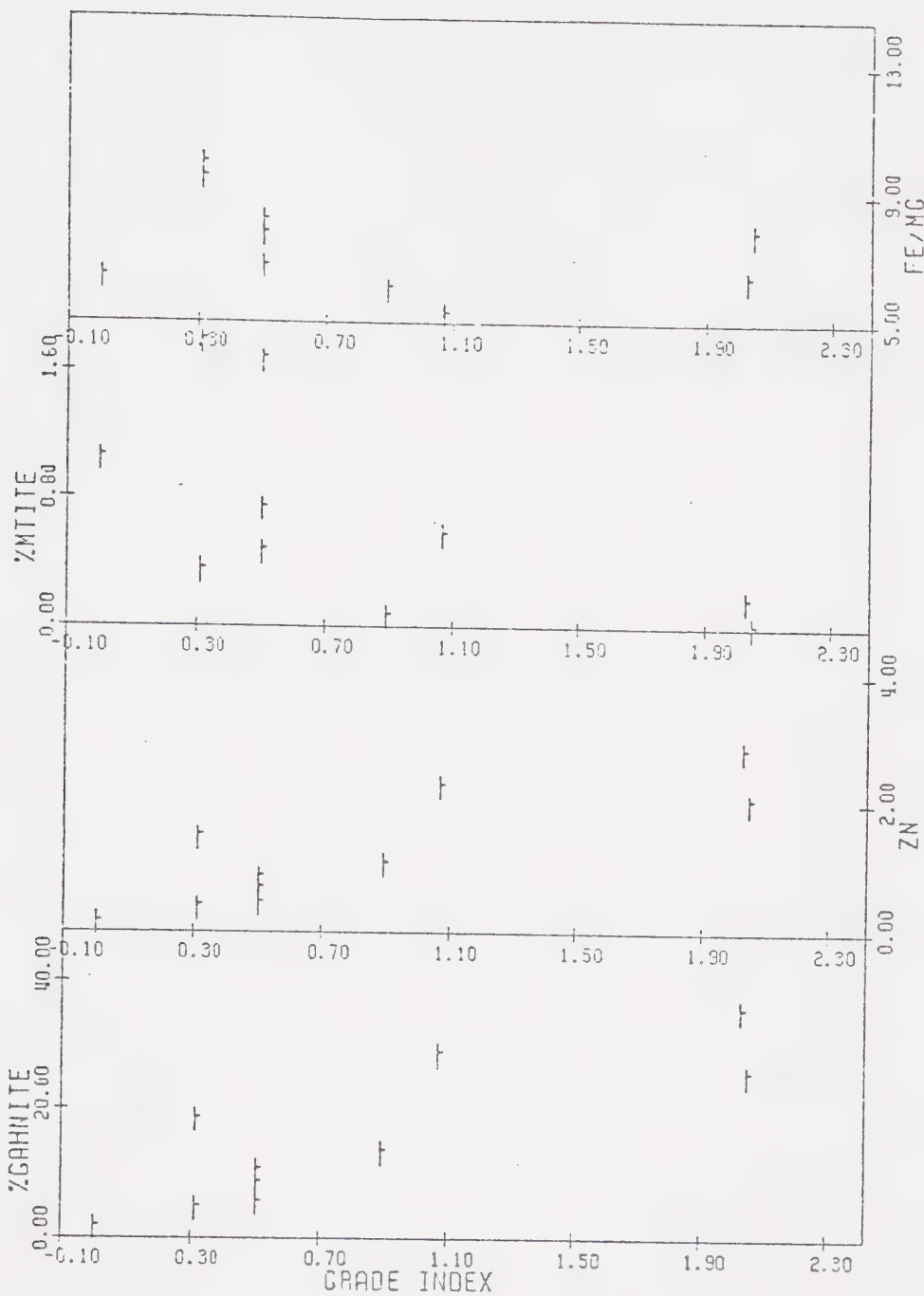


FIGURE 17a: Diagram illustrating the relationship between spinel composition (atomic proportions) and grade index for spinels from garnet free assemblages from the remobilised Archean paragneiss.

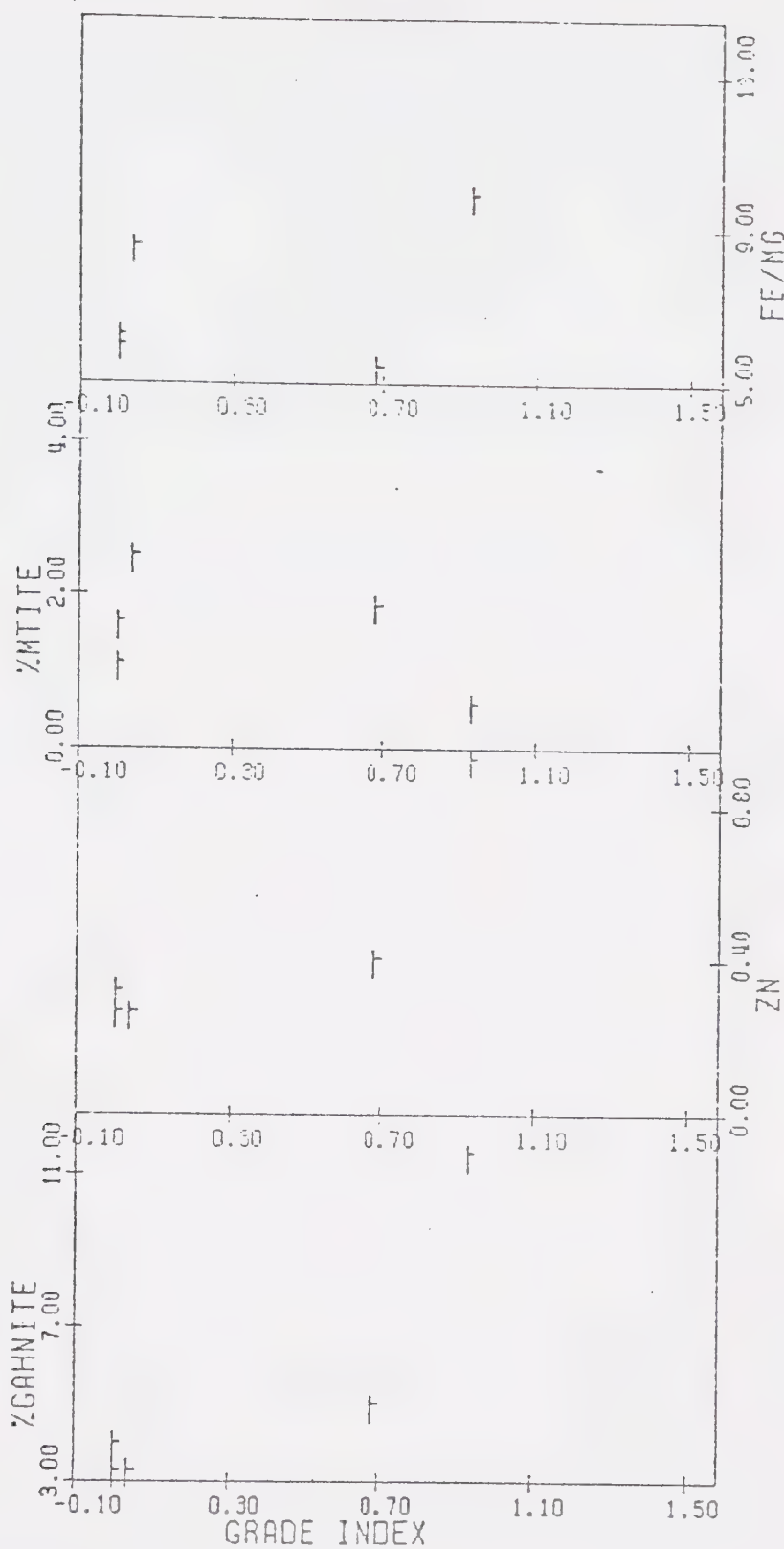


FIGURE 17b: Diagram illustrating the relationship between spinel composition (atomic proportions) and grade index for spinels from garnet bearing assemblages from the remobilised Archean paragneiss.

present only in trace amounts. The spinel occurs as rounded grains in large cordierite crystals, sometimes along with sillimanite prisms. They are homogeneous from core to rim and are usually less than 50 μm in diameter. Plate III shows the associations in which spinel occurs. The chromite rich ($\sim 20\%$) spinels occur within hydrothermally altered cordierite and are accompanied by diaspore.

Influence of Metamorphic Grade. There is a strong correlation between mole per cent gahnite in solid solution in the spinel phase, and the distance from the thermal dome. As distance increases and metamorphic grade decreases, mole per cent gahnite increases and modal spinel generally decreases. Figure 17 shows this relationship. No other component in the spinel shows such a correlation (e.g., Mg/Fe, V, Mn, Cr), which suggests that as the grade of the Hudsonian metamorphism decreased, it is the per cent reaction of spinel to cordierite that controlled the composition of the remaining spinel. This illustrates the gradual disappearance of a phase by continuous reaction. There is a gradual decrease in the Mg/Fe ratio, which is probably due to the distribution of the Mg into the cordierite and retention of the Fe and Zn in the spinel.

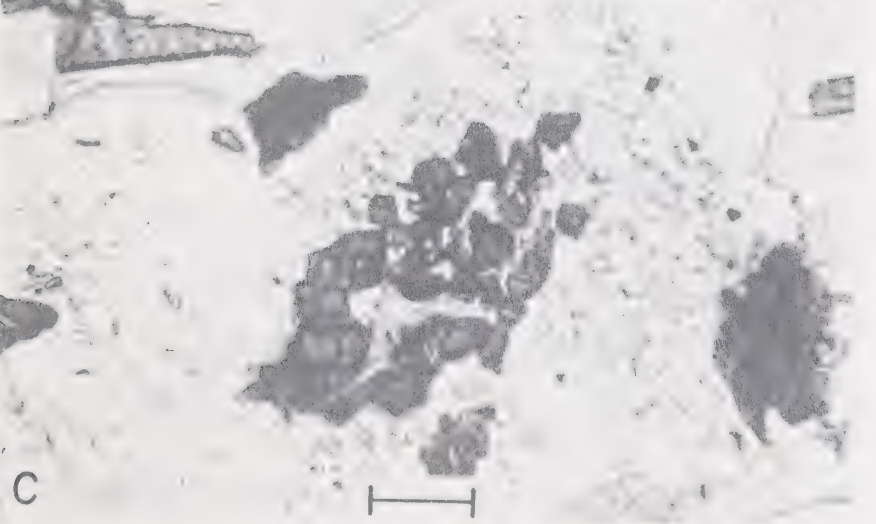
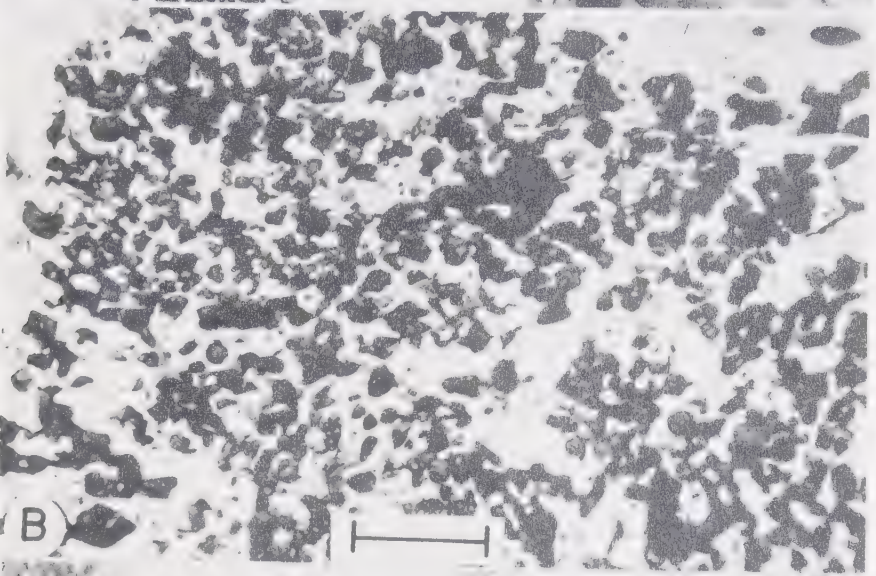
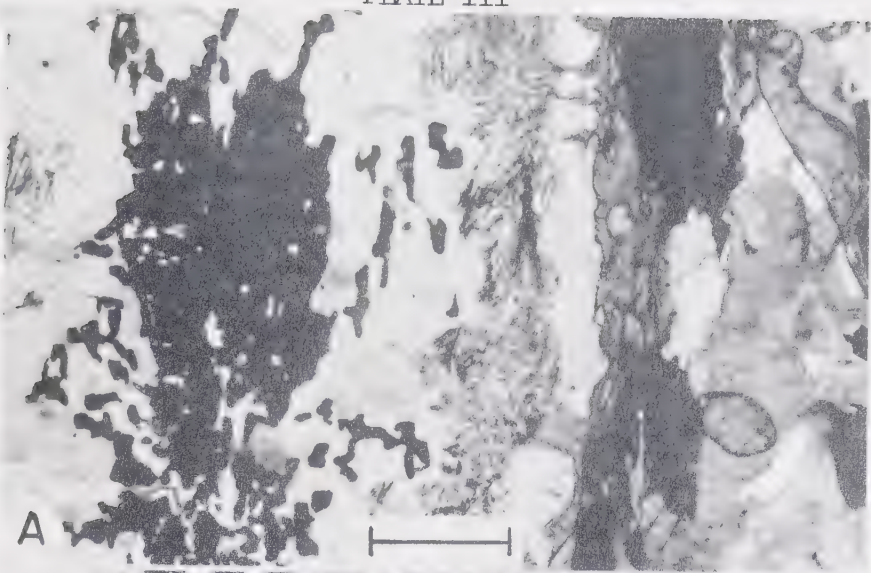
Comparative Discussion. The only study of spinel-cordierite relations in the literature is that

PLATE III

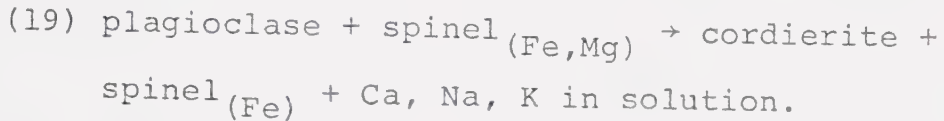
Spinel-cordierite-sillimanite relations in samples from the
remobilised Archean paragneiss.

- A. Sample 72345. Spinel-black, high relief and sillimanite-fine needles sitting in a large cordierite porphyroblast. On the right side of the photograph the cordierite shows pinitate alteration. The surrounding matrix is composed of quartz, microcline, plagioclase and biotite. Crossed nicols. Scale bar = 250 microns. Grade index = 0.0.
- B. Sample 72356. Spinel-black, dark grey in a large cordierite porphyroblast. Crossed nichols. Scale bar = 250 microns. Grade index = 0.
- C. Sample 73478. Small spinel grains (dark gray) in a twinned cordierite porphyroblast rimmed by quartz. The matrix is composed of K-feldspar and biotite. Partially crossed nicols. Scale bar = 50 microns. Grade index = 0.93.

PLATE III



of Henry (1974), on the garnet-cordierite gneisses near the Egersund-Ogna anorthosite intrusion in southwestern Norway. The pressure-temperature conditions deduced for that area are much higher than for this study area, but certain aspects are comparable. Henry noted that spinel occurred only in the cores of cordierite grains, and that the cordierite appeared to separate plagioclase from spinel. He deduced that the cordierite was produced by the reaction between spinel and plagioclase:



Henry's spinels are a hercynite-spinel solid solution with minor chromite and magnetite (< 5%). No gahnite molecule is reported, but low analytical totals suggest that it may be present.

As Henry's plagioclase-spinel reaction to cordierite proceeded, the residual spinel was richer in hercynite and chromite, and depleted in the spinel molecule. His most reacted spinels consisted of hercynite 75, chromite 7, spinel 15, and magnetite 3. In the Arseno Lake area, the least reacted spinel is hercynite 84.3, spinel 13.2, magnetite 1, and gahnite 1.5. Henry (1974) deduced temperatures in the range of 750 - 800° C. and a pressure of approximately 6.3 ± 0.5 kbar, using the method of Currie (1971, 1974). The temperature deduced for the Arseno Lake area is about 650 -

700° C. and a total pressure of 4 ± 0.5 kbar (see Part III). Thus the spinel-cordierite association in the Arseno Lake area may be similar in origin (via a spinel-plagioclase-cordierite reaction relationship) to that in the Egersund-Ogna area.

Garnet

Table 18 presents 6 garnet analyses from the remobilised Archean paragneiss. There is a tendency for Fe to decrease and Mg to increase with increasing grade. Ca is nearly constant and Mn is variable, but shows no trend with grade. The data is shown on Figure 18, although there is insufficient data to reliably predict the role of metamorphic grade in determining the garnet composition in the remobilised Archean paragneiss.

CONTROLS OF MINERAL CHEMISTRY IN THE REMOBILISED ARCHEAN PARAGNEISS

With the exception of the relic Al^{IV} content of biotite and cordierite from the remobilised Archean paragneiss, and the progressive increase in Zn in spinel, no trends in mineral composition are documented. The trends observed in biotite and cordierite from the cordierite-almandine-K-feldspar zone are absent from equivalent grade remobilised Archean paragneiss.

Metamorphic Grade

The increase in Zn in spinel with decreasing

TABLE 18: Microprobe analyses (weight %) and structural formulae (based on 24 oxygen ions) of GARNETS from remobilised Archean paragneisses

Sample Number	73478	73239	73252	72344	72345	72356
Grade Index	0.93	0.677	0.207	0.042	0	0
SiO ₂	35.84	36.33	38.11	37.68	36.39	36.51
Al ₂ O ₃	20.96	20.97	21.26	21.16	21.21	21.36
FeO*	37.05	35.97	33.83	35.43	34.25	35.98
MgO	2.25	3.44	4.31	2.13	3.78	4.23
MnO	2.59	2.10	2.48	4.85	2.95	1.51
CaO	0.89	0.94	0.92	0.98	1.41	0.98
Total	99.58	99.75	100.91	102.23	99.99	100.57
Si	5.877	5.900	6.032	5.999	5.936	5.855
Al ^{IV}	0.123	0.100	-----	0.001	0.064	0.145
Al ^{VI}	3.928	3.913	3.967	3.963	4.014	3.893
Fe	5.082	4.887	4.478	4.717	4.400	4.827
Mg	0.550	0.833	1.017	0.505	0.920	1.011
Mn	0.361	0.292	0.334	0.658	0.410	0.207
Ca	0.156	0.164	0.156	0.167	0.247	0.169
Σ X-site	6.149	6.176	5.985	6.147	5.977	6.214
Fe/Mg	9.24	5.87	4.403	9.34	4.78	4.77
mole % Alm	82.6	79.1	74.8	76.7	73.6	77.7
mole % Py	8.9	13.5	17.0	8.2	15.4	16.3
mole % Sp	5.9	4.7	5.6	10.7	6.9	3.3
mole %	2.6	2.7	2.6	2.7	4.1	2.7
Gr + An						

*total Fe as FeO

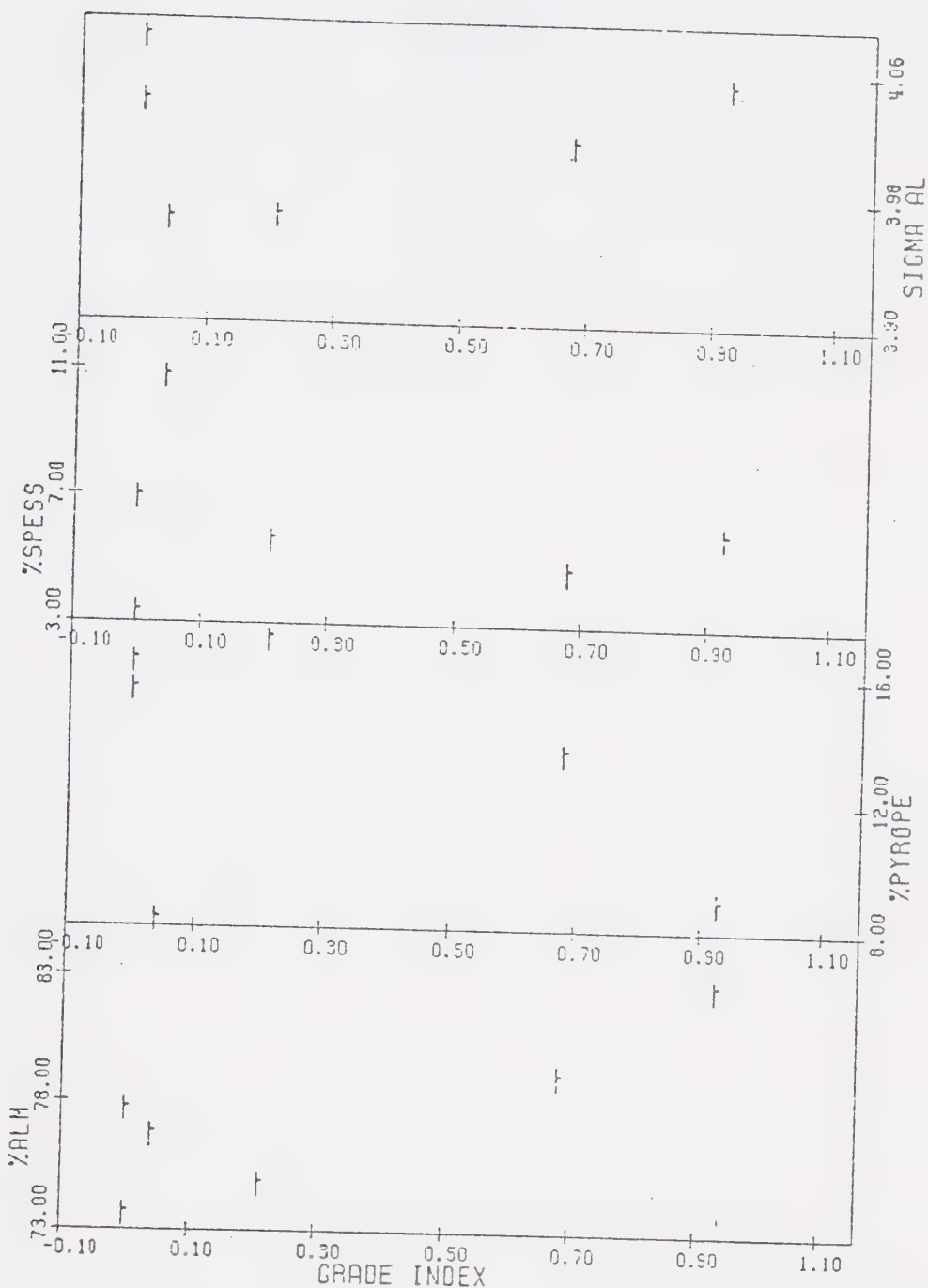
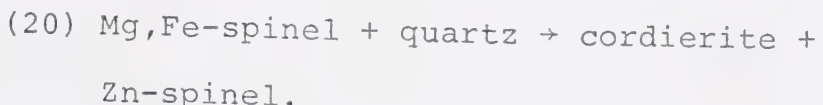


FIGURE 18: Diagram illustrating the relationship between garnet composition (atomic proportions) and grade index for garnets from the remobilised Archean paragneiss.

metamorphic grade is controlled by the grade of the Hudsonian metamorphism. Along with the increase in Zn, the amount of spinel decreases with decreasing grade. Since the spinel is only found within cordierite, the only apparent reaction that could have occurred was:



The absence of systematic variation in the other phases analysed suggests that the Hudsonian metamorphism was either not long enough, intense enough, or 'wet' enough to effect complete recrystallization of the pre-existing Archean metamorphic assemblages. Thus what is preserved is a partially re-equilibrated system where Hudsonian metamorphic trends have not developed and Archean metamorphic trends have not been completely obscured.

Conclusion

The results obtained from the remobilised Archean paragneiss have yielded two points of interest. First, the Zn content of spinel, as a function of the grade of the Hudsonian metamorphism, is a good example of the slow disappearance of a phase by a continuous reaction (18 above). It also illustrates the role of a single component in the stabilization of a phase. In the same way that manganese stabilizes garnet at low grade, the

presence of Zn apparently stabilizes spinel at the conditions of the cordierite zone. Second, it is important to note that certain compositional parameters (e.g., Al^{IV} in biotite and cordierite) first imposed on a mineral in one metamorphism, can persist even when the rocks are involved in a second metamorphic event where upper amphibolite grade conditions were reached. This may be a function of the composition of the fluid phase present during the Hudsonian metamorphism.

As discussed earlier (Part II, pp 34-36) a metamorphic fluid with a low activity of H₂O may restrict the rate of intergranular diffusion of many components and consequently will reduce the distance over which exchange of components such as Al, Fe, and Mg can proceed. As well, self diffusion of components to and from the tetrahedral sites of phases such as biotite and cordierite may be restricted by the energy necessary to break the Al-O bonds. Thus, the observed Al^{IV} content of biotite and cordierite in samples of the remobilised Archean paragneiss may have been preserved because the metamorphic fluid present was rich in CO₂ and there was insufficient energy to induce Al diffusion out of and Si diffusion into biotite and cordierite tetrahedral sites.

PART III: CONDITIONS OF METAMORPHISM

COMPARISON OF THE METAMORPHISM OF THE ARSENO LAKE AREA AND THE ABUKUMA PLATEAU

The sequence of mineral assemblages developed in the Arseno Lake area in the Snare Group metasediments is analogous to that observed in the metapelites from the Abukuma Plateau (Miyashiro, 1953, 1958, 1961; Shido, 1958; Shido and Miyashiro, 1959). (Table 19)

The Arseno Lake area, like the Abukuma Plateau, shows the following sequence of mineral assemblages (in each assemblage, the key index minerals are underlined):

1. Biotite - muscovite - chlorite - quartz.
2. Andalusite - biotite - muscovite - chlorite - quartz.
3. Andalusite - cordierite - biotite ± muscovite ± chlorite - quartz.
4. Sillimanite - cordierite - biotite - muscovite - quartz ± andalusite.
5. Sillimanite - cordierite - biotite - orthoclase - quartz.

In addition to the above prograde assemblages, the Arseno Lake area is characterised by a sixth prograde assemblage not found in the Abukuma Plateau:

6. Cordierite - biotite - almandine - orthoclase - quartz.

TABLE 19: Comparison of the Arseno Lake area with the Central Abukuma Plateau.

<u>CENTRAL ABUKUMA PLATEAU</u>		<u>ARSENOLAKE AREA</u>
chlorite + muscovite		chlorite + muscovite
biotite + muscovite		biotite + muscovite
spessartine rich garnet		spessartine rich garnet
andalusite + muscovite		andalusite + muscovite
cordierite + muscovite		cordierite
sillimanite + muscovite		sillimanite + muscovite
sillimanite + K-feldspar		sillimanite + K-feldspar
almandine rich garnet		almandine rich garnet
10-20 km wide		15 km wide
1.0-4.0 kbar	P range	2-3.1 kbar
300-800°C	T range	350-725°C
Igneous Association		
abundant granite		minor granite
" <u>in situ</u> migmatites		scarce <u>in situ</u> migmatite

Other major differences between this area, and the low pressure metamorphic belts in the Abukuma Plateau are:

1. Lithologies: The major rock type in the Abukuma region is metamorphosed basic volcanics with abundant hornblende. The Arseno Lake area is dominantly metapelite.
2. Peak metamorphic grade: As mentioned above, the Arseno Lake area recorded a higher peak temperature (as deduced from the assemblage cordierite-almandine-K-feldspar) than the Abukuma Plateau.
3. Amount of granitic material: There is a much higher proportion of granitic material exposed in the metamorphic belts of the Abukuma Plateau than in the Arseno Lake area. Also, as mentioned earlier, anatexis and in situ migmatites are rare in the Arseno Lake area.
4. Oxygen fugacity: Miyashiro (1953, 1958, 1961) reported the presence of magnetite and ilmenite from the andalusite-sillimanite facies series rocks of the Abukuma Plateau. Magnetite was not formed in the Arseno Lake area, therefore, f_{O_2} in this area must have been lower for a given set

of P_{total} -T conditions.

5. Composition of the metamorphic fluid:

Although Miyashiro (1953, 1958, 1961) suggested that $P_{\text{H}_2\text{O}}$ was lower than P_{total} in the Abukuma Plateau metamorphism, no quantitative estimates of the fluid composition were given. In the Arseno Lake area, preliminary fluid inclusion studies suggest that CO_2 was a significant component in the fluid phase, especially in the upper cordierite and the cordierite-almandine-K-feldspar zones.

RESTRICTIONS OF THE METAMORPHIC FLUID COMPOSITION IN THE ARSENO LAKE AREA

The composition of the metamorphic fluid present during the crystallization can be estimated from several types of observations. These are outlined below.

Fluid Inclusions

The study of primary fluid inclusions present in metamorphic assemblages may provide data on the composition of the fluid present during metamorphism. Under ideal conditions, the fluid trapped as primary inclusions may even be a sample of the fluid present during the crystallization of the host mineral (Roedder, 1965, 1972; Roedder and Skinner, 1968; Hollister and Burruss, 1976). In the upper cordierite zone, the cordierite-almandine-

K-feldspar zone, and the remobilised Archean paragneiss, primary fluid inclusions in quartz appear to be pure CO_2 , mainly in liquid form and commonly with small CO_2 gas bubbles included. Trains of secondary inclusions commonly contain an $\text{H}_2\text{O} + \text{CO}_2$ mixture and some H_2O rich secondary inclusions have been observed. Primary fluid inclusions in quartz from the lower cordierite zone and the biotite zone are nearly pure H_2O (Plate IV).

Thus, a change in composition of the fluid trapped in primary fluid inclusions has been observed across the Arseno Lake area, going from H_2O rich in the biotite zone to almost pure CO_2 in the cordierite-almandine-K-feldspar zone (Table 20).

Absence of Anatexis

A second observation which can provide information on the fluid composition is the amount of anatexis which has occurred in upper amphibolite grade metamorphism. Winkler and von Platen (1960), von Platen (1965), and Winkler (1970) have shown that pelites and graywackes can begin to melt at about 685° C . at 2 kbars = $P_{\text{H}_2\text{O}} = P_{\text{total}}$. At higher $P_{\text{H}_2\text{O}}$, the minimum melting temperature decreases. If, however, $P_{\text{H}_2\text{O}} < P_{\text{total}}$, then for a given P_{total} , the corresponding temperature at which melting begins increases. This effect was assessed by Kerrick (1972) for the system quartz-albite-orthoclase- $\text{H}_2\text{O}-\text{CO}_2$.

TABLE 20 : Compositions of primary fluid inclusions
observed in quartz

Sample Number	Grade Index	Composition Primary	Number of Phases	Mineral Assemblage Zone
7316	3.75	CO ₂	2	Cordierite muscovite
7273	3.27	H ₂ O	1	Biotite
73274	2.94	H ₂ O+CO ₂	2	Cordierite
7215	2.39	H ₂ O	1	Biotite
7269	2.24	H ₂ O	1	Biotite
73394	2.24	H ₂ O+CO ₂	2	Cordierite muscovite
72372	2.07	H ₂ O+CO ₂	2	Biotite
73376	2.03	CO ₂	2	Cordierite-sill-K-spar
7268	2.0	H ₂ O	1	Biotite RAP
7255	1.99	H ₂ O	1	Biotite
7256	1.95	H ₂ O	1	Cordierite
73331	1.85	H ₂ O	1	Almandine-cordierite-K-feldspar
73148	1.84	H ₂ O	1	Almandine-cordierite-K-feldspar
72388	1.44	CO ₂	1	Cordierite-sill-K-spar
7347	1.07	CO ₂	1	" " " "
72392	1.05	CO ₂	1	" " " "
73486	1.0	CO ₂	2	Almandine-cordierite-K-feldspar
73116	1.0	CO ₂	1	" "
73430	0.96	CO ₂	2	" "
73104	0.94	CO ₂	2	" "
73153	0.94	CO ₂	2	" "
73478	0.93	CO ₂	2	" " RAP
73483	0.93	CO ₂	2	" "
73479	0.91	CO ₂	2	Cordierite
73160	0.80	CO ₂	1	Almandine-cordierite-K-feldspar
73159	0.74	CO ₂	1	" "

TABLE 20 : Compositions of primary fluid inclusions
observed in quartz

Page 2

Sample Number	Grade Index	Composition (Primary)	Number of Phases	Mineral Assemblage Zone
7368	0.74	CO ₂ +H ₂ O	2	Cordierite
73163	0.44	CO ₂	2	Almandine-Cordierite-K-feldspar
73243	0.35	CO ₂	2	" "
73226	0.31	CO ₂	2	Cordierite-sil-K-spar RAP
73445	0.29	CO ₂	2	Calc silicate -
73228	0.29	CO ₂	1	Almandine-cordierite-K-feldspar
73252	0.21	CO ₂	2	" "
72343	0.01	CO ₂ +H ₂ O	2	" "
72356	0.0	CO ₂	2	" "
72345	0.0	CO ₂	2	" "

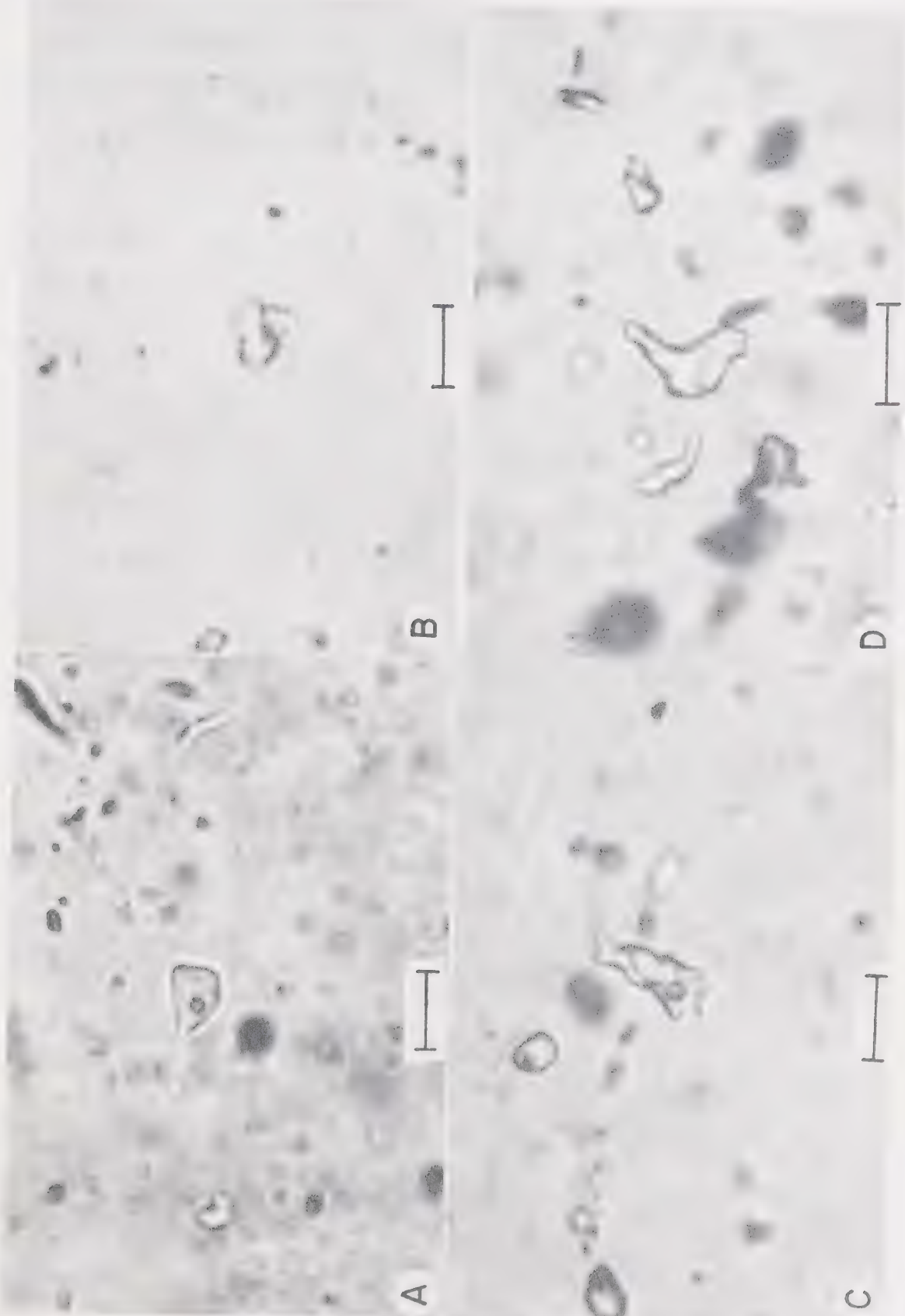
RAP = remobilised Archean paragneiss

PLATE IV

Fluid inclusions from samples from the almandine-cordierite-K-feldspar zone.

- A. Sample 72345. Two phase single component fluid inclusion. A small CO₂ vapor bubble sitting on a large volume of CO₂ liquid. The inclusion is found in a quartz grain. Plane polarised light. Scale bar = 2.5 microns.
- B. Sample 73483. Fluid inclusion in quartz grain. A single phase is present and the low relief suggests that it is H₂O. Plane polarised light. Scale bar = 2.5 microns.
- C. Sample 73483. Three two phase CO₂ inclusions like those in A. These fluid inclusions occur in the quartz grain shown in Plate 20. Plane polarised light. Scale bar = 2.5 microns.
- D. Sample 72356. Series of one phase CO₂ rich inclusions in a quartz grain adjacent to garnet. Plane polarised light. Scale bar = 2.5 microns.

PLATE IV



Scale of Equilibration

As discussed in the section on controls of mineral chemistry, the composition of the fluid phase is a major factor in determining the rate of transport of cations or cation complexes from a reaction site to a nucleation and growth site. Qualitative information on the solubility of various geologically important species is available (Mueller, 1967; Vidale and Hewett, 1973; Hofmann et al., 1974). Thus, we can predict that calcium and, to a lesser extent, magnesium are more soluble in a CO_2 rich fluid than an H_2O fluid. Conversely, potassium, sodium, iron, manganese, and titanium are more soluble in an H_2O rich fluid.

Thus, by examining the scale of equilibration of ferro-magnesian silicates, a qualitative inference may be drawn regarding the nature of the fluid present during equilibration. In the cordierite zone and the cordierite-almandine-K-feldspar zone, where equilibrium is established on a small scale, it can be inferred that the metamorphic fluid had a low mole fraction of H_2O .

Mineral Assemblages Present

In a metamorphic terrain, the mineral assemblages present and the width of the transition zone between two mineral assemblages on opposite sides of a discontinuous reaction, can provide information on the nature of the fluid phase. A sharp boundary (narrow transition zone)

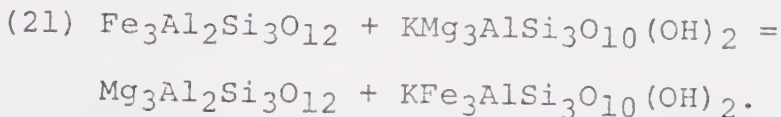
across a discontinuous dehydration reaction isograd could indicate that the composition of the metamorphic fluid was externally controlled. This is what is observed in the Arseno Lake area for the second sillimanite isograd reaction. There are very few samples which contain the equilibrium assemblage sillimanite + K-feldspar + quartz + muscovite + plagioclase. Again, this suggests that $P_{H_2O} < P_{total}$.

GARNET - BIOTITE - CORDIERITE GEOTHERMOMETRY

The widespread occurrence of phase assemblages including biotite, cordierite, and garnet as pairs, or with all three phases present, has long been of interest to metamorphic petrologists as a potential geothermometer and/or geobarometer.

Garnet-Biotite Geothermometry

The most common association of the above minerals is that of biotite plus garnet. This was the first mineral pair to be tested as a geothermometer. Saxena (1969) compiled compositional data on coexisting biotite and garnet from several metamorphic terrains covering a wide range of metamorphic grade. He examined the distribution of iron and magnesium between coexisting garnet and biotite by assuming an ion exchange equilibrium reaction:



The distribution coefficient on one cation ex-

change basis was:

$$K_D = X_{Bi} \times (1 - X_{Gt}) / (1 - X_{Bi}) \times X_{Gt},$$

where X_{Bi} = Fe/(Fe + Mg) in biotite. He then used regression and principal component analysis to study the chemical data on 93 coexisting biotite-garnet pairs. Eigenvalues and eigenvectors were used to obtain values of transformed distribution coefficients, which he found to be significant in distinguishing between rocks formed at different pressures and temperatures. Saxena arrived at a 'transformed distribution coefficient', obtained by principal component analysis, which is shown below:

$$\begin{aligned} \text{Transformed } K_D &= 0.5013 K_D - 0.442 X_{Gt}^{\text{Fe}} + \\ &0.1506 X_{Bi}^{\text{Fe}} - 0.3474 X_{Gt}^{\text{Mn}} + 0.0856 X_{Gt}^{\text{Ca}} - \\ &0.0333 X_{Bi}^{\text{AlIV}} - 0.3165 X_{Bi}^{\text{AlVI}} + 0.5488 X_{Bi}^{\text{Ti}}. \end{aligned}$$

The pressure dependence of the transformed K_D was neglected, and an attempt was made to relate the value of the transformed K_D to temperature of metamorphism. The calibration of the garnet-biotite geothermometer was based on three values of temperature, one each for charnockite (600° C.), upper amphibolite (500° C.), and epidote amphibolite (400° C.). In the light of present knowledge of the physical condition of upper amphibolite to granulite facies metamorphism, these calibration temperatures are too low, by approximately $150 - 200^\circ \text{ C.}$

Temperatures calculated using Saxena's method are

shown on Figure 19 and summarized in Table 21. These temperatures appear to be consistently too low. This is most probably due to:

1. Saxena's temperature calibration was based on estimated temperatures, not experimentally determined equilibria. This is complicated by problems in obtaining the temperature estimates used for calibration. For example, if the feldspar geothermometer of Barth (1934) is used, a maximum temperature of 600° C. is obtained, even though the temperature of equilibration may have been significantly higher (i.e. upper amphibolite-granulite metamorphism).
2. Errors were introduced in computing the transformed K_D because the terms related to the substitution of Mn, Ca, Ti, etc. for Fe and Mg were empirically determined. This problem could not be treated thermodynamically since no solid solution data for garnet and biotite were available to Saxena (1969).

More recent work on garnet-biotite geothermometry has been done by Thompson (1975 a, 1976 a,b). He synthesized all of the available data on garnet and biotite solid

TABLE 21 : Temperatures calculated using the relationships
 of Saxena (1969) and Thompson (1976b) for
 co-existing biotite and garnet

Sample Number	Grade Index	Thompson	Saxena	Recalibrated Saxena
73280	2.51	580	390	440
7248	2.39	420	305	355
73402	2.02	500	420	490
7255	1.99	505	330	380
73366	1.64	570	490	580
7345	1.00	540	480	570
73416	0.98	565	550	660
73478	0.93	550	390	440
73451	0.79	600	480	570
73239	0.68	600	515	620
73157	0.54	500	375	425
73202	0.46	620	405	560
73221	0.33	640	520	640
73252	0.21	615	525	640
72345	0.0	680	485	600
72356	0.0	655	495	620

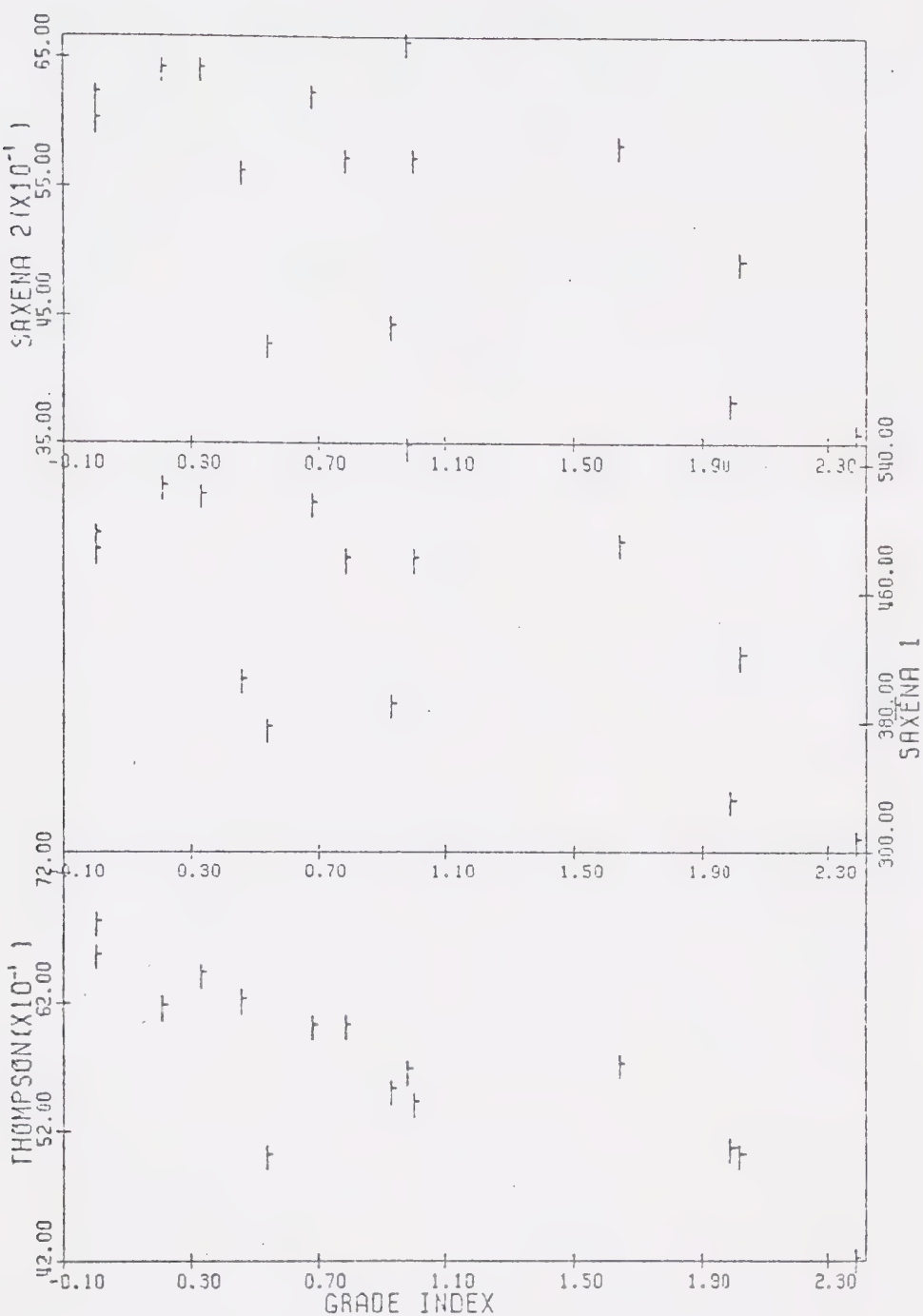


FIGURE 19: Diagram showing the relationship between temperatures ($^{\circ}$ C.) and grade index for garnet-biotite assemblages. Temperatures were calculated using the data of Thompson, 1976b (THOMPSON ($\times 10^{-1}$)), Saxena, 1969 (SAXENA 1), and the recalibrated data of Saxena (SAXENA 2 ($\times 10^{-1}$)).

solution and calculated the free energies of the exchange reactions. Using these data, he derived a relationship between the natural log of K_D and $1/T^0$ K.

Thompson's K_D is defined as:

$$K_D = x_{Gt}^{Fe} \times (1 - x_{Bi}^{Fe}) / x_{Bi}^{Fe} \times (1 - x_{Gt}^{Fe}),$$

where $x^{Fe} = Fe/(Fe + Mg)$. The relationship used in the Arseno Lake study is:

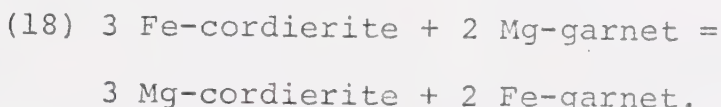
$$T^0 \text{ K.} = 1/3.239 \times 10^{-4} \ln K_D + 6.501 \times 10^{-4}^*.$$

The error assigned to the results is $\pm 50^\circ$ C. (Thompson, 1975a; Tracey *et al.*, 1975).

Temperatures calculated using this relationship are given in Table 21 and plotted on Figure 19.

Garnet-Cordierite Geothermometry

The second mineral assemblage to be investigated as a possible geothermometer was the assemblage garnet-cordierite-sillimanite-quartz. This system was first studied experimentally by Currie (1971). Currie considered the exchange reaction:



He assumed that both cordierite and garnet form an ideal solid solution of the iron and magnesium end members. He then conducted a series of experiments, using synthetic cordierite of varying Fe/Mg ratios, to investi-

*For derivation of this relationship, see Appendix: Numerical Methods.

gate the pressure dependence of the cordierite breakdown reaction:



Five weight per cent H_2O was added to all of the charges in order to facilitate reaction. From the experimental data, he constructed a series of isothermal P-X diagrams showing the composition of coexisting garnet and cordierite. The relationship between $T^\circ K.$ and K_D derived by Currie is:

$$T = 4515/(6.37 - \ln K),$$

where $K = X_{Co}^{Mg} \times X_{Gt}^{Fe}/X_{Co}^{Fe} \times X_{Gt}^{Mg}$. The estimated accuracy of this relationship is $\pm 50^\circ C.$ (Currie, 1971).

Application of this relationship to the cordierite-garnet data of this study produced the temperatures shown on Figure 20 and summarized in Table 22.

Hensen and Green (1971, 1972, 1973) investigated the stability of cordierite and garnet in model pelitic systems with varying $Al/(Fe + Mg)$ and $Mg/(Fe + Mg)$ ratios, in the presence of constant weight fractions of Na and K and varying amounts of Ca. The major difference between the assemblages they produced and natural assemblages is that the experiments were run in the absence of water and no MnO was included in the starting materials.

Results obtained by interpolation and extrapolation

TABLE 22 : Temperatures calculated using the relationships
 of Currie(1971), Hensen and Green (1973),
 Hutcheon et al (1975) and Thompson (1976b) for
co-existing garnet and cordierite

Sample Number	Grade Index	Thompson	Hutcheon et al	Currie	Hensen and Green
73402	2.02	545	360	875	650
73153	1.00	520	240	1042	500
73478	0.93	570	395	840	650
73239	0.68	565	385	850	680
73202	0.46	610	440	805	680
73221	0.33	630	430	815	680
73252	0.21	640	480	780	700
72345	0.0	660	510	765	690
72356	0.0	685	540	750	710

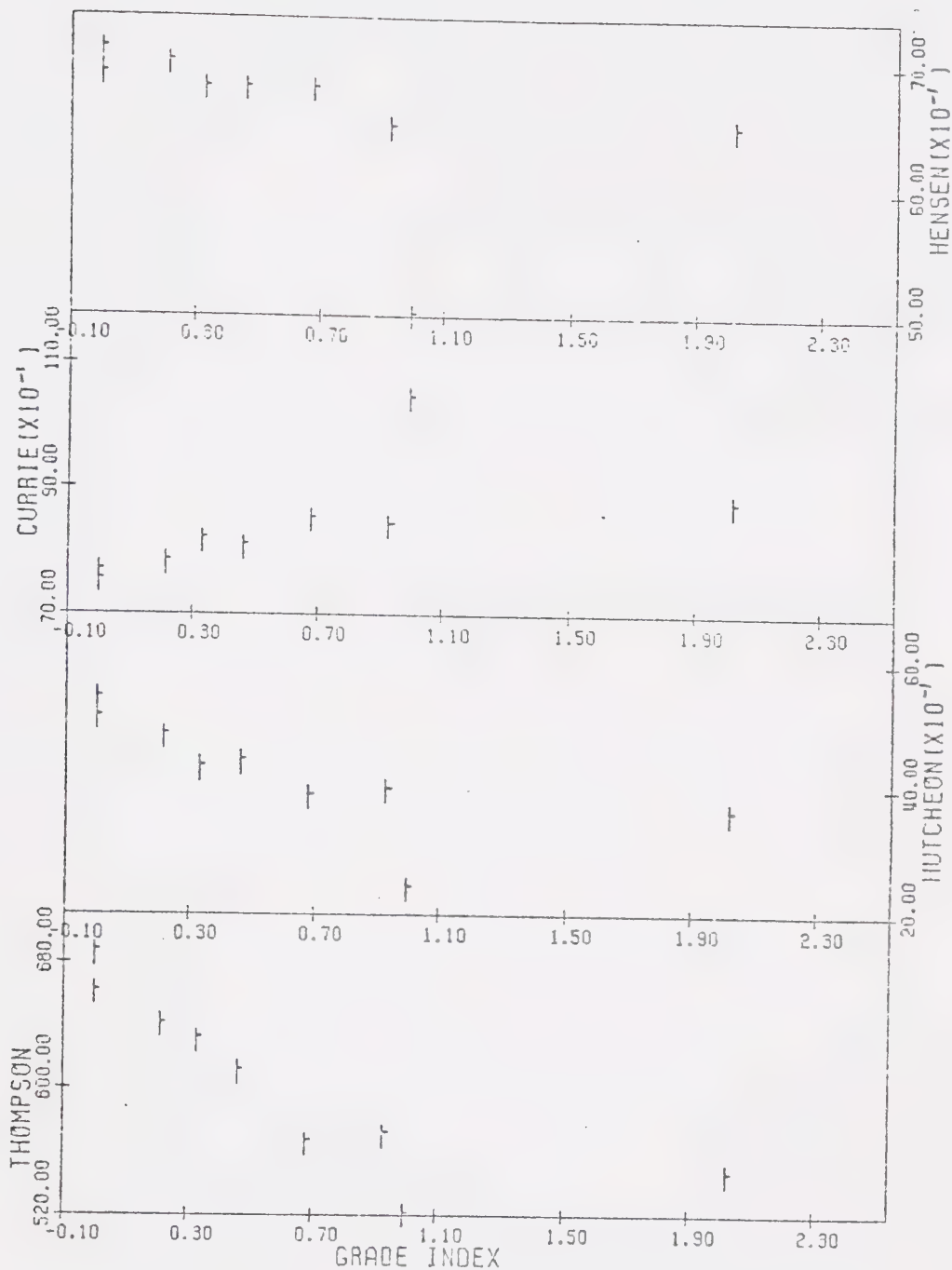


FIGURE 20: Diagram showing the relationship between temperatures ($^{\circ}$ C.) and grade index for garnet-cordierite assemblages. Temperatures were calculated using the data of Thompson, 1976b (THOMPSON), Hutcheon *et al.*, 1975 (HUTCHEON $\times 10^{-1}$), Currie, 1971 (CURRIE $\times 10^{-1}$), and Hensen and Green, 1973 (HENSEN $\times 10^{-1}$).

tion of the data of Hensen and Green (1973) are summarized in Table 22 and Figure 20. The error introduced by this extrapolation is probably at least $\pm 60^\circ$ C. and ± 500 bars.

Hutcheon et al. (1974), in an attempt to resolve the discrepancies between the data of Currie (1971) and Hensen and Green (1971), derived the phase relations of garnet and cordierite using the published data of Robie et al. (1967) and Froese (1973). Their treatment involved several assumptions which are summarized in Hutcheon et al. (1974). They derived the following expressions for P_{total} and T :

$$P = \frac{(AG_{(1)}^0 + 298AS_{(1)}^0 - AV_{(1)}^0)(R \ln K_{(2)} - AS_{(2)}^0) - (R \ln K_{(1)} - AS_{(1)}^0)(AG_{(2)}^0 + 298AS_{(2)}^0 - AV_{(2)}^0)}{(R \ln K_{(2)} - AS_{(2)}^0)AV_{(1)}^0 - (R \ln K_{(1)} - AS_{(1)}^0)AV_{(2)}^0}$$

$$T = \frac{(AG_{(1)}^0 + 298AS_{(1)}^0 - AV_{(1)}^0)AV_{(2)}^0 - (R \ln K_{(2)} + 298AS_{(2)}^0 - AV_{(2)}^0)AV_{(1)}^0}{(R \ln K_{(2)} - AS_{(2)}^0)AV_{(1)}^0 - (R \ln K_{(1)} - AS_{(1)}^0)AV_{(2)}^0}$$

The estimated accuracy of these expressions is temperature $\pm 75^\circ$ C. and pressure ± 500 bars. The results obtained by application of these relationships to the garnet-cordierite data from the Arseno Lake area are summarized in Table 22 and Figure 20.

Thompson (1975 a, 1976 a,b) investigated the potential use of the garnet-cordierite pair as a geothermometer. His synthesis of the available data of natural mineral pairs, as well as experimentally produced assemblages, produced the following expression relating T° K. and the distribution coefficient for iron

and magnesium between cordierite and garnet:

$$T = 1/(3.841 \times 10^{-4} \ln K_D + 2.936 \times 10^{-4}).$$

The results obtained by using this relationship are summarized in Table 22 and Figure 20.

Biotite-Cordierite Geothermometry

Thompson (1975 a, 1976 a,b) has compiled the available data on cordierite and biotite in an attempt to calibrate the continuous reaction between them in terms of pressure, temperature, and the activity of H₂O. He used experimentally determined and calculated pure iron and pure magnesium end member reactions and iron-magnesium exchange potentials, calculated from distribution coefficient data, to arrive at an expression relating temperature and the distribution of iron and magnesium between biotite and cordierite:



The following relationship between T and the distribution coefficient (K_D) for the above reaction was obtained:

$$T = 1/(3.691 \times 10^{-4} \ln K_D + 9.373 \times 10^{-4}).$$

This geothermometer is believed to be accurate to within $\pm 100^\circ \text{ C}$. (Thompson, 1975). The results obtained by using this relationship are presented in Table 23 and Figure 21.

TABLE 23 : Temperatures calculated using the relationship
 of Thompson (1976b) for co-existing biotite
 and cordierite

Sample Number	Grade Index	Thompson
73269	2.70	615
73394	2.22	600
73377	2.05	620
73376	2.03	600
73407	2.03	555
73402	2.02	565
73308	1.86	590
73131	1.28	570
72385	1.21	680
7347	1.07	630
7346	1.06	620
73153	1.00	565
73449	0.94	570
73162	0.92	575
73450	0.90	600
73453	0.89	580
73501	0.76	585
73239	0.68	535
73185	0.66	550
73238	0.56	535
73206	0.53	605
73155	0.53	575
73205	0.50	580
73208	0.50	580
73195	0.41	580
73221	0.33	555
73226	0.31	570
73227	0.29	580
73229	0.27	575
73252	0.21	580
73255	0.06	545
72345	0.0	540
72356	0.0	585

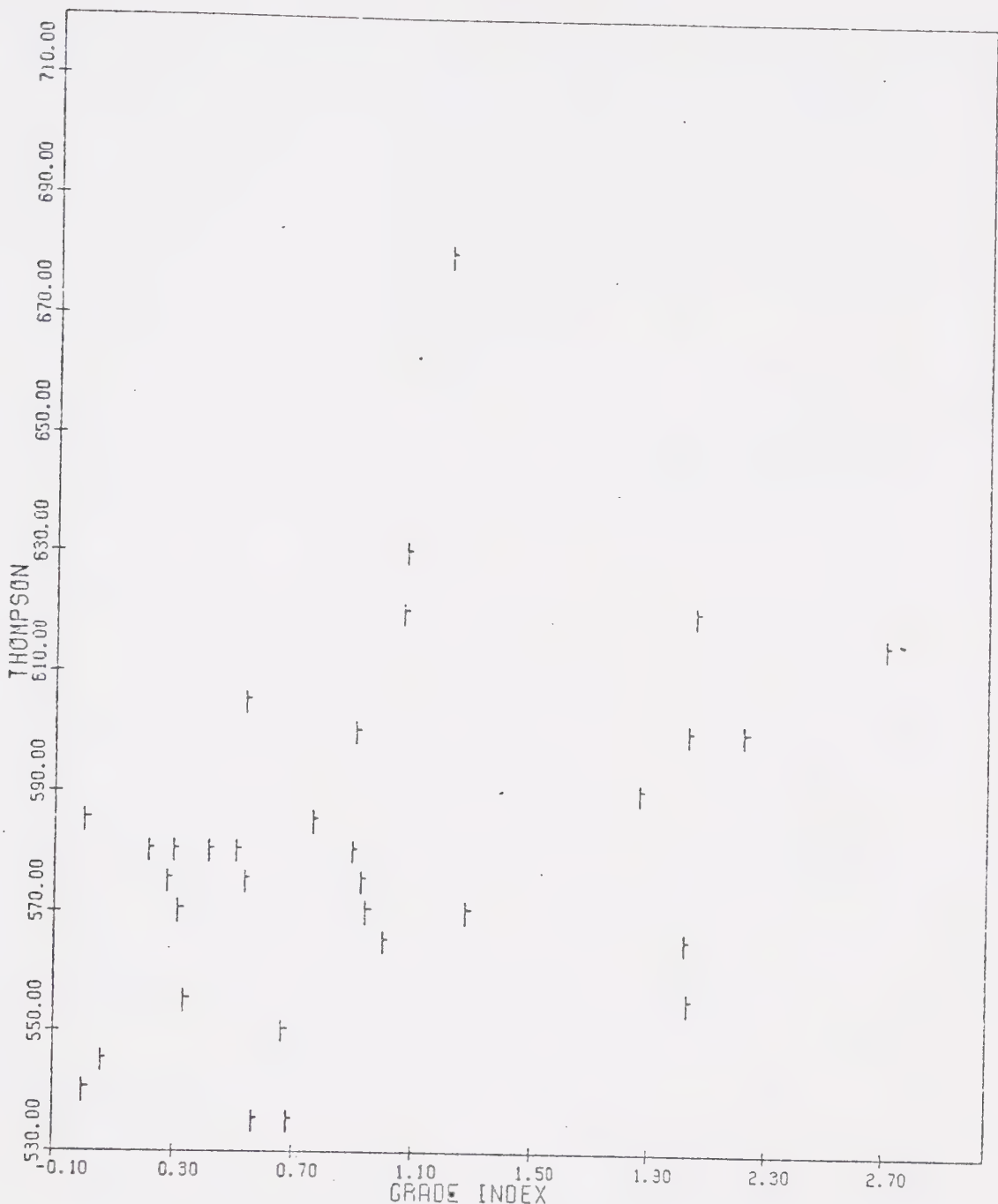


FIGURE 21: Diagram showing the relationship between temperatures ($^{\circ}$ C.) and grade index for biotite-cordierite assemblages. Temperatures were calculated using the data of Thompson, 1976b.

Evaluation and Discussion

Examination of the results obtained by application of the above discussed geothermometers provides information about the thermal gradient and the nature of the heat source. Before discussing these points, the geothermometers will be evaluated.

Garnet-Biotite. Both Saxena's (1969) expression and Thompson's (1975 a, 1976 a,b) expression indicate a trend of increasing temperature with increasing metamorphic grade. As will be shown below, the temperatures suggested by Saxena's expression are too low. However, this may result from the fact that the temperature estimates for various grades of metamorphism which were used for calibration were themselves too low, as discussed above. Figure 22 shows the temperatures obtained when Saxena's expression is calibrated with more recent temperature estimates for the granulite facies (750 - 850° C.), upper amphibolite facies (600 - 650° C.), and epidote-amphibolite facies (400 - 450° C.).

Both of the garnet-biotite thermometers discussed above appear to be useful for indicating relative changes in temperature within a metamorphic terrain. For those garnets where both core and rim analyses are available, it is interesting to compare the temperature calculated for the core formation and the temperature at which the rim equilibrated with biotite.

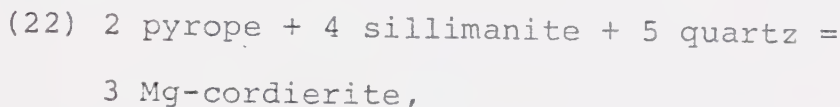
Comparison of core and rim temperatures may record the temperature decrease following the highest temperature conditions experienced by a sample. This approach may be valid if the amount of biotite is much greater than the amount of garnet in the specimen. In this case, the biotite could act as a reservoir of iron and magnesium, and any Fe-Mg exchange between biotite and garnet in response to declining temperature would be recorded in the garnet rim, but would have a negligible effect on the composition of the biotite.

The temperature decrease noted for garnets in the cordierite-almandine-K-feldspar zone ranges from 60° to 120° C. This magnitude of temperature decrease is consistent with the metamorphic evolution proposed for this study area. The garnets formed in the biotite zone, with Mn-rich cores, display prograde zoning (Grant and Wiebelen, 1971), and the calculated temperatures for the core and the rim suggest that the rim equilibrated at temperatures about 100° C. higher than the temperature of formation of the core.

Garnet-Cordierite. Four garnet-cordierite geothermometers have been applied to the Arseno Lake area. Three of them, Hensen and Green (1973), Hutcheon et al., (1974), and Thompson (1975 a, 1976 a,b), show increasing temperature with increasing metamorphic grade, although they differ in absolute value by approximately 250° for

a given sample. The fourth geothermometer, that of Currie (1971), is anomalous in that the temperatures show a decrease with increasing metamorphic grade, and the temperatures predicted are high enough to produce anatexis, even under conditions of $P_{H_2O} < P_{total}$. The problems encountered in using the Currie (1971) expression may result in part from the fact that the experimentally studied breakdown reaction of cordierite did not occur in the Arseno Lake area. A second contributing factor may be the range of the spessartine plus grossular components present in this area.

The differences between the temperatures obtained from Thompson's (1975 a, 1976 a,b) expression and the extrapolation of Hensen and Green's (1971, 1973) experimental error may be accounted for by the uncertainty of each calculation ($\pm 100^\circ C.$). It is, however, more difficult to assess the differences between the above geothermometers and that of Hutcheon et al. (1974). They may result, in part, from possible errors in the assumed values of ΔS° and ΔG for the reaction:



which was used in establishing their temperature equation.

As was the case with garnet-biotite geothermometry the temperature-composition of Hensen and Green (1971, 1973), Hutcheon et al. (1974), and Thompson (1975 a, 1976

a,b) appear to be valuable for indicating temperature changes within a metamorphic terrain, but further experimental work is required in order to obtain quantitative temperature measurements.

Biotite-Cordierite. The results obtained from Thompson's (1975 a, 1976 a,b) biotite-cordierite geothermometer across the study area show no temperature increase with increasing metamorphic grade. All of the temperatures lie in the range of 580° C. \pm 50° C. This is interpreted as the result of iron-magnesium exchange between biotite and cordierite with declining temperature in the late stages of metamorphism. The value $580^{\circ} \pm 50^{\circ}$ C. probably closely approximates the minimum temperature at which self-diffusion and intergranular or grain boundary transport of iron and magnesium could occur in this area.

Assumptions. All of the above geothermometers are based on two important assumptions, the validity of which cannot be assessed completely. The assumptions are:

1. All of the phases used in geothermometry exhibit ideal solution of all components in the crystalline solution (i.e., K_{DFe-Mg} is independent of composition). This appears to be valid for the aluminous garnets (Ganguly and Kennedy, 1974), but the necessary data for cordierite and biotite are not available at this time and further experimental work is needed.

2. The change in heat capacity (ΔC_p) for the iron-magnesium exchange reactions between mineral pairs is equal to zero. This assumption is perhaps more clearly seen in the definition of C_p :

$$\Delta C_p = T \frac{(\partial S)}{(\partial T)_p}$$

It follows from the above equality that if $\Delta C_p \neq 0$, then the exchange reaction does not behave ideally. The data necessary to assess this assumption are not presently available.

In addition, the nature and role of H_2O in the cordierite structure and its role in controlling Fe/Mg in cordierite must be investigated. Wood (1973) has suggested that H_2O dissolves more readily in iron cordierite and that the presence of water in cordierite will strongly influence the distribution coefficient for iron and magnesium between cordierite and garnet. This gives rise to a higher K_D as a result of a decreased $Fe/(Fe + Mg)$ ratio in cordierite. The other major problem to be investigated is the effect of Al^{IV} substitution for Si^{IV} in biotite, as well as the role of Ca, Mn, and Ti in determining the iron and magnesium distribution between biotite and coexisting ferro-magnesium silicates.

Conclusions. The change in temperature recorded by the garnet-cordierite and garnet-biotite

thermometers across this area, from the middle part of the biotite zone to the highest grade part of the cordierite-almandine-K-feldspar zone, was approximately 350° C. If the metamorphism was essentially isobaric, and the present erosional surface is used as an isobaric surface, then the thermal gradient around the heat source ranged from 50°/km towards the east, to 75 - 85°/km towards the south.

GARNET - CORDIERITE - PLAGIOCLASE GEOBAROMETRY

Two potential geobarometers involving garnet, cordierite, and plagioclase have recently been published (Currie, 1971; Hutcheon *et al.*, 1974; Ghent, 1975; Tracey *et al.*, 1975). The relationships of pressure and mineral composition data determined for several mineral associations are outlined below.

Garnet-Cordierite-Sillimanite-Quartz

The assemblage garnet-cordierite-sillimanite-quartz was first examined and calibrated as a geobarometer by Currie (1971). Currie concluded that if both garnet and cordierite form ideal solutions of their respective iron and magnesium end member molecules, then it should be possible to uniquely determine the pressure and temperature at which the garnet-cordierite pair equilibrated. He used the data of Richardson (1968) to obtain the equilibrium constant for the breakdown reaction of pure Fe-cordierite to garnet + sillimanite +

quartz (reaction 17).

A similar equilibrium constant was calculated for the Mg end member reaction. He proposed that the following relationship could be used to calculate P from the compositions of coexisting garnet and cordierite:

$$P = P^* + (\partial P/2) (x_{\text{Cd}}^{\text{Mg}} + x_{\text{Gt}}^{\text{Mg}}),$$

where $P = 3.138 \times 10^{-3} T \ln K_D$ and P^* is the equilibrium pressure at the calculated temperature for the pure Fe-cordierite breakdown reaction (Richardson, 1968). The results obtained by this method are believed to be accurate to within 500 bars (Currie, 1971). Table 24 shows the results calculated for the Arseno Lake area. All of the pressures calculated represent maximum pressures. It is most probable that the real pressure was lower because none of the samples from this area contained garnet coexisting with sillimanite. Other errors may be introduced by the presence of an average of 10 weight per cent spessartine + grossular end members in the garnets from this area.

Hutcheon et al. (1974) also investigated the potential of the garnet-cordierite pair, in the presence of quartz and sillimanite, as a geobarometer. Their approach was similar to that of Currie (1971), except that they attempted to account for the effect of Mn in cordierite and Mn + Ca in garnet. The relationship that they proposed is shown below:

$$P = \frac{(A G_{(1)}^0 + 293 A F_{(1)}^0 - A V_{(1)}^0)(R \ln K_{(2)} - A S_{(2)}^0) - (R \ln K_{(1)} - A S_{(1)}^0)(A V_{(2)}^0 + 293 A F_{(2)}^0 - A P_{(2)}^0)}{(R \ln K_{(1)} - A S_{(1)}^0) A V_{(2)}^0 - (P \ln K_{(2)} - A S_{(2)}^0) A V_{(1)}^0}$$

The pressures are believed to be accurate to ± 750 bars (Hutcheon et al., 1974).

More recently, Tracey et al. (1975) have re-examined the potential geobarometric usefulness of the garnet-cordierite-sillimanite-quartz assemblage. In their model, they have incorporated the data of Weisbrod (1973 a) in order to estimate the effect of Mn in garnet on the dependence of $K_{D_{Gt-Cd}^{Fe-Mg}}$. They constructed a series of isothermal sections for the temperature range 600 - 750° C., which show what the compositions of garnet would be in equilibrium with cordierite + sillimanite + quartz at various pressures. A compilation of these data is given in Figure 22. If the temperature of garnet-cordierite equilibration is known, pressure can be obtained by plotting the garnet composition on the diagram (Fig. 22) and interpolating the pressure. The accuracy is ± 1 kbar (Thompson, 1975 a).

Garnet-Plagioclase-Al₂SiO₅-Quartz

Ghent (1975), Tracey et al. (1975, in press), and Schmid and Wood (1976) have examined the assemblage garnet-plagioclase-Al₂SiO₅-quartz as a possible geobarometer. The pressure dependence of the distribution of Ca between garnet and plagioclase makes this assemblage potentially useful as a barometer if it can be calibrated.

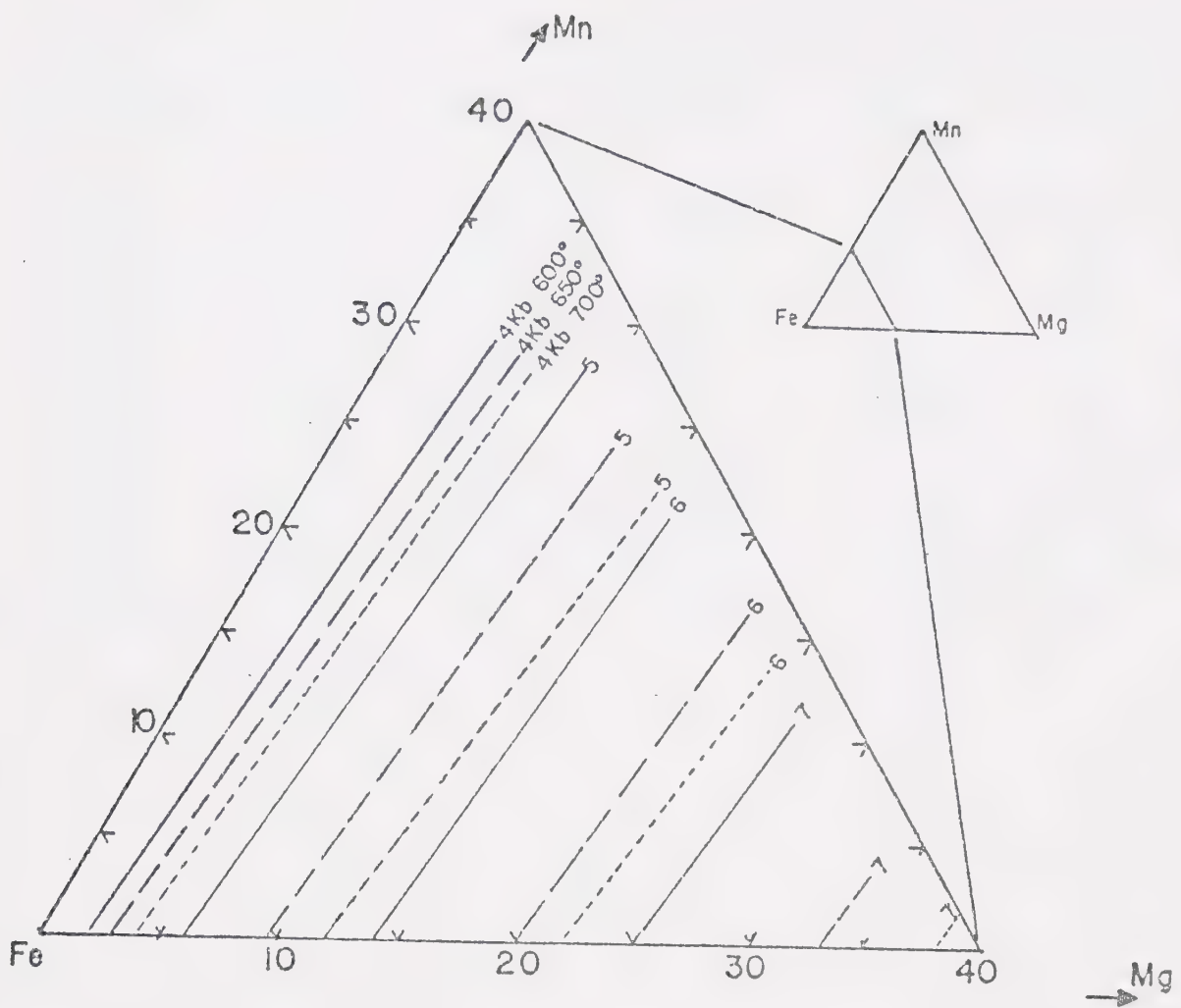


FIGURE 22: Diagram showing the calibration of the garnet- Al_2SiO_5 -quartz barometer. (Modified after Tracey *et al.*, 1975)

TABLE 24 : Pressures calculated using the relationships
 of Currie (1971), Hensen and Green (1973),
 Hutchison et al (1975) and Tracey et al (1975)
 for co-existing garnet and cordierite

Sample Number	Grade Index	Currie	Hutchison et al	Tracey et al	Hensen and Green
73402	2.02	5.76	2.50	6.0	7.5
73153	1.00	4.70	1.50	5.0	8.0
73478	0.93	5.24	2.71	5.5	8.0
73239	0.68	5.91	3.13	6.0	8.2
73202	0.46	5.70	3.27	5.8	8.5
73221	0.33	5.60	3.19	5.5	7.0
73252	0.21	5.60	3.76	5.5	8.0
73245	0.0	5.80	3.71	5.5	8.0
72356	0.0	5.74	3.97	5.5	8.1

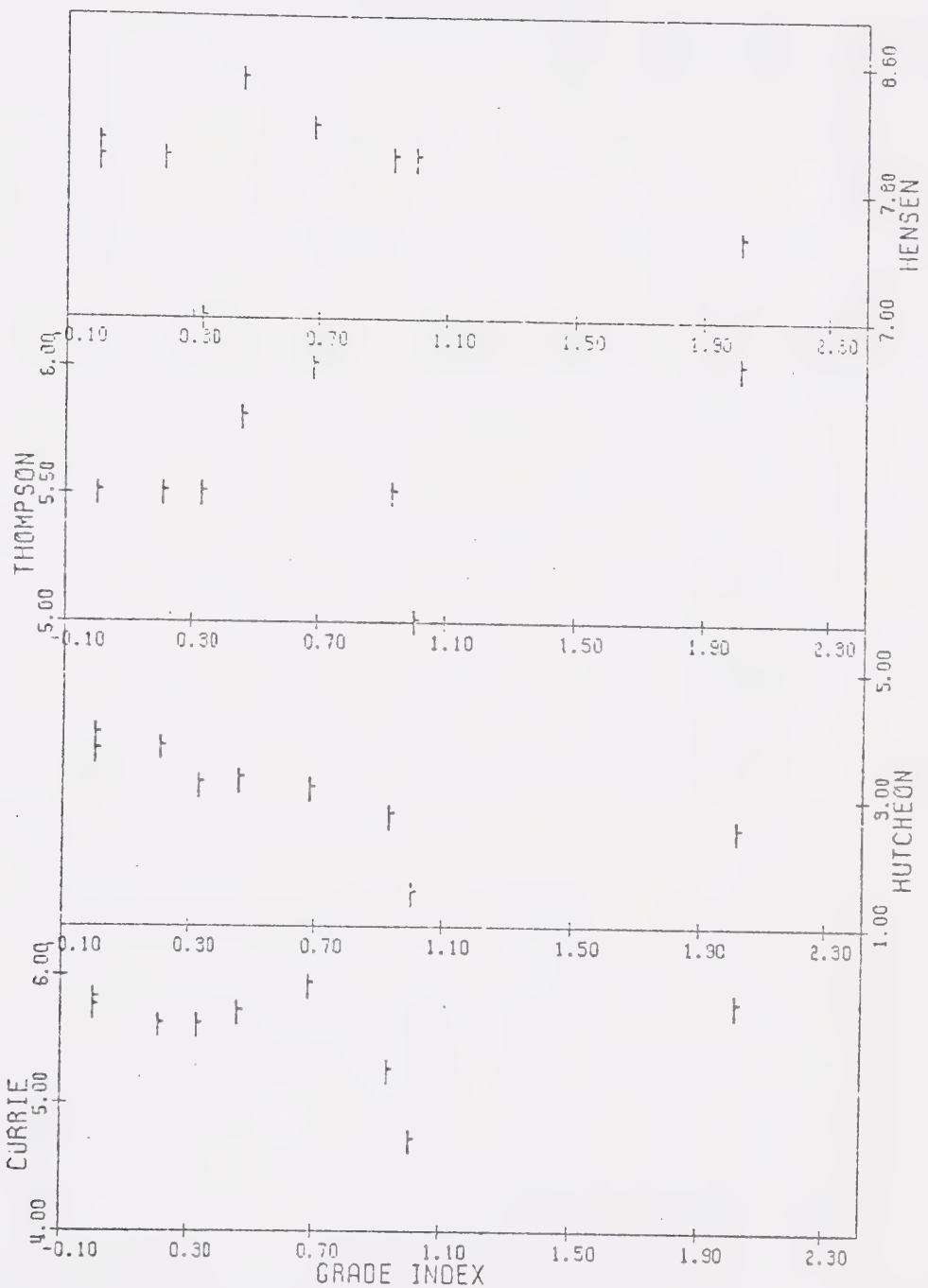


FIGURE 23: Diagram showing the relationship between pressure (kbar) calculated for garnet cordierite pairs and grade index. Pressures were calculated using the data of Currie, 1971 (CURRIE), Hutcheon et al., 1975 (HUTCHEON), Tracey et al., 1975 (THOMPSON), and Hensen and Green, 1972a (HENSEN).

Ghent (1975) used the experimental data of Hays (1967) and Hariya and Kennedy (1968) to calculate the following relationship:

$$G = 0 = \frac{3272}{T} + 8.3969 - \frac{0.3448 (P - 1)}{T} + \log K_D + 3 \log x_{\text{Gt}}^{\text{Ca}} - 3 \log x_{\text{Plag}}^{\text{Ca}}$$

for the reaction:



The above relationship assumes that there is ideal mixing between Ca and (Fe + Mg + Mn) in garnet. The data of Ganguly and Kennedy (1974) on ΔH_{mixing} between garnet end members would increase the estimated pressure for a given temperature. At present, the uncertainty of the calculated P is 'large' (Ghent, 1975). Tracey et al. arrived at similar conclusions regarding the use of this assemblage as a geobarometer.

Evaluation and Discussion

The mineral assemblages which occur in the Arseno Lake area permit the use of the garnet-cordierite geobarometer, with the restriction that the calculated pressures will represent maximum possible values, because Al_2SiO_5 is absent from the cordierite-garnet assemblage.

Garnet-Cordierite-Sillimanite-Quartz. The results obtained from the three pressure-composition relationships proposed by Currie (1971), Hutcheon et al. (1974), and Tracey et al. (1975) are presented in Table 24.

There is a very good agreement between the pressures obtained using the expressions of Currie (1971) and Tracey et al. (1975). The data of Hutcheon et al. (1974) yield much lower pressures which may result, in part, from the assumptions used in their derivation, coupled with the inclusion of Mn and Ca in the calculation of K_1 and K_2 . The other expressions do not consider the presence of Ca in garnet or Mn in cordierite. As will be shown below, the conditions of metamorphism deduced from other evidence appear to be in closer agreement with the calculated pressures using the method of Hutcheon et al. (1974). (Figure 23)

Conclusions. The present data available which relate to the pressure dependence of $K_{D\text{Gt}-\text{Cd}}^{\text{Fe-Mg}}$ and $K_{\text{DPlag-Gt}}^{\text{Ca}}$ are not sufficient to provide a quantitative geobarometer. However, the use of the above relationships appears to be able to show relative changes in pressure in a metamorphic terrain. Further experimental studies and thermochemical investigation of both the garnet-cordierite-sillimanite-quartz and the garnet-plagioclase- Al_2SiO_5 -quartz assemblages is likely to produce more reliable and accurate geobarometric data.

RESTRICTIONS OF PRESSURE AND TEMPERATURES OF METAMORPHISM

Recent experimental studies of several of the commonly observed metamorphic reactions have produced several equilibrium curves which have been used to construct

a pressure-temperature grid for the Arseno Lake area. The restrictions of maximum and minimum pressure and temperature are discussed below. (Figure 24)

The Aluminosilicate Phase Diagram

The position of the aluminosilicate triple point and the position of the andalusite-sillimanite inversion can provide maximum pressure constraints for the cordierite zone rocks of the Arseno Lake area. The location of the triple point has been investigated by several workers (Clark *et al.*, 1957; Bell, 1963; Khitarov *et al.*, 1963; Holm and Kleppa, 1966; Weill, 1966; Althaus, 1967; Richardson, Bell, and Gilbert, 1968; Anderson and Kleppa, 1969; Richardson, Gilbert, and Bell, 1969; Zen, 1969; Holdaway, 1971). The pressure and temperature of the triple point ranged from 8 kbar at 380° C. (Khitarov *et al.*, 1963) to 3.76 kbar and 501° C. (Holdaway, 1971).

It has been argued that the higher pressure values for the triple point are spurious (Zen, 1969; Holdaway, 1971) and may have resulted from improper calibration of the experimental apparatus, intense grinding of the starting mixture (which increases the free energy because of the large surface area contribution), and the presence of impurities, such as V and Fe, which increases the stability field for andalusite (Strens, 1968; Abs-Wurmbach and Langer, 1975). An additional contribution to the higher pressures for the triple point was the presence

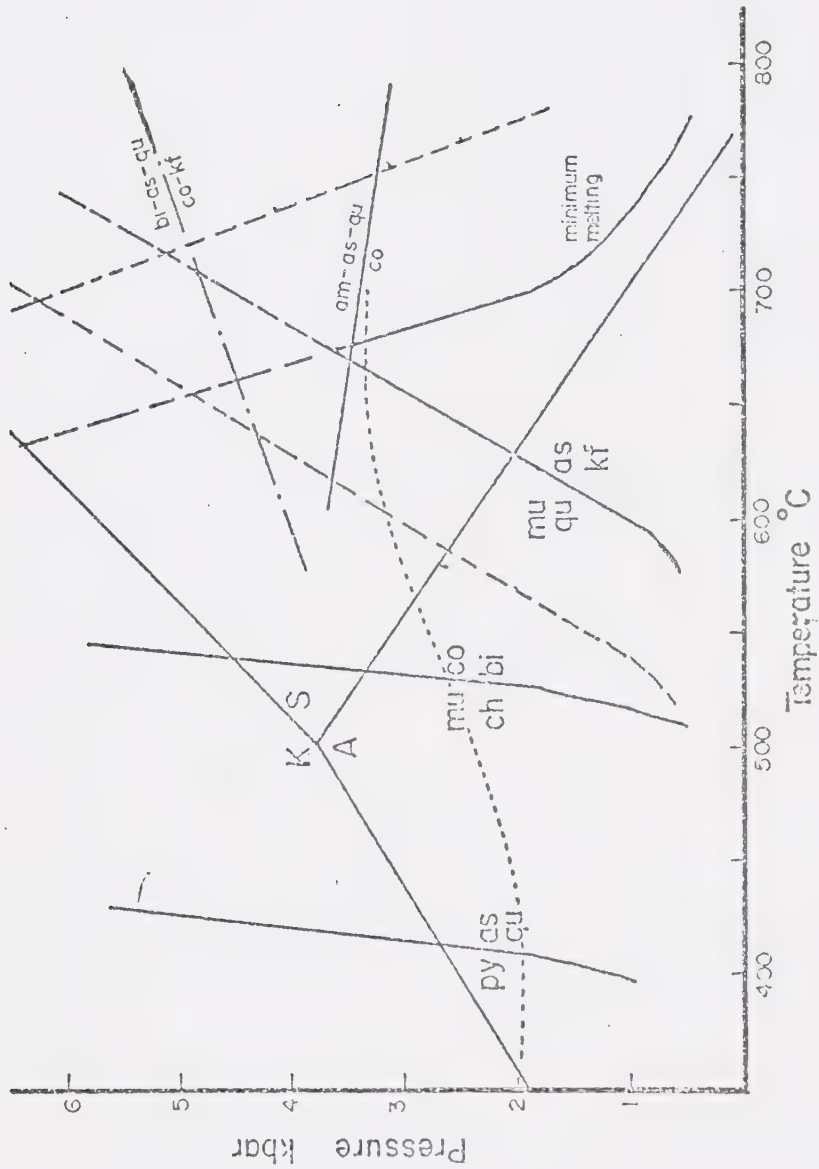


FIGURE 24: Diagram showing the experimentally determined equilibria used to define the pressure-temperature conditions of metamorphism in the Arseno Lake area. The dotted line shows the inferred P-T trajectory. py = pyrophyllite, as = aluminosilicate, qu = quartz, mu = muscovite, ch = chlorite, co = cordierite, kf = K-feldspar, am = garnet, A = andalusite, S = sillimanite, K = kyanite

of the fibrous variety of sillimanite used in studying the andalusite-sillimanite inversion. Holdaway (1971) suggested that the presence of fibrolite raises the entropy of the sillimanite in which it is included. This small entropy increase would be enough to displace the andalusite-sillimanite equilibrium to higher pressures by increasing the experimentally determined $\Delta S/\Delta T$ slope, because the entropy difference between andalusite and sillimanite is very small (0.7 cal./deg. mole, Pankratz and Kelley, 1964).

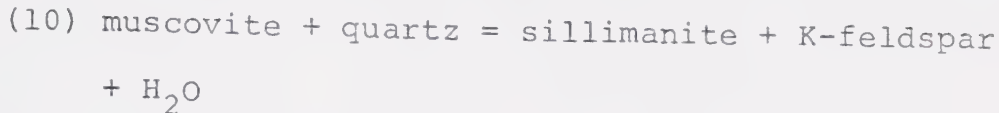
The experimental method employed by Holdaway minimized the effects of the problems discussed above, and for this reason, the aluminosilicate diagram reported by Holdaway (1971) was used in this study.

Dehydration Reactions

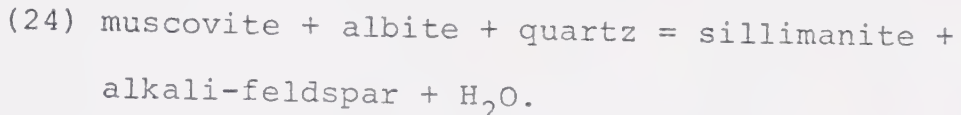
The most common type of reaction observed in pro-grade metamorphosed pelitic rocks is that of dehydration. Several dehydration reactions have been experimentally investigated. The most important of these, for this area, are discussed below.

Muscovite Breakdown. The decomposition of muscovite in the presence of quartz to sillimanite + K-feldspar + H_2O has been studied by Evans (1965), Velde (1965), Althaus *et al.* (1970), and Kerrick (1972). Evans' and Velde's experiments were conducted at $P_{H_2O} = P_{\text{total}}$; Kerrick studied the reaction under conditions of $P_{H_2O} <$

P_{total} . The experimentally determined reaction,



is probably modified in pelitic rocks by the presence of plagioclase. Evans and Guidotti (1965) suggested that the reaction that occurs in natural systems is:



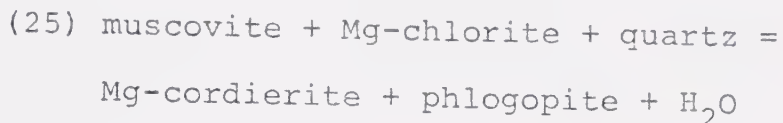
Under conditions of $P_{\text{H}_2\text{O}} = P_{\text{total}}$, the muscovite breakdown reaction is terminated at about 650° C. and 3.5 kbar by intersection with the wet granite solidus (minimum melt curve) (Winkler, 1965; Kerrick, 1972). At temperatures greater than about 650° C. and $P_{\text{H}_2\text{O}} > 3.5$ kbar, the dehydration of muscovite would be accompanied by anatexis and the formation of in situ migmatites.

The minimum pressure for the Arseno Lake area may be determined from the intersection of the muscovite decomposition curve with the andalusite-sillimanite boundary. At $P_{\text{H}_2\text{O}} = P_{\text{total}}$, these conditions are 2.1 kbar at 625° C. If $P_{\text{H}_2\text{O}} < P_{\text{total}}$, then the minimum pressure would increase and the corresponding temperature would decrease (see Kerrick, 1972).

Chlorite Breakdown. The stability of chlorite in the presence of quartz and quartz plus muscovite has been investigated by several workers. The phase relations of chlorite + muscovite + quartz are pertinent to this

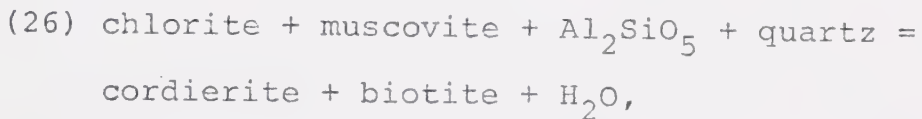
study because of their common occurrence in metapelites.

The results of Schreyer and Seifert (1969), Siefert (1970), and Bird and Fawcett (1973) are discussed below. All of these authors investigated the stability of chlorite in the system $K_2O-MgO-Al_2O_3-SiO_2-H_2O$ at $P_{H_2O} = P_{total}$, in the pressure range of 1.0 - 8.6 kbar. The equilibrium curve for the reaction:



is shown on Figure 24.

As discussed by Siefert and Bird and Fawcett, this equilibrium curve represents the maximum stability of muscovite + chlorite + quartz. The addition of FeO, which can substitute for Mg in chlorite, cordierite, and phlogopite, would alter the above phase relations in two ways, by the introduction of new phases and/or by altering the composition of phases already present, thereby changing the equilibrium conditions of the reactions. Siefert (1970) also discussed an additional reaction, which would occur in an iron bearing system:

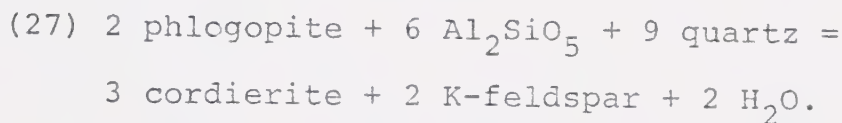


which would occur at lower temperatures than reaction (25).

Hirschberg and Winkler (1968) investigated the stability of chlorite in an iron bearing system and found that for a range of Mg/Fe ratios, the position of the

equilibrium curve was shifted very little, and was located at lower temperatures than the equivalent reaction in the iron free system. This curve probably represents the minimum temperature of formation of cordierite in the Arseno Lake area. The position of the cordierite isograd is therefore considered to be $525^\circ \pm 50^\circ$ C. The precise value of the temperature would be a function of the compositions of the chlorite, muscovite, biotite, and cordierite involved in the reaction, as well as the partial pressure of H_2O .

Biotite Breakdown. Biotite is stable from its first appearance as a product of the disappearance of chlorite, up to conditions above the dehydration of muscovite plus quartz. Schreyer and Siefert (1969) studied the reaction:



This reaction has a rather low $\partial P/\partial T$ slope and, as such, can provide a maximum pressure estimate for the higher grade portion of the Arseno Lake area. In an iron bearing system, the reaction would probably occur at lower pressures, if it is assumed that the effect of iron in this reaction is similar to its effect in the cordierite breakdown reaction, to garnet + sillimanite + quartz (Schreyer and Siefert, 1970; Weisbrod, 1973 b).

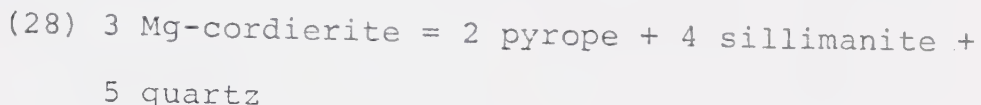
Anatexis

The absence of large scale anatexis in the Arseno Lake area is an additional control on the pressure and temperature conditions of metamorphism. Under conditions of $P_{H_2O} = P_{total}$, the minimum melting curve intersects the muscovite + quartz dehydration reaction at approximately 660° C. and 3.5 kbar. If an additional component (i.e., CO_2) was present in the fluid phase, then this intersection would move to higher values of pressure and temperature. Under the conditions of $X_{H_2O} = 0.6$, this intersection occurs at 690° C. and 6.25 kbar (Kerrick, 1972). Thus, if an estimate of X_{H_2O} in the fluid is available, the absence of anatexis (as provided by the scarcity of in situ migmatites) places a restriction on the conditions of metamorphism.

Cordierite Stability

The presence of cordierite in all but the most aluminum poor rocks up to the highest grade of metamorphism observed also provides restrictions on the conditions of metamorphism. Cordierite stability is a function of the Fe/Mg ratio. Several workers have investigated the stability of the pure iron and pure magnesium end member cordierite solid solution series. It has been shown that pure Fe-cordierite decomposes to almandine + sillimanite + quartz under conditions of $P_{total} = 3.7$ kbar at 550° C. to 3.3 kbar at 750° C. (Weisbrod,

1973 b). Pure Mg-cordierite is stable to much higher pressures and temperatures, but the reaction itself:



has not been determined experimentally because it is metastable over the temperature and pressure range of granulite and upper amphibolite grade metamorphism.

The reaction:



occurs at the breakdown of pure Mg-cordierite (Newton, 1972).

As mentioned in the discussion of biotite breakdown, the assemblage cordierite plus K-feldspar indicates the maximum pressure attained in the Arseno Lake area.

Oxygen Fugacity

The mineral assemblages from the Arseno Lake area provide an estimate of f_{O_2} during metamorphism. Magnetite has not been observed and in several thin sections, graphite was identified. The spinels from the remobilised Archean paragneiss contain less than 5 mole per cent magnetite. (The method of calculation of Fe_2O_3 in spinel is given in the Appendix.) With this information and an estimate of the temperature and pressure prevailing during metamorphism, it is possible to calculate the fugacity of oxygen.

Several methods are available to calculate this.

The first method is to assume that f_{O_2} was consistent with the stability of wustite. The range of f_{O_2} then would correspond to the conditions described by the magnetite-wustite buffer and the wustite-iron buffer for a given set of P_{total} -T conditions. The following two relations are from Eugster and Wones (1962):

(a) magnetite-wustite buffer:

$$\log f_{O_2} = \frac{-32730}{T} + 13.12 + \frac{0.083 (P - 1)}{T}$$

(b) wustite-iron buffer:

$$\log f_{O_2} = \frac{-27215}{T} + 6.57 + \frac{0.055 (P - 1)}{T}$$

The second method is to use the equilibrium data for the magnetite-hercynite solid solution series (Turnock and Eugster, 1962). Giving a maximum value of 5% Fe_3O_4 content to the spinels, and neglecting their Mg and Zn content as a first approximation, the f_{O_2} stability field at 650° C. would be:

$$24.7 \leq -\log f_{O_2} \leq 21.7, \text{ (by interpolation from T\&E, 1962)}$$

A third method is to use the data of French and Eugster (1965) on the C-O system. French and Eugster have shown that the C-O system operates as a buffer. The f_{O_2} for all P-T conditions was defined at the following value:

$$\log f_{O_2} = \frac{-20586}{T} - 0.044 + \log P - \frac{0.028 (P - 1)}{T}$$

The f_{O_2} results obtained from the above relationships are presented in Table 25.

TABLE 25 : Estimated limits of oxygen fugacity based on

Sample Number	Grade Index	Calculated Temperature	Estimated Pressure	M-W	WI	Mt Max	- Hc Min	C-O	maximum estimated fO_2
73377	2.05	620	3.0	-23.3	-23.7	-26.0	-22.9	-19.7	-23
7347	1.07	630	3.1	-24.7	-24.9	-25.9	-22.8	-20.7	-24
73153	1.0	550	3.1	-26.3	-26.3	-29.5	-25.4	-21.7	-26
73501	.76	585	3.2	-24.7	-24.9	-28.1	-24.5	-20.6	-24
73239	.68	565	3.0	-25.6	-24.8	-27.1	-24.1	-20.5	-24
73157	.54	575	3.0	-26.8	-26.7	-29.6	-26.7	-22.0	-26
73208	.50	580	2.9	-25.0	-25.1	-28.3	-24.7	-20.8	-25
73205	.50	580	2.85	-25.0	-28.2	-28.3	-24.7	-20.8	-25
73221	.33	630	3.2	-21.7	-22.4	-24.7	-21.7	-18.7	-21
72345	.0	660	3.5	-21.6	-22.4	-24.7	-21.7	-18.6	-21
72356	.0	680	3.5	-20.9	-21.8	-23.9	-20.9	-18.1	-20

M magnetite

W wustite

I iron

Mt-IIc magnetite-hercynite

Comparison of the maximum f_{O_2} likely to have occurred with the minimum f_{O_2} which would have been maintained by the C-O system, indicates that an additional component is needed in the fluid phase to buffer f_{O_2} to the values estimated for the Arseno Lake area.

French (1966) studied the system C-O-H and noted the following relationships:

1. When H is added to the C-O system, f_{O_2} decreases for a fixed total pressure and temperature.
2. For a given set of f_{O_2} -T conditions, an increase in pressure favors a more reduced gas phase, richer in CH_4 .
3. For a given set of f_{O_2} -P conditions, an increase in temperature favors a more oxidized gas phase, richer in H_2O and CO_2 .

From these observations, it is suggested that the H_2O released during the dehydration reactions dissociated and lowered the f_{O_2} in the overlying rocks in the Arseno Lake area to the approximate values shown on Table 25.

THE NATURE OF THE HEAT SOURCE

The metamorphism of the Snare Group and remobilised Archean ortho- and paragneisses, while analogous to the Abukuma facies series, is not strictly a regional event. As shown by the distribution of the observed

mineral assemblages (Fig. 4), the high grade metamorphism in the western half of the Arseno Lake area was superimposed upon a low grade greenschist facies (biotite zone) metamorphism, which extends along the whole length of the Snare Group sedimentary belt (Ross and McGlynn, 1965).

The cordierite-amphibolite facies assemblages form an asymmetric surface, with isograds more closely spaced in the south and southeast than in the north and northeast. The arrangement of isograds deduced from the observed spatial distribution of these mineral assemblages suggests that the high grade metamorphic area was formed around a Proterozoic pluton, emplaced at a depth of 10 - 14 km in the crust. This granitoid pluton would account for the updoming of the Archean basement ortho- and paragneisses observed in this area. As it cooled and crystallized, it would have acted as a long lived heat source and would have set up the thermal gradient suggested by the results obtained from garnet-biotite and garnet-cordierite thermometry.

The central part of the high grade terrain is thought to have formed nearest to the contact of the proposed pluton. The thermal center has been defined by the area bounded by samples 72356, 73178, and 72345. These three samples all contain spinel with less than 1.6 mole per cent gahnite and, as has been shown above,

represent spinel that equilibrated with cordierite at the highest temperatures. This choice for the thermal center is substantiated by the fact that these samples gave the highest relative temperatures when garnet-cordierite and garnet-biotite geothermometry was used.

The initial temperature of the pluton, the length of time that it could have provided heat to the host rocks, and the total quantity of heat available to the host rocks are functions of its composition, volume, and the amount of H_2O dissolved within it. A magma that was of granitoid composition, similar to the Hepburn Batholith, and which was undersaturated with H_2O , could have had an initial temperature in excess of 850 - 900° C. The rate that it would cool and the equilibrium thermal gradient that would be established would be a function of the mechanism of heat transfer and the volume of the pluton. If most of the heat was transferred by conduction, then the cooling period could be quite long and the peak temperatures reached in the host rocks could have reached the value of 680 - 700° C., as suggested by garnet-cordierite geothermometry near the thermal center.

THE CONDITIONS OF METAMORPHISM IN THE ARSENO LAKE AREA

The conditions of metamorphism in the Arseno Lake area are discussed below. The results which are presented are based on the restrictions outlined above and on the pressure-temperature values calculated using the P-T-X

relations for biotite, garnet, and cordierite. Table 26 summarizes the $P_{\text{total}} - P_{\text{H}_2\text{O}} - T$ conditions estimated from the biotite zone to the thermal center.

The Biotite Zone

Pressure and temperature conditions of the biotite zone appear to have ranged from approximately 350° C. at 2.0 kbar for the biotite isograd to 530° C. at 3 kbar, which marks the beginning of the cordierite zone. The conditions attained in the lower part of the biotite zone are limited in part by a single occurrence of andalusite found only 0.2 km above the biotite isograd. The sample is a fine grained graphitic slate containing several large porphyroblasts of andalusite, with quartz along the porphyroblast margins. This andalusite may have formed by the reaction:



which was investigated by Hemley (1967) and Kerrick (1968). At pressures greater than 2.6 kbar, kyanite would form instead of andalusite.

Garnets in the middle of the biotite zone yield temperatures of 420 - 505° C., using the garnet-biotite geothermometer of Thompson (1976 a,b). The pressure in the upper part of the biotite zone is limited by the absence of kyanite and the fact that andalusite is the stable Al_2SiO_5 polymorph. The conditions at the end of the biotite zone, at the cordierite isograd, are

TABLE 26: Pressure-temperature conditions of metamorphism for the Arseno Lake area.

Mineral zone	Temperature ¹ range	Pressure ² X_{H_2O} ³	Controls and restrictions ⁴
Chlorite	≤ 350	≈ 2	ch+mu/bi
Biotite	350-530	2.0-2.5	as triple point, py/as+qu on AS, ch+mu+qu/co+bi on AS
Cordierite andalusite	530-560	2.5-3.0	as triple point, ch+mu+qu/co+bi on AS, AS boundary
Cordierite sillimanite	560-600	3.0-3.2	ch+mu+qu/co+bi on AS, mu+qu/S+kf
Sillimanite K-feldspar	600-650	3.1-3.3	mu+qu/S+kf, bi+s+qu/co+kf
Almandine cordierite K-feldspar	≥ 630	≥ 3.2	bi+s+qu/co+kf, bi+s+qu/co+am+kf, co/am+s+qu

1-Temperatures are $\pm 50^{\circ}\text{C}$.

2-Pressures are ± 500 bars.

3-Where $X_{H_2O} < 1$, the probable error is ± 0.2 .

4-Abbreviations are the same as those in Figure 24.
The sequence of minerals is REACTANTS/PRODUCTS.

similarly limited by the observation that andalusite, and not sillimanite, accompanies cordierite and biotite as the product of reaction (8).

The Cordierite-Andalusite Zone

Pressure and temperature conditions of the cordierite-andalusite zone appear to have ranged from 530° C. at 3 kbar for the first appearance of cordierite, to approximately 560° C. at 3.2 kbar where sillimanite first appears. The limits on pressure are defined by the observed order of appearance:



At pressures greater than about 3.4 kbar, the equilibrium curve for the reaction:



as determined by Hirschberg and Winkler (1968), intersects the andalusite-sillimanite transition and the stable Al_2SiO_5 polymorph would be sillimanite. Therefore, the maximum pressure attained in the cordierite-andalusite zone was less than 3.4 kbar. The temperatures are probably accurate to within $\pm 20^\circ \text{ C}$. because the cordierite forming reaction has a large $\partial P/\partial T$ slope and the observed change in equilibrium temperature for experimental runs at two and four kilobars was 10° C . Similarly, the andalusite-sillimanite curve is insensitive

to variations in X_{H_2O} , because it is a phase transformation, not a dehydration reaction.

The Cordierite-Sillimanite Zone

Pressure and temperature conditions of the cordierite-sillimanite zone appear to have ranged from approximately 560° C. at 3.2 kbar to 625° C. at 3.25 to 3.3 kbar. The upper limit of the cordierite-sillimanite zone is defined as the second sillimanite isograd. The lower pressure-temperature estimate is probably accurate to $\pm 20^\circ$ C. and ± 400 bars, but the conditions for the second sillimanite isograd are less well determined. Evidence from fluid inclusions suggests that CO_2 was a significant component of the metamorphic fluid. On the basis of this evidence and the field observation that the cordierite + muscovite + sillimanite zone is quite narrow (≤ 0.75 km), the conditions estimated lie between those for the muscovite dehydration reaction at $P_{H_2O} = P_{total}$ and $P_{H_2O} = 0.6 P_{total}$ (Kerrick, 1972).

The Biotite-Cordierite-K-Feldspar-Sillimanite Zone

The biotite-cordierite-K-feldspar-sillimanite zone begins at the second sillimanite isograd and continues to the cordierite-almandine-K-feldspar zone. Pressure-temperature conditions appear to have varied from approximately 625° C. at 3.3 kbar to 670° C. at 3.5 kbar. In this zone, the assemblage biotite + sillimanite + quartz reacts to form cordierite +

K-feldspar (reaction 27). Maximum pressures are limited by the stability of cordierite + K-feldspar, and by the absence of the assemblage garnet + sillimanite + quartz, which would form at pressures greater than 3.7 kbar at 625° C. and 3.6 kbar at 670° C., in the system pure Fe-cordierite-almandine (Weisbrod, 1973 b). In the magnesium bearing system, this pressure limit would be higher (Hirschberg and Winkler, 1968). The uncertainties of these estimates are probably about $\pm 50^\circ$ C. and ± 400 bars.

Fluid inclusions in quartz from this zone are CO₂ rich, suggesting that X_{H₂O} < 1. The actual value of X_{H₂O} is not known and is critical in assessing the temperatures across this zone.

The Cordierite-Almandine-K-Feldspar Zone

Pressure-temperature conditions across the cordierite-almandine-K-feldspar zone apparently ranged from about 670° C. $\pm 50^\circ$ at 3.5 ± 0.5 kbar, to approximately 700° C. $\pm 50^\circ$ at 3.6 ± 0.5 kbar. All of the observed primary fluid inclusions from this area were essentially pure CO₂. Under these conditions, the biotite + sillimanite + quartz dehydration reaction to garnet + K-feldspar + H₂O \pm cordierite would have proceeded at lower temperatures than those suggested by Hess (1969, Fig. 3). The estimated temperatures are within the uncertainty of the temperatures calculated from garnet-biotite and

garnet-cordierite geothermometry.

Origin of the CO₂ Rich Fluid Phase

Fluid inclusion observations (see Table 20), as well as interpretation of the distribution of mineral assemblages, indicates that the metamorphic fluid in the high grade zones was composed mainly of CO₂. The origin and development of such a fluid in the Arseno Lake area is discussed below. The absence of graphite in many samples indicates that CO₂ was introduced to these samples from an external source. At the same time, a mechanism is needed which would permit the H₂O, which was released during dehydration reactions, to escape from the system. Three possible models are discussed below:

1. Due to the nature of the heat source for the metamorphism and its relatively localized nature, the H₂O which was evolved during dehydration reactions could have moved down the thermal gradient to the lower temperature regions of the gneiss dome.
2. The presence of large volumes of pre-Hudsonian high grade (granulite) metamorphites in the western part of the area may have acted as a sink for H₂O produced during the Hudsonian metamor-

phism. It also could have been a source for a relatively anhydrous fluid which could mix with the H_2O rich fluid. Such an anhydrous fluid might be rich in CH_4 and CO_2 , as shown by studies of fluid inclusions in granulite facies rocks (Touret, 1971; Hollister, 1975; Hollister and Burruss, 1976).

3. The emplacement of the heat source into the basal siliceous dolomite blanket present across the Aphebian sedimentary basin, would have initiated decarbonation reactions. The CO_2 evolved during this reaction series could then be flushed out of the system and up through the overlying argillaceous sediments, which were undergoing dehydration reactions. This would consequently affect the dilution of the H_2O in the fluid phase.
4. The formation of minor amounts of granitic melt would have preferentially taken in the H_2O in the fluid phase, thereby reducing X_{H_2O} .

As is shown in the block diagram (Fig. 25), the most likely mechanism for reducing X_{H_2O} below one is a

combination of 1. and 3. Thus CO₂ would have migrated down a thermal and pressure gradient, diluting the H₂O rich fluid which was formed during release of pore water and structural water in the overlying pelitic and psammitic metasediments.

The density difference between a supercritical H₂O rich fluid and a supercritical CO₂ rich fluid could also serve to deplete the metamorphic fluid of H₂O and increase CO₂ in the residual fluid.

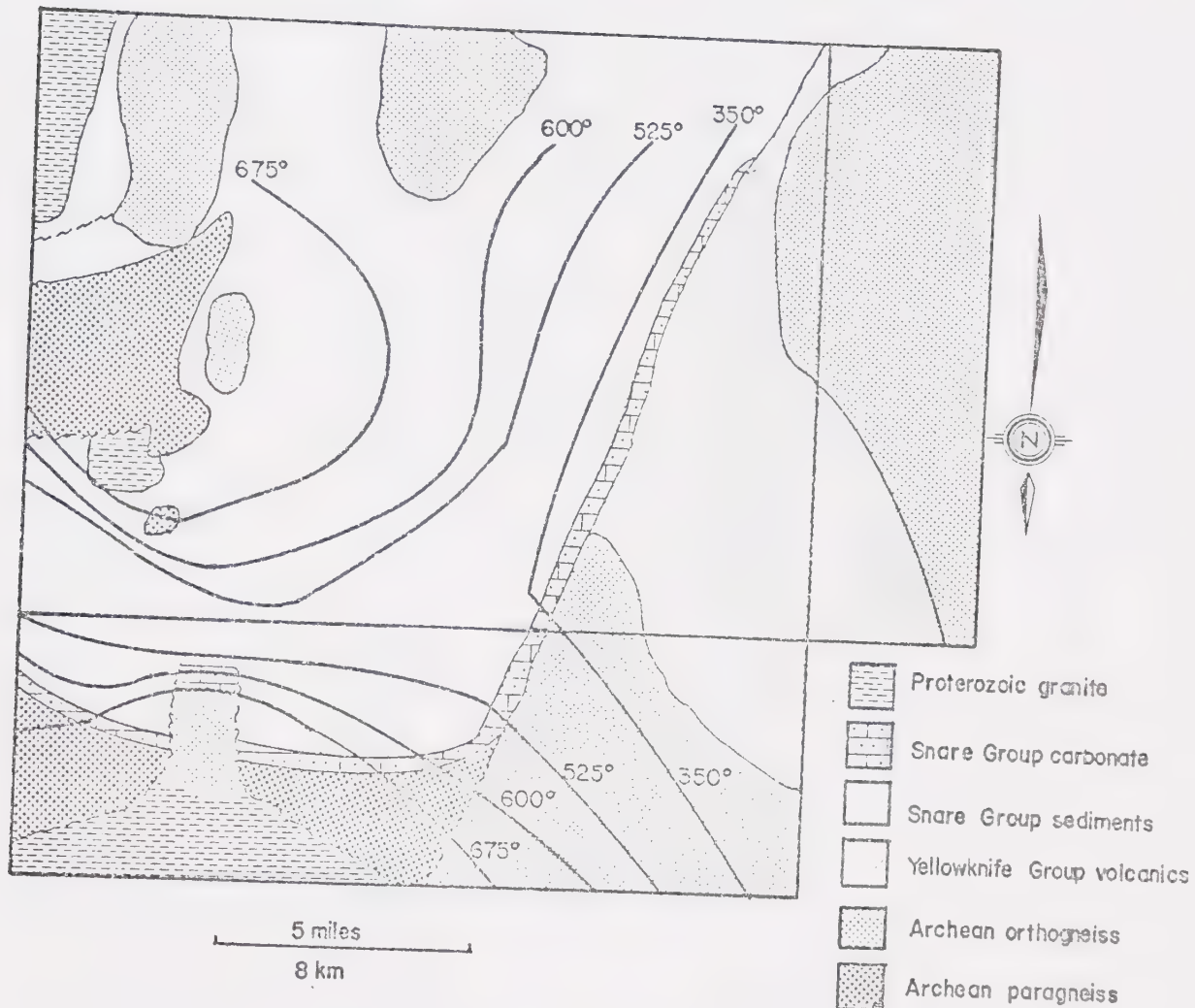


FIGURE 25: Block diagram showing the hypothetical distribution of lithologies and isotherms for the Arseno Lake area. Vertical exaggeration is x 10.

TABLE 27: Bulk rock analyses from the Arseno Lake area

Sample Number	727	7255G	72364	72345
Grade Index	2.87	1.99	1.20	0
SiO ₂	59.18	66.00	61.95	69.26
TiO ₂	1.25	0.65	0.75	0.73
Al ₂ O ₃	24.34	12.88	19.73	15.86
Fe ₂ O ₃	0.74	1.67	1.05	0.48
FeO	5.60	9.09	4.80	4.61
MnO	0.05	0.15	0.03	0.14
MgO	1.99	2.89	2.24	2.51
CaO	0.21	1.80	0.73	1.25
Na ₂ O	0.80	1.44	1.82	1.10
K ₂ O	3.10	1.84	3.96	2.72
P ₂ O ₅	0.14	0.12	0.07	0.21
H ₂ O-	0.16	0.21	0.34	0.24
H ₂ O+	2.32	1.43	1.84	1.04
S	ND	ND	0.42	ND
Total	99.88	100.17	100.28	100.15
Fe ⁺³ /Fe ⁺²	0.059	0.083	0.098	0.047
K/Na	2.55	0.84	1.43	1.63
Fe ⁺² /Mg	1.58	1.76	1.20	1.03
Zn*	ND	ND	ND	120
Cu*	ND	ND	ND	12
Co*	ND	ND	ND	320
Cr*	ND	ND	ND	200

*ppm

ND = not determined

G = spessartine rich garnet present

PART IV: SUMMARY AND CONCLUSIONS

The metamorphosed Proterozoic Snare Group sediments (Lord, 1942) and polymetamorphic remobilised Archean paragneisses from the Arseno Lake area were examined. Variation in mineral composition and the sequence of mineral assemblages from the Snare Group metasediments are typical of the 'low pressure' facies series of Miyashiro (1961). A comparison of the Arseno Lake area with the central Abukuma plateau was presented on Table 19 (Part III, Page 128).

The following isograds have been identified, based on the mineral assemblages observed in thin section and the spatial distribution of these assemblages across the study area.

- 1) Biotite in
- 2) Andalusite in
- 3) Cordierite in - muscovite + chlorite out
- 4) Sillimanite in - andalusite out
- 5) Sillimanite and K-feldspar in-muscovite
+ quartz out
- 6) Almandine and K-feldspar ± cordierite in -
biotite + sillimanite out

In the case of isograds 3-5, the reactant assemblages are totally consumed: Isograd 6 is marked as the first appearance of garnet + K-feldspar ± cordierite. Biotite is never completely consumed although it is not

found co-existing with sillimanite in the area above Isograd 6.

Individual reactions producing biotites, cordierite, and garnet have not been written in a quantitative manner because there is:

- 1) variation in reactant mineral composition (Fe/Mg, Al/Fe + Mg) resulting from variation in bulk rock composition
- 2) variation in reactant mineral composition due to the very small scale of equilibration (~1.5 - 2 mm) above the sillimanite isograd
- 3) variation in the rate of diffusion of components within individual phases (self-diffusion) and between phases (intergranular diffusion).

CONTROLS ON MINERAL COMPOSITION

The mineral chemical data presented in Part II provide information on the roles of the modifying controls on mineral composition. Discussion is limited to the ferromagnesian minerals biotite, cordierite and almandine, in the metamorphosed Snare Group. Spinel is an additional phase considered in the remobilised Archean paragneiss. For minerals such as rutile, ilmenite, and the alumino-silicates, andalusite and sillimanite, the permissive controls are sufficient to define their presence and composition.

Biotite. In the biotite zone, where biotite is the dominant ferro-magnesian phase, bulk rock composition is the major factor controlling biotite composition. The presence of chlorite as an additional Fe-Mg phase modifies the biotite composition to favor an Mg richer chlorite and an Fe rich biotite. As chlorite reacts with muscovite to produce biotite, there is a decrease in the Fe/Mg ratio of biotite.

In the cordierite zone, biotite composition is still mainly controlled by the bulk rock Fe/Mg ratio, but continuous Fe-Mg exchange between biotite and cordierite, and the breakdown of ilmenite to release Fe to the silicates, modifies the biotite composition. (see reaction 8 and 9, Part II, Page 73).

Biotite from the cordierite-almandine-K-feldspar zone has its composition controlled by Fe-Mg exchange with cordierite and with garnet. Growth rates and rates of intergranular and selfdiffusion are additional modifying controls in this zone. The CO_2 rich fluid phase present during the re-crystallisation of this zone restricted the rates of intergranular diffusion and resulted in small scale equilibration and heterogeneous biotite composition from grain to grain. The exact composition was a function of the local mineral assemblage around the biotite.

Cordierite. As discussed above, cordierite compositions in the cordierite zone is determined by a continuous

exchange reaction of Fe and Mg with biotite. For a given thin section, cordierite is homogeneous, but variations in bulk rock composition produce different cordierite compositions.

In the cordierite-almandine-K-feldspar zone, the most important control of cordierite composition was Fe-Mg exchange with biotite and garnet. As in the case of biotite from this zone, individual grains of cordierite are homogeneous, but there is a variation in Fe/Mg and Si/Al^{IV} between grains in the same sample. Here, too, the local mineral assemblage surrounding cordierite and the slow rate of intergranular diffusion controls the exact composition.

In samples from the remobilised Archean paragneiss, two reactions produced cordierite and these two types of cordierite show different compositions. This heterogeneity is attributed to slow rates of intergranular diffusion of Fe and Mg and to the nature of the phases producing cordierite. The first (reactions 12 and/or 16) results in cordierite similar to that from the cordierite-almandine-K-feldspar zone, and the major control of cordierite composition was Fe,Mg exchange with biotite. The situation is complicated by the preservation of the Al^{IV}/Si ratio, which appears to be a relic of the Archean metamorphism (Part II, page 102-107). The second cordierite producing reaction (reaction 19) resulted in cordierite with different Fe/Mg ratios and different Si/Al^{IV} ratios. The cordierite

composition here is determined by Fe-Mg exchange with spinel and by the amount of spinel which has reacted.

Garnet. The two types of garnet from the Arseno Lake area apparently reflect different controls of composition. Garnet formed in the biotite zone is characterised by high MnO content and displays prograde zoning with an increase in Mg and Fe and a decrease in Mn and Ca towards the rim. These garnets apparently nucleated because of the presence of Mn released by the breakdown of the pyrophanite component ($MnTiO_3$) of ilmenite. Thus, the MnO content may have permitted the formation of garnet. Its composition was then modified by exchange of Fe and Mg with biotite and chlorite. As temperature increased and the amount of MnO available decreased, the garnet became progressively enriched in Fe and Mg.

Garnet from the almandine-cordierite-K-feldspar zone is characterised by an Fe-Mg rich core and displays a retrograde increase of Mn and Ca towards the rim. This reflects slow, late stage Mg-Fe exchange with biotite and cordierite. This is somewhat complicated by the late reaction of garnet and K-feldspar + H_2O to produce retrograde biotite, as well as by Ca loss to plagioclase feldspar.

Spinel. The spinels observed in this study do not exhibit compositional zoning. This results in part from their fine grain size. These spinels show a progressive

Zn enrichment with decreasing grade of metamorphism. As discussed above, this Zn enrichment is apparently a direct result of the modal decrease in spinel at lower metamorphic grade, coupled with a strong site preference for zinc in spinel. Inspection of Figure 17 shows that the Zn content of spinel is independent of the Fe/Mg ratio and the magnetite content.

Thus, spinel composition is determined by the amount of spinel present, which is reflected in the Zn content, and by Fe-Mg exchange with the cordierite host in which it is preserved. The role of Zn in stabilizing spinel may be analogous to that of Mn in biotite zone garnets.

The Cordierite Amphibolite Facies

Figure 26 depicts the phase relations between microcline, sillimanite and the ferro-magnesian minerals observed in the A-K-F-M tetrahedron. Figures 27-28 present analysed co-existing minerals from the cordierite-almandine-K-feldspar zone and the remobilised Archean paragneisses plotted on the A'F'M' projection through K-feldspar. These diagrams show the progressive compositional changes of co-existing biotite-cordierite-garnet assemblages in response to changing metamorphic conditions. In both the cordierite-almandine-K-feldspar zone and the remobilised Archean paragneiss, the 3 phase triangles and 2 phase tie lines involving biotite, cordierite and/or garnet show a

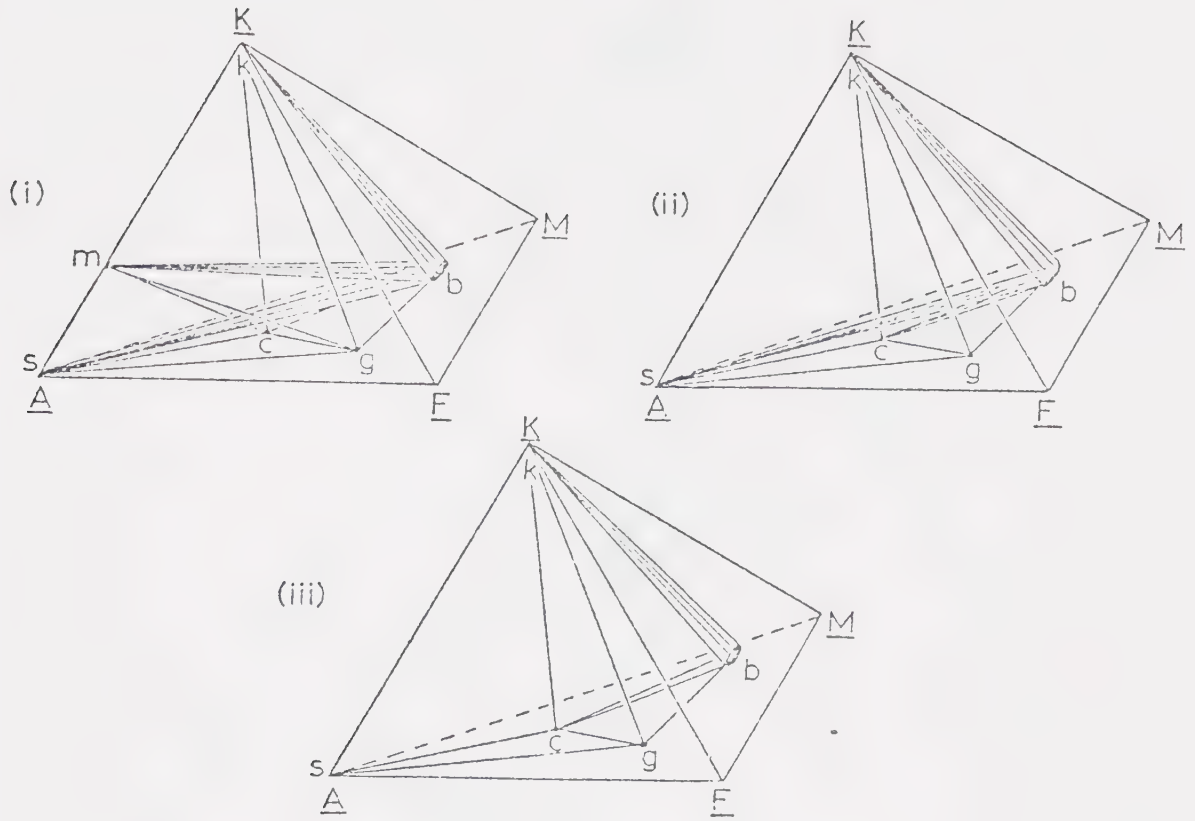


FIGURE 26: Diagram illustrating the phase relations in the AKFM tetrahedron between K-feldspar (k), muscovite (m), sillimanite (s), biotite (b), cordierite (c), and garnet (g):

- (i) at conditions below the muscovite + quartz breakdown
 - (ii) above the muscovite + quartz breakdown, below the biotite + sillimanite breakdown
 - (iii) above the biotite + sillimanite breakdown.
- (From Harris, 1976)

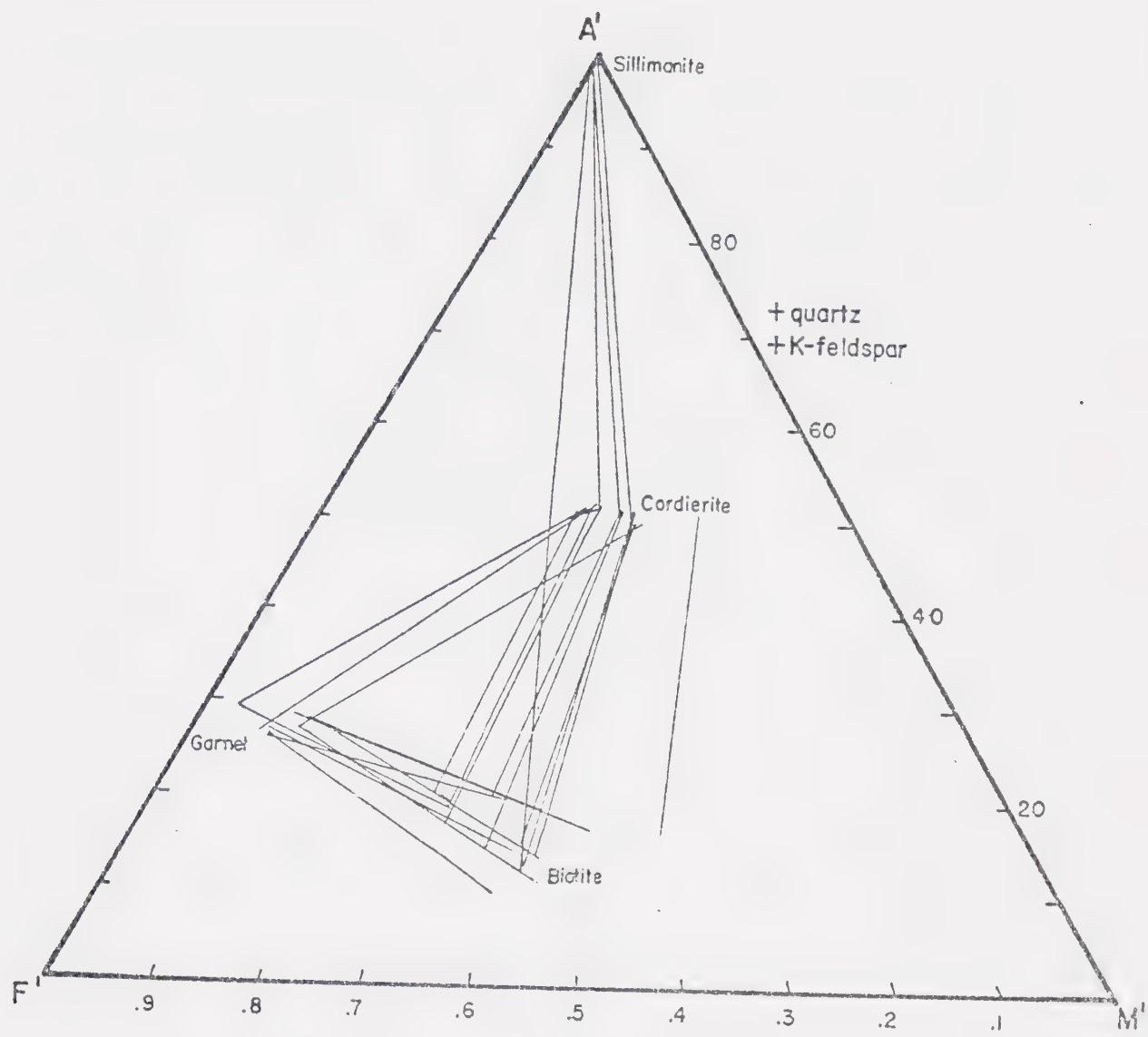


FIGURE 27: AKFM tetrahedron projected through K-feldspar (Thompson A'F'M' diagram) showing the compositional relationships between biotite-cordierite and garnet from the almandine-cordierite-K-feldspar zone.

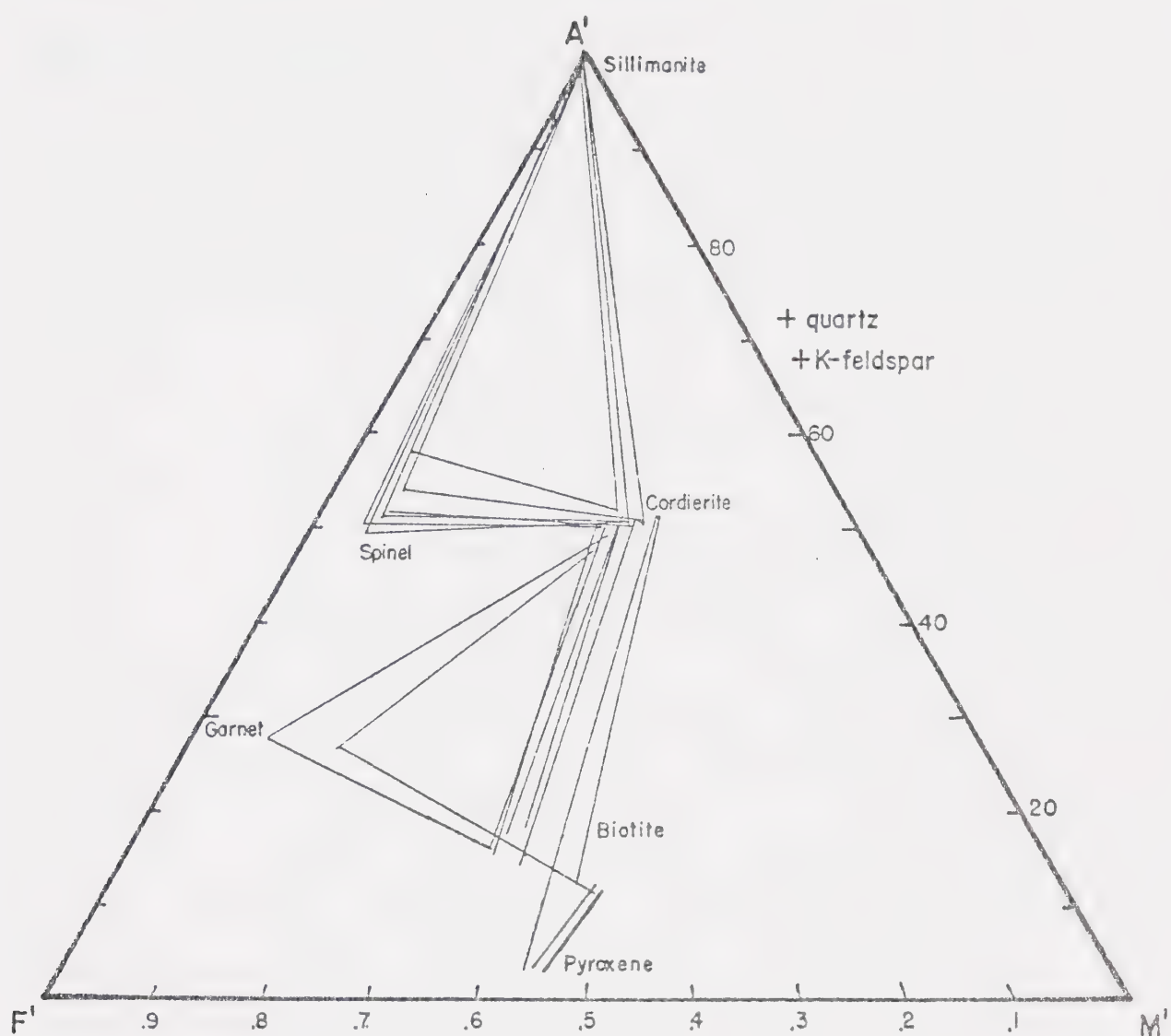


FIGURE 28: Thompson A'F'M' diagram showing the compositional relationships between cordierite, garnet, spinel, biotite, and orthopyroxene for samples from the remobilised Archean paragneiss.

progressive shift toward the Mg side of the diagram.

Geological Evolution

The data presented in this study, coupled with the data of Lord (1942), Hoffman (1970, 1973), and Leatherbarrow and Frith (1975), have been synthesized and interpreted to produce the following evolutionary scheme for the Arseno Lake area:

- 1) The Slave craton was originally developed as a series of granitic batholiths and greenstone belts. Kenoran intrusions and metamorphism produced local granulite grade assemblages of spinel-cordierite-garnet-orthopyroxene in the supracrustal sequence (Folinsbee, 1942).
- 2) In early to middle Aphébian time, uplift and erosion of this crystalline basement provided the clastic material deposited on the western margin of the Slave craton as the Epworth group sediments (Hoffman, 1970, 1973). In the Arseno Lake area, this sequence was deposited in a shallow marine to continental slope environment. Pressures deduced from metamorphic mineral assemblages suggest that the total sedimentary thickness exceeded 10-12 km.
- 3) The basal portions of this sequence were regionally metamorphosed to biotite zone conditions. The heat necessary to develop

these biotite-chlorite-muscovite assemblages can be accounted for by the higher heat flow associated with late Archean - early Proterozoic time.

- 4) A granitoid body was emplaced into the crystalline basement and caused the gneiss dome formation. The heat released by crystallisation and cooling of this body gave rise to the upper amphibolite grade mineral assemblages observed in the Arseno Lake area.

The higher heat flow, which caused the regional biotite zone metamorphism and the origin of the proposed granitoid pluton that intruded into the crystalline Archean basement, may be explained by the evidence of Proterozoic plate tectonic activity. Hoffman (1973) and Hoffman et al. (1974) have proposed the existence of an eastward dipping trench or Benioff zone in Proterozoic time which was situated west of the present Great Bear Lake, trending NE-SW. The Arseno Lake area lies ~ 300 km down-dip of this proposed structure and the granitoid intrusion may represent material melted above the Benioff zone and emplaced into the upper part of the crystalline basement. This is illustrated diagrammatically in Figure 29.

Scales of Equilibrium

The results presented in Part II have shown that within an area of high grade metamorphism, the scale of

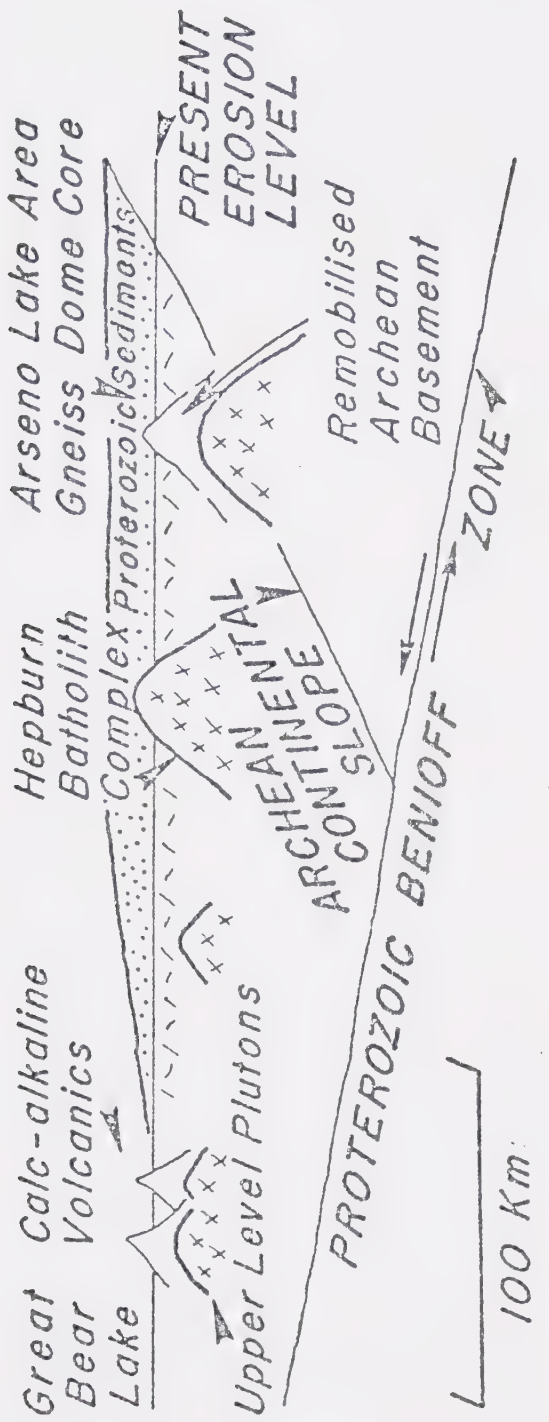


FIGURE 29: Diagram showing the proposed tectonic development of the Arseno Lake area.

equilibrium or intergranular homogeneity can vary as a function of the mineral phases participating and the mechanism by which components migrate between the equilibrating phases. Minerals such as cordierite and biotite are homogeneous on the scale of individual grains (up to 1-2 cm), and may be homogeneous throughout a single specimen if the rock itself has a homogeneous distribution of mineral species. Thus a rock with no metamorphic segregation, composed of biotite, cordierite, quartz and the feldspars, may have completely homogeneous biotite and cordierite and the scale of equilibration may be several centimeters. On the other hand, a rock with a heterogeneous distribution of mineral species will develop several sub-domains, each characterised by a distinct composition of biotite and cordierite. This situation of heterogeneous chemistry also arises where a relatively refractory or inhomogeneous phase occurs, for example where zoned garnets are present. In this case, the scale of equilibration is on the order of 5 mm and biotite compositions vary throughout the specimen as a function of the phase assemblage immediately surrounding it. Thus the local presence of ilmenite or rutile will produce a Ti richer biotite and the presence of garnet will produce an Mg richer, Fe,Mn poorer biotite.

The scale of equilibration is thus a function of the refractory nature of the local mineral assemblage and the rate of intergranular diffusion. In the Arseno Lake

area, the high grade gneisses from the cordierite-almandine-K-feldspar zone are characterised by small scales of equilibration, as evidenced by heterogeneity of biotites, and a CO_2 rich fluid, as evidenced by nearly pure CO_2 primary fluid conclusions.

BIBLIOGRAPHY

- ABS-WURMBACH, I. and LANGER, K., 1975. Synthetic Mn³⁺-kyanite and viridine, $(Al_{1-x}Mn^{3+})SiO_5$, in the system Al₂O₃-MnO-MnO₂-SiO₂. Contrib. Mineral. Petrol. 49, 21-38.
- ALBEE, A.L., 1965. Distribution of Fe, Mg, and Mn between garnets and biotite in natural mineral assemblages. Jour. Geol. 73, 155-164.
- ALTHAUS, E., 1967. The triple point andalusite-sillimanite-kyanite. Contrib. Mineral. Petrol. 16, 29-44.
- ALTHAUS, E., KAROTHE, E., NITSCH, K.H., and WINKLER, H.G.F., 1970. An experimental re-examination of the upper stability limit of muscovite plus quartz. Neues Jahrb. Mineralogie Monatsh. 7, 289-336.
- ANDERSON, D.E., 1974. Modelling of diffusion properties of silicates. Pp. 31-52 in Geochemical Transport and Kinetics (ed. Hofmann, A.W. et al.) Carnegie Institution of Washington Publication 634.
- ANDERSON, D.E. and BUCKLEY, G.R., 1973. Zoning in garnets - diffusion models. Contrib. Mineral. Petrol. 40, 87-104.
- ANDERSON, P.A.M. and KLEPPA, O.J., 1969. The thermochemistry of the kyanite-sillimanite equilibrium. Am. Jour. Sci. 267, 285-290.
- BARROW, G., 1983. On an intrusion of muscovite-biotite gneiss in the southeastern highlands of Scotland, and its accompanying metamorphism. Geol. Soc. London Quart. Jour. 49, 330-358.
- BARTH, T.F.W., 1934. Temperatur i lava og magmamasser, samt et nytt geologisk termometer. Naturen 58, 187-192.
- BARTH, T.F.W., 1962. Theoretical Petrology (Second Edition). New York and London: John Wiley & Sons.
- BELL, P.M., 1963. Aluminum silicate system: Experiments

- tal determination of the triple point. Science 139, 1055-1056.
- BERG, J.M., 1975. Quantitative regional geobarometry of the anorthositic Nain Complex, Labrador. In International Conference on Geothermometry and Geobarometry Extended Abstracts.
- BETHUNE, P. and LADURON, D., 1975. Diffusion processes in resorbed garnets. Contrib. Mineral. Petrol. 50, 197-204.
- BIRD, G.W. and FAWCETT, J.J., 1971. Some metamorphic reactions in the system $K_2O-MgO-Al_2O_3-SiO_2-H_2O$. Trans. Am. Geophys. Un. 52, 377.
- BIRD, G.W. and FAWCETT, J.J., 1973. Stability relations of Mg-chlorite-muscovite and quartz between 5 and 10 kb water pressure. Jour. Petrol. 14, 415-428.
- BOWEN, N.L. and TUTTLE, O.F., 1949. The system $MgO-SiO_2-H_2O$. Geol. Soc. Am. Bull. 60, 439-460.
- BROWN, E.H., 1967. The greenschist facies in part of Eastern Otago, New Zealand. Contrib. Mineral. Petrol. 14, 259-292.
- BROWN, E.H., 1971. Phase relations of biotite and stilpnomelene in the greenschist facies. Contrib. Mineral. Petrol. 31, 275-299.
- BUTLER, B.C.M., 1965. Compositions of micas in metamorphic rocks. Pp. 291-298 in Controls of Metamorphism (ed. Pitcher, W.S. and Flynn, G.W.) Edinburgh: Oliver and Boyd.
- BUTLER, B.C.M., 1967. Chemical study of minerals from the Moine schists of the Ardnamurchan area, Argyllshire, Scotland. Jour. Petrol. 8, 233-267.
- CARMICHAEL, D.M., 1969. On the mechanism of prograde metamorphic reactions in quartz-bearing pelitic rocks. Contrib. Mineral. Petrol. 20, 244-267.
- CARMICHAEL, D.M., 1970. Intersecting isograds in the Whetstone Lake area, Ontario. Jour. Petrol. 11, 147-181.
- CHINNER, G.A., 1959. Garnet-cordierite paragneisses. Yb. Carnegie Instn. Wash. 58, 112-113.

- CHINNER, G.A., 1960. Pelitic gneisses with varying ferrous/ferric ratios from Glen Clova, Angus, Scotland. Jour. Petrol. 1, 178-217.
- CHINNER, G.A., 1962. Almandine in thermal aureoles. Jour. Petrol. 3, 316-341.
- CLARK, S.P., JR., ROBERTSON, E.C., and BIRCH, F., 1957. Experimental determination of kyanite-sillimanite equilibrium relations at high temperatures and pressures. Am. Jour. Sci. 255, 628-640.
- CURRIE, K.L., 1971. The reaction 3 cordierite = 2 garnet + 4 sillimanite + 5 quartz as a geological thermometer in the Opinicon Lake region, Ontario. Contrib. Mineral. Petrol. 33, 215-226.
- CURRIE, K.L., 1974. A note on the calibration of the garnet-cordierite geothermometer and geobarometer. Contrib. Mineral. Petrol. 44, 35-44.
- DALLMEYER, R.D. 1972. Compositional controls on cordierite-bearing assemblages in high-grade regional metamorphism. XXIV Internat. Geol. Congress, Section 2, 52-63.
- DALLMEYER, R.D. and DODD, R.T., 1971. Distribution and significance of cordierite in paragneisses of the Hudson highlands, southeastern New York. Contrib. Mineral. Petrol. 33, 289-308.
- DAY, H.W., 1973. The high temperature stability of muscovite plus quartz. Am. Mineral. 58, 255-262.
- DEER, W.A., HOWIE, R.A., and ZUSSMAN, J., 1962. Rock-forming Minerals, Volume 1 (Ortho and Ring Silicates), Volume 3 (Sheet Silicates) and Volume 5 (Non-Silicates). London: Longmans, Green and Co.
- DEER, W.A., HOWIE, R.A., and ZUSSMAN, J., 1966. An Introduction to the Rock-forming Minerals. London: Longmans, Green and Co.
- DOUGAN, T.W., 1974. Cordierite gneisses and associated lithologies of the Guri area, northwest Guayana Shield, Venezuela. Contrib. Mineral. Petrol. 46, 169-188.
- DUNCOMB, P. and REED, S.B.J., 1968. The calculation of stopping power and backscatter effects in electron probe microanalyses. Nat. Bur. Stand. (U.S.), Spec. Publ. 298, 133-154.

- ESKOLA, P., 1915. On the relations between the chemical and mineralogical composition in the metamorphic rocks of the Orijarvi region. Bull. Comm. Geol. Finlante 44, 109-145.
- ESKOLA, P., 1920. The mineral facies of rocks. Norsk. Geol. Tidsskr. 6, 143-194.
- EUGSTER, H.P., 1959. Reduction and oxidation in metamorphism. Pp. 397-426 in Researches in Geochemistry (ed. Abelson, P.H.) New York: John Wiley & Sons.
- EUGSTER, H.P. and WONES, D.R., 1962. Stability relations of ferrounginous biotite, annite. Jour. Petrol. 3, 82-125.
- EVANS, B.W., 1965. Application of a reaction rate method to the breakdown equilibria of muscovite and muscovite plus quartz. Am. Jour. Sci. 263, 647-667.
- EVANS, B.W. and GUIDOTTI, C.V., 1965. The sillimanite-potash feldspar isograd in western Maine, U.S.A. Contrib. Mineral. Petrol. 12, 25-62.
- FOLINSBEE, R.E., 1940. Gem cordierite from the Great Slave Lake area. Am. Mineral. 25, 216.
- FOLINSBEE, R.E., 1941. The chemical composition of garnet associated with cordierite. Am. Mineral. 26, 50-53.
- FOLINSBEE, R.E., 1942. Zone facies of metamorphism in relation to the ore deposits of the Yellowknife-Beaulieu region. Ph.D. thesis, Univ. of Minnesota.
- FRENCH, B.M., 1966. Some geological implications of equilibrium between graphite and a C-H-O gas phase at high temperatures and pressures. Rev. Geophysics 4, 223-253.
- FRENCH, B.M. and EUGSTER, H.P., 1965. Experimental control of oxygen fugacities by graphite-gas equilibria. Jour. Geophys. Res. 70, 1529-1539.
- FRITH, R.A., 1973. The geology of the Bear-Slave boundary in the Indin Lake area, District of Mackenzie. Report Geol. Surv. Can. 1A.

- FRITH, R.A., FRITH, R., HELMSTAEDT, H., HILL, J., and LEATHERBARROW, R., 1974. Geology of the Indin Lake area (86B) District of Mackenzie. Report Geol. Surv. Can. 1A.
- FRITH, R.A. and LEATHERBARROW, R., 1975. Preliminary report of the geology of the Arseno Lake map area (86B-12), District of Mackenzie. Geol. Surv. Can., Paper 75-1, Part A, 317-321.
- FROESE, E., 1973. The oxidation of almandine and iron cordierite. Can. Mineral. 11, 991-1002.
- GANGULY, J. and KENNEDY, G.C., 1974. The energetics of natural garnet solid solution. I. Mixing of aluminosilicate end-members. Contrib. Mineral. Petrol. 48, 137-148.
- GHENT, E.D., 1975. Plagioclase-garnet-Al₂SiO₅-quartz: a potential geobarometer-geothermometer. International Conference on Geothermometry and Geobarometry, Extended Abstracts.
- GRANT, J.A., 1973. Phase equilibria in high-grade metamorphism and partial melting of pelitic rocks. Am. Jour. Sci. 273, 289-317.
- GRANT, J.A. and WEIBLEN, P.W., 1971. Retrograde zoning in garnet near the second sillimanite isograd. Am. Jour. Sci. 270, 281-296.
- GREENWOOD, H.J., 1961. The system NaAlSiO₄-H₂O-argon: total pressure and water pressure in métamorphism. Jour. Geophys. Res. 66, 3923-3946.
- GREENWOOD, H.J., 1963. Gas mixtures. Yb. Carnegie Instn. Wash. 62, 137-139.
- GREENWOOD, H.J., 1967. Mineral equilibria in the system MgO-SiO₂-H₂O-CO₂. Pp. 542-547 in Researches in Geochemistry II. (ed. Abelson, P.H.) New York: John Wiley & Sons.
- GREENWOOD, H.J., 1973. Thermodynamic properties of gaseous mixtures of H₂O and CO₂ between 450 and 800° C. and 0-500 bars. Am. Jour. Sci. 273, 561-571.
- GUIDOTTI, C.V., 1970. The mineralogy and petrology of the transition from the lower to upper sillimanite zone in the Oquossoc area, Maine. Jour. Petrol. 11, 277-336.

- GUIDOTTI, C.V., 1973. Compositional variation of muscovite as a function of metamorphic grade and assemblage in metapelites from northwest Maine. Contrib. Mineral. Petrol. 42, 33-42.
- HARIYA, J.F. and KENNEDY, G.C., 1968. Equilibrium study of anorthite under high pressure and high temperature. Am. Jour. Sci. 266, 193-203.
- HARKER, A., 1964. Petrology for Students. Cambridge: Cambridge University Press.
- HARRIS, N.B.W., 1976. The significance of garnet and cordierite from the Sioux Lookout region of the English River gneiss belt, northern Ontario. Contrib. Mineral. Petrol. 55, 91-104.
- HARTE, B., 1975. Determination of a pelitic petrogenetic grid for the eastern Scottish Dalradian. Yb. Carnegie Instn. Wash. 75, 438-446.
- HAYS, J.F., 1967. Lime-alumina-silica. Yb. Carnegie Instn. Wash. 65, 234-239.
- HEINRICH, K.F.J., 1967. The absorption correction model for microanalysis. Proc. Nat. Conf. Electron Microprobe Anal. 2nd. Paper No. 7.
- HEMLEY, J.J., 1967. Stability relations of pyrophyllite, andalusite and quartz at elevated pressures and temperatures. Am. Geophys. Union Trans. 48, 224.
- HENRY, J., 1974. Garnet-cordierite gneisses near the Egersund-Ogna anorthositic intrusion, southwestern Norway. Lithos 17, 207-216.
- HENSEN, B.J., 1971. Theoretical phase relations involving cordierite and garnet in the system MgO-FeO-Al₂O₃-SiO₂. Contrib. Mineral. Petrol. 33, 191-214.
- HENSEN, B.J. and GREEN, D.H., 1971. Experimental study of the stability of cordierite and garnet in pelitic compositions at high pressures and temperature. Part I. Compositions with excess alumino-silicate. Contrib. Mineral. Petrol. 33, 309-330.
- HENSEN, B.J. and GREEN, D.H., 1972. Experimental study of the stability of cordierite and garnet in pelitic compositions at high pressures and tempera-

- tures. Part II. Compositions without excess alumino-silicate. Contrib. Mineral. Petrol. 35, 331-354.
- HENSEN, B.J. and GREEN, D.H., 1973. Experimental study of the stability of cordierite and garnet in pelitic compositions at high pressures and temperatures. Part III. Synthesis of experimental data and geological applications. Contrib. Mineral. Petrol. 38, 151-166.
- HESS, P.C., 1969. The metamorphic paragenesis of cordierite in pelitic rocks. Contrib. Mineral. Petrol. 24, 191-207.
- HIETANEN, A., 1967. On the facies series in various types of metamorphism. Jour. Geol. 75, 187-214.
- HIRSCHBERG, A. and WINKLER, H.G.F., 1968. Stabilitätsbeziehungen zwischen chlorit, cordierit und almandin bei der metamorphose. Contrib. Mineral. Petrol. 18, 17-42.
- HOFFMAN, P.F., 1970. Study of the Epworth Group, Coppermine River area, District of Mackenzie. Pp. 144-149 in Report of Activities, Part A: April to October, 1969; Geol. Surv. Can., Paper 70-1.
- HOFFMAN, P.F., 1973. Evolution of an early Proterozoic continental margin: the Coronation geosyncline and associated aulacogens of the northwestern Canadian shield. Phil. Trans. Royal Soc. Lond. A. 273, 547-581.
- HOFFMAN, P.F., DEWEY, J.F., and BURKE, K., 1974. Aulacogens and their genetic relation to geosynclines, with a Proterozoic example from Great Slave Lake, Canada. Pp. 38-55 in Modern and Ancient Geosynclinal Sedimentation (ed. Dott, R.H., Jr. and Shaver, R.H.) Soc. Econ. Paleon. and Mineral., Special Pub. No. 19.
- HOFMANN, A.W., GILETTI, B.J., YODER, H.S., Jr., and YUND, R.A., 1974. Geochemical Transport and Kinetics Carnegie Institution of Washington Publication 634.
- HOLDWAY, M.J., 1971. Stability of andalusite and the aluminum silicate phase diagram. Am. Jour. Sci. 271, 97-131.

- HOLDAWAY, M.J., 1976. Mutual compatibility relations of the Fe^{+2} -Mg-Al silicates at 800° C. and 3 kb. Am. Jour. Sci. 276, 285-308.
- HOLDAWAY, M.J. and HASS, H., 1973. Equilibria in the system Al_2O_3 - SiO_2 - H_2O involving the stability limits of pyrophyllite, and thermodynamic data of pyrophyllite. Am. Jour. Sci. 273, 449-464.
- HOLLISTER, L.S., 1975. Granulite facies metamorphism in the coast range crystalline belt. Can. Jour. Earth Sci. 12, 1953-1955.
- HOLLISTER, L.S. and BURRUSS, R.C., 1976. Phase equilibria in fluid inclusions from the Khtada Lake metamorphic complex. Geochim. et Cosmochim. Acta 140, 163-175.
- HOLM, J.L. and KLEPPA, O.J., 1966. The thermodynamic properties of the aluminum silicates. Am. Mineral. 51, 1608-1622.
- HOSCHEK, G., 1969. The stability of staurolite and chloritoid and their significance in metamorphism of pelitic rocks. Contrib. Mineral. Petrol. 22, 208-232.
- HSU, L.C., 1968. Selected phase relationships in the system Al - Mn - Fe - Si - O - H : a model for garnet equilibria. Jour. Petrol. 9, 40-83.
- HUANG, W.L. and WYLLIE, P.J., 1974. Melting relations of muscovite with quartz and sanidine in the K_2O - Al_2O_3 - SiO_2 - H_2O system to 30 kilobars and an outline of paragonite melting relations. Am. Jour. Sci. 274, 378-395.
- HUTCHEON, I., FROESE, E., and GORDON, T.M., 1974. The assemblage quartz-sillimanite-garnet-cordierite as an indicator of metamorphic conditions in the Daly Bay complex, N.W.T. Contrib. Mineral. Petrol. 44, 29-34.
- KERRICK, D.M., 1968. Experiments on the upper stability limit of pyrophyllite at 1.8 kilobars and 3.9 kilobars water pressure. Am. Jour. Sci. 266, 204-214.
- KERRICK, D.M., 1972. Experimental determination of muscovite + quartz stability with $\text{P}_{\text{H}_2\text{O}} < \text{P}_{\text{total}}$. Am. Jour. Sci. 272, 946-958.

- KHITAROV, N.I., PUGIN, V.A., CHAO, P., and SLUTSKIY, A.B., 1963. Relations between andalusite, kyanite and sillimanite at moderate temperatures and pressures. Geochemistry (English Translation) 235-244.
- KRETZ, R. 1959. Chemical study of garnet, biotite, and hornblende from gneisses of southwestern Quebec, with emphasis on distribution of elements in coexisting minerals. Jour. Geol. 67, 371-402.
- KRETZ, R., 1974. Some models for the rate of crystallization of garnet in metamorphic rocks. Lithos 7, 123-136.
- LAL, R.K. and MOORHOUSE, W.W., 1969. Cordierite-gedrite rocks and associated gneisses of Fishtail Lake, Harcourt Township, Ontario. Can. Jour. Earth Sci. 6, 145-165.
- LAMBERT, R.St.J., 1959. The mineralogy and metamorphism of the Moine schists of the Morar and Knoydart districts of Inverness-shire. Trans. Royal Soc. Edinb. 63, 553-588.
- LAMBERT, R.St.J., 1965. The metamorphic facies concept. Min. Mag. 34, 283-291.
- LAMBERT, R.St.J., 1972. The metamorphic facies concept - continued. XXIV Internat. Geol. Cong., Section 2, 100-108.
- LEATHERBARROW, R., and FRITH, R.A., 1975. Gneiss domes along the boundary between the Bear and the Slave structural provinces (near Arseno Lake, N.W.T.). Geol. Soc. Am. Abst. 7, no. 6, 807.
- LORD, C.S., 1942. Snare River and Ingray Lake map areas, Northwest Territories. Geol. Surv. Can. Memoir 235.
- MATHER, J.D., 1970. The biotite isograd and the lower greenschist facies in the Dalradian rocks of Scotland. Jour. Petrol. 11, 253-275.
- McGLYNN, J.G. and ROSS, J.V., 1963. Arseno Lake map area, District of Mackenzie 86B/12. Geol. Surv. Can. Paper 63-26.
- MIYASHIRO, A., 1953. Calcium-poor garnet in relation to metamorphism. Geochim. et Cosmochim. Acta 4, 179-208.

- MIYASHIRO, A., 1958. Regional metamorphism of the Gosaisyo-Takanuki district in the central Abukuma Plateau. Jour. Fac. Sci. Tokyo Univ. Sec. II 11, 219-272.
- MIYASHIRO, A., 1961. Evolution of metamorphic belts. Jour. Petrol. 2, 277-311.
- MUELLER, R.F., 1967. Mobility of the elements in metamorphism. Jour. Geol. 75, 565-582.
- NEWTON, R.C., 1972. An experimental determination of the high-pressure stability limits of magnesian cordierite under wet and dry conditions. Jour. Geol. 80, 398-420.
- NIELSEN, P.A., 1975. Cordierite-garnet-spinel equilibria in polymetamorphic rocks from the Slave province of the Canadian Shield. Geol. Soc. Am. Abst. 7, No. 6, 829.
- OKRUSCH, M., 1971. Garnet-cordierite-biotite equilibria in the Steinach Aureole, Bavaria. Contrib. Mineral. Petrol. 32, 1-23.
- PANKRATZ, L.B. and KELLEY, K.K., 1964. High temperature heat contents and entropies of andalusite, kyanite and sillimanite. U.S. Bur. Mines Rept. Inv. 6370. 7 p.
- PHILIBERT, J., 1963. A method for calculating the absorption correction in electronprobe microanalysis. Pp. 379-392 in Third International Symposium on X-ray Optics and X-ray Microanalysis (ed. Pattee, H.H., Coslett, V.E., and Engstrom, A.) New York: Academic Press.
- PINSENT, R.H., 1971. Precambrian geology along the Fraser River between Mount Robson and Tête Jaune Cache, British Columbia. M.Sc. thesis, Univ. of Alberta.
- PINSENT, R.H. and SMITH, D.G.W., 1975. The development of carbonate-bearing biotite isograd assemblages from Tête Jaune Cache, British Columbia, Canada. Can. Mineral. 13, 151-161.
- RAMBERG, H., 1952. The Origin of Metamorphic and Metasomatic Rocks. Chicago: Univ. of Chicago Press.

RAMSAY, C.R., 1973a. Metamorphism and gold mineralisation of Archaean metasediments near Yellowknife, N.W.T., Canada. Ph.D. thesis, Univ. of Alberta.

RAMSAY, C.R., 1973b. Controls of biotite zone mineral chemistry in Archaean meta-sediments near Yellowknife, Northwest Territories, Canada. Jour. Petrol. 14, 467-488.

RAMSAY, C.R., 1973c. The origin of biotite in Archaean meta-sediments near Yellowknife, Northwest Territories, Canada. Contrib. Mineral. Petrol. 42, 43-54.

RAMSAY, C.R., 1974. The cordierite isograd in Archaean meta-sediments near Yellowknife, N.W.T., Canada - variations on an experimentally established reaction. Contrib. Mineral. Petrol. 47, 27-40.

RAMSAY, C.R. and MORTON, R.D., 1971. Hydrothermal retrogression of cordierite in the Bamble sector, south Norway. Neues Jahrb. Mineralogie Monatsh. 9, 398-403.

REED, S.J.B., 1965. Characteristic fluorescence corrections in electronprobe microanalysis. Brit. Jour. Appl. Phys. 16, 913-926.

REED, S.J.B. and WARE, N.G., 1975. Quantitative electron microprobe analysis of silicates using energy-dispersive X-ray spectrometry. Jour. Petrol. 16, 499-519.

REINHARDT, E.W., 1968. Phase relations in cordierite-bearing gneisses from the Gananoque area, Ontario. Can. Jour. Earth Sci. 5, 455-482.

RICHARDSON, S.W., 1968. Staurolite stability in a part of the system Fe-Al-Si-O-H. Jour. Petrol. 9, 467-488.

RICHARDSON, S.W., BELL, P.M., and GILBERT, M.C., 1968. Kyanite-sillimanite equilibrium between 700° and 1500° C. Am. Jour. Sci. 266, 513-541.

RICHARDSON, S.W., GILBERT, M.C., and BELL, P.M., 1969. Experimental determination of kyanite-andalusite and andalusite-sillimanite equilibria: the alumino-silicate triple point. Am. Jour. Sci. 267, 259-272.

ROBIE, R.A., BETHKE, P.M., and BEARDSLEY, K.M., 1967. Selected X-ray crystallographic data, molar volumes, and densities of minerals and related substances. U.S. Geol. Surv. Bull. 1248. 87 p.

ROEDDER, E., 1965. Liquid CO₂ inclusions in olivine-bearing nodules and phenocrysts from basalts. Amer. Mineral. 50, 1746-1782.

ROEDDER, E., 1972. Composition of fluid inclusions. Chapter JJ in Data of Geochemistry (ed. Fleischer, M.) 6th edition. U.S. Geol. Surv. Prof. Paper 440-JJ. 164 p.

ROEDDER, E. and SKINNER, B.J., 1968. Experimental evidence that fluid inclusions do not leak. Econ. Geol. 63, 715-730.

ROSS, J.V., 1962. Deposition and current direction within the Yellowknife Group at Mesa Lake, N.W.T., Canada. Bull. Geol. Soc. Am. 73, 1159-1162.

ROSS, J.V. and McGLYNN, J.C., 1965. Snare-Yellowknife relations, District of Mackenzie, N.W.T., Canada. Can. Jour. Earth Sci. 2, 118-130.

RUMBLE, D., 1971. Fe-Ti oxide minerals and the behaviour of oxygen during regional metamorphism. Yb. Carnegie Instn. Wash. 70, 157-165.

SAXENA, S.K., 1969. Silicate solid solutions and geothermometry. 3. Distribution of Fe and Mg between coexisting garnet and biotite. Contrib. Mineral. Petrol. 22, 259-267.

SAXENA, S.K. and HOLLANDER, N.B., 1969. Distribution of iron and magnesium in coexisting biotite, garnet, and cordierite. Am. Jour. Sci. 267, 210-216.

SCHMID, R. and WOOD, B.J., 1976. Phase relationships in granulitic metapelites from the Ivrea-Verbano zone (northern Italy). Contrib. Mineral. Petrol. 54, 255-280.

SCHREYER, W. and SEIFERT, F., 1969. Compatibility relations of the aluminum silicates in the systems MgO-Al₂O₃-SiO₂-H₂O and K₂O-MgO-Al₂O₃-SiO₂-H₂O at high pressures. Am. Jour. Sci. 267, 371-388.

- SCHREYER, W. and SEIFERT, F., 1970. Pressure dependence of crystal structures in the system $MgO-Al_2O_3-SiO_2-H_2O$ at pressures up to 30 kilobars. Physics Earth and Planetary Interiors 3, 422-430.
- SCHREYER, W. and YODER, H.S., 1961. Petrographic guides to the experimental petrology of cordierite. Yb. Carnegie Instn. Wash. 60, 147-152.
- SEIFERT, F., 1970. Low-temperature compatibility relations of cordierite in haplopelites of the system $K_2O-MgO-Al_2O_3-SiO_2-H_2O$. Jour. Petrol. 11, 73-99.
- SEIFERT, F., 1973. Stability of the assemblage cordierite-corundum in the system $MgO-Al_2O_3-SiO_2-H_2O$. Contrib. Mineral. Petrol. 41, 171-178.
- SHIDO, F., 1958. Plutonic and metamorphic rocks of the Nakoso and Iritono districts in the central Abukuma Plateau. Jour. Fac. Sci. Tokyo Univ. Sec. II 11, 131-217.
- SHIDO, F. and MIYASHIRO, A., 1959. Hornblendes of basic metamorphic rocks. Jour. Fac. Sci. Tokyo Univ. Sec. II 12, 85-102.
- SMITH, D.G.W. and GOLD, C.M., 1976. A scheme for fully quantitative energy dispersive microprobe analysis. Advances in X-ray Analysis (in press)
- SMITH, D.G.W., GOLD, C.M., and TOMLINSON, D.A., 1975. The atomic number dependence of the X-ray continuum intensity and the practical calculation of background in energy dispersive electron microprobe analysis. X-ray Spectrometry 4, 149-156.
- SMITH, D.G.W. and TOMLINSON, M.C., 1970. An APL language computer program for use in electron microprobe analysis. Kans. Geol. Surv. Comput. Contrib. 45. 28 p.
- SPRY, A., 1969. Metamorphic Textures. New York: Pergamon Press.
- STOCKWELL, C.H., McGLYNN, J.C., EMSLIE, R.F., SANFORD, B.V., NORRIS, A.W., DONALDSON, J.A., FAHRIG, W.F.,

- and CURRIE, K.L., 1970. Geology of the Canadian Shield. Pp. 43-150 in Geology and Economic Minerals of Canada (ed. Douglas, R.J.W.) Econ. Geol. Rept. Geol. Surv. Can. 1.
- STRENS, R.G.J., 1968. Stability of Al_2SiO_5 solid solutions. Min. Mag. 36, 839-849.
- TEX, E.D., 1971. The facies groups and facies series of metamorphism, and their relation to physical conditions in the Earth's crust. Lithos 4, 23-41.
- THOMPSON, A.B., 1975a. Cation exchange thermometry in metamorphic rocks. In International Conference on Geothermometry and Geobarometry, Extended Abstracts.
- THOMPSON, A.B., 1975b. Mineral reactions in calc mica schist from Gassetts, Vermont, U.S.A. Contrib. Mineral. Petrol. 153, 105-127.
- THOMPSON, A.B., 1976a. Mineral reactions in pelitic rocks: I. Prediction of P-T-X(Fe-Mg) phase relations. Am. Jour. Sci. 276, 401-424.
- THOMPSON, A.B., 1976b. Mineral reactions in pelitic rocks: II. Calculation of some P-T-X(Fe-Mg) phase relations. Am. Jour. Sci. 276, 425-454.
- THOMPSON, J.B., Jr., 1955. The thermodynamic basis for the mineral facies concept. Am. Jour. Sci. 253, 65-103.
- TILLEY, C.E., 1923. Contact metamorphism in the Comrie area of the Perthshire Highlands. Geol. Soc. London Quart. Jour. 80, 22-71.
- TILLEY, C.E., 1924. The facies classification of metamorphic rocks. Geol. Mag. 61, 167-171.
- TILLEY, C.E., 1926. Some mineralogical transformations in crystalline schists. Min. Mag. 21, 34-46.
- TOURET, J., 1971. Le facies granulite en Norvege Meridionale. II. Les inclusions fluides. Lithos 4, 423-436.
- TRACEY, R.J., ROBINSON, P., and THOMPSON, A.B., 1975. Garnet composition and zoning in the determination of temperature and pressure of metamorphism, central Massachusetts. In International

Conference on Geothermometry and Geobarometry,
Extended Abstracts.

- TRACEY, R.J., ROBINSON, P., and THOMPSON, A.B., in press. Garnet composition and zoning in the determination of temperature and pressure of metamorphism, central Massachusetts. Am. Mineral. (in press)
- TURNER, F.J., 1968. Metamorphic Petrology; Mineralogical and Field Aspects. New York: McGraw-Hill.
- TURNOCK, A.C. and EUGSTER, H.P., 1962. Fe-Al oxides: phase relationships below 1000° C. Jour. Petrol. 3, 533-565.
- VELDE, B., 1965. Phengite micas: synthesis, stability, and natural occurrence. Am. Jour. Sci. 263, 886-913.
- VERNON, R.H., 1972. Reactions involving hydration of cordierite and hypersthene. Contrib. Mineral. Petrol. 35, 125-137.
- VIDALE, R.J. and HEWETT, D.A., 1973. Mobile components in the formation of calc-silicate bands. Am. Mineral. 58, 991-997.
- VON PLATEN, H., 1965. Kristallisation granitscher schmelzen. Contrib. Mineral. Petrol. 11, 341-381.
- WANLESS, R.K., STEVENS, R.D., LACHANCE, G.R., and DELABIO, R.N., 1970. Age determinations and geological studies; K-Ar isotopic ages, part 9. Geol. Surv. Can. Paper 69-2A.
- WANLESS, R.K., STEVENS, R.D., LACHANCE, G.R., and EDMONDS, C.M., 1968. Age determinations and geological studies; K-Ar isotopic ages, report 8. Geol. Surv. Can. Paper 69-2A.
- WANLESS, R.K., STEVENS, R.D., LACHANCE, G.R., and RIMSAITE, J.Y.H., 1965. Age determinations and geological studies. Geol. Surv. Can. Paper 64-17, pt. 1.
- WANLESS, R.K., STEVENS, R.D., LACHANCE, G.R., and RIMSAITE, J.Y.H., 1966. Age determinations and geological studies; K-Ar isotopic ages, report 6. Geol. Surv. Can. Paper 65-17.
- WEILL, D.F., 1966. Stability relations in the Al_2O_3 -

SiO_2 system calculated from solubilities in the $\text{Al}_2\text{O}_3\text{-SiO}_2\text{-Na}_3\text{AlF}_6$ system. Geochim. et Cosmochim. Acta 30, 223-237.

WEISBROD, A., 1973a. Cordierite-garnet equilibrium in the system Fe-Mn-Al-Si-O-H. Yb. Carnegie Instn. Wash. 72, 515-518.

WEISBROD, A., 1973b. Refinements of the equilibrium conditions of the reaction Fe-cordierite = almandine + quartz + sillimanite ($+\text{H}_2\text{O}$). Yb. Carnegie Instn. Wash. 72, 518-521.

WINKLER, H.G.F., 1965. Petrogenesis of Metamorphic Rocks. New York: Springer-Verlag.

WINKLER, H.G.F., 1967. Petrogenesis of Metamorphic Rocks. (Revised second edition) New York: Springer-Verlag.

WINKLER, H.G.F., 1970. Wandel auf der gesteinmetamorphose. Geol. Rundsch. 57, 1002-1019.

WINKLER, H.G.F., 1974. Petrogenesis of Metamorphic Rocks. (Revised third edition) New York: Springer-Verlag.

WINKLER, H.G.F. and VON PLATEN, H., 1960. Experimentelle gesteinmetamorphose. III. Anatekische ultrametamorphose kalkhaltige tone. Geochim. et Cosmochim. Acta 18, 294-413.

WONES, D.R., 1963. Phase equilibria of "ferriannite", $\text{KF}_3^{+2}\text{Fe}^{+3}\text{Si}_3\text{O}_{10}(\text{OH})_2$. Am. Jour. Sci. 261, 581-596.

WONES, D.R. and EUGSTER, H.P., 1965. Stability of biotite: experiment, theory, application. Am. Mineral. 50, 1228-1272.

WOOD, B.J., 1973. $\text{Fe}^{2+}\text{-Mg}^{2+}$ partition between coexisting cordierite and garnet - a discussion of the experimental data. Contrib. Mineral. Petrol. 40, 253-258.

WYNNE-EDWARDS, H.R. and HAY, P.W., 1963. Coexisting cordierite and garnet in regionally metamorphosed rocks from the Westport area, Ontario. Can. Mineral. 7, 453-478.

YODER, H.S., Jr., 1952. The MgO-Al₂O₃-SiO₂-H₂O system and the related metamorphic facies. Am. Jour. Sci. 250A (Bowen Volume), 569-627.

ZEN, E-AN, 1969. The stability relations of the polymorphs of aluminum silicate: a survey and some comments. Am. Jour. Sci. 267, 297-309.

APPENDIX: METHODOLOGY

MINERAL ANALYSES

Equipment and Operating Conditions

The mineral analyses presented were obtained on an A.R.L. "EMX" microprobe which was fitted with an Ortec energy dispersive detector positioned at a distance of 270 mm from the sample, with an X-ray take-off angle of 52.5°. The associated electronic components were: a 450 research amplifier, a 454 timing filter amplifier, a 436 100 MHz discriminator, a 404A pulse pile-up rejector, and a 6220 MCA. The 6220 incorporates facilities for automatic correction of deadtime and pulse pile-up related counting losses. At a counting rate of 1000 pulses per second at 5.9 keV, the system had a full width half maximum (above background) of 154 eV. Data from the MCA was interfaced to an IBM 360/67 computer via a Texas Instruments Silent 700 ASR series, model 733, cassette tape terminal.

Analytical runs commenced and ended with the acquisition of a calibration standard spectrum. This spectrum permitted the calculation of shift and stretch of the standard and sample spectra. It was also used in the calculation of default standard intensities. The Fano factor and E_{noise} were also determined, which

allows the calculation of the FWHM of all peaks of interest.

Element concentrations were determined by comparison with silicate and oxide standards using the program EDATA, written by Smith, Gold, and Tomlinson (1975). At present, EDATA automatically and simultaneously searches for all of the elements from Na to Zn (except Ar) plus Zr and Ba. Recorded spectra are scanned by EDATA to seek and characterise peaks (energy, FWHM, intensity, and peak to background ratio). EDATA then corrects each spectrum by readjusting the intensity in each channel to those which would have been obtained with ideal instrument settings (i.e., 0.0 stretch and shift). Escape peaks are stripped using the method of Reed and Ware (1972). At this point, all intensities are normalised to a fixed probe current. The spectrum is then corrected for the continuum intensity using the method described by Smith *et al.* (1975) and Smith and Gold (1976). A peak free atomic number independent normalised background is multiplied by a factor related to the average Z of the unknown and then scaled to the unknown spectrum to take into account varying counting times and probe currents.

The spectrum is then corrected for overlap effects. Overlap coefficients are stored in a 22 x 22 matrix and are used to make corrections to analytical regions of interest by solving up to 21 simultaneous equations by the Gauss-Seidel iterative technique. Once overlap corrections

have been made, ZAF (matrix) corrections are performed. The atomic number correction employs the data of Duncomb and Reed (1968), the absorption correction uses the formulae of Philibert (1963) and Heinrich (1967), and the characteristic fluorescence correction uses the method of Reed (1965). For phases such as chlorite and the micas, the difference between 100% and the analytical total was assumed to be oxygen for the purpose of making matrix corrections.

For an unknown, the program continues iteratively through continuum, overlap, and ZAF corrections until present convergence limits have been achieved.

The present cut off for reporting the presence of an element is 300 ppm, and concentrations less than this are taken as zero. A useful measure of the success of this approach is the zero concentration reported for elements which are usually absent from each mineral group (i.e., K, Na in garnet; Zr, Ba in cordierite).

It should be stressed that all of the elements from Na to Zn (except Ar) plus Zr and Ba were analysed for in all of the mineral data presented. In all analyses presented, if an element is not reported, it is because that element was not detected at concentrations greater than 300 ppm.

F is reported for a few biotites and muscovites. F was measured using wavelength dispersive techniques on

a reconnaissance basis only. Where F is not reported, it was not determined.

The following operating conditions were used during analysis:

Analytical lines	$K_{\alpha(1,2)}$, $L_{\alpha(1,2)}$
Beam size	1 - 5 μm
Operation voltage	15 kV
Beam current	300 nanoamps
Probe current	30 - 35 nanoamps
Emission current	200 microamps
System livetime	400 seconds
Total time (live + deadtime)	450 - 520 seconds
Input count rate	\sim 3000 pulses per second

Precision and Accuracy of Energy Dispersive Analyses

The energy dispersive analyses presented in the text (Tables 2 - 18) are possibly slightly better than those which are normally achieved in conventional wavelength dispersive analysis. This is mainly a result of collecting data for all of the elements at the same point, simultaneously, over a relatively short time period. Thus, the problems of sample inhomogeneity are avoided, as are the potential uncertainties which may be introduced by spectrometer resetting and by long term contamination of the sample surface by a C rich film, in part derived by the breakdown of pump oils in the analysis chamber.

TABLE A - 1: Comparison of results obtained by energy dispersive and wavelength dispersive analysis of trace amounts of Zn and V for minerals from the Arseno Lake area

Mineral	Sample Number	Zn_E	Zn_W	$\frac{Zn_E}{Zn_W}$	V_E	V_W	$\frac{V_E}{V_W}$
Spinel	73376	13.280	n.d.		0.311	0.211	1.474
Biotite	73376	0.073	0.056	1.300	0.099	0.067	1.481
Cordierite	73376	0.104	0.080	1.300	-----	-----	
Ilmenite	73376	0.232	0.185	1.257	0.401	0.272	1.475
Spinel	73478	4.310	n.d.		0.051	0.035	1.457
Garnet	73478	0.096	0.080	1.200	-----	-----	
Cordierite	73478	0.129	0.104	1.231	-----	-----	
Biotite	73478	0.040	0.032	1.250	0.049	0.033	1.483
Ilmenite	72345	0.278	0.189	1.472	0.082	0.061	1.349
Spinel	72345	0.060	0.041	1.471	1.271	1.020	1.246
Garnet	72345	-----	-----		0.075	0.061	1.226
Cordierite	72345	-----	-----		0.061	0.048	1.271
Biotite	72345	0.183	0.092	1.983	0.031	0.024	1.275

----- = not detected

n.d. = not determined

E = energy dispersive analysis using EDATA for data reduction

W = wavelength dispersive analysis using PROBEDATA for data reduction

Minor elements (those present at the 0.2% or greater level) are probably comparable to the accuracy obtained by wavelength dispersive analysis. Elements below about 0.2% are unlikely to be as accurate as are wavelength dispersive analysis, because of a much lower peak/background ratio and high continuum intensity relative to true peak counts. Reed and Ware (1975) and Smith and Gold (1976) discuss the precision and accuracy of EDA and conclude that elements present in concentrations greater than 10 weight per cent usually have a coefficient of variation of less than 1% and never more than 3%. For elements present in concentrations between 1.0 and 10.0 weight per cent, the coefficient of variation ranges from 1 to 3.5% (Cocker, 1976).

Table A - 1 presents analyses of Zn and V present in minor and trace amounts in several phases using both energy dispersive and wavelength dispersive techniques. For these two elements, energy dispersive are greater than wavelength dispersive by a factor of 1.2 - 1.99 for Zn and 1.22 and 1.48 for V.

Comparative analyses of a variety of well characterised standards from the University of Alberta micro-probe laboratory are reported by Smith and Gold (1976).
Standards

A suite of nine standards was selected on the basis of homogeneity and composition, as determined by the

author and by results reported by several Geology 639 (Microprobe Analysis Theory and Technique) classes. Standards were used only for those elements for which they displayed homogeneity and where the element concentration in the standard exceeded that of the material being analysed. Table A - 2 lists the standards, their source, and the types of samples for which they were used. Table A - 3 lists the standard composition.

Sample Damage

Micaceous minerals from the chlorite zone and the lowest part of the biotite zone showed some damage caused by the electron beam, notably alkali migration away from the site of beam impact. This problem was most pronounced in the muscovites, due to their fine grain size, which required the use of a focussed beam ($0.5 - 1 \mu\text{m}$ in diameter) in order to avoid grain boundary effects and insure that the phase being analysed was the only phase in the volume excited by the electron beam. In coarser grained samples, this problem was overcome by scanning the beam over an area of the mineral being analysed. The normal area chosen was $19 \times 15 \mu\text{m}$. This corresponds to the smallest area which could be scanned using the beam scanning system available. This method of analysis generally eliminated alkali migration, and samples from the middle biotite zone through to the highest grade of metamorphism show little evidence of alkali migration.

TABLE A-2 : STANDARDS USED IN MICROPROBE ANALYSIS

MINERAL	NAME OF STANDARD (University of Alberta number)	REFERENCE	ELEMENTS
Feldspars	Hohenfels Sanidine (0279)	University of Alberta files	K, Al, Si, Ba
	Tiburon Albite (0009)	Evans	Na
	AN 80 Glass (0001)	Ribbe & Smith (1966)	Ca
Oxides	Ødegaarden Ilmenite (0152)	University of Alberta files	Ti, Fe
	Rhodonite (0269)	"	Mn
	Willemite (0332)	"	Zn
	Bayer Corundum (0076)	"	Al
	Periclase (0238)	"	Mg
All Silicates	Ødegaarden Ilmenite (0152)	University of Alberta files	Ti, Fe
	Rhodonite (0269)	"	Ca, Mn, (Si), Zn
	Hohenfels Sanidine (0279)	"	K, Na, Ba, (Si)
	Bayer Corundum (0076)	"	Al
	Periclase (0238)	"	Mg
	Quartz (0260)	"	(Si)

TABLE A-3 : Standard Compositions

STANDARD	Na	Mg	Al	Si	K	Ca	Ti	V	Mn	Fe	Zn	Ba	O
Willenite	0.07			12.89					3.77		54.16		29.12
Rhodonite	0.10	0.52	0.02	21.77	0.07	4.69			28.54	1.31	5.74		37.27
Bayer Corundum				52.93									47.07
Ødegaard Ilmenite			0.58	0.01					28.59	0.17	0.23	38.69	0.01
Hohenfels Saridine	2.23			9.93	30.23	10.05							31.72
Periclaste				60.32									39.68
Quartz							46.75						53.25
Tiburon Albitz	8.75			10.269	32.069	6.017							48.714
An 80 Glass	1.67			17.66	22.47				11.66				46.54

This problem can also be overcome on instruments where the energy dispersive detector can be placed closer to the sample. This allows much higher count rates at substantially lower probe currents. (At the University of Toronto, using a new Etec Autoprobe equipped with a movable detector, the equivalent count rate (3000 cps) used in this study can be obtained at 1% of the probe current required by the University of Alberta's probe laboratory.) This is essentially an inverse square relationship between sample to detector distance and probe current required to produce a constant count rate.

MAPS AND SAMPLING

Maps

Aerial photographs, 1:12,500 claim sheets, 1:50,000 NTS preliminary topographic maps, and the published map of Lord (1942) were used in the selection of traverses and served as the base maps for data plotting. The positions of quartzite and marble horizons were noted on the field maps and transferred to the final 1:50,000 geologic map. The geology shown on Map 1 is modified from the data of Lord (1942), McGlynn and Ross, (1963), and Frith and Leatherbarrow (1975).

Grade Index

In establishing a non-mineralogical index of metamorphic grade, it was first necessary to define and outline the highest temperature area of the thermal dome.

This area was defined by contouring the mole per cent gahnite ($ZnAl_2O_4$) in spinel data. There is a strong negative correlation between mole per cent gahnite in spinel and modal spinel. The gahnite content in spinel increased as modal spinel decreased. It was thus reasoned that the samples with the lowest gahnite content in spinel (and the highest modal spinel) had undergone the highest temperature equilibration with cordierite.

The reason for the relationship between gahnite content and modal spinel is most probably that Zn is much more stable in the spinel structure than in cordierite. At lower temperatures, a greater proportion of spinel would react with Si to form cordierite.

The Mg and Fe from the spinel could be readily incorporated in cordierite, but the Zn could remain in the spinel, causing a continuous increase in the gahnite content as modal spinel decreased. This is analogous to the Mn enrichment in retrograded garnets reported by Grant and Weiblen (1971).

Once the thermal high was outlined, the grade index of any sample was calculated as the distance from the thermal high to the sample, divided by the distance along the same line to the cordierite-almandine-K-feldspar isograd.

Thus, the grade index value increases with decreasing metamorphic grade. For the cordierite-almandine-K-feldspar zone, grade index varies from 0.0 - 1.0, the

cordierite zone from 1.0 - 2.7, and the biotite zone from about 2.0 - 4.0.

Samples

Samples of metasediments were collected from 893 localities along the Bear-Slave boundary and across the gneiss dome in the Bear Province. The locations of all samples are shown on Map 2. The samples were selected on the basis of the approximate bulk rock composition, as determined from hand specimen mineralogy, and are biased towards pelitic and basic chemistry, as these two general compositions show the best mineralogical variation with metamorphic grade.

Petrographic Methods

All samples were studied in thin section and a suite of 100 samples were selected for microprobe analysis on the basis of the mineral assemblages present and the absence of extensive weathering phenomena and secondary alteration. All samples selected for microprobe analysis were also examined in reflected light to select properly polished grains for analysis.

Mineral assemblage data for the unaltered samples are presented on Map 3 along with the metamorphic isograds deduced from mineral assemblage distribution.

FLUID INCLUSION STUDIES

The preliminary fluid inclusion work reported in this study was done using a normal petrographic micro-

scope with a x60 magnification objective and a x10 ocular. Standard petrographic thin sections and polished microprobe thin sections were studied in transmitted light, using the minimum aperature setting of the condenser stage to enhance relief and contrast.

The inclusions which contained both a liquid phase and vapor bubble were heated for a few seconds using a small hair dryer. If the vapor bubble homogenized with the liquid phase, it was then identified as a one component (CO_2), two phase inclusion. This is based on the low temperature ($\sim 30^\circ \text{ C.}$) required to cause homogenization of the CO_2 vapor - CO_2 liquid mixture. If the short heating to about 30° C. failed to homogenize the two phases, the inclusion was identified as a two component ($\text{H}_2\text{O} + \text{CO}_2$) inclusion. Only the data for primary fluid inclusions were used to estimate the composition of the metamorphic fluid.

Planar arrays of small vapor inclusions were observed in many of the sections studied. Dr. R. D. Morton (personal communication) has suggested that these inclusions are composed chiefly of H_2O and have probably formed after the main episode of metamorphism recorded in the Arseno Lake area. They are most likely related to the decline in temperature following the peak conditions reached by each sample.

TABLE A-4: Rb-Sr data for the samples plotted in figure
3.

Sample Number	Rb ppm	Sr ppm	$\text{Sr}^{87}/\text{Sr}^{86}$
73226	190	111	.85414
73180	73	150	.75597
73433	148	164	.77096
73486	107	182	.75506
73487	8	434	.71107
73488	156	138	.79913

TABLE A-5 : Microprobe analyses (weight %) and structural formulae (based on 20 oxygen ions) of aluminum silicate minerals from the Arseno Lake area

Sample Number	727	7259	7247	72351	73212	72329*	72329*	72321*	72321*
Grade Index	2.87	1.80	1.07	.50	.31	.68	.68	0.0	0.0
Mineral	andal	sill	sill	sill	sill	sill	sill	sill	fib
SiO ₂	36.18	36.78	36.74	37.18	35.92	37.98	36.81	37.27	35.37
Al ₂ O ₃	61.85	61.57	61.33	62.52	62.74	63.82	62.61	62.44	64.40
Fe ₂ O ₃ #	0.26	0.24	0.23	0.24	0.56	0.30	0.40	0.23	0.04
Cr ₂ O ₃	0.08	0.06	0.09	0.06	-----	-----	0.09	0.03	0.01
Mn ₂ O ₃	-----	-----	-----	-----	-----	-----	-----	0.01	0.01
V ₂ O ₃	-----	-----	0.10	-----	-----	nd	nd	nd	nd
MgO	98.37	98.65	98.29	100.01	99.22	102.10	100.00	100.01	99.86
Total									100.01
Si	3.974	4.025	4.025	4.012	3.916	4.018	3.979	4.023	3.826
Al	8.006	7.942	7.940	7.951	8.062	7.959	7.978	7.925	3.968
Fe	0.021	0.020	0.019	0.019	0.046	0.027	0.032	0.018	8.032
Cr	0.007	0.005	0.008	0.005	-----	-----	0.008	0.002	0.006
Mn	-----	-----	-----	-----	-----	-----	-----	0.001	0.001
V	-----	-----	0.008	-----	-----	nd	nd	0.002	0.001
Mg	-----	-----	-----	-----	-----	0.009	0.003	0.001	0.001

* analysed by wavelength dispersive method

total Fe as Fe₂O₃

nd not determined
----- not present (at concentration greater than 0.03 weight %)
andal andalusite
sill sillimanite
fib fibrolite

NUMERICAL METHODS AND SAMPLE CALCULATIONS

Calibration of Thompson's Geothermometry

The T- $\ln K$ relationships presented in the discussion of Thompson's (1975a; 1976a,b) garnet-biotite, garnet-cordierite, and biotite-cordierite geothermometers were calculated by this author. The three equations were determined by application of a least square linear regression analysis to the data presented by Berg (1975) and Tracey et al. (1975, in press). This was necessitated by the inability to obtain the equations directly from Thompson.

Calculation of Fe^{+3} in Spinel

The calculation of Fe^{+3} in spinel was done using an APL program, SPCALC, written by the author. An outline of this method follows:

1. The analysis was converted from weight per cent of the elements to moles of the elements.
2. The tetravalent, trivalent, and divalent cations were summed separately.
3. Twice the amount of the tetravalent cations was subtracted from the divalent sum (e.g., the spinel molecule Fe_2TiO_4).
4. One half the amount of the trivalent cations was subtracted from the divalent sum (e.g., spinel MgAl_2O_4).

5. Whatever divalent cation total remained after the subtractions was divided by three, and two-thirds of the remainder was assigned to Fe⁺³.

Thompson Geothermometry

A sample calculation (using the garnet-biotite geothermometer) is shown below. The garnet and biotite compositional data used are from Tables 10 and 12. (#73202)

	Fe	Mg	Fe/Fe+Mg	K _D	lnK _D	T°K	T°C
biot	2.656	1.952	.576		4.431	1.468	888
garn	4.488	0.763	.855				615

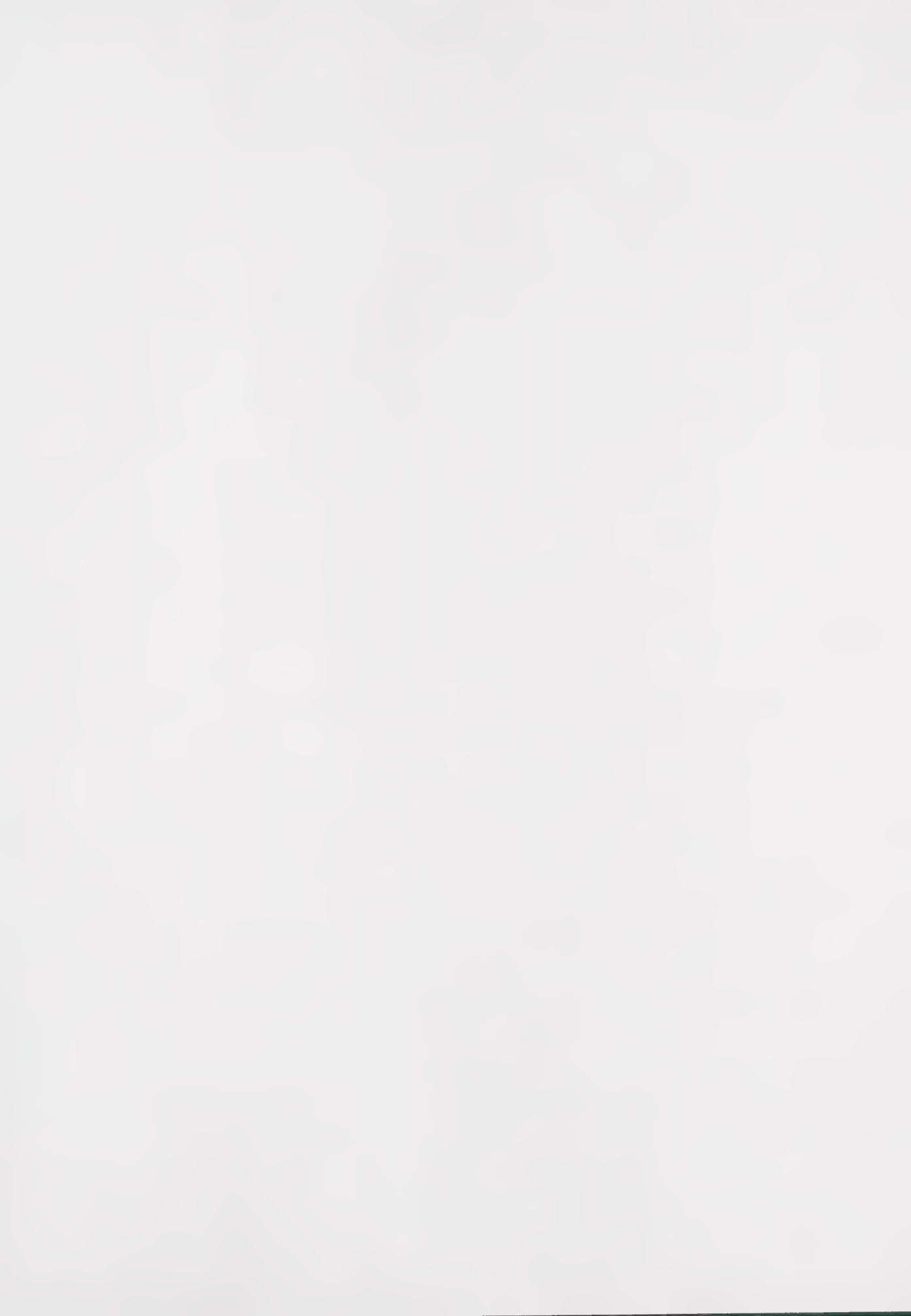
K_D is calculated as $x_{gt}^{Fe}x_{(1-x_{bi}^{Fe})}/(x_{bi}^{Fe}x_{(1-x_{gt}^{Fe})})$ where $x^{Fe}=Fe/(Fe+Mg)$.

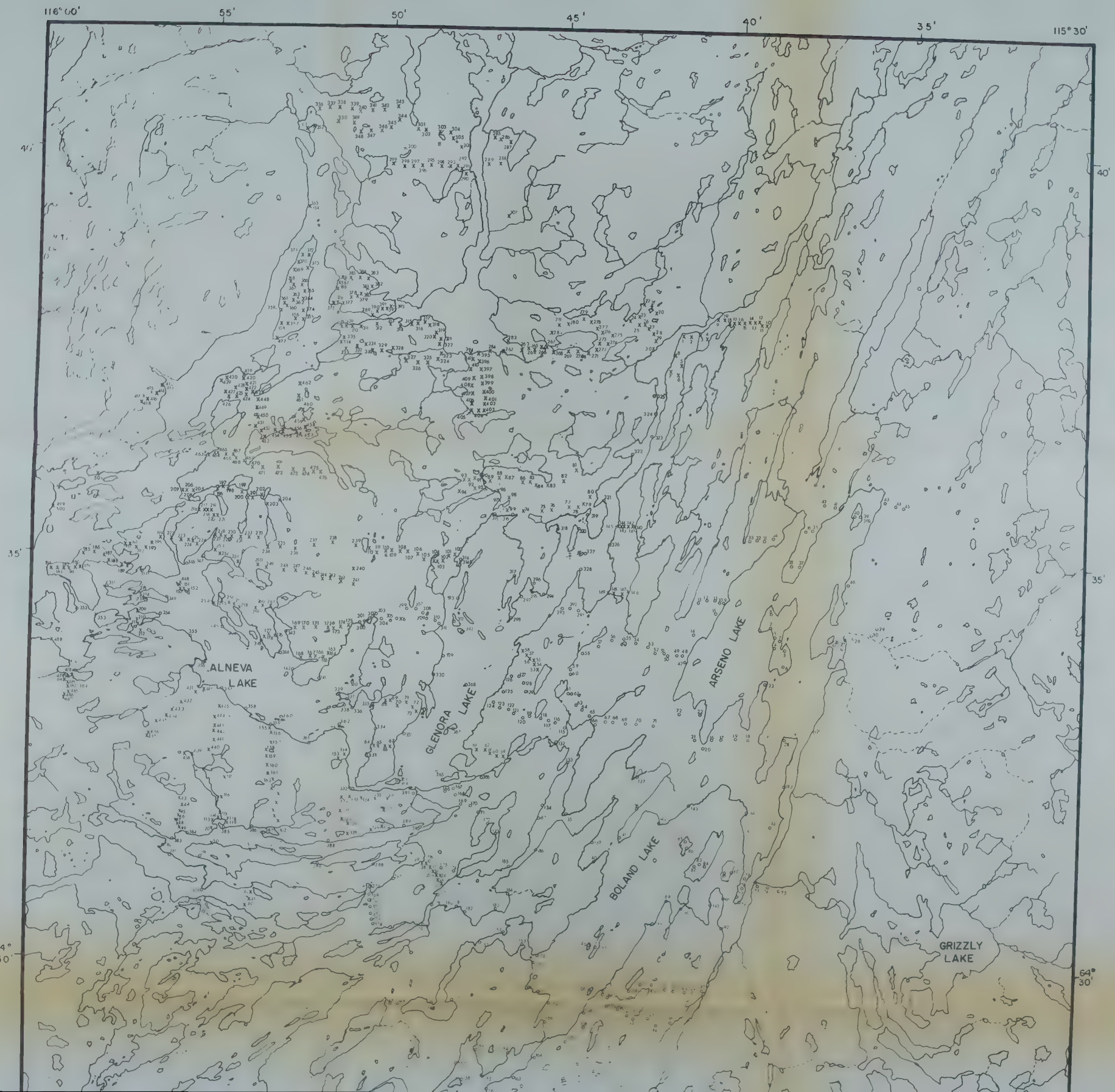
lnK_D is then put in the equation shown on page 142. The same procedure is followed for the garnet-cordierite and biotite cordierite thermometers. In all cases, the most Fe rich phase is used in the numerator (i.e. for garnet-biotite the numerator is $x_{gt}^{Fe}x_{(1-x_{bi}^{Fe})}$).

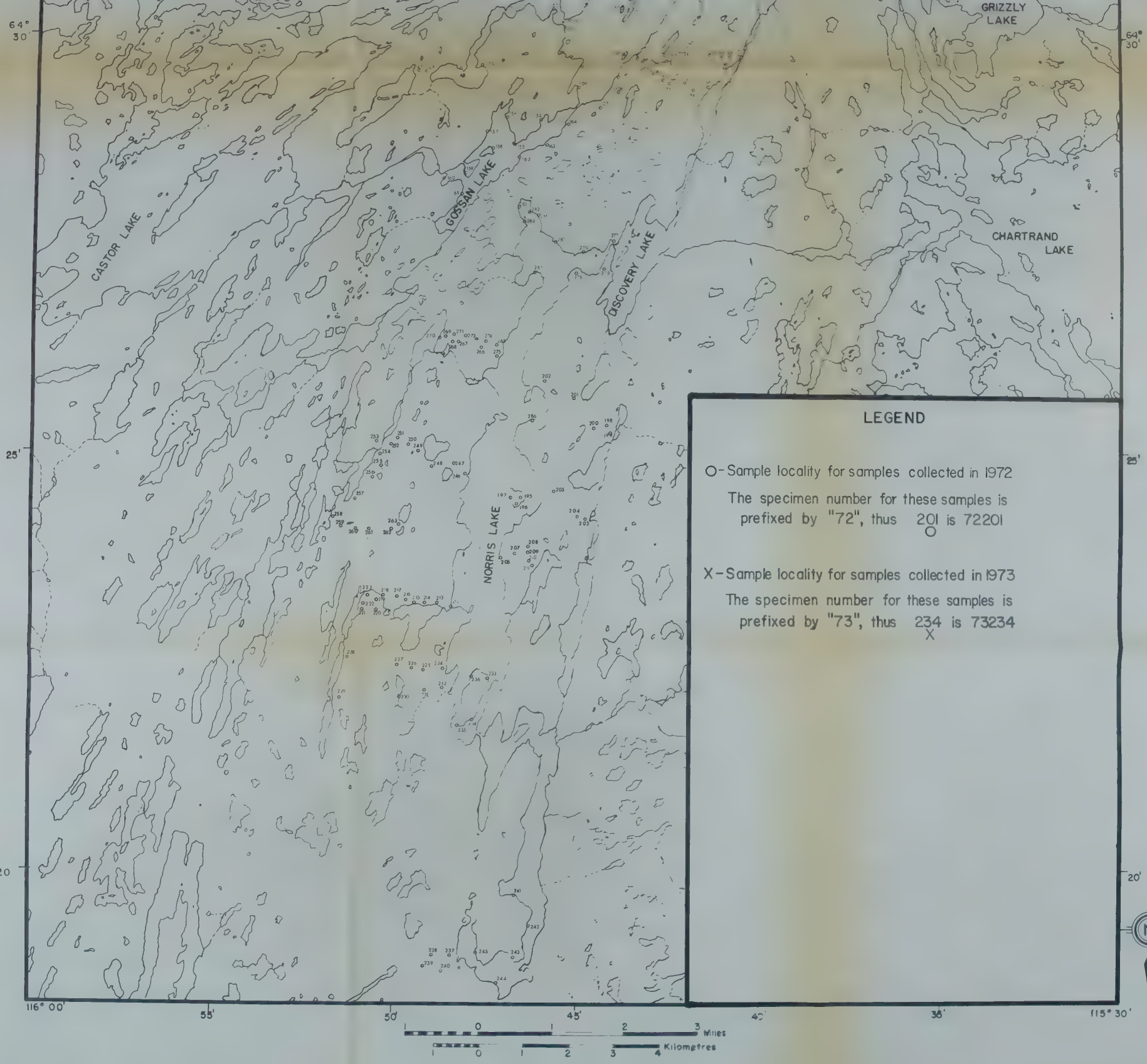
Currie Geothermometry

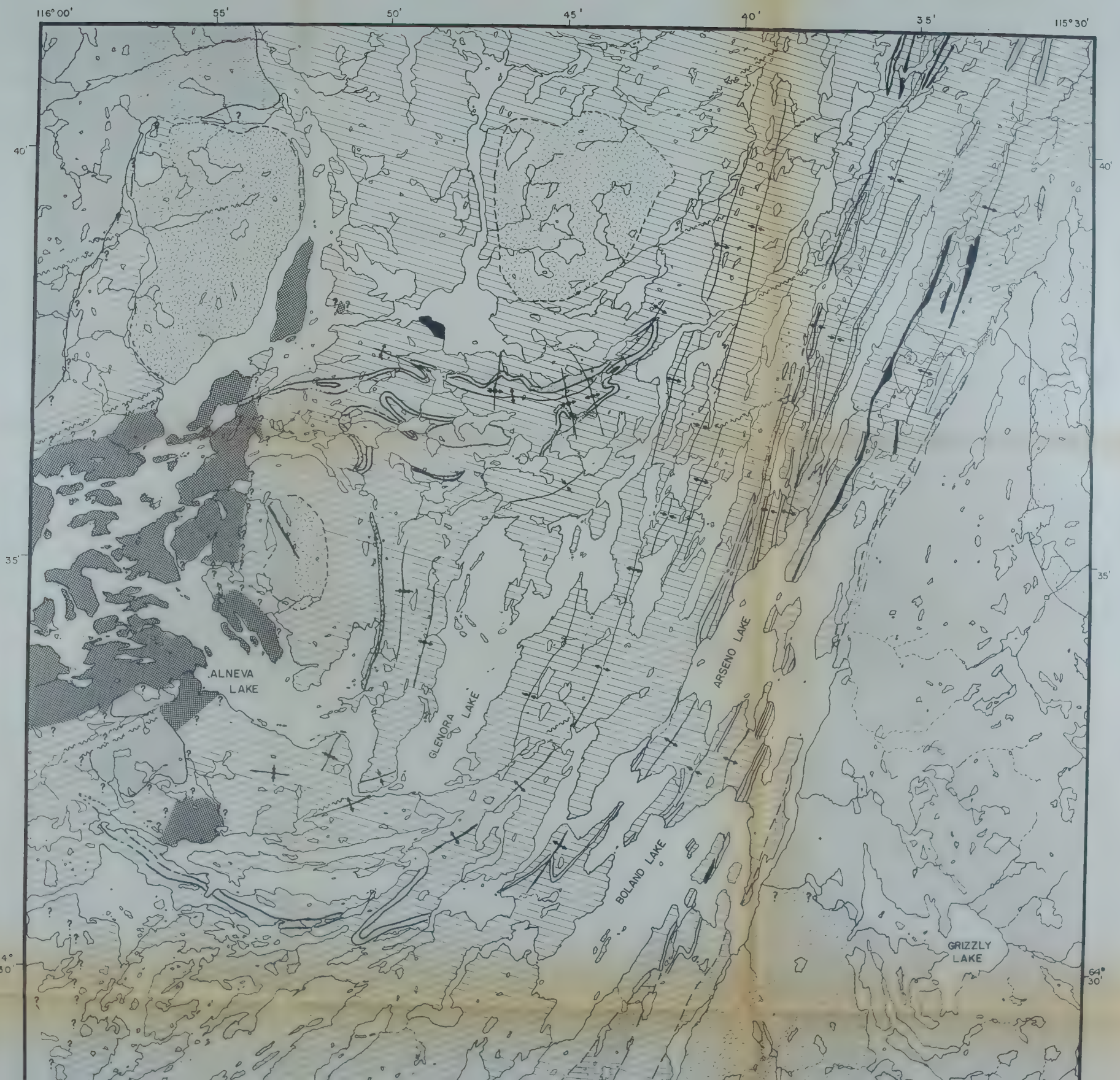
A sample calculation using the Currie (1971) thermometer (garnet-cordierite) is shown below. The data used are from Tables 11 and 12 (sample 202) and the equation used is shown on page 143.

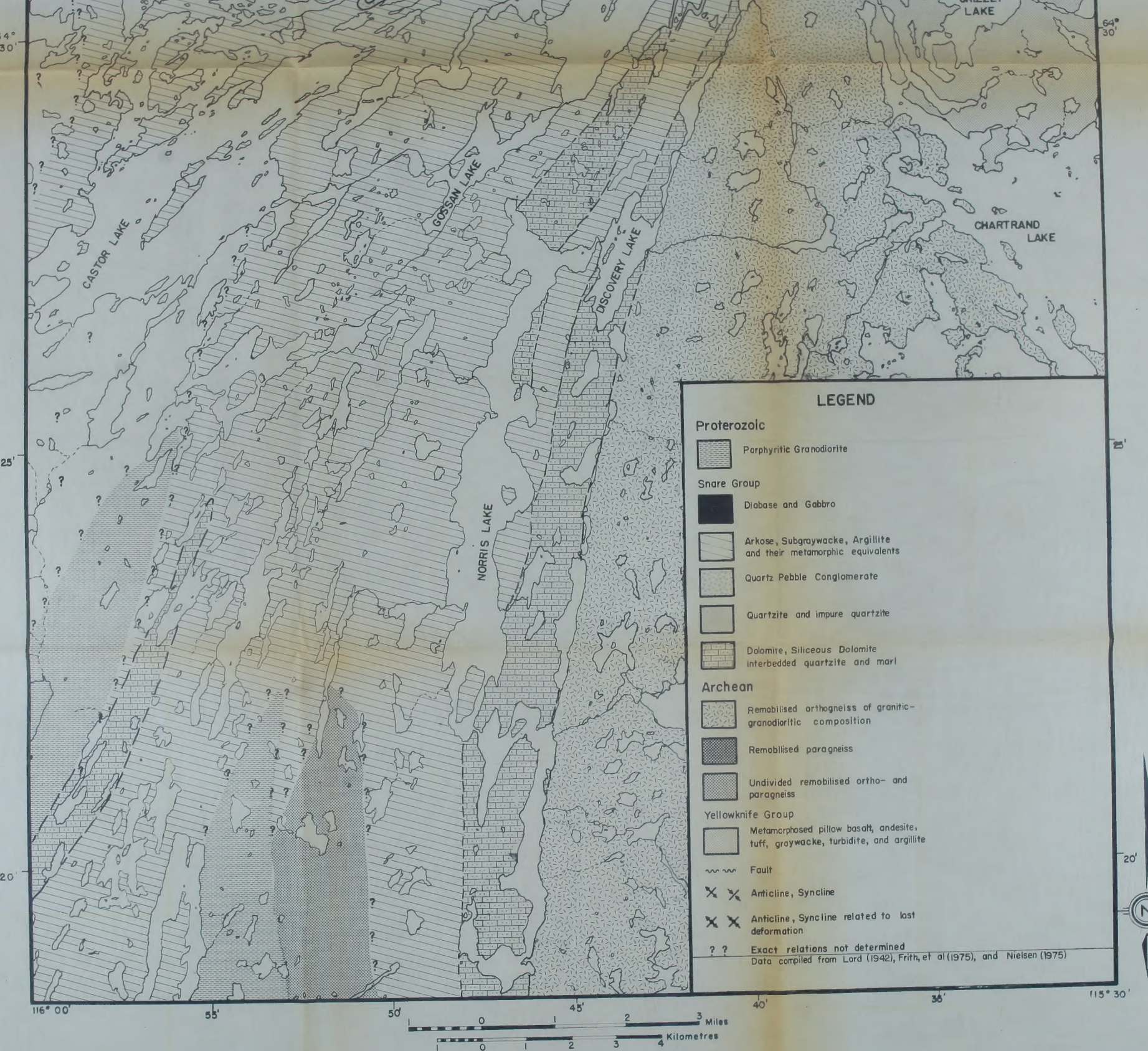
	Fe	Mg	Fe/Fe+Mg	K	lnK	T°K	T°C
cord	0.754	1.161	.394				
garn	4.488	0.763	.855	9.069	2.205	1084	811



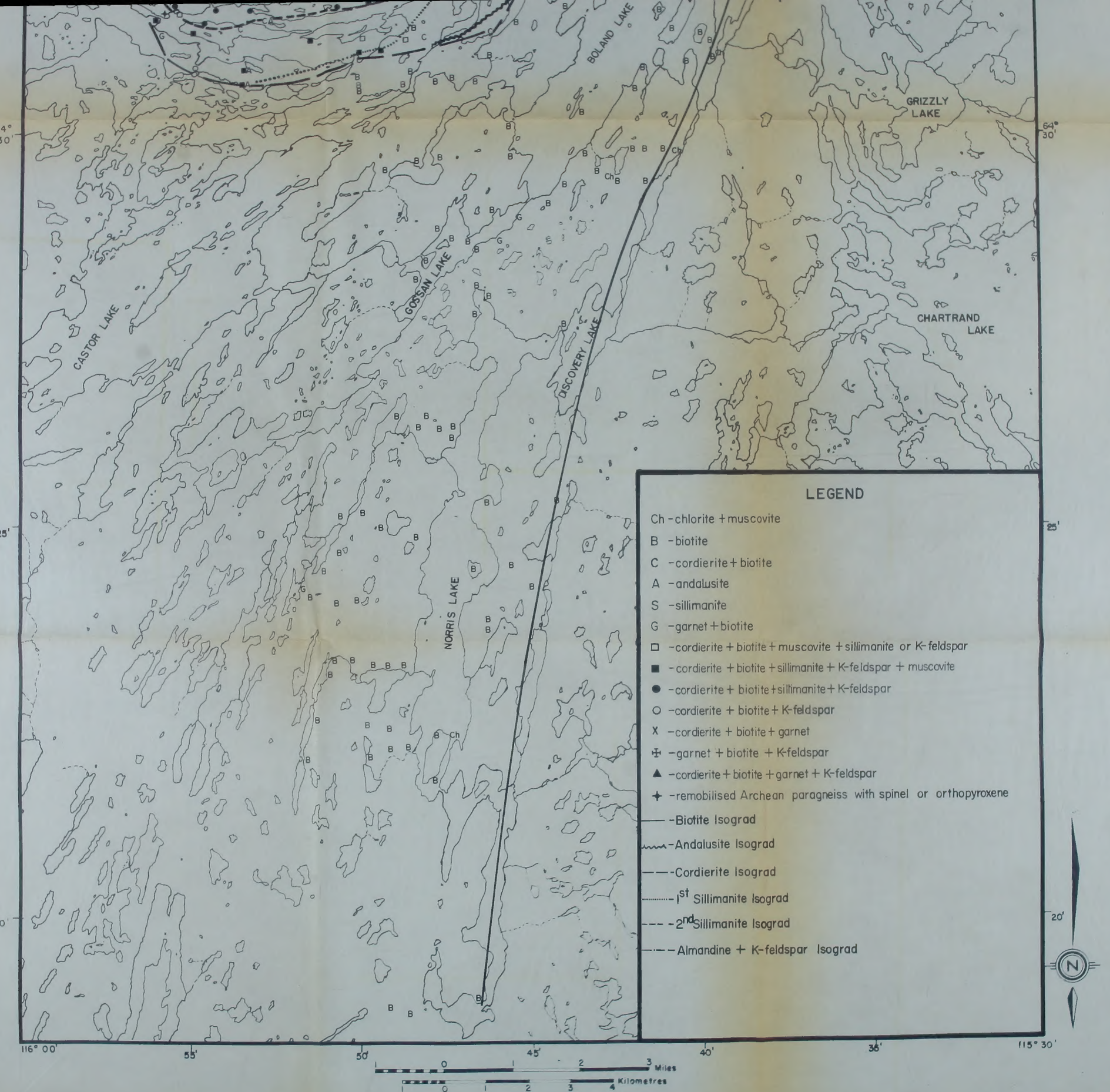












B30177